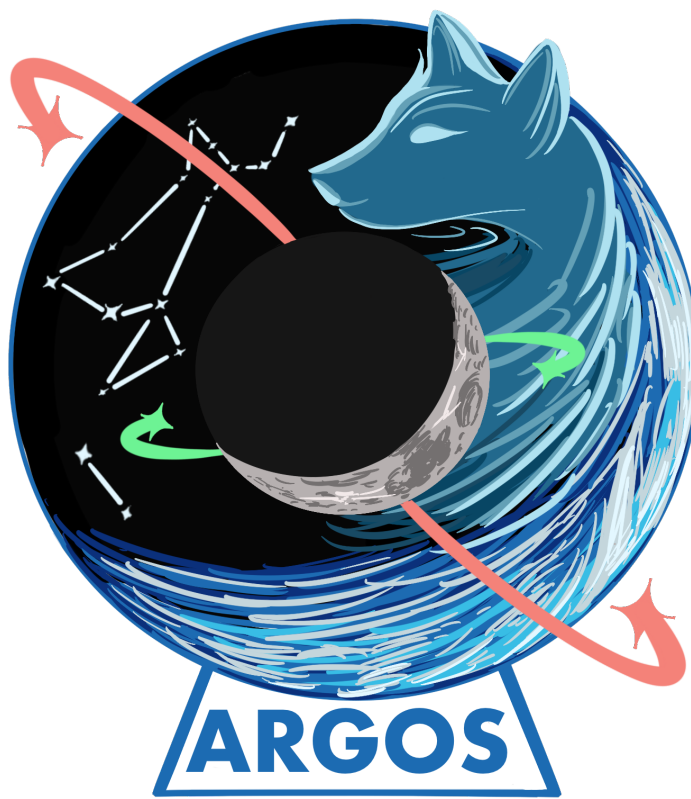


# MAE 342 Space System Design

## Final Design Report

**Team Name:** ARGOS

**Date:** May 7, 2024





## Abstract

The Advanced Relay for Geolunar Operational Support (ARGOS) mission is a four-satellite lunar mission designed to perform object tracking and establish a communications network in cislunar space. The mission has one 27U satellite each at Lagrange points L1 and L2 along with two 12U satellites in frozen lunar orbits, launched as payloads on Falcon 9 and Starship HLS rockets.

This report was written as a response to the Request for Proposal (RFP) and mimics the Pre-Phase A (Concept Studies) and Phase A (Concept and Technology Development) stages in the NASA Project Life Cycle. The RFP has three tiers of objectives, requirements, and constraints: 1. Tracking of cislunar objects for precision orbit determination. 2. Serving as a supplementary network for communication/data relay in the cislunar domain. 3. Demonstration of autonomous close proximity operations. The ARGOS mission satisfies tier 1 with sufficient access times (AT) and signal-to-noise ratios (SNR), as well as tier 2 with appropriate frequency bands and sufficient data rates. The ARGOS mission begins operations in 2026, is fully operational by 2028, and concludes in 2037 with a defined end-of-life procedure for each satellite with consideration for space sustainability. The mission holistically costs \$89.4 million, well under the maximum budget of \$400 million.

The mission has twelve subsystems, each with their own responsibilities. Guidance, Navigation, and Control defined the mission orbits. Attitude, Determination, and Control Systems designed satellite pointing and slewing methods and an actuator system. Payload determined the on-board sensors to perform object tracking. Launch Vehicles selected vehicles to use for satellite launch. Propulsion determined thrusters and fuel selections to enable satellite propulsion. Power and Electrical created a battery and solar panel system and managed a power budget for each satellite. Structures and Materials selected materials and managed the assembly of components within the satellite bus. Mechanisms selected components and interfaces to control moving parts on each satellite. Thermal performed heat transfer analysis and determined methods of thermal regulation. Communications designed critical communications components. Command and Data Handling designed the internal communication systems. Operations characterized the activities of each satellite and managed time and cost budgets.

Ultimately, Project ARGOS demonstrates technical, operational and budget compliance in establishing object-tracking and communication architecture in cislunar space, as outlined in the RFP. This will support and enhance the capabilities of NASA's Artemis campaign, as humanity aims towards further exploration of the Moon and beyond.



Table 1: Complete list of team members.

Name	Roles
Sidney Bae, '25	GNC, ADCS, and Payload
Sabrina Nicacio, '25	GNC, ADCS, and Payload
Albert Kreutzer, '25	GNC, ADCS, and Payload
Ariana Rausch, '24	GNC, ADCS, and Payload
Patrick Kozak, '24	GNC, ADCS, and Payload
Isabel Kim, '24	GNC, ADCS, and Payload
Mori Ono, '25	LV, Propulsion, and Power
Raphael Vogeley, '25	LV, Propulsion, and Power
Sarah Fry, '24	LV, Propulsion, and Power
Julia Hutto, '25	LV, Propulsion, and Power
Kazuki Tojo, '24	LV, Propulsion, and Power
Pia DiCenzo, '24	LV, Propulsion, and Power
Anna Solzhenitsyn, '25	SM, Mech, and Thermal
Candace Do, '24	SM, Mech, and Thermal
Evan Alfandre, '25	SM, Mech, and Thermal
Manali Badwe, '24	SM, Mech, and Thermal
Rihan Sajid, '25	SM, Mech, and Thermal
Ben Kim, '25	SM, Mech, and Thermal
Carrie Geisler, '25	Comms, CDH, and Ops
Jack Amen, '25	Comms, CDH, and Ops
Max Kreidl, '24	Comms, CDH, and Ops
Charlie Rogers, '24	Comms, CDH, and Ops
Zoe Koniaris, '25	Comms, CDH, and Ops
Andrew Robbins, '25	Comms, CDH, and Ops



## Acknowledgements

Team ARGOS would like to thank Professor Ryne Beeson, Professor Edgar Choueri, Michael Galvin, and course AIs Arjun Chhabra and Amlan Sinha for all of their instruction and insights throughout this course. We would also like to thank guest lecturers Cody Short, Vince Coppola, Joe Munder, Joe Throuthman, Thomas Grzymala, Dave Copeland, and Christopher DeBoy. Additionally, we would like to thank everyone at NASA Goddard for their hospitality, feedback, and expertise.



## Table of Contents

<b>1 Executive Summary</b>	<b>0</b>
1.1 Mission Overview . . . . .	0
1.2 Mission Objectives . . . . .	0
1.3 Mission Requirements . . . . .	1
1.4 Mission Constraints . . . . .	2
1.5 Mission Drivers . . . . .	4
1.6 Concept of Operations . . . . .	5
1.7 Key Design Decisions . . . . .	9
<b>2 Compliance</b>	<b>11</b>
2.1 Mission Requirements Compliance . . . . .	11
2.2 Mission Cost Compliance . . . . .	20
2.3 Mission Mass Compliance . . . . .	20
2.4 Mission Volume Compliance . . . . .	23
2.5 Mission Power Compliance . . . . .	25
2.6 Additional Compliance Budgets . . . . .	25
<b>3 Systems Integration</b>	<b>26</b>
<b>4 Operations Design</b>	<b>28</b>
4.1 Subsystem Overview . . . . .	28
4.2 Subsystem Objectives . . . . .	28
4.3 Subsystem Requirements . . . . .	28
4.4 Subsystem Constraints . . . . .	28
4.5 Subsystem Drivers . . . . .	29
4.6 Subsystem Design Approach . . . . .	29
4.7 Formal Analysis . . . . .	30
4.7.1 Pre-launch Timeline . . . . .	31
4.7.2 Transit Operational Procedure . . . . .	33
4.7.3 Nominal Operational Procedure . . . . .	35
4.7.4 Per-Orbit Activities . . . . .	37
4.7.5 ADCS Operational Procedure . . . . .	39
4.7.6 Eclipse Operational Procedure . . . . .	40
4.7.7 Station Keeping Operational Procedure . . . . .	41
4.7.8 End of Life (EOL) Operational Procedure by Satellite . . . . .	41
4.7.9 HOWLL Replacement Procedure - Risk Mitigation . . . . .	43
4.7.10 Risk Analysis and Mitigation . . . . .	44
4.7.11 Mission Budget . . . . .	48
<b>5 Launch Vehicle Design</b>	<b>50</b>
5.1 Subsystem Overview . . . . .	50
5.2 Subsystem Objectives . . . . .	50
5.3 Subsystem Requirements . . . . .	51
5.4 Subsystem Constraints . . . . .	52
5.5 Subsystem Drivers . . . . .	53



5.6	Subsystem Design Approach . . . . .	54
5.7	Formal Analysis . . . . .	56
5.7.1	Design Overview . . . . .	56
5.7.2	Primary Launch Vehicle Selection Overview . . . . .	57
5.7.3	Secondary Launch Vehicle Selection Overview . . . . .	59
5.7.4	Backup Launches . . . . .	59
5.7.5	Further Launch Vehicle Compliance . . . . .	62
<b>6</b>	<b>GNC Design</b> . . . . .	<b>63</b>
6.1	Subsystem Overview . . . . .	63
6.2	Subsystem Objectives . . . . .	63
6.3	Subsystem Requirements . . . . .	64
6.4	Subsystem Constraints . . . . .	65
6.5	Subsystem Drivers . . . . .	66
6.6	Subsystem Design Approach . . . . .	66
6.7	Formal Analysis . . . . .	68
6.7.1	Access Times . . . . .	68
6.7.2	Station-Keeping . . . . .	70
6.7.3	Conjunction Analysis . . . . .	71
6.7.4	DeltaV Verification . . . . .	71
<b>7</b>	<b>Propulsion Design</b> . . . . .	<b>74</b>
7.1	Subsystem Overview . . . . .	74
7.2	Subsystem Objectives . . . . .	75
7.3	Subsystem Requirements . . . . .	75
7.4	Subsystem Constraints . . . . .	77
7.5	Subsystem Drivers . . . . .	77
7.6	Subsystem Design Approach . . . . .	78
7.6.1	Thruster Selection, Operation and Layout . . . . .	79
7.6.2	Nozzles . . . . .	80
7.6.3	Propellant Storage and Management . . . . .	81
7.7	Formal Analysis . . . . .	82
7.7.1	Thruster Selection . . . . .	82
7.7.2	Thruster Operation and Layout . . . . .	83
7.7.3	Nozzles . . . . .	86
7.7.4	Propellant Storage and Management . . . . .	89
<b>8</b>	<b>ADCS Design</b> . . . . .	<b>94</b>
8.1	Subsystem Overview . . . . .	94
8.2	Subsystem Objectives . . . . .	94
8.3	Subsystem Requirements . . . . .	95
8.4	Subsystem Constraints . . . . .	96
8.5	Subsystem Drivers . . . . .	97
8.6	Subsystem Design Approach . . . . .	97
8.7	Formal Analysis . . . . .	99
8.7.1	Control Modes . . . . .	99



8.7.2 Disturbances . . . . .	99
8.7.3 Spacecraft Control . . . . .	102
8.7.4 Hardware Determination . . . . .	103
8.7.5 Control Algorithms . . . . .	106
8.7.6 Mass and Volume Budget Compliance . . . . .	107
<b>9 Payload Design</b>	<b>108</b>
9.1 Subsystem Overview . . . . .	108
9.2 Subsystem Objectives . . . . .	108
9.3 Subsystem Requirements . . . . .	108
9.4 Subsystem Constraints . . . . .	109
9.5 Subsystem Drivers . . . . .	109
9.6 Subsystem Design Approach . . . . .	110
9.7 Formal Analysis . . . . .	111
9.7.1 PACK . . . . .	113
9.7.2 HOWLL and WOOF . . . . .	118
<b>10 Communications Design</b>	<b>123</b>
10.1 Subsystem Overview . . . . .	123
10.2 Subsystem Objectives . . . . .	124
10.3 Subsystem Requirements . . . . .	124
10.4 Subsystem Constraints . . . . .	125
10.5 Subsystem Drivers . . . . .	126
10.6 Subsystem Design Approach . . . . .	127
10.7 Formal Analysis . . . . .	127
10.7.1 Conceptual Architecture and Frequency Band Selection . . . . .	127
10.7.2 X-Band and K-Band Hardware Selection . . . . .	129
10.7.3 Continuing Design Evolution . . . . .	130
10.7.4 HOWLL Hardware Augmentation . . . . .	130
10.7.5 WOOF Hardware Augmentation . . . . .	130
10.7.6 Summary After Adjustments . . . . .	131
<b>11 Command and Data Handling Design</b>	<b>133</b>
11.1 Subsystem Overview . . . . .	133
11.2 Subsystem Objectives . . . . .	133
11.3 Subsystem Requirements . . . . .	135
11.4 Subsystem Constraints . . . . .	136
11.5 Subsystem Drivers . . . . .	137
11.6 Subsystem Design Approach . . . . .	138
11.7 Formal Analysis . . . . .	140
11.7.1 Hardware Analysis . . . . .	140
11.7.2 Data Budget . . . . .	141
11.7.3 Image Processing . . . . .	144
11.7.4 Software Considerations . . . . .	145
11.7.5 Compliance . . . . .	146
<b>12 Power Design</b>	<b>147</b>



12.1 Subsystem Overview . . . . .	147
12.2 Subsystem Objectives . . . . .	147
12.3 Subsystem Requirements . . . . .	148
12.4 Subsystem Constraints . . . . .	148
12.5 Subsystem Drivers . . . . .	149
12.6 Subsystem Design Approach . . . . .	150
12.7 Formal Analysis . . . . .	150
12.7.1 Eclipse Analysis . . . . .	150
12.7.2 Power Load and Operational Mode Determination . . . . .	151
12.7.3 Power Storage . . . . .	154
12.7.4 Power Generation . . . . .	155
12.7.5 Power Distribution and Management . . . . .	156
<b>13 Mechanisms Design</b> . . . . .	<b>158</b>
13.1 Subsystem Overview . . . . .	158
13.2 Subsystem Objectives . . . . .	158
13.3 Subsystem Requirements . . . . .	158
13.4 Subsystem Constraints . . . . .	159
13.5 Subsystem Drivers . . . . .	159
13.6 Subsystem Design Approach . . . . .	160
13.6.1 Satellite Dispenser . . . . .	160
13.6.2 Solar Array Release . . . . .	161
13.6.3 Solar Array Deployment . . . . .	161
13.6.4 Solar Array Articulation . . . . .	161
13.6.5 Other Considered Mechanisms . . . . .	162
13.7 Formal Analysis . . . . .	163
13.7.1 Satellite Dispenser . . . . .	163
13.7.2 Solar Array Release . . . . .	164
13.7.3 Solar Array Deployment . . . . .	165
13.7.4 Solar Array Articulation . . . . .	167
13.7.5 Budget Compliance . . . . .	169
<b>14 Thermal Design</b> . . . . .	<b>172</b>
14.1 Subsystem Overview . . . . .	172
14.2 Subsystem Objectives . . . . .	172
14.3 Subsystem Requirements . . . . .	172
14.4 Subsystem Constraints . . . . .	174
14.5 Subsystem Drivers . . . . .	174
14.6 Subsystem Design Approach . . . . .	175
14.6.1 Thermal Environments and Extremes . . . . .	175
14.6.2 Subsystem Temperature Requirements . . . . .	176
14.6.3 Minor Underlying Assumptions . . . . .	177
14.7 Formal Analysis . . . . .	177
14.7.1 External Coating . . . . .	179
14.7.2 Conductive Elements . . . . .	181
14.7.3 Heater . . . . .	182



14.7.4 Internal Heat Radiator . . . . .	183
14.7.5 Temperature Sensor . . . . .	184
14.7.6 Louver . . . . .	185
14.7.7 Budget Analyses . . . . .	186
<b>15 Structures and Materials Design</b> . . . . .	<b>187</b>
15.1 Subsystem Overview . . . . .	187
15.2 Subsystem Objectives . . . . .	187
15.3 Subsystem Requirements . . . . .	187
15.4 Subsystem Constraints . . . . .	188
15.5 Subsystem Drivers . . . . .	189
15.6 Subsystem Design Approach . . . . .	189
15.6.1 Materials . . . . .	190
15.6.2 Structures . . . . .	190
15.7 Formal Analysis . . . . .	191
15.7.1 Materials Selection . . . . .	191
15.7.2 Radiation Shielding . . . . .	192
15.7.3 Solar Panel Array Material . . . . .	193
15.7.4 Material Outgassing . . . . .	194
15.7.5 HOWLL Structural Design and Analysis . . . . .	195
15.7.6 PACK-C Structure Design and Analysis . . . . .	203
15.7.7 Verification Tests . . . . .	205
15.7.8 Compliance with Subsystem Objectives, Requirements, and Constraints . . . . .	206
<b>16 References</b> . . . . .	<b>208</b>
<b>A Appendix</b> . . . . .	<b>222</b>
A.1 General Mission Information . . . . .	223
A.2 Compliance . . . . .	224
A.3 Launch Vehicle . . . . .	225
A.4 GNC . . . . .	229
A.4.1 Orbit Literature Review Trade Study . . . . .	229
A.4.2 Access Times . . . . .	230
A.4.3 Station-Keeping . . . . .	233
A.4.4 Conjunction Analysis . . . . .	240
A.4.5 Insertion DeltaV . . . . .	249
A.5 Propulsion . . . . .	252
A.5.1 Propulsion Method Trade Study . . . . .	252
A.5.2 Monopropellant Thruster Trade Study . . . . .	253
A.5.3 Propellant Tank Sizing . . . . .	255
A.5.4 Pressurant Tank Sizing . . . . .	255
A.5.5 System Sizing . . . . .	256
A.6 Payload . . . . .	257
A.7 Communications . . . . .	258
A.7.1 Link Margin: Calculated Variables . . . . .	258
A.8 Command and Data Handling . . . . .	260



---

A.9 Power . . . . .	261
A.10 Mechanisms . . . . .	262
A.11 Structures and Materials . . . . .	265
A.11.1 Advanced Standard for CubeSats . . . . .	265
A.11.2 HOWLL Analysis Results . . . . .	265
A.11.3 PACK-C Analysis Results . . . . .	265
A.11.4 Falcon 9 Rideshare Environments . . . . .	266
A.11.5 Verification of Requirements and Constraints . . . . .	268
<b>B Contributions Table</b>	<b>274</b>
<b>C Contributions Description</b>	<b>276</b>

## List of Acronyms

- ADCS:** Attitude Determination and Control Systems
- AdvCAT:** STK's Advanced Conjunction Analysis Tool
- ARGOS:** Advanced Relay for Geolunar Operational Support
- AT:** Access Time
- BOL:** Beginning-of-Life
- CA:** Conjunction Analysis
- CAD:** Computer-Aided Design
- CDH/C&DH:** Command and Data Handling
- CDS:** CubeSat Design Specification
- CFS:** Core Flight System
- CLPS:** Commercial Lunar Payload Services
- COMMS:** Communications
- ConOps:** Concept of Operations
- COTS:** Commercial Off-the-Shelf
- CSD:** Canesterized Satellite Dispenser
- CR3BP:** Circular Restricted Three Body Problem
- CVCM:** Collected Volatile Condensable Material
- DOD:** Depth of Discharge
- EBAD:** Ensign-Bickford Aerospace and Defense
- EFO:** Elliptical Frozen Orbit
- ELO:** Elliptical Lunar Orbit
- EOL:** End-of-Life
- ESPA:** Evolved Secondary Payload Adapter
- FDR:** Final Design Review
- GNC:** Guidance Navigation and Control
- GTO:** Geo-Transfer Orbit
- HLS:** Human Landing System
- HOWLL:** Homing Orbital Waypoint L1-Linkage
- HPGP:** High Performance Green Propellant

**HRC:** High Resolution Camera

**IS:** Infrared Sensor

**ITAR:** International Traffic in Arms Regulations

**LEO:** Low Earth Orbit

**LLO:** Low Lunar Orbit

**LV:** Launch Vehicle

**Mech:** Mechanisms

**MEP:** Micro-electrospray Propulsion

**NASA:** National Aeronautics and Space Administration

**NRHO:** Near Rectilinear Halo Orbit

**MIPS:** Million Inputs Per Second

**OBC:** On-board Computer

**ORC:** Objectives, Requirements, and Constraints

**PACK:** Pathfinding Array for Cislunar Kinematics

**PACK-C:** Pathfinding Array for Cislunar Kinematics - Circular

**PACK-E:** Pathfinding Array for Cislunar Kinematics - Elliptical

**PCB:** Printed Circuit Board

**PDR:** Preliminary Design Review

**PMAD:** Power Management and Distribution system

**PSLV:** Polar Satellite Launch Vehicle

**RFP:** Request for Proposal

**SADA:** Solar Array Drive Assembly

**SIMPLEx:** Small, Innovative Missions for Planetary Exploration

**SM:** Structures & Materials

**SMA:** Shape Memory Alloy

**SMPC:** Shape Memory Polymer Composite

**SNR:** Signal to Noise Ratio

**SSO:** Sun-Synchronous Orbit

**STK:** Systems Tool Kit

**TCM:** Telemetry and Command Module

**TLI:** Trans-Lunar Injection



**TML:** Total Mass Loss

**TRL:** Technology Readiness Level

**MOI:** Moment of Inertia

**WOOF:** Wide-range Orbital Operations Facilitator

## List of Symbols

- $\alpha$  - Absorptivity  
 $\epsilon$  - Emissivity  
 $\sigma$  - Stefan-Boltzmann Constant  
 $I$  - Operating current of each satellite  
 $\alpha$  - Angular acceleration  
 $\tau$  - Torque  
 $T_g$  - Maximum gravity torque  
 $\mu$  - Moon's gravity coefficient  
 $R$  - Orbit radius  
 $R$  - Albedo (Thermal)  
 $S$  - Solar flux at Earth distance  
 $\theta$  - Maximum deviation of the Z-axis from local vertical  
 $I$  - Moment of inertia  
 $I_x$  - Moment of inertia in x-direction  
 $I_y$  - Moment of inertia in y-direction  
 $I_z$  - Moment of inertia in z-direction  
 $F_s$  - Solar constant  
 $c$  - Speed of light  
 $A_s$  - Surface area  
 $c_{ps}$  - Location of the center of solar pressure  
 $c_g$  - Center of gravity  
 $q$  - Reflectance factor  
 $I$  - Angle of incidence of the sun  
 $L$  - Nozzle length  
 $R_e$  - Nozzle exit radius  
 $R_t$  - Nozzle throat radius  
 $A_e$  - Nozzle exit area  
 $A_t$  - Nozzle throat area  
 $\alpha$  - Nozzle cone angle

$\lambda$  - Effective momentum ratio  
 $L^*$  - Chamber characteristic length  
 $V_c$  - Chamber volume  
 $A_c$  - Chamber area  
 $L_1$  - Chamber cylindrical length  
 $L_c$  - Chamber convergent length  
 $\gamma$  - Ratio of specific heat  
 $p_c$  - Chamber pressure  
 $M_e$  - Exit Mach number  
 $p_e$  - Exit pressure  
 $C_F$  - Thrust coefficient  
 $I_{sp}$  - Specific impulse  
 $c^*$  - Characteristic velocity  
 $t$  - propulsion burn time  
 $\Delta V$  - spacecraft delta-V  
 $T$  - thrust  
 $g$  - acceleration of gravity  
 $m_p$  - propellant mass  
 $m_i$  - pressurant mass  
 $V_p$  - propellant volume  
 $V_i$  - pressurant volume  
 $\rho_p$  - propellant density  
 $\rho_i$  - pressurant density  
 $\sigma$  - maximum allowable tank material stress  
 $P_p$  - propellant pressure  
 $P_i$  - pressurant pressure  
 $R$  - gas constant  
 $M$  - molar mass  
 $k$  - specific heat ratio  
 $r$  - tank radius  
 $l$  - tank length



$t_c$  - cylindrical tank wall thickness

$t_s$  - spherical endcap tank thickness



## List of Figures

1	Concept of Operations Image . . . . .	6
2	Cost Budget Compliance . . . . .	20
3	System Block Diagram for Each ARGOS Satellite . . . . .	27
4	Nominal Operational Procedure Functional Flow Diagram . . . . .	37
5	Initial Risk Matrix . . . . .	45
6	Risk Matrix After Mitigation . . . . .	47
7	Mission Budget Breakdown . . . . .	49
8	Overview of Cumulative LV Subsystem Design Process . . . . .	54
9	Astroscopic Deployment Orbit (Left) and Maneuvers to Enter Mission Orbit (Right) . . . . .	61
10	ARGOS Satellites and Tier 1 Tracking Objects . . . . .	68
11	Insertion to PACK Orbits from Deployment Orbit . . . . .	72
12	Propulsion Subsystem Design Approach Block Diagram . . . . .	79
13	Improvement of the thruster layout for increased separation and adjustment of thrust centre to align with mass centre. . . . .	80
14	CAD model of the Bradford Space HPGP 1N thruster. Model obtained from [76]. . . . .	80
15	Figure from [8] contrasting regulated vs. blowdown pressure-regulated systems . . . . .	82
16	Thruster separations on all satellites. . . . .	84
17	Thruster configurations studied by Nehrenz and Sorgenfrei [81]. . . . .	85
18	Detumbling time of two thruster configurations. From [81]. . . . .	86
19	Nozzle geometry and its parameters. From [86]. . . . .	87
20	Chamber geometry and its parameters. From [87]. . . . .	87
21	Plume exhaust analysis. From [89]. . . . .	89
22	Propellant Tank Feed System Design, with time $t$ , total spacecraft delta-V $\Delta V$ , specific impulse $I_{sp}$ , total impulse $I_t$ , thrust $T$ , acceleration of gravity $g$ , mass $m$ (with subscripts p and i for propellant and pressurant respectively, volume $V$ , density $\rho$ , tank material stress $\sigma$ , pressure $P$ , gas constant $R$ , molar mass $M$ , specific heat ratio $k$ , tank radius $r$ , tank length $l$ , cylindrical tank wall thickness $t_c$ and spherical tank wall thickness $t_s$ [8] . . . . .	90
23	Propellant Tank Feed System Design [8], [92], [93] . . . . .	92
24	Image of a ring baffle within a propulsion tank. Reproduced from [93] . . . . .	93
25	4-RW Tetrahedral Structure [97]. . . . .	98
26	Firing of Thrusters for Momentum Dumping along each Axis. . . . .	101
27	Sensors for ARGOS Satellites . . . . .	111
28	The signal-to-noise ratio of the from the circular orbit PACK satellite (black) and the elliptical orbit PACK satellite when targeting space object lunar gateway . . . . .	113
29	The signal-to-noise ratio of the 90mm Camera attached to our PACK-C and PACK-E satellite and pointed at the LLO-1 space object with a sample rate of 1 hour. The black line represents SNR from PACK-C, while the green line is from PACK-E. . . . .	113
30	The signal-to-noise ratio of the 90mm Camera attached to our PACK-C and PACK-E satellite and pointed at the LLO-2 space object with a sample rate of 1 hour. The black line represents SNR from PACK-C, while the green line is from PACK-E. . . . .	115
31	The signal-to-noise ratio of the 90mm Camera attached to our PACK-C and PACK-E satellite and pointed at the LLO-3 space object with a sample rate of 1 hour. The black line represents SNR from PACK-C, while the green line is from PACK-E. . . . .	116



32	The signal-to-noise ratio of the 90mm Camera attached to our PACK-C and PACK-E satellite and pointed at the LG space object with a sample rate of 1 hour. The black line represents SNR from PACK-C, while the green line is from PACK-E. . . . .	117
33	SNR of i-SIM 90 camera attached to HOWLL/WOOF pointing at L1 Halo. Note: Green corresponds to WOOF, and blue corresponds to HOWLL . . . . .	118
34	SNR of the i-SIM 90 camera attached to HOWLL/WOOF pointing at GTO to L1 Halo during the Low Thrust Spiral Phase. Note: Green corresponds to WOOF, and Blue corresponds to HOWLL . . . . .	119
35	SNR of the i-SIM 90 camera attached to HOWLL/WOOF pointing at GTO to L1 Halo after insertion. Note: Green corresponds to WOOF, and blue corresponds to HOWLL . . . . .	120
36	SNR of the i-SIM 90 camera attached to HOWLL/WOOF pointing at GTO to L2 Halo during the Low Thrust Spiral Phase. Note: Green corresponds to WOOF, and blue corresponds to HOWLL . . . . .	121
37	SNR of the i-SIM 90 camera attached to HOWLL/WOOF pointing at GTO to L2 Halo after insertion. Note: Green corresponds to WOOF, and blue corresponds to HOWLL . . . . .	121
38	The block diagram for the Communications subsystem, showing its relationship to the other subsystems comprising the mission. . . . .	123
39	The finalized conceptual architecture diagram for the Communications subsystem, showing the links present in the mission design as well as the frequency bands able to be transmitted through. . . . .	132
40	C&DH System Block Diagram . . . . .	134
41	Overview of Design Approach through each Design Cycle . . . . .	139
42	Data Budget for Storage and Transmission needs for Each Subsystem . . . . .	144
43	Rocket Lab CSD and Example of Dispensing [151] . . . . .	164
44	Frangibolt and Locations . . . . .	165
45	Recovery Process of SMPC Smart Hinge [159] . . . . .	166
46	CAD of the Solar Array on PACK satellites (solar arrays in blue, hinge brackets in red) . . . . .	167
47	Various external coating options . . . . .	180
48	Various conductive elements options . . . . .	181
49	Various heater options . . . . .	183
50	Various internal heat radiator options . . . . .	184
51	Various temperature sensing options . . . . .	184
52	Commercial OSR to be modified . . . . .	185
53	SM design approach. Green designates stages completed for PDR, and yellow designates stages completed for FDR. . . . .	189
54	Radiation shielding thicknesses for various materials [208]. . . . .	192
55	Stiffener Diagram [210]. . . . .	193
56	Free-vibration test results [210]. . . . .	194
57	Exploded view of 27U primary structure. . . . .	196
58	Models of secondary structures. . . . .	196
59	HOWLL solar array configurations. Solar arrays are shown in blue, and hinge brackets and Frangibolts in red. . . . .	197
60	HOWLL internal layout. . . . .	198



61	Simplified model of HOWLL for analysis.	200
62	HOWLL static load analysis results for YZ load case.	201
63	Visualization of HOWLL low-frequency vibrational modes.	202
64	Exploded view of PACK-C primary structure.	203
65	PACK solar array configurations. Solar arrays are shown in blue, and hinge brackets and Frangibolts in red.	204
66	PACK-C internal layout.	204
67	Mass stackup for all subsystem components for each satellite.	224
68	Volume stackup for all subsystem components for each satellite.	224
69	Comparison of Secondary Payload Launch Vehicle Options and RocketLab Electron	225
70	NASA Moon Launch Manifest	226
71	Full PSLV-XL vs. Falcon 9 Comparison	227
72	Trade Study for Lagrange Point Orbits	229
73	Trade Study for Lunar Orbits	229
74	Access Times from PACK-C to LG and LLO Objects	230
75	Access Times from PACK-E to LG and LLO Objects	230
76	Access Times to LLO-2 Object from HOWLL and WOOF	230
77	Access Times from HOWLL to L1 and L2 Objects	231
78	Access Times from WOOF to L1 and L2 Objects	231
79	Access Times from WOOF to LG	231
80	Access Times to GTotoL1 Object from HOWLL and WOOF	232
81	Access Times to GTotoL2 Object from HOWLL and WOOF	232
82	Access Times from HOWLL to WOOF and PACK for Communication Purposes	232
83	Propulsion Method Trade Study (1 of 2)	252
84	Propulsion Method Trade Study (2 of 2)	252
85	Monopropellant Thruster Trade Study (1 of 4)	253
86	Monopropellant Thruster Trade Study (2 of 4)	253
87	Monopropellant Thruster Trade Study (3 of 4)	254
88	Monopropellant Thruster Trade Study (4 of 4)	254
89	Propellant Tank Calculations (1 of 5)	255
90	Propellant Tank Calculations (2 of 5)	255
91	Propellant Tank Calculations (3 of 5)	255
92	Propellant Tank Calculations (4 of 5)	255
93	Propellant Tank Calculations (5 of 5)	255
94	Pressurant Tank Calculations (1 of 2)	255
95	Pressurant Tank Calculations (2 of 2)	256
96	Propulsion Subsystem Total Mass and Volume	256
97	Data Specifications for Sirius OBC&TCM	260
98	Power storage specifications for each satellite	261
99	Power storage calculations for each satellite	261
101	Release Mechanism Ranked Trade Study [226] [171] [227] [228] [229]	263
103	HOWLL static load analysis visualization for XY load case.	265
104	HOWLL static load analysis visualization for XZ load case.	265
105	PACK static load analysis visualization for XY load case.	266
106	PACK static load analysis visualization for XZ load case.	266
107	Quote for PACK y-plus frame	270



100	Specifications on the EBAD TiNi Frangibolt . . . . .	272
102	CubeSat paramaters from the Advanced Standard for Cubesats [156]. . . . .	273



## List of Tables

1	Complete list of team members.	2
2	Selected “Operations” Mission-Level Requirements [6]	2
3	HOWLL Concept of Operations	6
4	PACK Concept of Operations	7
5	WOOF Concept of Operations	8
6	Mission Level Requirements	11
7	Subsystem mass budgets and compliances for HOWLL	21
8	Subsystem mass budgets and compliances for WOOF	21
9	Subsystem mass budgets and compliances for PACK-C	22
10	Subsystem mass budgets and compliances for PACK-E	22
11	Mass margins for all four satellites.	23
12	Subsystem volume budgets and compliances for HOWLL	23
13	Subsystem volume budgets and compliances for WOOF	24
14	Subsystem volume budgets and compliances for PACK-C	24
15	Subsystem volume budgets and compliances for PACK-E	25
16	Detailed Pre-Launch Timeline and Activities	31
17	Transit Operational Procedure for All Satellites	34
18	Assignment of Space Objects to Satellites for Tracking	35
19	Nominal Operational Procedure for All Satellites	36
20	Steps for Attitude Determination and Control	40
21	Eclipse Operational Procedure	40
22	HOWLL EOL Operational Procedure	42
23	PACK EOL Operational Procedure	42
24	WOOF EOL Operational Procedure	42
24	WOOF EOL Operational Procedure	43
25	HOWLL Replacement Procedure	43
26	LV Subsystem Requirements Summary	51
27	The Updated LV Requirement	52
28	Comparison of Primary LV Launch Options	58
29	Comparison of Secondary Payload Launch Options	61
30	GNC Subsystem Requirements	65
31	Orbital Parameters for PACK Satellites	67
32	Initial Conditions for HOWLL and WOOF in CR3BP	67
33	Average Monthly Access Times	69
34	PACK Satellite Target vs Perturbed	70
35	ARGOS Satellites DeltaV Requirements	73
36	Selected requirements for the propulsion subsystem [6]. The below requirements are for PACK, but the same edits with different quantitative values were made for HOWLL and WOOF as well.	76
37	Nozzle and chamber parameter values	88
38	Propellant and Pressurant Storage Parameters [8], [79]	89
39	Cylindrical Propellant Tank Dimensions [79]	91
40	Spherical Pressurant Tank Dimensions [79]	91
41	Propulsion Subsystem Mass Budget Compliance [79]	93



42	Propulsion Subsystem Volume Budget Compliance [79] . . . . .	93
43	Selected requirements for the ADCS subsystem [6]. . . . .	95
44	Different control modes needed for each spacecraft . . . . .	99
45	External perturbations acting on each satellite. . . . .	100
46	Satellite Operation Times . . . . .	102
47	Moment of Inertia for stowed configuration . . . . .	102
48	Moment of Inertia for deployed configuration . . . . .	103
49	Torque for stowed configuration . . . . .	103
50	Torque for deployed configuration . . . . .	103
51	COTS IMU trade study [99] . . . . .	104
52	COTS Star Tracker trade study [99] . . . . .	104
53	COTS Sun Sensor trade study [99] . . . . .	105
54	COTS Control Board trade study [99] . . . . .	105
55	COTS Reaction Wheel trade study [99] . . . . .	106
56	Compliance Requirements for Satellite Specifications . . . . .	107
57	Mass and Volume Constraints by Satellite . . . . .	109
58	STK Sensor Specifications . . . . .	111
59	Space Object Tracking Allocation . . . . .	112
60	Tracking requirements for LLO-1 . . . . .	114
61	Tracking requirements for LLO-2 . . . . .	115
62	Tracking requirements for LLO-3 . . . . .	116
63	Tracking requirements for LG . . . . .	117
64	SNR Requirements for L1 Halo . . . . .	118
65	SNR Requirements for GTO to L1 Halo . . . . .	120
66	SNR Requirements for GTO to L2 Halo . . . . .	121
67	COMMS Subsystem Requirements . . . . .	125
68	Constraints for HOWLL, WOOF, and PACK Satellites . . . . .	125
69	The compliance table for the communication subsystem's various constraints. . . . .	127
71	The preliminary link budget analysis for potential S-band communication systems. . . . .	128
70	Details of typical frequency bands as defined by the IEEE. [116] . . . . .	128
72	Input variables for link margin calculations . . . . .	129
73	The details of our selected communications hardware upon the conclusion of the FDR. . . . .	130
74	The strength of the various communication links in the mission upon the conclusion of the FDR. . . . .	130
75	Mass and volume budgets on HOWLL, before and after the addition of an additional X-band communication system to the satellite. . . . .	131
76	Mass and volume budgets on WOOF, before and after the addition of an X-band communication system to the satellite. . . . .	131
77	C&DH Subsystem Requirements . . . . .	136
78	Constraints for HOWLL, WOOF, and PACK Satellites . . . . .	136
79	Performance Metrics of Top 3 Choices for On-Board Computers . . . . .	140
80	Image Sizing Summary . . . . .	145
81	Specifications and Margins for Sirius OBC/TCM . . . . .	146
82	Power Subsystem Requirements . . . . .	148
83	Eclipse and Sun Time Data for ARGOS Satellites . . . . .	150



84	PACK Power Budget Matrix . . . . .	152
85	HOWLL/WOOF Power Budget Matrix . . . . .	153
86	ARGOS Power Storage Requirements . . . . .	154
87	ARGOS Battery Pack Specifications . . . . .	155
88	ARGOS Power Generation Data . . . . .	156
89	Specifications of Pumpkin Space Systems EPSM 1 [143], [148] . . . . .	156
90	Mechanisms Subsystem Requirements . . . . .	159
91	Dimensions of Scaled 27U CSD . . . . .	163
92	Scaled down HoneyBee Robotics SADA . . . . .	168
93	Estimated Costs for Mechanisms . . . . .	169
94	Mechanisms Mass Compliance . . . . .	170
95	Mechanisms Volume Compliance . . . . .	170
96	Mechanisms Power Compliance . . . . .	171
97	Subsystem Requirements . . . . .	173
98	Environmental Heating Conditions . . . . .	176
99	Temperature Requirements for ARGOS Satellite Components . . . . .	177
100	Temperature Regulation Calculations for PACK Body . . . . .	178
101	Temperature Regulation Calculations for HOWLL/WOOF Body . . . . .	178
102	Temperature Regulation Calcs for Solar Panel Nodes . . . . .	178
103	Mass, Volume, Cost Budget Analysis . . . . .	186
104	Selected SM requirements. . . . .	188
105	Properties of aluminum 6061, aluminum 7075, and carbon fiber [202] [203] . . . . .	191
106	Mechanical properties of aluminum 6061 at elevated temperatures [205] . . . . .	191
107	Outgassing Properties of PCB and Viscoelastic Tape [211] [210] . . . . .	195
108	Maximum dimensions of a 27U CubeSat according to the Advanced Standard for CubeSats [156]. . . . .	195
109	Material properties of Al-6061 and FR-4 [202], [213]. . . . .	199
110	Static load cases for analysis. . . . .	200
111	Results from static load analysis. . . . .	201
112	Fundamental frequencies and corresponding effective masses of 27U bus in stowed configuration. . . . .	202
113	Vibrational modes of 27U bus in deployed configuration. . . . .	202
114	Maximum dimensions of a 12U CubeSat according to the Advanced Standard for CubeSats [156]. . . . .	203
115	Results from static load analysis. . . . .	205
116	Fundamental frequencies and corresponding effective masses of 12U bus. . . . .	205
117	Vibrational modes of 27U bus in deployed configuration. . . . .	205
118	Verification Tests [214] . . . . .	206
119	Comparison of Environmental Loads Across Selected LVs . . . . .	228
120	Design Specifications for High-Resolution Camera . . . . .	257
121	System Comparison and Evaluations for High-Resolution Camera . . . . .	257
122	Design Specifications for Infrared Sensor . . . . .	257
123	System Comparison and Evaluations for Infrared Sensor . . . . .	258
124	Comparison of Various CubeSat Deployment Systems . . . . .	262
125	General Characteristics of Various Solar Array Release Mechanisms . . . . .	262
126	Specific Characteristics of Various Solar Array Release Mechanisms . . . . .	263



---

127	Characteristics of Various Solar Array Drive Assemblies . . . . .	264
128	Shock Test Environment [202] . . . . .	266
129	Random Vibration Environment [214] . . . . .	267
130	Maximum Payload Emission [214] . . . . .	267
131	Temperature Environments [214] . . . . .	267
132	Sinusoidal Vibration Environment [214] . . . . .	267
133	Pressure Requirements [214] . . . . .	268
134	Verification of technical requirements . . . . .	268
135	Verification of constraints . . . . .	269
136	Verification of environmental requirements . . . . .	269
137	SM subsystem cost breakdown of HOWLL satellite . . . . .	270
138	SM subsystem cost breakdown of WOOF satellite . . . . .	271
139	SM subsystem cost breakdown for each PACK-C and PACK-E satellite . . . . .	271
140	Team Contributions . . . . .	274



# 1 Executive Summary

## 1.1 Mission Overview

Following the Request For Proposal (RFP) and the Preliminary Design Report (PDR), Advanced Relay for Geolunar Operational Support (ARGOS) seeks to increase the viability for and number of missions in the cislunar domain. This goal manifests in two main pathways. First, the mission seeks to develop architecture that will track cislunar objects for orbit determination and improved navigation. Second, the mission seeks to enhance current cislunar communication and data transmission relays with novel architecture. Since the PDR, the third goal of close-proximity operations for repurposing, recycling, mitigating space debris has been relinquished.

With increasingly more inexpensive price tags on payload launches, miniaturization of spacecraft, and a new look at the Moon as a stepping stone toward Mars and deep space, the cislunar domain has been a subject of increasing interest in the last few decades [1] [2]. This developing attention is met by challenges of operating in the cislunar domain, the first of which is the complex gravitational environment. Due to the influence of both the Earth and the Moon, there is no closed-form solution for the trajectory of the spacecraft that can be derived using orbital mechanics. Therefore, small differences in spacecraft trajectories will lead to chaotic, increasingly divergent orbits [3]. So, to mitigate this problem, satellites in the cislunar domain need consistent tracking, stationkeeping (orbit correction), and communication to facilitate the former. The addressing of these challenges would aid the viability of missions in this domain and proliferate spacecraft operations. Therefore, ARGOS seeks to fulfill the mission of tracking space objects and augment the communication abilities. The ARGOS mission stresses the fulfillment of object tracking and orbit determination as the primary goal, and ARGOS seeks to fulfill the development of communication architecture as a secondary goal, albeit a significant one.

The mission has undergone its final round of revisions since the PDR, most notably that the third high-level objective in the RFP, close-proximity operations, has been abandoned. The goals and concepts of operations, otherwise, have largely remained the same since the PDR; ARGOS is still a four-satellite mission with two at L1 and L2 respectively and two in low lunar orbit. The primary 27U satellite, named Homing Orbital Waypoint L1-Linkage (HOWLL), will operate in a halo orbit around L1 point, and the secondary 27U satellite, named the Wide-range Orbital Operations Facilitator (WOOF), will operate in a similar orbit around the L2 point. Two 12U satellites that belong to the Pathfinding Array for Cislunar Kinematics (PACK) will be in frozen lunar orbits, one circular and one elliptical. The mission will begin full operations by 2027 and continue running until 2030-2037.

## 1.2 Mission Objectives

The ARGOS mission aims to address the three objectives from the given Request for Proposal [1] to enhance and develop operations in Cislunar space especially with the growing interest and increasing amount of traffic in the domain. These three objectives were ranked in importance in the following order:

- **1. Mission Level Tier 1 Objective:** Improve the tracking of Cislunar objects (as defined by the Tier 1 Object Catalog [4]) for precision orbit determination, which may be followed by navigation for operating space objects (SO) or hazard avoidance / debris mitigation for



non-cooperating or non-active SO (debris or derelicts).

- **2. Mission Level Tier 2 Objectives:** Create a supplementary network for communication and data relay between Cislunar architectures and in particular from Lunar-based assets to Earth-based resources.
- **3. Mission Level Tier 3 Objectives:** Demonstrate autonomous close proximity operations (e.g., navigation) of non-active objects in the Cislunar domain for repurposing, recycling, debris mitigation, or industrial space-based manufacturing.

Due to the desire to ensure the full satisfaction of the basic primary objectives, the ARGOS team decided to prioritize the completion of the first two RFP mission objectives and not address the tertiary objective. As such, the designs for all subteams have been geared towards meeting the first two Mission Level Objectives and this report will serve as a final verification on the requirements for these subteams to meet these objectives to completion and with margin. For the Primary Objective, the tracking and orbit determination will be addressed by the ARGOS team. Navigation will not be discussed by the team, but the design choices and ARGOS setup could theoretically perform this task.

### 1.3 Mission Requirements

Mission requirements derive directly from the MAE 342 Request for Proposal (RFP) [1]. There have been no changes to the mission-level requirements since the previous design iteration (the Preliminary Design Report, or PDR). Significant changes to mission-level requirements during the PDR design cycle played a crucial role in enabling a closed loop in this final design iteration. For the purpose of conceptually summarizing the mission requirements, they can be subdivided into the three major categories of Operations requirements, Tracking (Tier 1) requirements, and Communications (Tier 2) requirements.

1. **Operations:** These requirements relate to the timeline and cost-related guidelines outlined in the RFP. Specifically, the RFP states that the mission should be fully operational from 2030 to 2037. Furthermore, the mission must cost less than \$400 million. Related to this cost limitation are the mass and volume budgets for mission spacecraft, as compliance to pre-specified spacecraft size guidelines allows for feasible and cost-effective launches. Specific requirement labels corresponding to Operational requirements include:
  - *Functional:* MISS-F-001 through MISS-F-005, MISS-F-014, MISS-F-015, MISS-F-016, MISS-F-018
  - *Performance:* MISS-P-013
  - *Constraint:* MISS-C-001, MISS-C-002, MISS-C-010 through MISS-C-018
  - *Environmental:* MISS-E-001 through MISS-E-006
2. **Tracking:** The primary objective for this mission relates to the tracking of objects in low lunar orbit (LLO), Lagrange Halo orbits around L1 and L2, and lunar and libration point orbits. These requirements relate to the functionality and performance of the tracking mechanisms themselves, but also to the prioritization of tracking over communications requirements. Specific requirement labels corresponding to Operational requirements include:



- *Functional:* MISS-F-019, MISS-F-020, MISS-F-021
- *Performance:* MISS-P-014 through MISS-P-028
- *Constraint:* MISS-C-007, MISS-C-009

**3. Communications:** The secondary objective for this mission concerns the ARGOS Mission's responsibility to facilitate communications between Earth-based and cislunar resources. Specifically, the ARGOS Mission spacecraft are tasked with serving as a communications relay network among cislunar spacecraft as well as between cislunar spacecraft and Earth-based resources. Specific requirement labels corresponding to Communications requirements include:

- *Functional:* MISS-F-008 through MISS-F-013, MISS-F-017
- *Constraint:* MISS-C-008

The below table provides a subset of mission-level requirements, and a full summary 73 mission-level requirements can be accessed directly in the ARGOS Mission Requirements spreadsheet [5], under the "Mission-Level Requirements" tab.

Table 2: Selected "Operations" Mission-Level Requirements [6]

Requirement ID	Requirement	Rationale	Verification, Validation Method	TraceUp
MISS-F-001	The mission shall begin operations by 2027	The RFP requires that the mission begin operations by 2030	Satisfaction of Trace Down Requirements	RFP-F-001
MISS-P-013	The mission components shall spend at most 2 consecutive hours charging/generating power during the transit period	Mission time may need to be split into periods of recharging spacecraft batteries / orienting spacecraft to generate power from solar panels etc. This may impact the amount of time available to conduct mission operations.	Power system charging / discharging requirement	RFP-P-001, RFP-P-002, RFP-P-005, RFP-P-006, RFP-P-009, RFP-P-010, RFP-P-011, RFP-P-012
MISS-C-001	The mission components must cost at most \$400 million in total	Typical cost for a NASA Discovery-class mission	Cost budget breakdown	RFP-C-001
MISS-E-001	The mission components must be capable of operating in the radiative environment of $10^8$ to $10^{20}$ eV/n (TBC) for the duration of the mission	The radiative environment could affect electronics and spacecraft structures, impeding operations	Simulation / Radiation Testing	RFP-E-001

## 1.4 Mission Constraints

Mission constraints serve to narrow the viable design options for ARGOS mission systems. These constraints have essentially remained the same since the PDR, but design developments since then have revealed a greater understanding of the impacts of those constraints. Cost remains the most important constraint, as it determines the acceptable scale and complexity for spacecraft systems and launch vehicle options. It is also a factor that must be minimized in order to maximize mission feasibility and flexibility, as any reduction in expenses makes the introduction of greater redundancies less costly.



dancy a more affordable option to reduce risks to mission success. The mission timeline is the next most critical factor in developing the ARGOS mission architecture, as the selected spacecraft components and launch vehicles must be ones that are ready and available before RFP deadlines that dictate mission success. The combination of mass and volume is the third most important factor, with this constraint receiving a lower importance given that these limits are largely self-imposed with the exception of Artemis Program rideshare payloads, and generally exist out of a need to minimize cost. Limits on mass and volume also translates to limiting the capabilities for each subsystem that can be placed on each satellite. This limit then drives further constraints on individual subsystems. The impacts of these constraints are discussed below in this importance-based order. However, it is also clear that these constraints are interrelated with each other, making it difficult to isolate the impact of these constraint factors on their own:

1. **Cost:** Initial efforts to stay within the \$60 million recommended limit for a NASA Small, Innovative Missions for Planetary Exploration (SIMPEx)-class mission (RFP-C-001) proved impractical due to the difficulty of fulfilling mission-critical technical tasks such as tracking Cislunar space objects and conducting relay communications with the low-cost components that could be acquired with that budget. Rescaling the spacecraft to a larger mass and volume also meant that primary payload launches would have to be contracted, imposing a significant launch cost. For this reason, the cap was lifted to the \$400 million hard limit of a NASA Discovery-class mission (RFP-C-002). With the mission cost only reaching \$89.4 million, cost has not presented an imminent difficulty. However, the increased cost cap must not be crossed in mission design, and the relatively low costs expended opens the opportunity for backup or replacement satellites and launches to reduce mission risk through redundancy while staying under budget.
2. **Timeline:** Aside from the recommendation to continue full operations of the mission architecture from 2032 to 2037, the RFP's deadlines for ARGOS (RFP-F-001, RFP-F-002, RFP-F-003) are hard limits that cannot be adjusted during mission development. Timeline limitations have significant impacts on design, most notably for launch vehicles selection. Because of when Artemis Program missions are scheduled, the number of available launches is limited. This constraint is particularly apparent for backups launches, which require a minimum lead time to prepare following an unexpected mission failure.
3. **Mass and Volume:** HOWLL and WOOF were limited to 54 kg of mass and 42,577 cm<sup>3</sup> of internal volume, and PACK to 24 kg and 19,071 cm<sup>3</sup>. The internal volume encompasses all components except for the outer structure of the satellites. These mass and volume limits were in turn subdivided among the various subsystems and thus limiting the size of equipment that each could install on the ARGOS spacecraft. The revision of mass and volume requirements enabled enough of an increase in capabilities for heavily mass-dependent subsystems such as propulsion to meet compliance with Objectives, Requirements, and Constraints (ORC) while preserving a significant margin in both mass and volume. However, it should be noted that mass proved to be a much tighter constraint for the smaller PACK satellites. One of the nuances with volume that became particularly important to resolve was the placement of components with varying geometries within the spacecraft itself. This often required close coordination between subsystems as this was a tighter constraint than whether total internal volume in general was left.
4. **Constraints on Individual Subsystems:** Under the constraints of cost as well as mass and



volume, the Communications, C&DH, and Power made selections of specific components, and the Operations team devised the development of operations duty cycles. Subsystems development had to adhere to these new constraints: electricity usage during various modes of the mission, the data storage available onboard, and the data rate per transmission cycle all needed to be considered so that the selected components and the duty cycles could still provide enough resources and time for each subsystem. This also worked in reverse as the selection of these components was driven by the needs of other subsystems, such as the temperature ranges that the thermal subsystem must keep components within.

## 1.5 Mission Drivers

Our primary mission drivers, outlined below in approximate order of importance, have been adjusted based on finalized calculations while remaining consistent with the Preliminary Design Report (PDR). These drivers are derived from our mission requirements.

### 1. Mission Timeline

The mission timeline is of critical due to the requirement for operational architecture by 2027 and full operational capability by 2030. This constraint significantly impacts various subsystems and shapes the overall concept of operations.

Initiating and executing operations within our mission architecture significantly influences material durability, manufacturing and testing processes, integration of redundancies, technology readiness levels (TRL), and power requirements across all mission stages. It also dictates launch vehicle availability, satellite trajectories, and material durability in the harsh cislunar environment.

### 2. Communication Capabilities

Communication capabilities are fundamental to our mission's primary goal of tracking cislunar objects for orbit determination and hazard mitigation. Additionally, communication is essential for establishing an effective data relay network in areas of cislunar space lacking direct, continuous lines of sight with Earth [1]. Reliable and advanced communication technology selection directly impacts mission success through bandwidth, data rate, signal-to-noise ratio, and mission longevity.

### 3. Maneuverability and Station-Keeping

Maneuverability and station-keeping are crucial for achieving our goal of autonomous operation with minimal adjustments. Choosing stable orbits and maintaining desired precise orbits are vital. Balancing thrust and specific impulse capabilities of propulsion is essential for optimizing mission efficiency, along with precision orientation facilitated by the Attitude Determination and Control System (ADCS) to meet all mission requirements.

### 4. Temperature

Temperature control is critical due to the harsh conditions of cislunar space. Material selection, active and passive systems, and heat regulation mechanisms are imperative to maintaining operational conditions within acceptable ranges, especially considering that many of the onboard systems are delicate and require rigid temperature ranges to fully operate.



## 5. Propulsive Delta-V

Propulsive Delta-V is essential for achieving mission objectives by enabling satellite positioning, orientation, and maneuvering. It significantly impacts the size of the architecture, with its large size and additional mass, and requires efficient propulsion systems to fulfill mission requirements.

## 6. Size

Size considerations, encompassing mass and volume, are crucial for cost efficiency and meeting launch vehicle payload constraints. Adhering to these constraints while optimizing operational capabilities poses a challenge. This was moved lower in priority due to increased allowable mass and volume from the transition to larger spacecrafts. These constraints impact all of the subsystems as they need to be constrained by the size and mass budgets for each subsystem.

## 7. Radiation/Space Debris Tolerance

While the ARGOS mission carries various delicate electrical components, actuators, and circuits, it is of extreme importance to select hardware components across a variety of systems that are (a) radiation-hardened and (b) robust enough to withstand impacts from micrometeoroids, space debris, and charged particles [7]. Selecting radiation-hardened components and robust hardware is vital to withstand space conditions and impacts from micrometeoroids and space debris. This influences hardware selection and verification processes, as well as the requirements for subsystems like Communications and Command & Data Handling.

## 8. Vacuum/Microgravity Tolerance

Functioning effectively in vacuum and microgravity environments presents unique challenges, influencing spacecraft material selection, mechanism design, and propulsion system choice. In a vacuum, potential issues include material out-gassing, cold welding, propellant storage complications, and limited avenues for heat transfer within the spacecraft [7]. While significant, these considerations have been less influential in our design process due to the extensive availability of space-grade materials.

### 1.6 Concept of Operations

None of the core content within the Concept of Operations (ConOps) changed since the last design cycle. However, some information that was unclear or left out (but was reflected in operational procedures) has been clarified or added. For example, much of the Activate Subsystems stage and the Ground Station Confirmation was not properly conveyed in the previous ConOps. Additionally, specific activities during Mission Duration are now specified. It was previously stated that the 27U satellites had no dispenser; the Mechanisms team since determined a dispenser. This change is reflected in the ConOps. Additionally, the end of life result of heliocentric orbit or lunar impact is now specified.

An abbreviated version of our ConOps is shown and described in this figure.

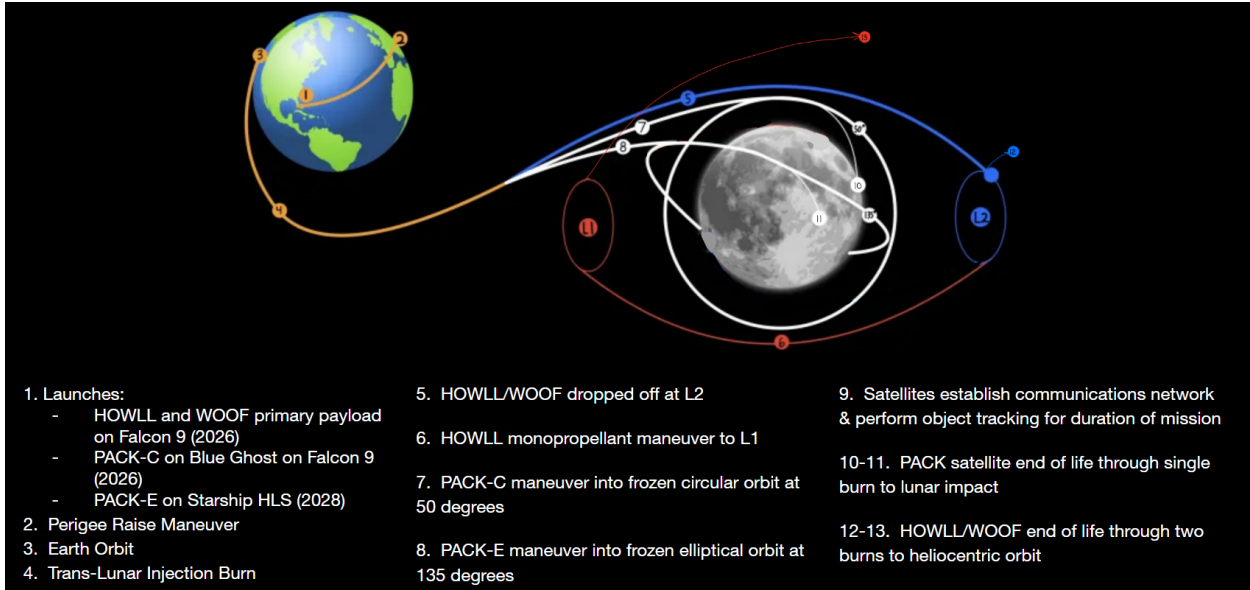


Figure 1: Concept of Operations Image

The full Concept of Operations is outlined by satellite below, with both PACK satellites described together.

Table 3: HOWLL Concept of Operations

Stage	Event	Description
1	Launch	Falcon 9 launches 27U satellites HOWLL and WOOF as a Primary Payload Launch in late 2026 on a Trans-Lunar Injection.
2	Deployment	Satellites are dispensed from their respective dispensers. HOWLL and WOOF are deployed on a Trans-Lunar Injection near L2.
3	Activate Subsystems	Activate all subsystems while relying on batteries. Release mechanism to deploy solar arrays and begin to generate power. Perform thermal regulation. Establish communication with WOOF. Verify satellite health.
4	Outbound Trajectory Correction Maneuvers	Use onboard monopropellant thrusters to guide HOWLL towards L1 equilibrium point.
5	Halo Orbit Insertion	Fire thrusters & directly inject HOWLL into a Halo Orbit around L1.
6	Lower Halo Orbit Maneuver	Decay Halo Orbit to as tight around L1 as possible using anti-directional thrust maneuvers.



7	Ground Station Confirmation	Repeat satellite health assessment. Establish communication with the ground station. Communicate health assessment and orbital insertion confirmation with ground station. Relay WOOF's health assessment and orbital insertion confirmation to ground station.
8	Mission Duration	Satellite continually iterates through nominal operational procedure for the majority of mission life. Performs nominal mission activities of object tracking, power generation, satellite maintenance, and communications. Continually relays communications and data transfers from PACK-E, PACK-C, and WOOF to ground station. Yearly station-keeping to maintain L1 Halo Orbit through small burns.
9	Cessation of station-keeping	Relays WOOF and PACK end-of-life confirmation to ground station. HOWLL enters end-of-life procedures last. All controlled maneuvers are stopped.
10	Final impulsive maneuvers	Impulse to decay away from Earth-Moon system in unstable orbit. Second impulse to avoid Earth-Moon system reentry.
11	Stable heliocentric orbit	Maintains communications with ground station. HOWLL enters stable heliocentric orbit.

Table 4: PACK Concept of Operations

Stage	Event	Description
1	Launch	PACK-C is launched as a secondary payload (free 12U) on Blue Ghost on a Falcon 9 in 2026. PACK-E is launched as a secondary payload (free 12U) on Starship HLS in late 2028.
2	Deployment	Satellites are dispensed from their respective dispensers. PACK-C is deployed in an elliptical lunar 2000x673km orbit at a 50 degree inclination. PACK-E is deployed in an elliptical lunar 505x2000 orbit at a 135 degree inclination.
3	Activate Subsystems & Generate Power	Activate all subsystems while relying on batteries. Release mechanism to deploy solar arrays and begin to generate power. Perform thermal regulation. Establish communication with HOWLL. Verify satellite health.
4	Outbound Trajectory Correction Maneuvers	Use onboard monopropellant thrusters to guide each of the 12U PACK satellites towards LLO.
5	Low-Lunar Orbit Insertion	Fire thrusters & directly inject PACK satellites into frozen orbits with one PACK satellite at a 50 degree inclination and the other at a 135 degree inclination.




---

6	Ground Station Confirmation	Repeat satellite health assessment. Communicate health assessment and orbital insertion confirmation to HOWLL, which relays to ground station.
7	Mission Duration	Satellite continually iterates through nominal operational procedure for the majority of mission life. Performs nominal mission activities of object tracking, power generation, satellite maintenance, and communications. Yearly station-keeping to maintain frozen orbits through small burns; both satellites have independent station-keeping.
8	Cessation of station-keeping	All controlled maneuvers are stopped.
9	Final impulsive maneuver	Satellites perform single retrograde burn.
10	Lunar surface impact	Maintains communications with HOWLL throughout orbital decay to track and relay to ground station where impact occurs. PACK satellites impact the lunar surface. HOWLL confirms lunar surface impact to ground station.

---

Table 5: WOOF Concept of Operations

---

Stage	Event	Description
1	Launch	Falcon 9 launches 27U satellites HOWLL and WOOF as a Primary Payload Launch in late 2026 on a Trans-Lunar Injection.
2	Deployment	Satellites are dispensed from their respective dispensers. HOWLL and WOOF are deployed on a Trans-Lunar Injection. Activate subsystems, begin to generate power, and establish communication with HOWLL.
3	Activate Subsystems & Generate Power	Activate all subsystems while relying on batteries. Release mechanism to deploy solar arrays and begin to generate power. Perform thermal regulation. Establish communication with HOWLL. Verify satellite health.
4	Outbound Trajectory Correction Maneuvers	Use onboard monopropellant thrusters to guide the 27U WOOF towards L2 equilibrium point.
5	Halo Orbit Insertion	Fire thrusters & directly inject WOOF into a Halo Orbit around L2.
6	Ground Station Confirmation	Repeat satellite health assessment. Communicate health assessment and orbital insertion confirmation to HOWLL, which relays to ground station.



7	Lower Halo Orbit Maneuver	Decay Halo Orbit to as tight around L2 as possible using anti-directional thrust maneuvers.
8	Mission Duration	Satellite continually iterates through nominal operational procedure for the majority of mission life. Performs nominal mission activities of object tracking, power generation, satellite maintenance, and communications. Yearly station-keeping to maintain L2 Halo Orbit through small burns.
9	Cessation of station-keeping	All controlled maneuvers are stopped.
10	Final impulsive maneuvers	Impulse to decay away from Earth-Moon system in unstable orbit. Second impulse to avoid Earth-Moon system reentry.
11	Stable heliocentric orbit	Maintains communications with HOWLL throughout end-of-life to relay progress to ground station. WOOF enters stable heliocentric orbit. HOWLL confirms stable orbit entry to ground station.

## 1.7 Key Design Decisions

The ARGOS team underwent 5 major mission-level design iterations to satisfy the aforementioned objectives, requirements, and constraints. Through our design process, we balanced sufficient redundancy to achieve mission success while also ensuring to not over-design and incur unnecessary costs. Additionally, unexpected challenges forced necessary design evolution. The 5 major design iterations are as follows:

- 1. Initial Mission Design:** The initial mission level design consisted of 1 12U HOWLL satellite orbiting at L1 and 4 6U PACK satellites in LLO. Much like our current mission infrastructure, the PACK satellites were responsible for tracking and relaying cislunar communication in their respective regions. The HOWLL was a communication relay for all mission architecture to and from Earth. The increased transmission requirements informed the larger size of the HOWLL satellite.
- 2. WOOF Addition:** A 12U Satellite, WOOF, was added to our mission architecture to focus on tracking objects in the L2 Halo Orbit and the GTO to L2 Halo trajectory. GNC and payload subsystem analysis indicated a satellite positioned in an L2 orbit would be better suited to meet mission objectives than the 4 PACK satellites alone. The increased distance from HOWL to WOOF informed the selection of the larger 12U size to support more powerful communication hardware.
- 3. PACK Reduction from 4 to 2:** Informed predominantly by analysis from the GNC subsystem, the number of PACK satellites was reduced from 4 to 2. Preliminary assessment indicated that 2 PACK satellites would provide more than sufficient coverage of LLO objects. Thus, it was nonsensical to include expensive redundant architecture. While budget was not yet the foremost concern, streamlining our design was an obvious step. Further, should PACK satellites fail, the rest of the mission can continue operating while a replacement is launched and positioned appropriately.



4. **Satellite Size Increases:** The fuel mass and volume required to complete our necessary maneuvers were too large for the original 6U and 12U size configurations. We decided to change our PACK satellites to 12U and WOOF and HOWLL to 27U. This allowed us to accommodate the increased propellant to satisfy mission  $\Delta v$  requirements. Unfortunately, the increase in satellite size meant we could no longer launch all mission architecture with free Artemis launches. We thus evolved our LV selection to pay for a primary payload launch on the Falcon 9 system. This significantly increased our expected mission budget such that we could no longer fall under the original goal of \$60 million. Our budget requirement evolved to consider the less stringent bound of \$400 million.
5. **HOWLL & WOOF Standardization:** Our final iteration standardized the design of HOWLL and WOOF satellites. All other satellites rely on HOWLL to communicate with Earth, making it a single point of failure. To mitigate this risk, WOOF will be designed with the same capabilities as HOWLL to move to L1 and replace its functionality should HOWLL fail. The additional hardware on WOOF to provide the same capabilities as HOWLL was relatively inexpensive and easy to integrate. WOOF already had space for sufficient propellant to travel from L2 to L1, given that both HOWLL and WOOF were dropped off near the L2 point. HOWLL has to transfer from L2 to L1 to reach its desired orbit. This redundancy plan would simply use the same trajectory for WOOF, making this design evolution straightforward.



## 2 Compliance

### 2.1 Mission Requirements Compliance

The following table depicts the compliance of Project ARGOS with mission requirements. Mission requirements MISS-F-006 to MISS-F-007, MISS-P-001 to MISS-P-010, MISS-C-003 to MISS-C-006 and MISS-C-008 were removed and MISS-F-019 to MISS-F-021, MISS-P-014 to MISS-P-028, MISS-C-010 to MISS-C-019 were added due to changes in the mission architecture throughout the design process. The reasons for each removal and addition are depicted in the Mission Requirements Google Spreadsheet [6]. Overall, there is satisfactory compliance of the vast majority of requirements, with some minor items remaining to address. Specifically, environmental requirements must undergo pre-launch testing and debris tracking must be researched further.

Table 6: Mission Level Requirements

Requirement ID	Requirement	Status	Verification Details
MISS-F-001	The mission shall begin operations by 2027	Met	Analysis performed in Sections 4.7.1-4.7.6
MISS-F-002	The mission shall be fully operational by 2030	Met	Analysis performed in Sections 4.7.1-4.7.6
MISS-F-003	All mission components must remain operational throughout 2030 and 2031	Met	Analysis performed in Sections 4.7-15.7
MISS-F-004	All mission components should remain operational from 2032 to 2037	Met	Analysis performed in Sections 4.7-15.7
MISS-F-005	All components of the mission architecture must have an end of life disposal plan	Met	Analysis performed in Section 4.7.7
MISS-F-008	Mission components should be capable of communication with spacecrafts in Low Lunar Orbit	Met	Analysis performed in Sections 10.7.1-10.7.5
MISS-F-009	Mission components should be capable of communication with spacecraft in L1 Halo Orbit	Met	Analysis performed in Sections 10.7.1-10.7.5

Continued on next page



Table 6 – continued from previous page

Requirement ID	Requirement	Status	Verification Details
MISS-F-010	Mission components should be capable of communication with spacecraft in L2 Halo Orbit	Met	Analysis performed in Sections 10.7.1-10.7.5
MISS-F-011	Mission components should be capable of communication with spacecraft in transfer orbits between the Earth and the lunar regime	Met	Analysis performed in Sections 10.7.1-10.7.5
MISS-F-012	The mission should provide a communication relay to spacecraft within the appropriate frequency bands for the orbits utilized by the mission: 2-40 MHz	Met	Analysis performed in Sections 10.7.1-10.7.5
MISS-F-013	The mission components shall collect and transmit telemetry data back to Earth	Met	Analysis performed in Sections 10.7.1-10.7.5
MISS-F-014	The mission components shall operate at 1% autonomy	Met	Analysis performed in Sections 4.7-15.7
MISS-F-015	The mission components shall have propellant/thrust available to conduct mission operations for the duration of the mission	Met	Analysis performed in Sections 7.7.1-7.7.4
MISS-F-016	The mission shall have power available to conduct mission operations for the duration of the mission	Met	Analysis performed in Sections 12.7.1-12.7.5
MISS-F-017	The mission components shall communicate with each other to relay relevant data and commands	Met	Analysis performed in Sections 10.7-11.7

Continued on next page



Table 6 – continued from previous page

Requirement ID	Requirement	Status	Verification Details
MISS-F-018	Mission components shall have the ability to detect/forecast potential collisions in their nominal orbit up to a period of 3 days in the future	Partially met	Analysis performed in Section 7.7.1-7.7.4 verify collision avoidance, although collision detection has not been verified
MISS-F-019	PACK satellites shall be capable of tracking all three LLO objects and Lunar Gateway (LG) in NRHO from Tier 1 of the mission catalog	Met	Analysis performed in Sections 6.7, 9.7
MISS-F-020	The HOWLL satellite shall be capable of tracking the L1/L2 Halo and GTO to L1/L2 Halo objects from Tier 1 of the mission catalog	Met	Analysis performed in Sections 6.7, 9.7
MISS-F-021	The WOOF satellite shall be capable of tracking the L1/L2 Halo, GTO to L1/L2 Halo, and Lunar Gateway objects from Tier 1 of the mission catalog	Met	Analysis performed in Sections 6.7, 9.7
MISS-P-011	The mission should provide a data relay to spacecraft at an uplink data rate of at least 2 Mbps	Met	Analysis performed in Sections 10.7.1-10.7.5
MISS-P-012	The mission should provide a data relay to spacecraft at a downlink data rate of at least 5 Mbps	Met	Analysis performed in Sections 10.7.1-10.7.5
MISS-P-013	The mission components shall spend at most 2 consecutive hours charging/generating power during the transit period	Met	Analysis performed in Sections 4.7.2, 12.7.1-12.7.5

Continued on next page



Table 6 – continued from previous page

Requirement ID	Requirement	Status	Verification Details
MISS-P-014	PACK satellites shall be capable of tracking all three LLO objects and Lunar Gateway from Tier 1 of the mission catalog for at least the cumulative access time specified in the catalog	Met	Analysis performed in Sections 6.7, 9.7
MISS-P-015	The HOWLL satellite shall be capable of tracking the L1/L2 Halo and GTO to L1/L2 Halo objects from Tier 1 of the mission catalog for at least the cumulative access time specified in the catalog	Met	Analysis performed in Sections 6.7, 9.7
MISS-P-016	The WOOF satellite shall be capable of tracking the L1/L2 Halo, GTO to L1/L2 Halo, and Lunar Gateway objects from Tier 1 of the mission catalog for at least the cumulative access time specified in the catalog	Met	Analysis performed in Sections 6.7, 9.7
MISS-P-017	PACK satellites shall be capable of tracking all three LLO objects and Lunar Gateway from Tier 1 of the mission catalog for at least the monthly access time specified in the catalog	Met	Analysis performed in Sections 6.7, 9.7
MISS-P-018	The HOWLL satellite shall be capable of tracking the L1/L2 Halo and GTO to L1/L2 Halo objects from Tier 1 of the mission catalog for at least the monthly access time specified in the catalog	Met	Analysis performed in Sections 6.7, 9.7

Continued on next page



Table 6 – continued from previous page

Requirement ID	Requirement	Status	Verification Details
MISS-P-019	The WOOF satellite shall be capable of tracking the L1/L2 Halo, GTO to L1/L2 Halo, and Lunar Gateway in NRHO objects from Tier 1 of the mission catalog for at least the monthly access time specified in the catalog	Met	Analysis performed in Sections 6.7, 9.7
MISS-P-020	PACK satellites shall be capable of tracking all three LLO objects and Lunar Gateway from Tier 1 of the mission catalog with at least the signal-to-noise ratio specified in the catalog	Met	Analysis performed in Sections 6.7, 9.7
MISS-P-021	The HOWLL satellite shall be capable of tracking the L1/L2 Halo and GTO to L1/L2 Halo objects from Tier 1 of the mission catalog with at least the signal-to-noise ratio specified in the catalog	Met	Analysis performed in Sections 6.7, 9.7
MISS-P-022	The WOOF satellite shall be capable of tracking the L1/L2 Halo, GTO to L1/L2 Halo, and Lunar Gateway in NRHO objects from Tier 1 of the mission catalog with at least the signal-to-noise ratio specified in the catalog	Met	Analysis performed in Sections 6.7, 9.7
MISS-P-023	PACK satellites shall be capable of tracking all three LLO objects and Lunar Gateway from Tier 1 of the mission catalog with at least the monthly maintained signal-to-noise ratio specified in the catalog	Met	Analysis performed in Sections 6.7, 9.7

Continued on next page

Table 6 – continued from previous page

Requirement ID	Requirement	Status	Verification Details
MISS-P-024	The HOWLL satellite shall be capable of tracking the L1/L2 Halo and GTO to L1/L2 Halo objects from Tier 1 of the mission catalog with at least the monthly maintained signal-to-noise ratio specified in the catalog	Met	Analysis performed in Sections 6.7, 9.7
MISS-P-025	The WOOF satellite shall be capable of tracking the L1/L2 Halo, GTO to L1/L2 Halo, and Lunar Gateway in NRHO objects from Tier 1 of the mission catalog with at least the monthly maintained signal-to-noise ratio specified in the catalog	Met	Analysis performed in Sections 6.7, 9.7
MISS-P-026	PACK satellites shall be capable of tracking all three LLO objects and Lunar Gateway from Tier 1 of the mission catalog with at least the integrated signal-to-noise ratio specified in the catalog	Met	Analysis performed in Sections 6.7, 9.7
MISS-P-027	The HOWLL satellite shall be capable of tracking the L1/L2 Halo and GTO to L1/L2 Halo objects from Tier 1 of the mission catalog with at least the integrated signal-to-noise ratio specified in the catalog	Met	Analysis performed in Sections 6.7, 9.7

Continued on next page



Table 6 – continued from previous page

Requirement ID	Requirement	Status	Verification Details
MISS-P-028	The WOOF satellite shall be capable of tracking the L1/L2 Halo, GTO to L1/L2 Halo, and Lunar Gateway in NRHO objects from Tier 1 of the mission catalog with at least the integrated signal-to-noise ratio specified in the catalog	Met	Analysis performed in Sections 6.7, 9.7
MISS-C-001	The mission components must cost at most \$400 million in total	Met	Analysis performed in Section 4.7.10
MISS-C-002	The mission components should cost at most \$60 million in total	Not met	Analysis performed in Section 4.7.10
MISS-C-007	The mission shall ensure the necessary resources for the functional and performance capabilities of tracking the space objects in Tier 1 of the catalog before allocating resources for tracking the space objects in Tier 2 of the catalog	Met	Analysis performed in Sections 4.7, 6.7, 9.7, 10.7
MISS-C-009	The mission shall ensure the necessary resources for the functional and performance capabilities of the primary ORC before allocating resources for the secondary ORC	Met	Analysis performed in Sections 4.7, 6.7, 9.7, 10.7
MISS-C-010	Each PACK satellite shall have a volume of at most 19071 cm <sup>3</sup> at the beginning of mission operations	Met	Analysis performed in Sections 15.7.5-15.7.8

Continued on next page



Table 6 – continued from previous page

Requirement ID	Requirement	Status	Verification Details
MISS-C-011	The HOWLL satellite shall have a volume of at most 42577 cm <sup>3</sup> at the beginning of mission operations	Met	Analysis performed in Sections 15.7.5-15.7.8
MISS-C-012	Each PACK satellite should not exceed 12U volume	Met	Analysis performed in Sections 15.7.5-15.7.8
MISS-C-013	Each PACK satellite must not exceed 24 kg mass	Met	Analysis performed in Sections 15.7.5-15.7.8
MISS-C-014	The HOWLL satellite should not exceed 27U volume	Met	Analysis performed in Sections 15.7.5-15.7.8
MISS-C-015	The HOWLL satellite must not exceed 54 kg mass	Met	Analysis performed in Sections 15.7.5-15.7.8
MISS-C-016	The WOOF satellite should not exceed 27U volume	Met	Analysis performed in Sections 15.7.5-15.7.8
MISS-C-017	The WOOF satellite must not exceed 54 kg mass	Met	Analysis performed in Sections 15.7.5-15.7.8
MISS-C-018	The WOOF satellite shall have a volume of at most 42577 cm <sup>3</sup> at the beginning of mission operations	Met	Analysis performed in Sections 15.7.5-15.7.8
MISS-C-019	The mission shall communicate directly to Earth ground stations	Met	Analysis performed in Sections 10.7.1-10.7.6
MISS-E-001	The mission components must be capable of operating in the radiative environment of 10 <sup>8</sup> to 10 <sup>20</sup> eV/n for the duration of the mission	Partially met	Analysis performed in Sections 4.7-15.7, although pre-launch tests are required for full verification
MISS-E-002	The mission must operate within the temperature range of 0 °C to 45 °C for the satellite body	Partially met	Analysis performed in Sections 4.7-15.7, although pre-launch tests are required for full verification

Continued on next page



Table 6 – continued from previous page

Requirement ID	Requirement	Status	Verification Details
MISS-E-003	All mission components must be capable of operating in the unstable and inconsistent gravitational environment in Cislunar space through the duration of the mission	Partially met	Analysis performed in Sections 4.7-15.7, although pre-launch tests are required for full verification
MISS-E-004	HOWLL and WOOF must withstand the Launch Vehicle vibrational environment of $0.03 g^2/\text{Hz}$ at 800-925Hz/5.57 GRMS during transit from Earth to the chosen orbit	Partially met	Analysis performed in Sections 4.7-15.7, although pre-launch tests are required for full verification
MISS-E-005	PACK must withstand the Launch Vehicle vibrational environment of $0.034 g^2/\text{Hz}$ at 800-925Hz/5.13 GRMS during transit from the Earth to the desired orbit	Partially met	Analysis performed in Sections 4.7-15.7, although pre-launch tests are required for full verification
MISS-E-006	All mission components must withstand the Launch Vehicle g-force load environment of axial -4 to $7 g$ and lateral $\pm 3.0 g$ during transit from the Earth to the desired orbit	Partially met	Analysis performed in Sections 4.7-15.7, although pre-launch tests are required for full verification
MISS-E-007	HOWLL and WOOF must withstand the maximum Launch Vehicle g-force load environment of axial $\pm 10 g$ and lateral $\pm 16 g$ during transit from the Earth to the deployment orbit	Partially met	Analysis performed in Sections 4.7-15.7, although pre-launch tests are required for full verification
MISS-E-008	All mission components must withstand the external vacuum environment for the duration of the mission	Met	Analysis performed in Sections 4.7-15.7



## 2.2 Mission Cost Compliance

The following table indicates the state of compliance for each subsystem to their total allocated cost budget. Notably, the cost budget was designed in close alignment with Table 20-9 from the SMAD (see Section 4.7.10 for more details), which takes into account both Research, Development, Testing, and Evaluation (RDT&E) and production. Therefore the only costs which are not directly included in this budget are satellite replacement. However, given the large positive margins for every subsystem, our mission will remain in compliance with the cost budget even in the unlikely event one of our satellites needs to be replaced.

		Cost Allocated (\$)	Cost Consumed (\$)	Cost Margin (%)	Compliant?
<b>Spacecraft Bus Subsystems</b>	Payload	52,000,000	5,800,000	89%	Yes
	Comms	48,000,000	1,029,800	98%	Yes
	SM	8,000,000	200,000	98%	Yes
	Mech	20,000,000	746,572	96%	Yes
	Thermal	4,000,000	400,000	90%	Yes
	Power	28,000,000	2,000,000	93%	Yes
	CD&H	24,000,000	400,000	98%	Yes
	ADCS	24,000,000	1,000,000	96%	Yes
	Prop	12,000,000	1,200,000	90%	Yes
<b>Wraps Subsystems</b>	Ops	32,000,000	4,580,000	86%	Yes
	GNC	8,000,000	610,000	92%	Yes
	LV	4,000,000	610,000	85%	Yes
<b>Other Wraps Costs</b>	Integration, Assembly, & Test (IA&T)	24,000,000	2,780,000	88%	Yes
	Ground Systems Equipment (GSE)	12,000,000	1,320,000	89%	Yes
<b>Launch Costs</b>	Falcon 9 Primary Launch	100,000,000	67,000,000	33%	Yes
<b>TOTAL</b>		400,000,000	89,676,372	78%	Yes

Figure 2: Cost Budget Compliance

## 2.3 Mission Mass Compliance

The following tables indicate the state of compliance of each subsystem to their allocated mass budget for each satellite. All subsystems are compliant with their mass budgets.

Allocated mass budgets were determined through a combination of values from literature (Table 10-10 in Section 10.3 of SMAD [8]) and an iterative process in which subsystems estimated their total mass and conducted mass trades. The consumed masses were calculated by adding the masses of all subsystem components, and the mass stackups for each satellite are detailed in Appendix A.2.



Subsystem	Allocated Mass (kg)	Consumed Mass (kg)	Compliant?
Operations	0	0	Yes
Launch Vehicle	0	0	Yes
GNC	0	0	Yes
Propulsion	7.70	6.60	Yes
ADCS	3.25	2.96	Yes
Payload	4.00	4.00	Yes
Communications	1.50	1.20	Yes
Command and Data Handling	0.30	0.26	Yes
Power	4.00	3.88	Yes
Mechanisms	2.25	0.95	Yes
Thermal	1.50	1.08	Yes
Structures and Materials	10.75	9.50	Yes
<b>Total</b>	<b>35.25</b>	<b>30.48</b>	<b>Yes</b>

Table 7: Subsystem mass budgets and compliances for HOWLL.

The maximum mass of HOWLL is 54 kg as defined by Requirement MISS-C-015. Respective to this maximum mass, we have 77.1% margin, which is more than adequate (SMAD recommends 5-25% [8]).

Subsystem	Allocated Mass (kg)	Consumed Mass (kg)	Compliant?
Operations	0	0	Yes
Launch Vehicle	0	0	Yes
GNC	0	0	Yes
Propulsion	7.70	6.59	Yes
ADCS	3.25	2.78	Yes
Payload	4.00	4.00	Yes
Communications	1.50	0.87	Yes
Command and Data Handling	0.30	0.26	Yes
Power	4.00	3.88	Yes
Mechanisms	2.25	0.95	Yes
Thermal	1.50	1.08	Yes
Structures and Materials	10.75	9.50	Yes
<b>Total</b>	<b>35.25</b>	<b>29.96</b>	<b>Yes</b>

Table 8: Subsystem mass budgets and compliances for WOOF.

WOOF's maximum mass is 54 kg (Requirement MISS-C-017). WOOF has 80.2% mass margin.



Subsystem	Allocated Mass (kg)	Consumed Mass (kg)	Compliant?
Operations	0	0	Yes
Launch Vehicle	0	0	Yes
GNC	0	0	Yes
Propulsion	5.30	4.63	Yes
ADCS	3.00	2.78	Yes
Payload	1.50	1.40	Yes
Communications	0.60	0.55	Yes
Command and Data Handling	0.30	0.26	Yes
Power	2.00	1.63	Yes
Mechanisms	2.25	1.77	Yes
Thermal	0.75	0.28	Yes
Structures and Materials	7.25	5.79	Yes
<b>Total</b>	<b>22.95</b>	<b>19.14</b>	<b>Yes</b>

Table 9: Subsystem mass budgets and compliances for PACK-C.

The maximum mass of PACK-C is 24 kg (Requirement MISS-C-0013). PACK-C has 25.4% mass margin.

Subsystem	Allocated Mass (kg)	Consumed Mass (kg)	Compliant?
Operations	0	0	Yes
Launch Vehicle	0	0	Yes
GNC	0	0	Yes
Propulsion	5.3	2.82	Yes
ADCS	3.00	2.78	Yes
Payload	1.50	1.40	Yes
Communications	0.60	0.55	Yes
Command and Data Handling	0.30	0.26	Yes
Power	2.00	1.63	Yes
Mechanisms	2.25	1.77	Yes
Thermal	0.75	0.28	Yes
Structures and Materials	7.25	5.79	Yes
<b>Total</b>	<b>22.95</b>	<b>17.33</b>	<b>Yes</b>

Table 10: Subsystem mass budgets and compliances for PACK-E.

The maximum mass of PACK-E is 24 kg (Requirement MISS-C-0013). PACK-E has 38.5% mass margin.

The following table summarizes the mass margins for the four satellites.



Satellite	Mass Margin (%)
HOWLL	77.1
WOOF	80.2
PACK-C	25.4
PACK-E	38.5

Table 11: Mass margins for all four satellites.

Literature suggests that up to 10% of spacecraft mass is typically dedicated to wire harness mass, which is currently unaccounted for in our mass stackups [9]. SMAD also suggests that up to 2% of mass will be secondary structures, which have not all been designed (see Section 15 for details). Even after adding the wiring and secondary structures mass, we still have plenty of margin for any mass changes during future design phases.

## 2.4 Mission Volume Compliance

The following tables demonstrate whether each subsystem is compliant with their allocated volume budget for each satellite. All subsystems are compliant with their volume budgets. Detailed volume stackups for each satellite are in Section A.2.

Subsystem	Allocated Volume (cm <sup>3</sup> )	Consumed Volume (cm <sup>3</sup> )	Compliant?
Operations	0	0	Yes
Launch Vehicle	0	0	Yes
GNC	0	0	Yes
Propulsion	5300	5157.82	Yes
ADCS	2000	1709.51	Yes
Payload	5000	4434.14	Yes
Communications	1000	770.632	Yes
Command and Data Handling	1400	1319.51	Yes
Power	2000	1423.76	Yes
Mechanisms	1000	661.044	Yes
Thermal	2000	1890.09	Yes
Structures and Materials	3000	3643	Yes
<b>Total</b>	<b>42,577</b>	<b>21,009</b>	<b>Yes</b>

Table 12: Subsystem volume budgets and compliances for HOWLL

The maximum volume possible of HOWLL is  $42577\text{g}/\text{cm}^3$  (Requirement MISS-C-014). Our HOWLL satellite has a 125% volume margin.



Subsystem	Allocated Volume (cm <sup>3</sup> )	Consumed Volume (cm <sup>3</sup> )	Compliant?
Operations	0	0	Yes
Launch Vehicle	0	0	Yes
GNC	0	0	Yes
Propulsion	5300	5157.82	Yes
ADCS	2000	1709.51	Yes
Payload	5000	4434.14	Yes
Communications	1000	507.967	Yes
Command and Data Handling	1400	1319.05	Yes
Power	2000	1423.76	Yes
Mechanisms	1000	661.044	Yes
Thermal	2000	1890.09	Yes
Structures and Materials	3000	3643	Yes
<b>Total</b>	<b>42,577</b>	<b>20,746.38</b>	<b>Yes</b>

Table 13: Subsystem volume budgets and compliances for WOOF

The maximum volume possible of WOOF is  $42577\text{g}/\text{cm}^3$  (Requirement MISS-C-016). Our WOOF satellite has a 125% volume margin.

Subsystem	Allocated Volume (cm <sup>3</sup> )	Consumed Volume (cm <sup>3</sup> )	Compliant?
Operations	0	0	Yes
Launch Vehicle	0	0	Yes
GNC	0	0	Yes
Propulsion	3700	3500.07	Yes
ADCS	1600	1555.91	Yes
Payload	2900	2871.82	Yes
Communications	650	601.15	Yes
Command and Data Handling	1400	1319.1	Yes
Power	300	143.76	Yes
Mechanisms	1600	1527.25	Yes
Thermal	1250	1085.17	Yes
Structures and Materials	3000	2333.2	Yes
<b>Total</b>	<b>19,071</b>	<b>14,937.43</b>	<b>Yes</b>

Table 14: Subsystem volume budgets and compliances for PACK-C

The maximum volume possible of PACK-C is  $19071\text{g}/\text{cm}^3$  (Requirement MISS-C-012). Our PACK-C satellite has a 56% volume margin.



Subsystem	Allocated Volume (cm <sup>3</sup> )	Consumed Volume (cm <sup>3</sup> )	Compliant?
Operations	0	0	Yes
Launch Vehicle	0	0	Yes
GNC	0	0	Yes
Propulsion	3700	1932.18	Yes
ADCS	1600	1555.91	Yes
Payload	2900	2871.82	Yes
Communications	650	601.15	Yes
Command and Data Handling	1400	1319.1	Yes
Power	300	143.76	Yes
Mechanisms	1600	1527.25	Yes
Thermal	1250	1085.17	Yes
Structures and Materials	3000	2333.2	Yes
<b>Total</b>	<b>19,071</b>	<b>13,369</b>	<b>Yes</b>

Table 15: Subsystem volume budgets and compliances for PACK-E

The maximum volume possible of PACK-E is  $19071\text{g}/\text{cm}^3$  (Requirement MISS-C-012). Our PACK-E satellite has a 56% volume margin.

## 2.5 Mission Power Compliance

Due to the variety in power consumption of available components for the different subsystems of the missions and as per Joe Troutman's lecture detailing Satellite Electrical Power System Design [10], the ARGOS power subsystem was designed based on the power draws of the selected components from other subsystems and their respective duty cycles. For clarification, this means that a power budget in the sense that the power subsystem allotted a specific maximum power draw for each other subsystem was not created. A more detailed analysis of power loads and duty cycles for determination of the operational modes constraining the power subsystem design can be found in Section 12 which outlines Power Subsystem Design. Power compliance is thus inherent to the design of the power subsystem, including its batteries and solar arrays. The only thing actually constraining the power subsystem is the other constraining budgets, namely those of mass and volume, and the final design adheres to what was allotted for each.

## 2.6 Additional Compliance Budgets

Please refer to Section 4.7.4 and Section 8.6 for comments regarding the compliance budgets related to time allocation during nominal operations, Section 11.7.2 for comments regarding the compliance budgets related to data transmission and receiving as well as data storage, and Section 6.7.4 for comments regarding Delta-V budgets.



### 3 Systems Integration

A system block diagram (SBD) is shown in Figure 3. The subsystems are split into two main categories: mission planning subsystems and spacecraft subsystems. LV is denoted in the SBD as a mission planning subsystem because the deployment from the launch vehicle is being controlled by the Mechanisms subsystem, so LV is mainly responsible planning which launch vehicle we will utilize and not focused on any parts of the spacecraft for which there will be interface connections. The lone integration requirements to the LV subsystem involve deployment of each satellite from the launch vehicle, which involves the deployment mechanism, C&DH command of the operation, and SM layout design to ensure the bus supports connection to the launch vehicles selected.

The spacecraft systems section of the SBD is color-coded by type of interface for the five major interfaces anticipated on each spacecraft. Orange connections represent power transfer interface connections stemming from the Power subsystem. Red connections represent thermal protection from the Thermal subsystem to other subsystems. Purple connections represent data transfer connections stemming from the C&DH subsystem. Green connections represent physical connections giving structural support to each subsystem stemming from the S&M subsystem. Blue connections represent pointing requirements that require integration through the ADCS subsystem.

The major interfaces run by Power, Thermal, SM, C&DH, and ADCS have been analyzed in all operational modes to ensure compliance with mission and subsystem-level requirements. The power interface has been verified to be operational in both nominal sunlit operation and during eclipse times, as well as after deployment from the launch vehicle. The thermal interface has been analyzed and verified at the worst-case hot and cold temperature environments using a multi-node analysis. The data transfer (C&DH) interface contains sufficient storage and processing power for our mission requirements in data collection mode, data transmission mode, and safe mode. Pointing requirements have been analyzed to ensure the satisfaction of each subsystem's pointing needs. The SM subsystem has designed a layout for each satellite that incorporates all the components and accounts for the placement needs of each subsystem. Within the layout design, space has been kept available for the power and data transfer wiring that will need to connect all components requiring power and data transfer, which will consume a non-negligible amount of volume.

The mechanisms subsystem has considerable integration needs for each mechanism designed. The solar panel control mechanism has been designed to integrate within the solar panels designed by the thermal subsystem, the sensor covers have been designed to fit the imaging components chosen by the payload subsystem, and the LV deployment mechanism has been designed with the LV subsystem to ensure compliance with each selected launch vehicle.

The propulsion system is tasked with providing thrust for both GNC orbit determination and station keeping as well as for ADCS in desaturating the reaction wheels. This impacted the design decision for the thrusters, which are useful for both navigation and attitude applications. Another key integration task between the SM and propulsion subsystems was ensuring the propulsion was through the center of mass of the satellite to avoid unwanted torques caused by the thrusters during orbit-changing burns. Since the center of mass may not be directly in the center of the spacecraft geometrically, this required communication between the two subsystems to ensure compliance.

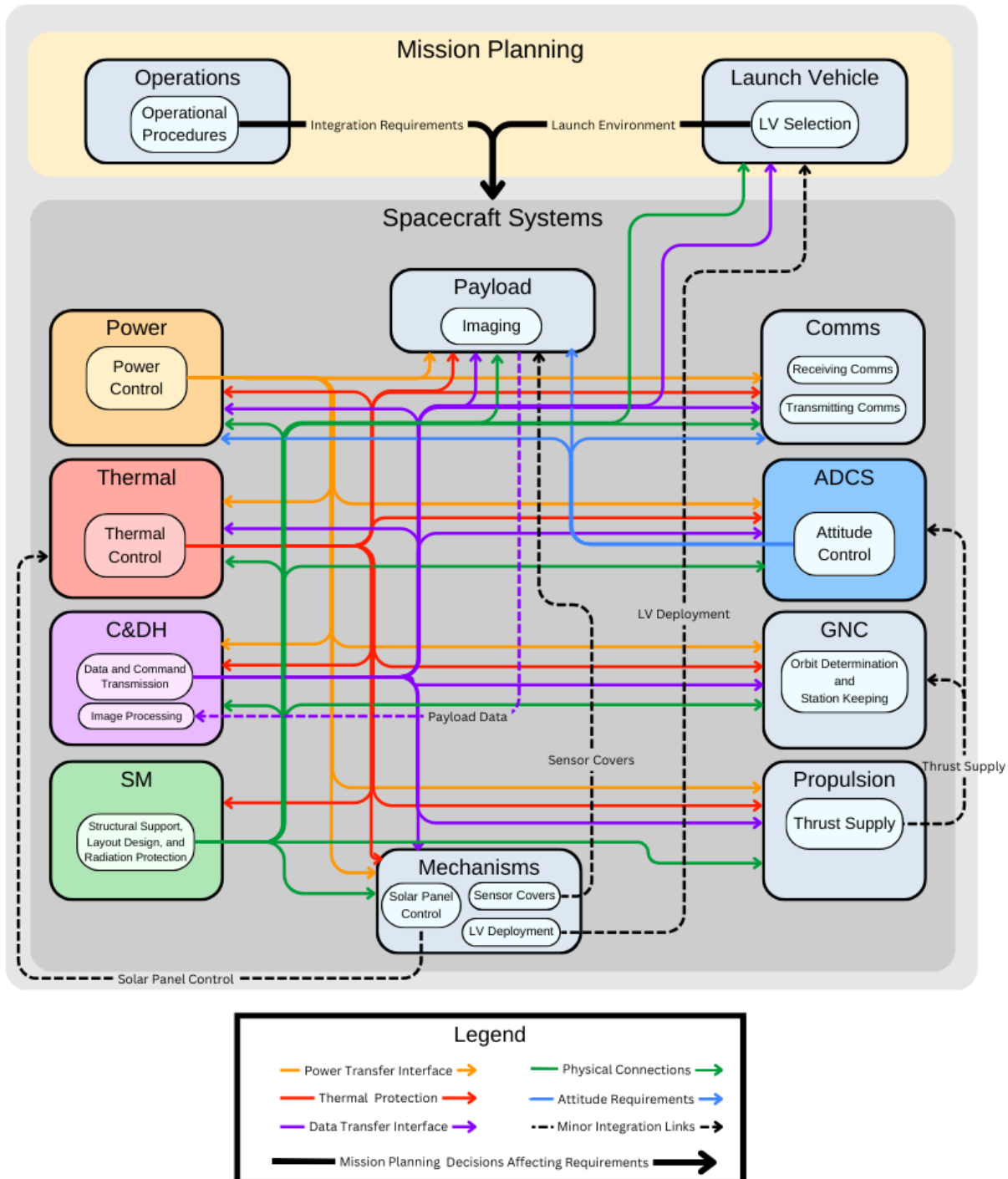


Figure 3: System Block Diagram for Each ARGOS Satellite



## 4 Operations Design

### 4.1 Subsystem Overview

The primary responsibility of the Operations subsystem (Ops) is to define the necessary operating modes for each satellite, followed by the operating procedures for each mode. Ops is also responsible for distributing the mission cost budget between all the subsystems, and defining the mission timeline from development to End of Life (EOL). This includes developing the pre-launch timeline, working closely with the Launch Vehicle (LV) subsystem to determine the launch schedule, and developing a per-orbit timeline of nominal satellite activities. Finally, Ops is responsible for risk categorization and mitigation at both a subsystem and mission level.

### 4.2 Subsystem Objectives

The Ops objectives involve the development of operational procedures, detailed cost and schedule breakdowns, and risk and compliance analysis. The full objectives are listed below.

1. Define operational modes
2. Define operational procedures for each mode
3. Define subsystem-level budget distribution
4. Define pre-launch and launch schedule
5. Assess and mitigate sources of risk
6. Assess Request for Proposal (RFP) Objectives, Requirements, and Constraints (ORC) compliance

### 4.3 Subsystem Requirements

The Ops requirements include defining operational modes and procedures for each phase of the mission, allocating the mission cost budget and analyzing cost compliance, defining launch and pre-launch timelines, and finally consolidating and mitigating sources of risk. The only change to the Ops requirements since the Preliminary Design Review is the refinement of requirement OPS-C-001, which limits the number of single points of failure within the mission architecture to five, all of which must be classified as "very unlikely". The full requirements can be seen in the Ops tab of the Requirements Spreadsheet [11].

### 4.4 Subsystem Constraints

The primary constraint for the Ops subsystem is time. The RFP designates that the mission must begin operations by 2027, be fully operational by 2030, and remain operational through 2031. These requirements constrain the timeline within which pre-launch and launch activities must take place. Further, the RFP defines a monthly duration for which each object in the catalog must be tracked, which constrains how much time each of our satellites must spend on object tracking per one orbit.

The secondary constraint for the Ops subsystem is the per-orbit needs of each subsystem. For instance, the Payload subsystem requires the satellites to be pointed at the catalog objects for a



certain duration and with a certain frequency for object tracking. Similarly, the Communications (Comms) subsystem requires the satellites to point to HOWLL and the ground station for certain durations to transfer data, and the Attitude Determination and Control System (ADCS) requires a certain amount of time to point the satellite.

The tertiary constraint for the Ops subsystem is cost, with a maximum mission cost of 400 million dollars. This constraint is not a significant concern since the maximum mission cost is very generous. However, if this maximum cost is exceeded, there is a substantial risk our mission would not be funded, which the Ops team must keep in mind at all times.

Finally, Ops has a constraint to keep the number of single points of failure for the mission equal to or below five, which all must be classified as very unlikely, in order to keep the risk of total mission failure acceptably low.

## 4.5 Subsystem Drivers

As indicated above by the Ops constraints, cost and time are two of the most important drivers for the operational design, as these factors determine our choice of launch provider and drive the development of the mission schedule. Mass and volume have also driven several budget trades with total mission cost, including the decision to fund a primary launch and increase the total budget from 67 million to 400 million, in order to provide each critical subsystems such as Payload and Propulsion (Prop) with the additional mass and volume they needed to meet their requirements.

Our design was also driven by the per-orbit needs of each subsystem. As indicated in our subsystem constraints, several subsystems have constraints on when and for how long during each orbit the satellite needs to be pointed in a certain direction. These constraints acted as design drivers in the development of our nominal operational procedures and per-orbit timeline to ensure each subsystem was able to perform their essential activities.

Finally, the limit of five very unlikely single points of failure drove the rigor of our risk mitigation. Ops worked closely with the LV, Mechanisms (Mech), Prop, Power, Command and Data Handling (CD&H), and Comms subsystems to develop risk mitigation for all identified single points of failure to ensure all were able to be downgraded in likelihood to "very unlikely."

## 4.6 Subsystem Design Approach

All ARGOS mission subsystem reports were thoroughly reviewed by the Operations team in order to create cohesive, in-depth, and accurate operational procedures [12] [13] [14] [15] [16] [17] [18] [19] [20] [21] [22]. When reviewing the subsystem reports, we kept track of the actions the satellites needed to perform according to each subsystem, the assumptions subsystems made about how the satellite functioned, the need of various subsystems, and how the subsystems had to balance each other. For example, in order to create the transit operational procedure, specific information had to be sought from relevant subsystems. The types of orbits were noted from the GNC report. The choice of launch vehicle and deployment location were taken from the LV report. The mechanism report noted that there was a mechanism that would activate the satellite subsystems upon dispensing. The ADCS report discussed tumbling and stabilization after dispensing. Propulsion



and GNC reports provided information about thrusters and maneuvering into orbit. All of this information was synthesized by the Ops team and turned into the formal analysis section below.

Due to the frequency of attitude determination and control maneuvers, the Ops team created a nominal ADCS subsystem operational procedure 4.7.5. When pointing or attitude adjustments are more broadly referenced in other operational procedures, the ADCS procedure is the full version of what is meant. This information was the basis for all of the operational procedures listed 4.7.4 4.7.6 4.7.2 4.7.8 4.7.9. The HOWLL replacement procedure 4.7.9 was developed by the Ops team; the entire ARGOS mission had to make the conscious design choice to make the HOWLL and WOOF satellites as physically similar as possible in order to accommodate this method of risk mitigation. The per-orbit activities section was developed from the nominal operational procedure, using duration estimates from the GNC, Comms, ADCS, Power, CDH, Mech, Thermal, and Payload subsystems [12] [13] [14] [17] [19] [20] [21] [22].

The pre-launch timeline was created using information across several different sources from literature such as the SpaceX user's guide [23] and sources specific to 27U class satellites [24], but primarily from the CubeSat 101 reference document [25] produced by the NASA CubeSat Launch Initiative. The sources were synthesized and adapted to fit the needs of the ARGOS mission. An Air Force Institute of Technology article on the Rapid Build and Space Qualification of CubeSats **debes2011rapid** and the CubeSat Design Specification document by The CubeSat Program [26] were also consulted for creation of the pre-launch timeline. Steps of the pre-launch timeline that mention individual CubeSats are iterated for each CubeSat in accordance with the launch cadence.

Ops also collaborated with all other ARGOS mission subsystems to determine the most important risks presented by each subsystem. These risks were compiled by the Ops team into a risk matrix to visualize the most high-level risks, which were then analyzed for their impact and potential mitigation. Single points of failure were also identified. The risk information was then compiled into a risk matrix, which was refined after risk mitigation methods were considered.

Finally, the Ops team generated a final budget for this point in the mission life cycle. This section indicates the new cost budget allocated to each subsystem following the change in launch costs, the expected cost of each subsystem design, and subsequently the current margin. For subsystems which do not purchase physical components for the satellite (such as GNC and Ops), the expected cost was estimated using parametric modeling provided in the SMAD [8].

The Ops team formal analysis satisfies all subsystem objectives, requirements, and constraints as described above. The Ops team defined operational modes and associated procedures, defined a system-level budget, defined a pre-launch schedule and worked with the LV team on the launch schedule (provided in the LV section of the FDR Report), and assessed and mitigated high level risk. RFP ORC compliance at the mission level is assessed in the Compliance section of this report; the Ops team provided input, oversight, and edits. The Ops team additionally satisfied our time and cost based constraints.

## 4.7 Formal Analysis

The Ops team developed a pre-launch timeline to outline the activities that must take place before the satellites can be launched, and at what cadence these activities occur. As described in the design approach section, it synthesizes information from a variety of CubeSat sources in addition to



the launch vehicle provider's requirements and schedule. The pre-launch schedule was reconciled and integrated with the Launch Vehicle team's launch cadence.

#### 4.7.1 Pre-launch Timeline

Table 16: Detailed Pre-Launch Timeline and Activities

Step	Activity/Action	Timespan
1	<b>Concept Development and CubeSat Design</b>	Feb - May 2024
	GNC Subsystem Design and Development	(4 months)
	ADCS Subsystem Design and Development	(4 months)
	Payload Subsystem Design and Development	
	Launch Vehicles Subsystem Design and Development	
	Propulsion Subsystem Design and Development	
	Power and Electrical Subsystem Design and Development	
	SM Subsystem Design and Development	
	Thermal Subsystem Design and Development	
	Mechanisms Subsystem Design and Development	
	CDH Subsystem Design & Development	
	(Tele)Communications Subsystem Design & Development	
	Operations Subsystem Design and Development	
2	<b>Merit and Feasibility Reviews</b>	May - Jun 2024
	Reviewers assess the ARGOS mission's RFP needs addressal	(1-2 mo)
	Reviewers assess mission quality of investigation	
	Reviewers assess technical implementation feasibility	
	ARGOS developers review feedback and iterate	
3	<b>Mission Coordination</b>	Jul 2024 - Jul/Dec 2025
	Manage integration schedules	(9-18 mo)
	Ensure CubeSats meet launch requirements	<i>begins 18 months before each</i>

Continued on next page



**Table 16 – continued from previous page**

Step	Activity/Action	Timespan
	Teleconference for mission coordination	<i>scheduled launch</i>
	Create CubeSat to dispenser interface documentation	
	Mission integration analysis inputs	<i>8 months before launch</i>
	SpaceX contract signature milestone	<i>10 months before launch</i>
	SpaceX mission integration kickoff milestone	<i>10 months before launch</i>
4	<b>Licensing</b>	Jul - Dec 2024
	Obtain communications and sensor licenses	(4-6 mo)
	Obtain any additional necessary licenses	<i>concurrently with steps 4 through 8</i>
5	<b>CubeSat Hardware Fabrication and Testing</b>	Jul 2024 - May / Jul 2025
	Fabricate HOWLL, PACK, & WOOF	(9-12 mo)
	Conduct Random Vibration Testing	<i>concurrently with steps 4 through 8</i>
	Perform Thermal Vacuum Bakeout	
	Execute Shock Testing	
	Perform Visual Inspection	
6	<b>Ground Station Testing</b>	Jul 2024 - May / Jul 2025
	Complete ground station design/develop	(9-12 mo)
	Test ground station with CubeSats	<i>concurrently with steps 4 through 8</i>
7	<b>Mission Readiness Reviews</b>	May / Jul 2025 - Jul / Sept 2025
	Assess compliance with design/development	(1-2 mo)
	Assess CubeSats performance	<i>concurrently with steps 4 through 8</i>
	ARGOS developers review feedback and iterate	
	Payload operations for SpaceX launch provider	<i>1 month before launch</i>

Continued on next page



**Table 16 – continued from previous page**

Step	Activity/Action	Timespan
	SpaceX launch campaign planning and mission integration	<i>10 months before launch</i>
8	<b>CubeSat to Dispenser Integration and Testing</b>	Sept 2025
	Deliver CubeSats to integration site	(1 day)
	Conduct additional CubeSat tests	<i>concurrently with steps 4 through 8</i>
	Ship dispenser loaded with CubeSat	
9	<b>Dispenser to Launch Vehicle Integration</b>	Sept 2025
	Perform final cleaning and inspection	<i>(1 day) begins 0.5 to 4 months prior to launch depending on launch vehicle provider; dependent on completion of dispenser integration</i>
	Integrate dispenser onto launch vehicle	
10	<b>Launch</b>	2026 - 2028
	Launch WOOF and HOWLL as primary payloads on Falcon 9	(24 hrs) in 2026
	Launch PACK-C on Blue Ghost 2 as a secondary payload launch	(24 hrs) in 2026
	Launch PACK-E as a secondary payload on Starship HLS	(24 hrs) in 2028
11	<b>Mission Operations</b>	2026 - 2037
	Begin mission operations	<i>(first launch to end of mission life cycle)</i>

#### 4.7.2 Transit Operational Procedure

The transit operational procedure defines the activities performed by each satellite in between launch and the start of nominal operations.



Table 17: Transit Operational Procedure for All Satellites

Step Number	Action
1	<p><b>Within Launch Vehicle</b></p> <p>HOWLL and WOOF are launched on a Falcon 9 as a Primary Payload Launch in late 2026 on a Trans-Lunar Injection.</p> <p>PACK-C is launched as a secondary payload (free 12U) on Blue Ghost on a Falcon 9 in 2026.</p> <p>PACK-E is launched as a secondary payload (free 12U) on Starship HLS in late 2028.</p>
2	<p><b>Satellite Dispensing/Deployment</b></p> <p>Dispense all satellites from their respective Rocket Lab Canisterized Satellite Dispensers.</p> <p>Deploy PACK-C in an elliptical lunar 2000x673km orbit at a 50 degree inclination.</p> <p>Deploy PACK-E in an elliptical lunar 505x2000km orbit at a 135 degree inclination.</p> <p>Deploy HOWLL and WOOF satellites on a Trans-Lunar Injection.</p> <p>Use ADCS zero-momentum three-axis control systems to stop tumbling.</p>
3	<p><b>Activate Subsystems &amp; Generate Power</b></p> <p>Mechanism to turn on the satellite is activated upon release from dispenser.</p> <p>Rely on batteries for 50 minutes (out of 1.5-2 hour capacity) after deployment before solar panels deploy.</p> <p>Deploy solar arrays from stowed position by releasing Frangibolts.</p> <p>Perform nominal ADCS operational procedure to point solar arrays to maximize power generation.</p>
4	<p><b>Thermal Regulation</b></p> <p>Use thermocouple to monitor temperature of satellite's components.</p> <p>Use radiator to radiate heat.</p>
5	<p><b>Health Assessment &amp; Confirmation</b></p> <p>Verify all subsystems are turned on and performing as desired using CDH subsystem. Run health diagnostic.</p> <p>Use sun sensor, star tracker, and CDH system to collect positional data. Engage nominal ADCS operational procedure.</p>
6	<p><b>Satellite Pointing</b></p>

Continued on next page



**Table 17 – continued from previous page**

Step Number	Action
	Perform ADCS operational procedure to point the satellite so the antenna is pointed at HOWLL (if PACK or WOOF) or the Earth (if HOWLL) to allow communication transmission.
7	<p><b>Communications &amp; Data Transmission</b></p> <p>Transmit communication to ground (through HOWLL if applicable) confirming satellite deployment, health, and position.</p>
8	<p><b>Orbit Insertion/Initialization</b></p> <p>ADCS orients satellite in direction to propel.</p> <p>HOWLL and WOOF use thrusters to maneuver to enter L2. WOOF enters its final position in a Southern L2 Halo orbit.</p> <p>HOWLL applies a secondary burn to transfer from L2 to its final position in L1 in a Northern L1 Halo orbit.</p> <p>PACK-E and PACK-C both complete single impulsive burns to reach their desired orbits. PACK-C is in a circular lunar frozen orbit with a 3737.4 km semi-major axis and 50 deg inclination. PACK-E is in an elliptical lunar frozen orbit with a 3737.4 km semi-major axis and 135 deg inclination.</p> <p>Perform ADCS operational procedure: Initial attitude determination, stabilization, and motion control using three-axis control.</p> <p>Repeat health assessment &amp; confirmation steps; verify &amp; communicate that desired orbit has been achieved.</p>
9	<p><b>Begin Nominal Operations</b></p>

#### 4.7.3 Nominal Operational Procedure

To contextualize the object tracking in the nominal operational procedure, this table defines which satellites track which objects. Two satellites track each object for redundancy and due to the strength of their respective sensors.

Satellite	Space Object
HOWLL, WOOF	L1 Halo, L2 Halo, GTO to L1 Halo, GTO to L2 Halo
PACK-C, PACK-E	LLO 1-3, LG

Table 18: Assignment of Space Objects to Satellites for Tracking

The differences between satellites for nominal operational procedure are quite minimal, so the procedure is presented in one table for all mission satellites. The main distinctions as relevant to nominal operations are that HOWLL serves as the communications relay between the ground station and all other ARGOS mission satellites.



Table 19: Nominal Operational Procedure for All Satellites

Step Number	Activity/Action
1	<b>Object Tracking</b> Satellite uses sensors to collect observational tracking data on surrounding objects. Satellite uses CDH subsystem to process and store tracking data.
2	<b>Power Generation</b> ADCS system points satellite to maximize power generation through solar arrays. Battery charges for PACK satellites.
3	<b>Satellite Maintenance</b> Satellite runs health diagnostic: monitors temperature, component functionality. Satellite uses sun sensor and star tracker to determine its attitude. Once per year, satellite performs station keeping maneuvers (less than 5 m/s per year) using ADCS and propulsion systems. HOWLL sends health diagnostic and observational data to ground station. Thermocouple continually monitors temperature and determines passive radiative mode of high vs low.
4	<b>Communications</b> Satellite points at HOWLL/ground station. Satellite transmits tracking, health, and attitude data to the ground station (through HOWLL if applicable) and potentially uploads new commands.

Here is the nominal operational procedure visualized as a functional flow diagram:

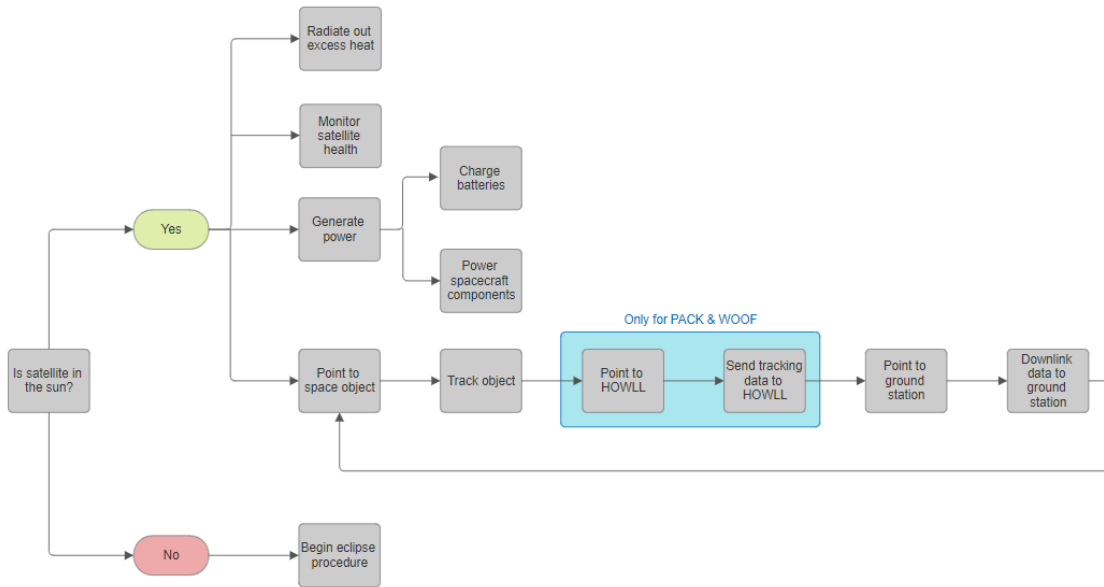


Figure 4: Nominal Operational Procedure Functional Flow Diagram

#### 4.7.4 Per-Orbit Activities

In addition to the nominal operational procedure, the Ops team created a per-orbit operational procedure/timeline. This outlines, in order, the activities each satellite would perform in one orbit and expresses the duration of the activity as a percentage of the orbit. This orbit is assumed to be the most basic orbit experienced by the satellite. For example, the 27U satellites only infrequently experience eclipse, so eclipse was excluded from this timeline. Additionally, station-keeping is only performed by each satellite approximately once a year, so it was excluded as well.

## **HOWLL Per-Orbit Activities:**

1. Object Tracking – 13% of orbit
    - (a) Control gimbal to direct payload sensor towards space object. If not enough range of motion, perform attitude adjustment
    - (b) Articulate solar arrays to maximize power generation
    - (c) Perform object tracking
  2. On-Board Computer Operations – <1% of orbit
    - (a) Process and compress object tracking data
    - (b) Perform satellite health confirmation
  3. Communications – 3.33% of total orbit
    - (a) Perform ADCS maneuver to point communications antenna towards PACK satellites
    - (b) Articulate solar arrays to maximize power generation



- (c) Receive communications/data package from PACK
  - (d) Perform ADCS maneuver to point communications antenna towards WOOF satellite
  - (e) Articulate solar arrays to maximize power generation
  - (f) Receive communications/data package from WOOF
  - (g) Perform ADCS maneuver to point communications antenna towards ground station
  - (h) Send data to ground station: object tracking, health confirmation, attitude measurements, from all satellites
4. ADCS Disturbance Correction – 20% of orbit
    - (a) Constant but minimal use of reaction wheels
    - (b) Use thrusters to desaturate reaction wheels if necessary
  5. Dedicated Power Generation – remainder of orbit, approx. 63%
    - (a) Perform attitude adjustment and solar panel articulation to maximize power generation

**PACK Per-Orbit Activities:**

1. Object Tracking – 13% of orbit
  - (a) Control gimbal to direct payload sensor towards space object If not enough range of motion, perform attitude adjustment
  - (b) Articulate solar arrays to maximize power generation
  - (c) Perform object tracking
2. On-Board Computer Operations – <1% of orbit
  - (a) Process and compress object tracking data
  - (b) Perform satellite health confirmation
3. Communications – 3.33% of orbit
  - (a) Perform ADCS maneuver to point communications antenna towards HOWLL
  - (b) Articulate solar arrays to maximize power generation
  - (c) Send communications/data package to HOWLL
4. Eclipse and safe mode – 15% of orbit
  - (a) Cease operations other than monitoring satellite health and attitude
  - (b) Turn on heater and radiator passively turns to low radiative mode
  - (c) Turn subsystems back on and articulate solar panels to generate power at end of eclipse
5. ADCS Disturbance Correction – 20% of orbit
  - (a) Constant but minimal use of reaction wheels



- (b) Use thrusters to desaturate reaction wheels if necessary
- 6. Dedicated Power Generation – remainder of orbit, approx. 48%
  - (a) Perform attitude adjustment and solar panel articulation to maximize power generation

### WOOF Per-Orbit Activities:

- 1. Object Tracking – 13% of orbit
  - (a) Control gimbal to direct payload sensor towards space object If not enough range of motion, perform attitude adjustment
  - (b) Articulate solar arrays to maximize power generation
  - (c) Perform object tracking
- 2. On-Board Computer Operations – <1% of orbit
  - (a) Process and compress object tracking data
  - (b) Perform satellite health confirmation
- 3. Communications – 3.33% of orbit
  - (a) Perform ADCS maneuver to point communications antenna towards HOWLL
  - (b) Articulate solar arrays to maximize power generation
  - (c) Send communications/data package to HOWLL
- 4. ADCS Disturbance Correction – 20% of orbit
  - (a) Constant but minimal use of reaction wheels
  - (b) Use thrusters to desaturate reaction wheels if necessary
- 5. Dedicated Power Generation – remainder of orbit, approx. 63%
  - (a) Perform attitude adjustment and solar panel articulation to maximize power generation

Every time an attitude adjustment is performed, the solar arrays are articulated to maximize power generation at the given attitude. Within the non-eclipse orbit, the solar panels generate power 90% of the time [17]. The 10% of time they do not generate significant power is not dependent on specific orbital activities, but rather the incidental position of the other point of communication relative to the sun (i.e. if HOWLL is pointed at a PACK satellite but the sun is in the least favorable position and the solar panels cannot be articulated enough to generate power during the communication). For further description of how power is distributed among operational activities refer to the FDR Report Power subsection.

#### 4.7.5 ADCS Operational Procedure

A full operational procedure was designed specifically for the ADCS subsystem due to how frequently attitude adjustments are performed by each satellite. Every time an attitude adjustment or pointing is mentioned in an operational procedure, this operational procedure is the full description of the action. The various onboard mechanisms, such as the gimbal on the payload sensor



and the actuators on the solar arrays, help to reduce the reliance on ADCS and allow for greater simultaneous activities than would have otherwise been possible (i.e. solar arrays can be actuated more towards the sun while the communications antenna can be gimbaled towards the ground station while the greater satellite body can be in an intermediate attitude).

Table 20: Steps for Attitude Determination and Control

Step	Action
1	Use sun sensor and star tracker to collect attitude data.
2	Process data, estimate attitude, and calculate adjustments to be made through CDH subsystem and the TRIAD algorithm with extended Kalman Filter [13].
3	Perform attitude adjustments using single-gimbal control moment gyroscopes and reaction wheels.
4	Engage thrusters to momentum dump to correct reaction wheel saturation if necessary.

#### 4.7.6 Eclipse Operational Procedure

All ARGOS mission satellites experience eclipse. Therefore, this operational procedure applies to all four ARGOS mission satellites, with varying degrees of frequency of use. The PACK-C and PACK-E satellites experience eclipse for approximately 45 minutes every 5.695 hour orbit, with an additional approximately 5 hour eclipse about once a year due to the Earth. The HOWLL and WOOF satellites experience eclipse for about 3 to 5 hours at varying frequencies, spanning for a few days to several weeks between eclipses. This operational procedure applies to all of these eclipses, regardless of length. The Power subsystem further discusses power needs while in eclipse in their section of the FDR report.

Table 21: Eclipse Operational Procedure

Step	Action
1	<b>Recognize Eclipse</b> Onboard computer, in combination with historical data collected by sensors, monitors orbit progress and recognizes when an eclipse is about to begin.
2	<b>Engage Safe Mode</b> Temporarily power down payload sensors and stop object tracking. Temporarily cease communications. Temporarily cease continuous ADCS satellite pointing.

Continued on next page



**Table 21 – continued from previous page**

Step	Action
	<p>Turn on heater.</p> <p>Radiator passively turns from high to low radiative mode.</p> <p>Perform regular health diagnostics throughout eclipse duration: monitor temperature, component functionality, and orbital position.</p>
3	<p><b>Exit Eclipse</b></p> <p>Onboard computer measures time and turns all subsystems back on after the duration of the eclipse.</p> <p>Solar arrays begin to generate power again, verifying eclipse cessation.</p> <p>Assess solar panel integrity by verifying normal power generation in case of Thermal Elastic Shock.</p> <p>Satellite communicates health diagnostic through HOWLL to ground station.</p> <p>Satellite returns to nominal operational procedure.</p>

#### 4.7.7 Station Keeping Operational Procedure

A simple operational procedure was outlined for station-keeping. All satellites have station-keeping needs on the order of about 5 m/s or less (with the Lagrange point Halo orbit satellites having larger station-keeping deltaV needs than the frozen orbit satellites). This procedure is for all satellites.

Station keeping operations:

- On-board computer determines station-keeping must occur based on elapsed time since last occurrence / Command to station-keep is received from the ground station
- Reaction wheels orient the spacecraft so that thrusters are in position to station keep
- Satellite performs a small burn to maintain orbit
- Send communication to ground station confirming completion of station-keeping burn
- Return to nominal operational procedure

#### 4.7.8 End of Life (EOL) Operational Procedure by Satellite

To ensure that our mission planning is comprehensive, we determined end of life procedures for each satellite. HOWLL and WOOF perform two burns to enter heliocentric orbit. Both PACK satellites do one impulsive maneuver to impact upon the lunar surface. Since HOWLL is the communications relay between the other satellites and the ground station, it performs its end of life procedure last of the four satellites.



Table 22: HOWLL EOL Operational Procedure

Step	Action
1	Ground station sends command to HOWLL to begin EOL procedure
2	Thrusters fire, performing single impulse maneuver
3	Satellite decays away from Earth-Moon system in unstable orbit
4	Communications with ground station are maintained throughout end of life
5	Thrusters fire, performing second maneuver to change orbital energy appropriately and avoid re-entry into Earth-Moon system
6	Zero Velocity Curves are constructed and monitored by ground crew to ensure HOWLL has entered a stable heliocentric orbit

Table 23: PACK EOL Operational Procedure

Step	Action
1	Ground station sends command to HOWLL to begin EOL procedure
2	HOWLL sends command to PACK satellites to begin EOL procedure
3	Satellite orbital position is monitored
4	When satellite reaches its apoapsis, fire thrusters to perform single retrograde burn
5	Orbit continuously decays
6	Communications through HOWLL to ground station are maintained throughout end of life
7	PACK impacts the lunar surface
8	Ground station confirms impact with last available position data received

Table 24: WOOF EOL Operational Procedure

Step	Action
1	Ground station sends command to HOWLL to begin EOL procedure
2	HOWLL sends command to WOOF to begin EOL procedure
3	Thrusters fire, performing single impulse maneuver
4	Satellite decays away from Earth-Moon system in unstable orbit



Table 24: WOOF EOL Operational Procedure

Step	Action
5	Communications through HOWLL to ground station are maintained throughout end of life
6	Thrusters fire, performing second maneuver to change orbital energy appropriately and avoid re-entry into Earth-Moon system
7	Zero Velocity Curves are constructed and monitored by ground crew to ensure WOOF has entered a stable heliocentric orbit

#### 4.7.9 HOWLL Replacement Procedure - Risk Mitigation

As is further explained in the risks section of this report 4.7.10, HOWLL is a single point of failure for our mission due to its function as the communications relay between the ground station and all other satellites. Therefore, the Ops team created a replacement procedure for HOWLL. Due to the overwhelming similarities between HOWLL and WOOF (with the only physical differences being slightly different propulsive capacities, as explained in the propulsion subsystem), WOOF will move to L1 to replace HOWLL in the event of an unrecoverable failure on HOWLL. A new satellite would then be inserted at L2 to replace what was formerly WOOF.

The key problem in this replacement procedure is that only the satellite at L1 can communicate with the ground station. Barring relying on external cislunar communications architecture, there is no way for the ground station to contact the PACK or WOOF satellites in the event of a HOWLL failure. The former WOOF satellite can only reach the ground station once close to L1 [21]. The satellites, without uploaded commands from the ground station, must independently determine a critical HOWLL failure and WOOF must insert itself in HOWLL's previous orbit.

Table 25: HOWLL Replacement Procedure

Step	Action
1	WOOF and PACK tries to communicate through HOWLL; communication is not received
2	WOOF and PACK repeatedly attempt to communicate to HOWLL for a duration greater than the maximum eclipse time any satellite experiences (over 5 hours)
3	WOOF and PACK satellites contact each other and mutually confirm HOWLL is unresponsive
4	It is determined that HOWLL is not in communication and therefore has had a major failure
5	WOOF performs an attitude adjustment to point thrusters in desired direction for propulsion

Continued on next page



Table 25 – continued from previous page

Step Number	Action
6	WOOF applies a burn to transfer from L2 to L1; enters its new position in a Northern L1 Halo orbit (copies HOWLL's orbit insertion/initialization procedure <a href="#">4.7.2</a> )
7	WOOF communicates to PACK that it is the new L1 communications relay
8	WOOF communicates to ground station that it is the new L1 communications relay
9	WOOF uses payload sensor to perform object tracking on HOWLL; processes and compresses data and communicates it to ground station
10	If possible (depending on HOWLL failure), ground station instructs HOWLL to enter end of life procedure; HOWLL enters heliocentric orbit
11	Pre-launch timeline is repeated to manufacture a replacement 27U satellite to insert at L2
12	New 27U satellite is launched as a primary payload on a Falcon 9 as soon as possible on a trans-lunar injection
13	Transit Operational Procedure is repeated for the new 27U satellite, inserted in a Southern L2 Halo orbit

#### 4.7.10 Risk Analysis and Mitigation

The Ops team worked with all other subsystems during the design cycle leading up to PDR to understand the most important risks for each subsystem, and classify those risk using a risk matrix that takes into consideration both likelihood and impact. The initial risk matrix which was constructed from these discussions is provided in the figure below. Risk level is indicated by color where red is high, orange is medium-high, yellow is medium, light green is low-medium, and green is low.



	Negligible	Minor	Moderate	Significant	Severe
Very Likely					
Likely					
Possible		Single event effects from radiation Solar flare radiation	Secondary payload launch delay Data budget exceeded Timeline delays	Blue ghost lander failure Power system overload Design team communication failure	
Unlikely		Gimbal failure	Structural damage during launch Uncontrolled nozzle exhaust plume Battery failure TID radiation design limit exceeded	Uncontrolled propellant tank sloshing Uncontrolled nozzle exhaust plume Battery failure TID radiation design limit exceeded	Solar array failure Sensor failure Solar array deployment failure Comms hardware failure
Very Unlikely			Primary payload launch delay	Solar array articulation failure	Launch vehicle explosion Propulsion feed system failure Failure to dispense cubesats Conductive surfaces disconnect OBC failure \$400 million budget exceeded

Figure 5: Initial Risk Matrix

In the final design cycle, Ops worked to mitigate all medium-high risks such that they could be downgraded to medium risks. This risk mitigation process is described below.

- Blue Ghost Lander Failure:** The possibility of the Blue Ghost Lander failing was initially classified as possible, due to its low Technology Readiness Level (TRL) of TRL 6, and significant, as its failure would require PACK-C to use extra propellant to enter its final orbit, reducing the propellant available for station keeping and shortening the mission lifetime. It was determined that there are no other lunar landers on the market which fulfill our needs and have a higher TRL, therefore this risk was unable to be successfully mitigated, and remained classified as medium-high.
- Power System Overload:** The possibility of a power system overload was initially classified as possible due to the various power draws of different subsystems at different times, and significant, as an overdraw could permanently damage the power system. Discussions with the Power team revealed that they already have shunts in place to prevent overdraw, and therefore the possibility of this risk was downgraded to unlikely, which downgraded the risk to a medium level.



3. **Design team communication failure:** The possibility of a design team communication failure was initially classified as possible, due to the large size of the overall team and the number of subsystems working concurrently. The impact was classified as significant, since each subsystem shares critical mission resources, and the failure to communicate a critical design decision which impacts other subsystems could lead to designs which are incompatible. The preparation for the team PDR and Final Design Review (FDR) saw a significant increase in cross-subsystem communication, and the successful resolution of small design differences. Therefore this risk was downgraded to "unlikely" and an overall risk level of medium.
4. **Solar array failure:** The possibility of the entire solar array failing was initially classified as unlikely, but severe since the inability to generate power would be fatal to our mission. Further discussion with the Power team led to the understanding that the solar array is made up of individual solar panels, which are made up of solar cells. Therefore, the possibility of an individual cell or panel failing to generate power is significantly more likely than the possibility that the entire array fails. With this revised understanding of the power generation architecture, this risk was downgraded to "very unlikely" and an overall risk level of medium.
5. **Sensor failure:** The possibility of the payload sensors failing was initially classified as unlikely, due to the flight heritage of the chosen sensors, but severe, since the inability to track objects with one of our satellites would make it impossible to meet our primary mission objective. A discussion with the Payload team revealed there was insufficient mass and volume margin onboard all the satellites to carry backup sensors in the case of failure. However, it was determined that each catalog object is being tracked by two satellites, therefore even if the sensors on one satellite fail, we are still able to track that object. With this new understanding we downgraded the impact of sensor failure to "significant", which reduced the overall risk level to medium.
6. **Solar array deployment failure:** The possibility of the solar array failing to deploy was initially classified as unlikely due to the flight heritage of the chosen mechanisms, but severe, since the inability to deploy our solar array would make it impossible to generate enough power, and be fatal to our mission. Discussion with the Mech subsystem revealed that the chosen deployment mechanisms for the solar array - Frangibolts - are internally redundant, therefore decreasing the likelihood that the solar array fails to deploy. With this new information, the likelihood was downgraded to "very unlikely," which reduced the overall risk level to medium.

#### 7. Comms hardware failure:

The possibility of the Comms hardware failing was initially classified as unlikely due to the flight heritage of the chosen hardware, but severe, since the failure of the X-band antenna on HOWLL would eliminate our ability to send data to the ground, and the failure of the K-band antenna on HOWLL would eliminate our ability to communicate with or collect data from the other three satellites. It was determined at a mission level that WOOF would be altered to be nearly identical to HOWLL, such that if the HOWLL satellite fails, WOOF can be maneuvered from L1 to L2 and act as the new HOWLL satellite. From a Comms perspective, this means if the X-band antenna fails on HOWLL, WOOF will replace HOWLL and reinstate our communication with the ground. Conversely, if the K-band antenna fails on HOWLL, it was determined that the PACK satellites



can send their data to WOOF using their K-band antennas, and then WOOF can send the data to HOWLL using its X-band antenna. Therefore, there is now redundancy in the Comms hardware which eliminates previous single points of failure and reduces the impact of the failure to moderate. Therefore this risk was successfully mitigated and downgraded to a medium level.

As evidenced above, all medium-high risks were able to be successfully mitigated and downgraded to medium risks with the exception of the possibility of a Blue Ghost Lander failure. The updated risk matrix after mitigation of these risks is provided in the figure below.

	Negligible	Minor	Moderate	Significant	Severe
Very Likely					
Likely					
Possible		Single event effects from radiation  Solar flare radiation	Secondary payload launch delay  Data budget exceeded  Timeline delays	Blue ghost lander failure	
Unlikely		Gimbal failure	Structural damage during launch  Comms hardware failure	Uncontrolled propellant tank sloshing  Uncontrolled nozzle exhaust plume  Battery failure  TID radiation design limit exceeded  Power system overload  Design team communication failure  Sensor failure	
Very Unlikely			Primary payload launch delay	Solar array articulation failure	Launch vehicle explosion  Propulsion feed system failure  Failure to dispense cubesats  Conductive surfaces disconnect  OBC failure  \$400 million budget exceeded  Solar array deployment failure  Solar array failure

Figure 6: Risk Matrix After Mitigation

The risk mitigation performed during this design cycle also reduced the single points of failure



within our mission architecture. The initial six single points of failure and their current state is listed below.

1. **Launch vehicle explosion:** The Falcon 9 has a failure rate of only 0.92 percent, and has had no failures since 2016. Therefore this risk is very unlikely, however it still exists and presents a single point of failure for our mission.
2. **Cubesat dispenser failure:** It was determined that the RocketLab Canisterized Satellite Dispenser (CSD) has double and triple internal electrical redundancies, so the risk that our cubesats do not dispense is very unlikely but nonzero, and still represents a single point of failure for our mission.
3. **Propulsion feed system failure:** The failure rate of the propulsion feed system was determined to be very low, making this risk very unlikely but nonzero and still represents a single point of failure for our mission.
4. **Solar array failure/ deployment failure:** As discussed above, the solar array is redundant, and the deployment mechanism is internally redundant. Therefore, this risk is very unlikely, however the failure to deploy the solar array is still a single point of failure.
5. **On-board Computer (OBC) failure:** The mean time to failure for our chosen OBC is several decades, and it is internally redundant, so the risk of failure is very unlikely. However this risk still represents a single point of failure.
6. **Comms hardware failure:** As discussed above, the Comms hardware has been updated such that it is now redundant and no longer a single point of failure for our mission.

Therefore, our mission has five remaining single points of failure. However, all five are classified as "very unlikely" due to internal redundancies for high TRL, so we are very confident in the improbability of one of these risks occurring.

#### 4.7.11 Mission Budget

The maximum total mission budget as defined by the RFP is 400 million dollars. The recommended total mission budget is a more conservative value of 60 million dollars, however, it was determined relatively early in our mission design that this value was too restrictive to be feasible, as the mass and volume needs of our subsystems required a larger spacecraft bus than could be launched using free ride-share programs.

The 400 million dollars for our total mission cost was split 70/30 in accordance with recommendations from the SMAD [8] as well as the 2019 Development of Small Satellite Cost Model **SSCM19**, with 30 percent of the budget allocated to "Wraps" costs and the remaining 70 percent allocated to the development of satellite buses and payloads. Here, "Wraps" is a term taken from the SMAD which encompasses nonphysical expense factors such as systems engineering, integration and test, etc. Ops, Guidance, Navigation and Control (GNC) and LV were all classified as Wraps subsystems for the purpose of our budget distribution, while the remaining nine subsystems contribute to satellite bus and payload development. Additionally, a portion of the Wraps budget was set aside for Integration, Assembly, and Test (IA&T) costs, as well as Ground Systems Equipment (GSE).



With these categories established, the budget was further distributed to each of the twelve subsystems in accordance with recommendations from Table 20-9 in the SMAD. Notably, Table 20-9 accounts for both RDT&E costs as well as production costs, so the only mission expense which is not accounted for by this cost model is satellite maintenance or replacement. Ops informed each subsystem of their allocated cost budget early in the design cycle, and from that point each subsystem was individually responsible for updating the budget spreadsheet with their anticipated subsystem costs, as well as notifying us with any concerns about exceeding their budget allocation. The final budget distribution, including the allocated and actual costs of each subsystem, as well as their percent margin, is provided in the figure below.

		<b>Percent of Total Budget</b>	<b>Cost Budget TOTAL</b>	<b>Estimated Expenses</b>	<b>Current Margin</b>
<b>Spacecraft Bus Subsystems</b>	Payload	13%	\$52,000,000	\$5,800,000	89%
	Comms	12%	\$48,000,000	\$1,029,800	98%
	SM	2%	\$8,000,000	\$200,000	98%
	Mech	5%	\$20,000,000	\$746,572	96%
	Thermal	1%	\$4,000,000	\$400,000	90%
	Power	7%	\$28,000,000	\$2,000,000	93%
	CD&H	6%	\$24,000,000	\$400,000	98%
	ADCS	6%	\$24,000,000	\$1,000,000	96%
	Prop	3%	\$12,000,000	\$1,200,000	90%
<b>Wraps Subsystems</b>	Ops	8%	\$32,000,000	\$4,580,000	86%
	GNC	2%	\$8,000,000	\$610,000	92%
	LV	1%	\$4,000,000	\$610,000	85%
<b>Other Wraps Costs</b>	Integration, Assembly, & Test (IA&T)	6%	\$24,000,000	\$2,780,000	88%
	Ground Systems Equipment (GSE)	3%	\$12,000,000	\$1,320,000	89%
<b>Launch Costs</b>	Falcon 9 Primary Launch	25%	\$100,000,000	\$67,000,000	33%
	<b>TOTAL</b>	100%	\$400,000,000	\$89,676,372	78%

Figure 7: Mission Budget Breakdown

## 5 Launch Vehicle Design

### 5.1 Subsystem Overview

It is the responsibility of the Launch Vehicle (LV) subsystem to safely deliver the Homing Orbital Wolf L-1 Linkage (HOWLL) communications satellite and the Pathfinding Array for Cislunar Kinematics (PACK) lunar coverage satellites to the determined orbit to allow transition to in-space operations. The subsystem must determine an appropriate launch vehicle capable of carrying the spacecraft to an orbit that would allow movement into operational orbit using system propulsion. The launch environment must be characterized in order to ensure that adverse effects are not suffered as a result of launch, and practical considerations such as cost, launch cadence, readability, and readiness must be considered. The LV subsystem is essential to the mission architecture of Advanced Relay for Geolunar Operational Support (ARGOS).

Communication between subsystems is essential to the success of LV because of the nature of the reliance of the mission on successful launch as a first step. Communication with the Operations subsystem is needed for discussions regarding mission architecture such as launch schedules and orbital trajectories. Analysis pertaining to the transition of the spacecraft from deployment orbit to final mission orbit must be conducted in collaboration with the Guidance, Navigation, and Control (GNC) subsystem. Viable deployment orbit will be considered in discussion also with the Propulsion subsystem in order to verify the  $\Delta V$  means of the spacecraft. Structures and Materials (SM) must work to minimize the dry mass of the spacecraft and is, in addition to Thermal, responsible for accounting the effect of the launch environment on the spacecraft. The Mechanisms subsystem must select a mechanism capable of deploying the spacecraft from the launch vehicle once delivered to deployment orbit.

### 5.2 Subsystem Objectives

No major changes to the Launch Vehicle objectives have been made in the last design cycle. The objective regarding power distribution was clarified to refer to the responsibility of the Launch Vehicle subsystem to ensure mission compliance with launch vehicle integration requirements related to electrical power as well as interface and telecommunication specifications. Minimizing launch costs was clarified to be a focus of the selection of launch providers specifically, with another objective added referring to the selection of launch times. The primary concern of the LV subsystem is to ensure a safe delivery of the satellites to deployment orbit. Any objective that is critical to the success of the mission is ranked above objectives that regard more efficiently or effectively fulfilling the mission architecture. Though the mass, volume, and interfacing requirements have a much larger margin than before the mission architecture was last changed, these requirements are still the most important to be fulfilled because they allow for launch to take place. The objectives are summarized as follows:

- Meeting mass, volume, and interfacing requirements for ARGOS satellites as payload on respective launch vehicles
- Delivery of HOWLL, WOOF, and PACK satellites avoiding destructive loads or exposure to the launch environment causing launch failure
- Launch integration of the launch vehicle enabling reliable spacecraft in-space operations following deployment



- Delivery of the HOWLL satellite to the required trajectory allowing for delivery of the spacecraft by propulsion to the mission orbit within propellant margin, allowing for the achievement of communication relay mission objectives
- Delivery of the WOOF satellite to the required trajectory allowing for delivery of the spacecraft by propulsion to the mission orbit within propellant margin, allowing for the achievement of communication relay mission objectives
- Delivery of the PACK satellites to the required trajectory allowing for delivery of the spacecraft by propulsion to the mission orbit within propellant margin, allowing for the achievement of communication relay mission objectives
- Effective distribution of power to necessary subsystems during transit and orbital insertion of the spacecraft while complying with any launch restrictions on electronics
- Timely completion of the mission architecture by accounting for setbacks including with the launch provider and launch failure within launch scheduling and redundancy
- Minimizing launch-related costs with selection of low-cost launch providers
- Timely completion of the mission architecture with selection of appropriate launch times in the developed launch schedule

### 5.3 Subsystem Requirements

The LV subsystem has a total of 29 requirements that can be found in full in the LV tab of the “[Requirements Spreadsheet](#)” Google Sheet [11]. These requirements are organized and summarized into the following categories:

Table 26: LV Subsystem Requirements Summary.

Req. ID (LV-###)	Description	Objective Category
LV-F-001, LV-F-002, LV-F-003, LV-P-001, LV-P-002	The LV subsystem shall conduct a successful launch by 2027 and complete the mission architecture by 2029 with backup launch capability.	Mission Architecture and Timeline
LV-F-004, LV-F-005, LV-F-006, LV-F-011, LV-F-012, LV-F-013, LV-F-014	The LV subsystem shall select an LV that can support the mass, volume, and integration requirements of ARGOS satellites.	LV Mass, Volume, Interfacing
LV-F-007, LV-F-008, LV-F-009, LV-C-001, LV-C-002	The LV subsystem shall limit costs to \$75 million while mitigating LV-related risks.	LV Cost, Reliability, and Readiness
LV-F-010, LV-F-015, LV-F-016, LV-F-017, LV-F-018	The LV subsystem shall characterize the environmental loads during launch and transit.	Environmental Loads Characterization
LV-E-001, LV-E-002, LV-E-003, LV-E-004, LV-E-005, LV-E-006, LV-E-007	The ARGOS mission spacecraft shall be able to withstand the environmental loads during launch and transit.	Environmental Loads Compliance

The LV subsystem is compliant with all remaining requirements, although the Environmental Loads Compliance category was fulfilled primarily with analysis from other subsystems. Most of the requirements have been kept, but a couple of modifications have been made. For requirement LV-F-010, 10 km was selected as the minimum separation between satellite deployment and



known Cislunar objects, as verification of this value could now be achieved using analysis methods examined by the GNC team. This requirement is listed below:

Table 27: The Updated LV Requirement

Requirement ID	Requirement	Rationale	Verification Method	Trace-Up/Down
LV-F-010	ARGOS satellite deployment shall be conducted with a minimum 10 km separation from known cislunar objects	Setting a minimum distance standard during deployment will minimize the risk of colliding with another spacecraft	Analysis/simulation of deployment orbits	MISS-F-018

The former LV-E-007, the requirement regarding the ability of mission components to survive depressurization, was ultimately abandoned due to the lack of a clear method for verifying compliance. The analysis methods that could be found proved to be too complex given the scope of the subsystem, such as a Jet Propulsion Laboratory method that involved modeling the payload and payload fairing before conducting a computational fluid dynamics simulation that would then enable particle transport modeling simulations [27].

## 5.4 Subsystem Constraints

No changes to constraints have been made. The primary constraints on Launch Vehicle continue to be mass and volume and timeline, though cost has been deemphasized. The constraints added in the PDR, export controls and information, continued to be considered in this design cycle as backup launches were being considered under the same constraints as the central launches were. Not-yet-determined information regarding CLPS missions used for additional PACK satellite launches as needed will be discussed in the design section of this report. The constraints are summarized as follows:

- **Mass and volume:** The capacity of the launch vehicle will primarily determine its compatibility with the mission architecture.
- **Launch environment:** Considerations including g-force load, vibration, heat, and radiation must be able to be withstood by the spacecraft structure and equipment.
- **Mission timeline:** Planned launches must comply with the overall mission deadline of beginning operations by 2027 and being operational by 2030.
- **Available information:** Launch vehicle specifications available to the public and lack of flight heritage for use of ensuring compliance with mission needs limit selection for ARGOS primary payload launches.
- **Artemis missions:** Predetermined launch schedules and trajectories on Artemis missions limit selections for secondary payload launches that comply with mission deadlines and spacecraft deployment.
- **Onboard propulsion capability:** Planned deployment must comply with the  $\Delta V$  values and engine thrust that can be achieved by spacecraft propulsion.
- **Mission cost:** Team-wide constraints like available budget limit viable launch vehicle options as the launch vehicle is the most expensive singular component of the mission.



- **Export Control Laws:** Federal laws limit or complicate the use of foreign launch vehicles for U.S. spacecraft.

## 5.5 Subsystem Drivers

No changes to the subsystem drivers have been made. They are summarized as follows:

- **$\Delta V$  and Orbits:** Desired orbital insertion and the subsequent  $\Delta V$  requirement is determined by GNC and the spacecraft's  $\Delta V$  availability is determined by Propulsion. Only vehicles that meet these requirements can be considered for primary payload launches. Mission planning will determine if considered launch vehicles are capable of meeting orbital needs of primary payloads
- **Reliability:** This is important to keep in mind in launch vehicle selection, as a launch failure would present a mission-critical obstacle.
- **Readiness:** Some launch vehicle options, especially the Artemis Program ones available for rideshares, are mostly in early stages of operation or are still under development. Launch timeline problems could arise if failures or delays occur in the introduction of the launch vehicle, further delaying subsequent launches.
- **Volume and Mass of Secondary Payloads:** Though the decision was made to use at least one primary payload launch, restrictions must still be met for subsequent secondary payload launches for PACK-C/E. Restrictions are also important for the sale of available additional space on primary payload launches. Exceeding mass and volume allocations on the Artemis rideshare will require more than one primary payload launch and prevent the use of Artemis launches as backup in case PACK-C/E suffer a mission-critical failure. Additionally, volume and mass allowances are also determined by support of power and propulsion during in-space operations.
- **Cost:** Though the decision was made to use at least one primary payload launch, cost is still considered in the decision making. Though it provides more flexibility, the use of launch vehicles other than an Artemis Program-related rideshare dramatically increases the cost of the mission.



## 5.6 Subsystem Design Approach

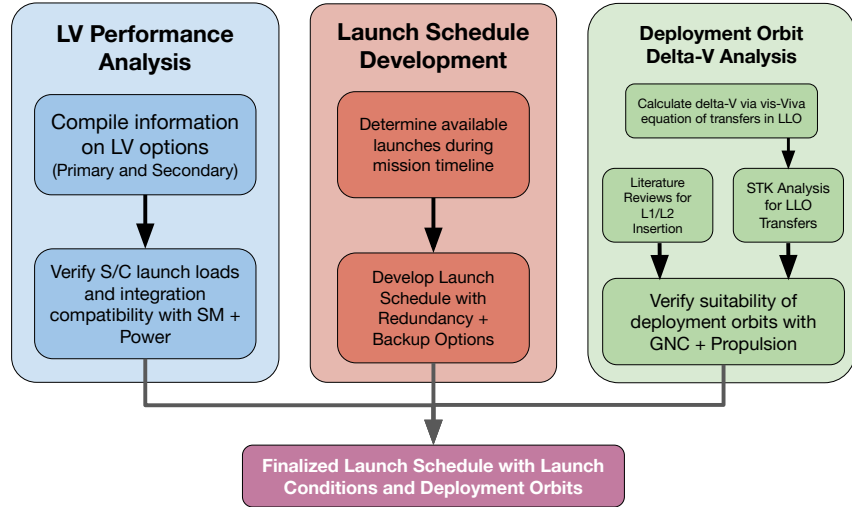


Figure 8: Overview of Cumulative LV Subsystem Design Process

The redimensioning of HOWLL and WOOF as 27U, 54 kg spacecraft and PACK-C/E as 12U, 24 kg spacecraft were the final changes that reprioritized the metrics were examined in deciding between various launch vehicle options. As such, the launch vehicle team's priorities have shifted to ensuring more rigorous analysis of the subsystem's compliance with requirements and conducting analyses that minimize the risks and uncertainties associated with the selected launch vehicles.

The mission-critical nature of launch vehicle failures and severe launch delays is what motivated the LV team to examine backup and alternative launch options. On top of this, a major system failure of an ARGOS satellite would also necessitate the use of additional launch vehicles to carry the replacement satellite to a deployment orbit that would provide enough of a boost for the spacecraft to maneuver itself into the orbit intended for mission operations. The added redundancy of a backup launch is particularly important due to the reduction of PACK satellite numbers from four to two during the PDR design cycle, which would mean a more severe drop in capacity from the loss of one satellite. This is further compounded by the fact that the original mission architecture had two satellites in each orbit, meaning that the observational capabilities provided by that orbit would still be maintained at a lower capacity, meaning that there was built-in redundancy into the core mission architecture.

The lower mass and volume of the PACK-C/E satellites placed strict limitations on the propellant available for spacecraft orbital maneuvers, but allowed their placement as rideshare payloads on NASA Artemis missions at no additional cost to the ARGOS budget and in orbits much closer to the final desired mission orbit. At the same time, this exposed the two satellites to the risks involved in using the Blue Ghost lander and Starship Human Landing System (HLS) as orbital transfer vehicles to Lunar orbit. Both have yet to prove their success in Cislunar operations, and Starship HLS' development has been set at a particularly ambitious timeline that is 13 months shorter than the average major NASA project, creating significant potential for delays [28] [29].



Despite these shortcomings, the combination of these two options allows the quickest completion of the ARGOS mission architecture while minimizing onboard  $\Delta V$  requirements. Therefore, alternative launch options in the case of delays or cancellations and backup options in the case of launch failures were examined with regard to compliance for both.

To ensure the deployment of PACK satellites into a Lunar orbit similar to the one already proposed for the spacecraft deployment orbit, the launch vehicle team considered only Artemis-related Lunar lander missions that offered deployment opportunities in Lunar orbit prior to their landing attempt. Uncertainties regarding the exact lander used for upcoming missions meant that the information on a range of options was considered, with the PACK satellites verified for compliance with specified requirements. The best options out of the CLPS lander options for PACK-C/E were evaluated based on their impacts on spacecraft  $\Delta V$  consumption for mission orbit insertion maneuvers.

The use of the Falcon 9 greatly mitigates launch related risks for HOWLL and WOOF, as the launch vehicle offers a 99.2% success rate [30]. However, the reliance on HOWLL for the communication relay architecture and the importance of WOOF in fulfilling critical tracking and communication objectives in L2 means that the ability to launch a replacement option was also considered. On account of the additional \$67 million required for launching another Falcon 9 backup, opportunities for reducing the launch costs for ARGOS were examined by calculating the costs that could be taken on by potential ridesharing spacecraft customers and the market demand for such a launch [31]. Alternative launch options were also considered in 5.7.2 and their launch capacity assessed according to publicly available payload capacity calculators, but the Falcon 9 ultimately proved to be the lowest risk option.

Subsequent analysis focused on evaluating whether the already selected launch vehicle options remained viable despite concerns that were discussed over the past design cycle, and evaluating the ability of the spacecraft to endure any launch-related environmental conditions that had not received detailed analysis up to this point. This meant an examination of the 7-day minimum separation requirement for Falcon 9 rideshare vehicles, acceptable minimum distances from other Cislunar objects during spacecraft deployment, and an assessment of depressurization effects during launch.

Analysis was attempted to verify that deployment of HOWLL at L2 and transfer to L1 is more  $\Delta V$  efficient than a deployment directly at L1 which was previously concluded with literature review. This analysis was attempted by following an STK tutorial for a mission to Sun-Earth L1 and changing the target points and central bodies, however geometry for the Lagrange points would not configure and the program would crash after the addition of the maneuver to the respective Lagrange point in the target sequence. The range of values provided in the PDR for direct transfer to L1, direct transfer to L2 halo, and transfer to L2 Halo via lunar flyby were deemed sufficient in confirming the choice of deployment of HOWLL and WOOF via a Lunar flyby trajectory.

The analysis conducted for the Launch Vehicle subsystem confirms that the subsystem meets all of its ORC. The launch vehicle selection and timeline accommodates the mass, volume, and integration needs of HOWLL, WOOF, and PACK and enables operations to commence by the deadline for initial operations in 2027, and enables complete operations by the 2029 deadline. The launch vehicle selection also helped minimize the  $\Delta V$  requirements as much as possible for the onboard propulsion system. Additionally, the cost, reliability, and readiness of the launch vehicle options



were assessed and balanced in their selection to minimize overall mission risks. Furthermore, a wide range of environmental loads during launch and transit have been characterized as listed in Table 119, and the subsequent analysis and design conducted by the SM, Mechanisms, and Thermal teams have ensured the ability of the spacecraft to endure launch.

## 5.7 Formal Analysis

### 5.7.1 Design Overview

HOWLL and WOOF are launched by a SpaceX Falcon 9 Block 5 from Cape Canaveral Air Force Station in Florida. This launch is anticipated to take place first, as HOWLL and WOOF are the two satellites equipped to relay data between the PACK-C/E satellite and the NSN on Earth. This means that the launch will be scheduled for 2026 before the scheduled launch of PACK-C. The specific launch date will have greater flexibility as HOWLL and WOOF are the primary payload and not on an Artemis Program rideshare, so the launch schedule can be better adjusted to ARGOS mission needs while avoiding the risk of delays commonly encountered by a program with as ambitious a scope as Artemis [28].

The Falcon 9 initially enters a circular, 200 km altitude Earth parking orbit. The orbit is at an  $28.5^\circ$  inclination to achieve the maximum boost in velocity possible from the rotation of the Earth for the launch site at Cape Canaveral, which is followed by a Trans-Lunar Injection (TLI) burn that increases the characteristic energy,  $C_3$ , to the  $-1.5 \text{ km}^2/\text{s}^2$  of TLI [32]. Once HOWLL and WOOF are separated from the second stage upon completion of the burn, they will be on a trajectory to flyby the Moon and conduct maneuvers at perilune: this thus enables the spacecraft to take advantage of a gravitational assist and the Oberth Effect to minimize onboard  $\Delta V$  requirements [33].

PACK-C is launched as a payload onboard the Blue Ghost 2 mission, a part of the Commercial Lunar Payload Services (CLPS). As a 12U secondary payload, PACK-C's use of an Artemis Program-associated launch vehicle means that the satellite can be deployed without increasing mission costs per the RFP [1]. The spacecraft and its dispenser are placed below the Blue Ghost spacecraft's bottom deck, where a  $69 \times 45 \times 45 \text{ cm}$  volume with a 50 kg mass limit is provisioned for attaching larger payloads such as scientific instruments, rovers, or CubeSat dispensers [34]. The space provides considerable margin for the  $45.4 \times 27.1 \times 26.3 \text{ cm}$  dispenser and 29.1 kg combined mass of the satellite and dispenser [34]. Alternatively, the dispenser can be mounted to the Elytra Dark Transfer Vehicle, which serves as the transfer vehicle for the Blue Ghost 2 lander [35]. While mounting the satellite to Elytra is not considered as the primary option because of the comparative lack of public information regarding the available attachment spaces, it may be reconsidered as more information is made available in the process of reserving a space on the spacecraft; the appeal is the potential flexibility that would be provided by the maneuvering capabilities of the Elytra.

The Blue Ghost lander is launched with PACK-C onboard into a TLI by a Falcon 9 Block 5 at some point in 2026. The Blue Ghost 2 mission will then enter Lunar orbit prior to attempting a landing on the Moon, providing an opportunity to deploy satellite secondary payloads. A  $673 \times 2000 \text{ km}$  altitude orbit is the intended deployment orbit for PACK-C. The Lunar Pathfinder mission that is already scheduled to be a rideshare payload on Blue Ghost 2 will have a  $673 \times 7331 \text{ km}$  orbit [36]. With this in mind, the Blue Ghost 2 mission architecture can be adapted to accommodate PACK-C with relatively little disruption, as an apolune-reducing burn will be the only added



maneuver needed after Lunar Pathfinder is deployed and the before the orbit is further reduced in preparation for Blue Ghost's Lunar landing. The relatively high perilune of the deployment orbit is key to minimizing PACK-C's onboard  $\Delta V$  requirements, as less  $\Delta V$  is necessary for the circularization burn needed for the 2000 km altitude orbit required for mission operations.

Starship HLS will carry PACK-E as a secondary payload as part of Artemis IV in September 2028 [37]. Though no public information regarding launch opportunities or a Payload User's Guide have been released for the Artemis IV Starship HLS, one of the NASA Goddard Space Flight Center panelists for the Team ARGOS FDR indicated that such an opportunity was being planned. Such an opportunity would also be consistent with the ridesharing opportunities offered on Artemis I and II and supported by the massive cargo mass and volume capacities offered by Starship HLS [38] [39]. Deployment for PACK-E would take place at a 200 x 3495 km altitude orbit following Starship HLS' departure from the Lunar Gateway as Starship HLS makes maneuvers in preparation for landing on the Moon [40]. The 3495 km apolune will be that of the final mission orbit, but the 200 km altitude perilune has been selected because of the need for Starship to minimize its orbit in preparation for landing on the Moon.

### 5.7.2 Primary Launch Vehicle Selection Overview

The Falcon 9 was selected from a wide range of launch vehicle options that will be available in 2026 to launch the HOWLL and WOOF satellites, which are too large to use free rideshare launches. Not included in this analysis were the range of operational Russian and Chinese launch vehicles that would be physically able to deliver HOWLL and WOOF to a TLI, as U.S. entities are barred from using launch vehicles from either country [41][42][43]. More generally, U.S. commercial satellite owners are allowed to launch using foreign launch vehicles, but U.S. government satellites are mandated to launch on American launch vehicles [44].

Several launch vehicles were eliminated on a case-by-case basis, generally with regard to the lack of information available for analyzing compliance with the assessment criteria:

1. H3: A Japanese launch vehicle, its lack of a Payload User's Guide made it impossible to obtain information that would be useful for the SM and Power subteams to assess whether the spacecraft was compatible with the rocket's launch environmental load and integration specifications [45].
2. GSLV and LVM3: These Indian launch vehicles also lack a Payload User's Guide for detailed loading and integration specifications.
3. Vulcan Centaur: While it demonstrated the ability to launch payloads to TLI on its debut launch, that launch has been its only launch to date, limiting the ability to assess its reliability [46].
4. Other launch vehicles capable of delivering payloads to TLI have yet to launch, which limits the information available about their reliability.

This limited the launch vehicles in consideration to the Falcon 9, Falcon Heavy, Polar Satellite Launch Vehicle-XL (PSLV-XL), and Electron with the Photon Kick Stage. These were evaluated along the criteria in Table 28 in order to downselect launch options. A three-color scale is used with green signifying that the launch vehicle meets ARGOS mission architecture needs without



qualification, yellow indicating that needs are generally met but with greater risk, and red indicating that needs are not met:

Table 28: Comparison of Primary LV Launch Options

LV	Mass to TLI (kg)	Export Controls	Information	Reliability	Cost
Falcon 9 Block 5 RLTS	2708 kg (2082-3398 kg 95% confidence margin) [47]	U.S. Manufactured [48]	Up-to-date User's Guide for Primary and Rideshares [48]	274/274 (Block 5) 328/331 (Falcon 9) [30]	\$67 million [31]
Falcon Heavy (Side Booster RTLS, Core ASDS)	11922 kg (10007-14124 kg 95% confidence margin) [47]	U.S. Manufactured [48]	Up-to-date User's Guide for Primary and Rideshares [48]	9/9 [30]	\$97 million [31]
PSLV-XL	593 kg (208-1034 kg 95% confidence margin) [47]	Export waivers acquired for U.S. companies [43]	User's Guide for older PSLV variant [49]	24/25 (PSLV-XL) 57/60 (All PSLV) [30]	\$31 million [30]
Electron with Photon Kick Stage	(28-57 kg 95% confidence margin) [47]	U.S. Manufactured [50]	Up-to-date User's Guide and Photon Information [50] [51]	1/1 (Variant) 43/47 (Total) [30]	\$11.9 million [52] [53]

The Mass to TLI is evaluated with the Silverbird Astronautics calculator [47]. A 200 km parking orbit is assumed for all launch vehicles with a final C3 of  $-1.5 \text{ km}^2/\text{s}^2$ . With the Silverbird Astronautics calculator, the following assumptions are made: a declination equivalent to that of the launch site latitude, a two-burn trajectory, the more precise GCS shutdown mode, a mix of raw data and data derived from the User's Guide, and an upper stage disposal when possible. The only exception to this was Electron, where an optimal trajectory and 165 km parking orbit was used to follow the precedent of the Lunar-bound CAPSTONE mission carried by the Electron, which used multiple orbit raising maneuvers by the kick stage before the final TLI [50] [51].

The comparison of factors reaffirms the use of the Falcon 9 for the primary payload launch of HOWLL and WOOF and a potential backup launch in the case that either spacecraft fails before the conclusion of the mission. All of the assessed criteria are met, ensuring that the Falcon 9 can deliver HOWLL and WOOF to TLI with approval from U.S. regulators and a high degree of confidence in reliability. PSLV-XL does cost roughly half of the Falcon 9, but it is ultimately affected by the risk involved in obtaining an International Traffic in Arms Regulations (ITAR) waiver, while it is uncertain that Electron has the performance necessary to deliver the combined mass of either HOWLL or WOOF along with their respective dispensers to TLI (43.75 kg) [43]. For more details on the comparison between PSLV-XL and Falcon 9, Figure 71 provides further details. Compared to Falcon Heavy, Falcon 9 is more affordable and has a stronger flight heritage [31].

The Falcon 9's lift capability far exceeds the needs for launching only HOWLL and WOOF to the Moon, and thus the use of the lower-capacity first stage recovery option of a Return to Launch Site (RTLS) will be assumed. However, this may be adjusted to a landing on an Autonomous Spaceport Drone Ship (ASDS) if there is especially high demand for rideshare payloads. An assessment of ridesharing potential is further explored in (5.7.3).



### 5.7.3 Secondary Launch Vehicle Selection Overview

The RFP specifies that only one 12U spacecraft is able to launch each year for free as a secondary payload on an Artemis Program related launch. Given the time required to fabricate, test, and qualify the spacecraft, not to mention the time required to negotiate a ridesharing deal, it is unlikely that either of the PACK satellites are able to launch in 2025. Additionally, the two satellites will have limited utility without HOWLL, meaning there is little use in considering launches available even earlier. While the selected options are discussed in further detail below, the Figure<sup>69</sup> provides a comparison of a wider set of secondary payload options in early parts of subsystem development.

The Blue Ghost 2 mission currently offers additional payload capacity for deploying satellites in Lunar orbit in 2026 [35]. When considering the current mission timeline, this provides sufficient time to prepare PACK-C for launch while ensuring that a significant portion of ARGOS mission architecture is established early on. Additionally, the Lunar Pathfinder's orbit properties were particularly favorable to accommodating PACK-C, meaning that the spacecraft could be added to the Blue Ghost 2 mission without significant disruption [36]. While other missions contracted under the CLPS are planned after Blue Ghost 2, the lack of downselection regarding the lander for the missions makes them more difficult to plan for.

Figure 70 indicates the lack of Artemis Program launches in 2027 with a selected launch and transit vehicle means that the Artemis IV Starship HLS launch becomes the next preferred option for launching PACK-E [37]. An SLS Block 1B as another launch option is also involved in the Artemis IV mission architecture, but with deployment limited to TLI as noted in 69, that option would increase spacecraft  $\Delta V$  requirements considerably [54]. The Blue Moon HLS on New Glenn is also scheduled for its first uncrewed test in 2028, but this option is eliminated on the basis that neither the lander nor launch vehicle have been tested, introducing a greater degree of uncertainty regarding reliability [37].

### 5.7.4 Backup Launches

For HOWLL and WOOF, which are planned to launch on a Falcon 9 in 2026, alternative and replacement options involve an additional primary payload launch by contracting a Falcon 9. The contract could be signed a mere 8 months in advance for this launch, which is a short enough time frame for the replacement launch to be planned between the failure of the originally planned launch in 2026 and the deadline for beginning in-space operations in 2030 [55]. The launch vehicle has a 99.2% success rate, so it is unlikely that the launch will be needed due to the failure of the original Falcon 9 launch [30]. The replacement launch would more likely be used in the event of either HOWLL or PACK suffering a mission-critical failure.

The cost of this replacement launch would cost an additional \$67 million on top of the \$67 million of the original launch, however a significant portion could be recouped by selling available space to other payloads bound for a TLI trajectory. The effective payload capacity will be reduced by the adapters needed to mount additional payloads. However, the reduction will be proportionally small: a MOOG Evolved Secondary Payload Adapter (ESPA) that could support 6 satellites of 450 kg each for a total of 2,700 kg would only amass 136 kg [24]. Coupled with the mass of HOWLL and WOOF, there would still be over 2,400 kg of capacity remaining for a Falcon 9 RTLS launch. Based on the current SpaceX rideshare rate, \$6,000/kg to a Sun Synchronous Orbit (SSO), at least



\$14.4 million could be regained [56]. Given that the Falcon 9 RTLS generally delivers around 5,000 kg to SSO and the relative difficulty of delivering spacecraft to TLI, it would also be reasonable to double prices to \$12,000/kg to recoup around \$30 million [57]. Particularly high demand could enable the use of a Falcon 9 ASDS with its capacity to TLI of around 3,700 kg [47].

Another possibility is for HOWLL and WOOF replacements to be launched as secondary payloads themselves. Astrobotic offers delivery at \$300,000/kg directly to the more ΔV intensive Lunar orbit [58]. Even at this price point, one that is likely to be significantly higher than the price point for delivery to TLI, it would only cost around \$13.1 million to deliver the 43.75 kg satellite-dispenser combination for each satellite. Intuitive Machines' Nova-C lander is stacked on an ESPA ring that can support up to 1000 kg of payload as excess launch capacity, which would be more than enough to accommodate the satellite, dispenser, and potential interfaces to attach the dispenser to the ESPA ring's port [59]. The primary drawback for Nova-C is the 20 month timeline from contract to launch, which could push the launch of the replacement into 2028 [59]. iSpace's Hakuto-R lander appears to offer similar capabilities, having carried NASA's Lunar Flashlight as a rideshare to a Lunar transfer trajectory [60]. It should be noted that it was only a 6U CubeSat, requiring only around 22% of the volume of HOWLL and WOOF. While being a secondary rideshare customer will make the launch of the replacements dependent on the timeline of the primary payload, this could significantly reduce launch costs even if they cannot launch for free as with payloads on Artemis Program missions that are in accordance with the RFP guidelines.

Cost is not one of the main priorities of the LV subsystem ORC given the significant cost margin of the mission, but it is still important to consider and to keep to a minimum. Though the need to replace HOWLL and WOOF would be a huge hurdle in the completion of the mission architecture, ridesharing provides a promising pathway to minimizing the impact of launch vehicle price on achieving compliance with mission requirements.

Alternative and replacement options for PACK-C and E involve launches as secondary payloads on Artemis Program missions. Launching PACK satellites on one of eleven NASA CLPS missions between 2027 and 2029 – three in 2027, two in 2028, and six in 2029 – provide extensive options for several situations that would require their use [37]. Depending on the lead time required, all of them could potentially be used to replace PACK-C in the case of a launch or Blue Ghost failure, or a spacecraft failure soon after deployment. If complications with deploying PACK-E from a human spaceflight mission arise, Starship HLS and Artemis IV face delays that threaten their ability to launch by the end of 2029, or if secondary payload deployment on Starship HLS is ultimately not offered, the multiple CLPS missions from 2027 to 2029 provide promising alternative options.

Table 29: Comparison of Secondary Payload Launch Options

Lander	Peregrine [58]	Griffin [58]	Blue Ghost [34]	Nova-C [59]	APEX 1.0 [61]
Mass	70-100 kg to surface	625 kg to surface	50 kg (Option 4)	650 kg (200 km) 715 kg (2000 km)	300 kg to surface
Volume / Attachment Area	0.2-0.5 m <sup>2</sup> (per deck)	0.2-0.5 m <sup>2</sup> (per deck)	69 x 45 x 65 cm for (Option 4)	10 m <sup>2</sup>	TBD
Power (in transit)	22.95 W	22.95 W	270 W (total)	200 W (total)	TBD
Interface	Requires proven release mechanism design	Requires proven release mechanism design	Proprietary and standard deployment mechanisms	Cubesat deployment mechanisms	TBD
Communications	229.5 kbps	229.5 kbps	2 kbps	4 Mbps on surface	TBD
Deploy in Orbit	Yes	Yes	Yes	Yes	Yes

The landers that will be used on the missions have not been announced, however, making it difficult to plan for a particular CLPS launch. The possible landers are the Astrobotic Peregrine or Griffin, Firefly Blue Ghost, Intuitive Machines Nova-C, and Draper APEX 1.0 [62]. The comparison table above suggests that the CLPS options satisfactorily meet the key metrics to ensure that PACK-C/E can be attached to the landers and deployed in Lunar orbit without modification. The only exception is APEX 1.0, for which information on most metrics remains unavailable. However, the fact that the other landers do meet the requirements suggest that APEX 1.0 will be competitive given its need to compete for the same CLPS contracts. Even if APEX 1.0 does not accommodate ridesharing for PACK-C/E, the 11 mission opportunities and the availability of other landers suggests that there will be a number of other missions that can still accommodate the role of the backup launch. Out of the available options, Nova-C is ideal for a PACK-C backup launch, as the lander initially enters a circular 2000 km orbit as part of the standard mission profile [59]. As such, PACK-C can be deployed directly into its mission orbit.

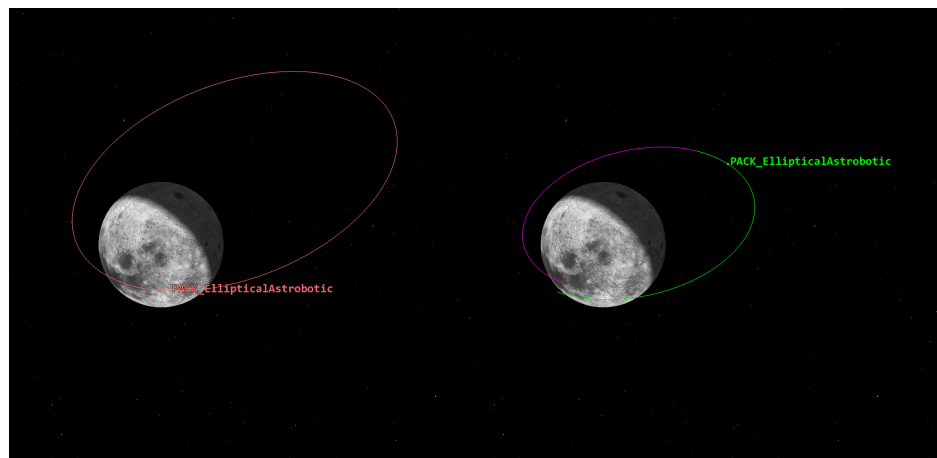


Figure 9: Astrobotic Deployment Orbit (Left) and Maneuvers to Enter Mission Orbit (Right)

The Astrobotic Peregrine and Griffin landers are assessed to be the best suited for deploying PACK-E, as they initially enter a 100 x 8700 km altitude Lunar orbit with nonstandard payload



deployment upon request [58]. This highly-elliptical orbit reduces the  $\Delta V$  requirements to enter the final  $505 \times 3495$  km altitude mission orbit. STK Astrogator analysis reveals that a burn at periapsis to enter a  $100 \times 3495$  km orbit and then a burn at apoapsis to enter the final mission orbit requires a total of 191.9 m/s of  $\Delta V$ , compared to 131 and 96.4m/s of  $\Delta V$  for PACK-C/E in the primary ARGOS mission architecture. The addition of an intermediate  $100 \times 3495$  km orbit as the Astrobotic lander gradually reduces their apoapsis would reduce PACK-E's insertion  $\Delta V$  requirements to only 49.1 m/s. Less  $\Delta V$  used for orbital insertion means more  $\Delta V$  available for stationkeeping, extending the spacecraft's operational lifetime.

### 5.7.5 Further Launch Vehicle Compliance

A few additional areas of concern are regarding the launch vehicles and their trajectory profiles are examined in further detail to assess methods for mitigation or to better understand the degree of risk involved.

The Falcon 9 Rideshare Payload User's Guide specifies that payloads must not conduct propulsive maneuvers for seven days after deployment. At first glance, this is a source of potential concern because the transfer time from Earth to an L2 Halo orbit is 8.35 days, and a Lunar flyby maneuver must take place before arrival at L2, likely within the seven day limit [33]. However, the specification is not anticipated to be a concern for HOWLL and WOOF. This restriction exists primarily to allow the 18th Space Defense Squadron (18 SDS) time to catalog the deployed rideshare spacecraft [55]. This is particularly critical in Earth orbit, where there are over 47,000 human-made objects that the 18 SDS is responsible for tracking. With far fewer objects in Lunar orbit, that challenge of tracking objects is greatly reduced, and thus the possibility that an exception can be granted is more feasible [63]. If that is not in play, however, launching HOWLL and WOOF alone will circumvent the issue, as the requirement only exists for SpaceX Transporter-style missions with many payloads. While launch costs cannot be recouped, it will ensure that a key regulatory hurdle can be avoided.

The GNC subsystem team conducted analysis on collision risks with existing space objects around the Moon from August 2027 to April 2030 using STK's Advanced CAT tool. The LV team built upon this analysis further by applying the GNC team's analysis, whose methodology is discussed in further detail in Section 6.7.3, to the PACK-C/E deployment orbits. For the deployment orbits of both PACK-C and PACK-E, neither the Tier 1 tracking objects nor the other ARGOS mission spacecraft came within 10 km of the spacecraft within the deployment orbit from April 2026 to April 2037, indicating that there is no major risk of a collision with existing spacecraft. As the LV-F-010 requirement that pertains most closely to this analysis only covers Cislunar objects, the object environment of HOWLL and WOOF are not examined at deployment, as that takes place much closer to Earth.



## 6 GNC Design

### 6.1 Subsystem Overview

The Guidance, Navigation, and Control (GNC) team is tasked with researching, analyzing, and determining the desired trajectories and orbits that best suit the mission. For this mission, the GNC team is in charge of finding optimal orbits for the mission satellites HOWLL (Homing Orbital Waypoint L1-Linkage), WOOF (Wide-range Orbital Operations Facilitator), and PACK (Pathfinding Array for Cislunar Kinematics).

In the case of the ARGOS (Advanced Relay for Geolunar Operational Support) mission, orbits will be chosen to enhance the Cislunar communication network and track objects listed in the Tier 1 Object Catalog [4]. Some of the considerations that go into the decisions of the orbits for PACK, HOWLL, and WOOF are stability, access to Tier 1 objects for tracking, access to other Earth and Cislunar architecture for communication, and required deltaV for satellites' life-cycle. The GNC team will also have to ensure that this mission does not present a hazard to any current or future missions by performing collision risk assessments. Additionally, to make sure the ARGOS program does not add to the amount of space debris and crowd Cislunar space, at the end of its mission, the team will plan decommissioning trajectories that will safely take the satellites out of their mission orbits and ensure the debris does not continue in operational orbits. A more detailed explanation of these satellites and their chosen trajectories are restated in Section 6.6 of this report.

Because the GNC team is essentially determining the entire mission trajectory, it is heavily interconnected with many of the other subteams. The GNC team will have to work in close conjunction with the Launch Vehicle and Propulsion teams to minimize deltaV expenditure and ensure the chosen orbits are feasible with the propulsion tank mass and volume allocation. Depending on what orbits the GNC team chooses, this will also heavily affect the Thermal and Power teams. The Thermal team will need to ensure they can protect the satellites from wildly varying Cislunar temperatures, and the Power team will need to ensure their chosen architecture can store enough power to make it through longer ranges of eclipse times. Additionally, to successfully maintain the desired orbits for the lifetime of the mission, the GNC team will need to work with the Communications teams to make sure their chosen orbits allow for an enhanced communication network and ensure there is enough relay from the satellites to Earth on their current positions so any adjustments can be made if necessary.

### 6.2 Subsystem Objectives

The objectives for the GNC team have mainly stayed the same since the PDR subteam report [12]. The objectives derived from the tertiary mission objective will no longer be included since the ARGOS mission will prioritize only the first two RFP objectives. The objectives are included below for the completeness of the report.

#### GNC Objectives derived from the Primary RFP Objective: Tracking

- Determine suitable orbits for satellites to track Cislunar objects defined in the Tier 1 Object category.
- Determine orbits that can be feasibly reached with Launch Vehicle and insertion deltaV constraints.



- Maintain the chosen orbits through correction or station-keeping maneuvers throughout the mission lifetime.
- Have navigation capabilities to avoid hazardous or non-active space objects.
- Perform collision risk assessments to ensure chosen orbits for mission do not present a hazard to current and future missions.

#### GNC Objectives derived from the Secondary RFP Objective: Communication

- Ensure the satellites have proper reach and secure seamless communication network across Cislunar space.
- Choose orbits with eclipse times in mind to ensure communication between satellites is consistent, accessible, and frequent throughout the mission lifetime.
- Ensure the chosen orbits allow for accessible communication with Earth-based resources from Lunar-based assets.

#### Additional GNC objectives:

- Choose orbits with good stability to minimize deltaV expenditure (trajectory and station-keeping burns) and elongate the lifetime of the satellites while still meeting the mission requirements.
- Determine an end-of-life trajectory for all satellites in the mission architecture so ARGOS satellites do not become hazardous debris in active Cislunar orbits once they are no longer operational.

### 6.3 Subsystem Requirements

The requirements have mainly stayed the same since the PDR report. The only requirements updated with actual values are GNC-F-005 and GNC-F-006 for station-keeping and GNC-P-002 for collision risk assessment through conjunction analysis (CA). The complete list of requirements can be found in the "GNC" tab of the "Requirements Spread-sheet" Google Sheet [6].

These requirements can be categorized into five different objectives. Table 30 below summarizes the grouping of these requirements. The first column contains the requirement ID. As they all start with "GNC-", this part of the ID was excluded for brevity. The second column provides a high-level description of the category, and the third column identifies the objective the requirement intends to satisfy.



Req. ID (GNC ###)	Description	Objective Category
F-001 - F-004, P-001, P-003 - P-005,	The GNC team shall plan trajectories that allow ARGOS satellites to be placed in compliance with the mission level timeline requirements	Mission Timeline Compliance
F-008, P-006 - P-011	The GNC team shall choose orbits that allow for the Tier 1 Tracking Requirements to be met	Tracking
F-009, F-010	The GNC team shall choose orbits that provide an enhanced communication network in Cislunar Space	Communication
C-001 - C-004	The GNC team shall choose orbits that minimize delta-V expenditure as to comply with mass and volume constraints for fuel	DeltaV
F-005 - F-007, F-011, F-012, P-002, E-001	The GNC team will perform station-keeping and other correction maneuvers to maintain the desired mission trajectories and will ensure that no further space debris is created (CA, EOL, etc.)	Sustainability of Mission and Cislunar Domain

Table 30: GNC Subsystem Requirements

## 6.4 Subsystem Constraints

The GNC subsystem constraints are difficulties the GNC team faces in achieving the objectives listed in the [6.2](#) section. The only change that has been made since the previous iteration is that the constraint for reliability has been removed since while a challenge, it does not necessarily pose a constraint on the GNC team. The remaining constraints are both derived from the overall mission and GNC-focused, and an organized overview is as follows:

- **Launch Constraints:** The choice of the launch vehicle will dictate the options for the launch date and the initial trajectory planning needed to transition the mission's payload toward the desired orbits.
- **Satellite Deployment Constraints:** The deployment point of each satellite impacts the GNC trajectories and navigation towards the desired orbits.
- **Fuel and Power Constraints:** The total fuel and power available for maneuvers and station-keeping are fundamental constraints. These limitations dictate the feasibility of reaching and maintaining the desired orbits.
- **Communication and Tracking Constraints:** The systems' communication capabilities will limit the placement of satellites as necessary for the efficient operation of the full communication network, a primary objective of the ARGOS mission. Similarly, the sensors determined by the payload subsystem impact GNC's decision on satellite orbit placement to ensure that all objects that need to be tracked are reachable.
- **Interference and Compatibility Constraints:** Ensuring compatibility with other Cislunar missions and avoiding interference with existing satellites and debris requires precise orbit selection and constant monitoring for collision avoidance.



## 6.5 Subsystem Drivers

The GNC subsystem drivers have mainly stayed the same since the last report. The focus centers on deltaV expenditure, continuous object tracking, compliance with the mission timeline, and simplicity. A sub-driver for end of life was added under the deltaV expenditure driver since this was a large component of the deltaV literature analysis.

### DeltaV Expenditure:

- *Transfer to Orbit*: Ensuring precise satellite deployment into designated orbits to minimize fuel use and optimize trajectory for reduced DeltaV.
- *Station-Keeping/Stability of Orbit*: Maintaining satellites in stable orbits with minimal energy, emphasized by recent research and simulations of Cislunar space dynamics.
- *End of Life*: Planning decommissioning trajectories for satellites after end of operations to alleviate concerns about increasing amount of traffic and debris in Cislunar space.

### Continuous Tracking and Communication:

- *Tracking Ability*: Ensuring sufficient access times to objects and tracking abilities for monitoring objects to be tracked.
- *Communication Network*: Maintaining access between satellites in ARGOS architecture for sustained communication in complex Cislunar missions.
- *Eclipse Avoidance*: Focusing on maintaining continuous solar power and thermal management to prevent system disruptions (collaboration with the Power team, see analysis in Section 12)

### Mission Timeline:

- Adjustments to the timeline are crucial to align with launch windows, aiming for operational readiness by 2027 and full functionality by 2030.

### Simplicity:

- Given the complexities of Cislunar space and the Three-Body Problem, the GNC team prioritizes simplifying mission architecture by minimizing satellite numbers and trajectories and aiming for achievable orbits.

These mission drivers guide GNC's decisions on orbit placement for the HOWLL, WOOF, and PACK satellites. DeltaV remains the largest expenditure, significantly influencing the ARGOS mission's mass budget.

## 6.6 Subsystem Design Approach

To reiterate the decided GNC design in detail, the following orbits were chosen for the four ARGOS satellites:

- HOWLL: 27U satellite in a Northern L1 Halo orbit
- WOOF: 27U satellite in a Southern L2 Halo orbit



- PACK-C: 12U satellite in a circular frozen lunar orbit
- PACK-E: 12U satellite in an elliptical frozen lunar orbit

The orbital parameters of each satellite can be found in Tables 31 and 32 below. The reasons for choosing these orbits can be found in more detail in the GNC Appendix Section A.4.1.

Table 31: Orbital Parameters for PACK Satellites

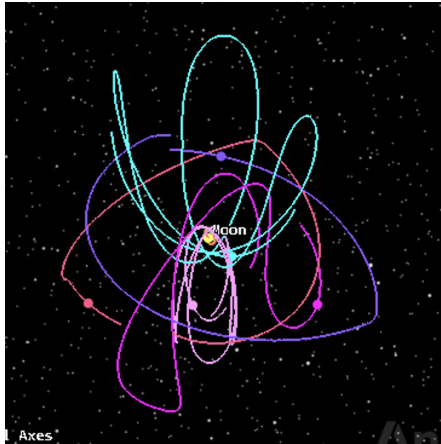
Satellite	Semimajor Axis	Eccentricity	Inclination	Argument of Perigee	RAAN
PACK-C	3737.4 km	0	50 deg	0 deg	0 deg
PACK-E	3737.4 km	0.4	135 deg	0 deg	0 deg

Table 32: Initial Conditions for HOWLL and WOOF in CR3BP

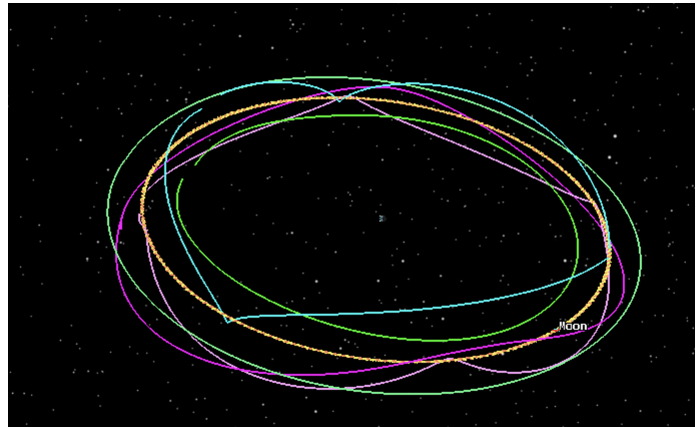
Satellite	X	Y	Z
HOWLL	0.8967003948	0	0.1993274947
WOOF	1.103326911	0	-0.1977059649
Satellite	vX	vY	vZ
HOWLL	0	0.1911749687	-3.17E-12
WOOF	0	-0.2178975724	0
Satellite	Jacobi Constant	Stability Index	Period (TU)
HOWLL	3.001771733	1.90931159	1.948571459
WOOF	3.019976114	7.640941065	2.681588563

The main goal of this final design report is to verify the requirements on the chosen orbit as much as possible through STK analysis. These requirements include access time, SNR, station keeping, conjunction analysis, eclipse times, and deltaV. Note that SNR is being analyzed by the Payload team, and eclipse times are being analyzed by the Power Team. Both these teams have verified that the orbits chosen by the GNC team will be suitable to meet their mission operations and requirements. There is only a small note for issues with SNR for the GTotoL2 object. Further detail on these two components can be found in Sections 9 and 12.

Using Professor Ryne Beeson's Pydylan software, the initial conditions for HOWLL and WOOF in CR3BP were solved for, corrected, and converted to the J2000 Earth Inertial Frame [64] [65]. These solutions were then exported as a bsp file, allowing all satellites (ARGOS and Tracking) to be simulated in one STK scenario as shown below in Figure 10.



(a) Moon Inertial Frame



(b) Earth Inertial Frame

Figure 10: ARGOS Satellites and Tier 1 Tracking Objects

Now that all satellites are in the same scenario, this report will continue access time verification, specifically for the objects that HOWLL and WOOF will be tracking. Additionally, access times can be analyzed between ARGOS satellites to ensure that access to HOWLL is sufficient for communication purposes.

STK simulation will also be used to perform conjunction analysis using STK's Advanced Conjunction Analysis Tool (AdvCAT) to ensure that the ARGOS architecture is not placed in a risky area in Cislunar space. The GNC team will also perform station-keeping and insertion simulation for the PACK satellites to attempt to verify the values from literature.

## 6.7 Formal Analysis

### 6.7.1 Access Times

Access time (AT) analysis has been done for HOWLL and WOOF since the last PDR since the trajectories of these two satellites were able to be converted to the J2000 Earth Inertial Frame [64] [65]. The satellites HOWLL and WOOF are both in charge of tracking are the L1, L2, GTOTOL1, and GTOTOL1 objects. In addition to these, WOOF is also in charge of tracking the Lunar Gateway (as this is particularly of concern when the Lunar Gateway is too far from the PACK satellites to track). It was found that, for an analysis of eight months, HOWLL and WOOF have constant access to all of the objects mentioned above. Additionally, since meeting the AT requirements was potentially a concern for the LLO-2 object, the access time from HOWLL and WOOF to the LLO-2 object were also calculated to serve as an additional method of redundancy to meet the access time requirements. The compilation of AT analysis can be found in Table 33 below, and the STK reports for the access times can be found in the GNC Appendix Section A.4.2.



	Required Monthly AT (days)	Monthly AT from PACK-C (days)	Monthly AT from PACK-E (days)	Monthly AT from HOWLL (days)	Monthly AT from WOOF (days)	Meets Requirements?
LLO-1	≥18 days	17.9198	19.8893			Yes
LLO-2	≥18 days	15.3211	14.4929	30.625	30.625	Yes*
LLO-3	≥18 days	17.9931	20.1078			Yes
LG	≥18 days	28.7264	28.7107		30.625	Yes
L1	≥15 days			30.625	30.625	Yes
L2	≥12 days			30.625	30.625	Yes
GTO to L1	≥15 days			30.625	30.625	Yes
GTO to L2	≥12 days			30.625	30.625	Yes

Table 33: Average Monthly Access Times

As one can see, all of the tracked objects' monthly AT requirements are met. For the most part, each object can meet its monthly access time requirements with just one of the ARGOS satellites. However, all objects will be designated to two different ARGOS satellites to add a form of redundancy. The \* in the second row simply is a note that PACK-C and PACK-E cannot meet the minimum monthly access times for LLO-2 on their own, but the superposition of these two satellites will allow for the AT requirements to be met. There is an additional requirement on the access times for these tracked objects for there to be a cumulative access time of three years over the mission lifetime. For the most part, this requirement is less demanding than the monthly AT requirements as since the mission will be operational for approximately 7-9 years, the cumulative AT demands that ARGOS satellites have access to the tracked objects for about 40% of the operation time. This requirement is more relaxed for the LLO and L1 tracked objects as their monthly AT requirements come out to demand about 60% and 50%, respectively. So, since the monthly AT requirement for these objects are satisfied, the cumulative AT requirement is also satisfied. However, for the L2 and GTOToL2 objects, which only require a minimum of 12 days out of the month, which comes out to be about 38% of operational time, it needs to be checked that the cumulative AT requirement can be met. In this case, the cumulative AT requirement has been met since HOWLL and WOOF have essentially constant access to these two objects. In summary, the GNC team has chosen orbits that satisfy all their AT requirements for the Tier 1 Object Catalog.

To ensure that the chosen orbits also allow for a strong Cislunar communication network, access times from HOWLL to WOOF and PACK were computed to ensure that any information coming from WOOF and PACK would be able to be reliably relayed from HOWLL to Earth. From this analysis (which can be found in the GNC Appendix Section A.4.2), HOWLL has constant access to WOOF, which is critical since the Communications Team depends on nearly constant access between these two satellites. HOWLL has access to PACK-C 93.7% of the time and access to PACK-E 89.3% of the time. This is sufficient for the ARGOS communication network. Note that all access times were taken over a series of multiple months, but as these months for all satellites produced essentially identical patterns between each month, these access times were generalized to the mission lifetime.



### 6.7.2 Station-Keeping

Station-keeping values were also desired to be simulated in STK. This was loosely done for the PACK satellites by simulating a target satellite using STK's TwoBody propagator and another "real" satellite using STK's higher fidelity HPOP propagator. Because the HPOP propagator includes perturbations from idealities, the "real" satellite slowly drifts from the target satellite over time. PACK-E perturbed from its desired orbit much faster than PACK-C did. As such, it was deemed that PACK-E needed a station-keeping maneuver every two weeks, and PACK-E needed a station-keeping maneuver every month. These station-keeping maneuvers were simulated by targeting the original Keplerian parameters of the target satellite. As such, since Keplerian elements cannot define HOWLL and WOOF, station-keeping simulation could not be done for these two satellites, and the deltaV values for station-keeping will remain from literature.

The station-keeping values were significantly higher than the literature values were suggesting and what was expected. The perturbations were very small, but this still led to extremely high deltaV values, especially for PACK-E. The simulation could not converge when all values for PACK-C were targeted at the same time, so the deltaV required for the PACK-C station-keeping was all done separately (i.e., one for eccentricity, one for inclination, one for RAAN, and one for semi-major axis). Since PACK-C is ideally a circular orbit, the change in Argument of Periapsis did not matter, and as such, a burn to correct this was not made. The perturbed parameters after one month for PACK-C and after two weeks for PACK-E can be found below in Table 34.

Table 34: PACK Satellite Target vs Perturbed

Satellite	Semimajor Axis	Eccentricity	Inclination	Argument of Perigee	RAAN
PACK-C Real After 1 Month	3737.05 km	0.000176	49.705 deg	356.354 deg	1.56328 deg
PACK-C Target	3737.4 km	0	50 deg	0 deg	0 deg
PACK-E Real After 2 Weeks	3737.24 km	0.399737	134.913 deg	2.19209 deg	4.2214 deg
PACK-E Target	3737.4 km	0.4	135 deg	0 deg	0 deg

The total deltaV for the PACK-C burns was 2.33 m/s. While this number seems reasonable, this is a value that would be required every month, producing a total required station-keeping deltaV of about 28 m/s per year, which is greater than the near 0 m/s per year expected from literature [66]. The simulation converged when the desired orbit for PACK-E was targeted, so a two burn maneuver was used to target all of them. This produced a significantly larger deltaV than expected, totaling about 32.83 m/s for both burns. This would result in a station-keeping requirement of about 400 m/s per year, which is far off from the literature on elliptical frozen orbits [67] where the orbit for PACK-E was found. It is noted, however, that this value is close to what is expected for a nominal elliptical lunar orbit [66] that does not exhibit frozen qualities. As such, the GNC team has conjectured that the gravity model of the Moon in STK does not account for the special "frozen" gravity gradients. This would also explain the much faster perturbation from the circular frozen orbit and higher deltaV values than expected for PACK-C. All maneuver summaries are in the GNC Appendix Section A.4.3.

Additionally, these burns may not have been optimal, especially since only one or two burns were performed to reach the correct orbital elements. It may be optimal to perform many tiny correction burns, but these multi-burn simulations did not converge since there were too many



control variables to trade over. In conclusion, because these values found in STK are not even in the same ballpark as those found in literature, it has been deemed that the STK simulations could not verify the literature values due to the potential low fidelity of the simulation and setup. Therefore, literature values will continue to be taken as the station-keeping values for the total deltaV estimate of the satellites.

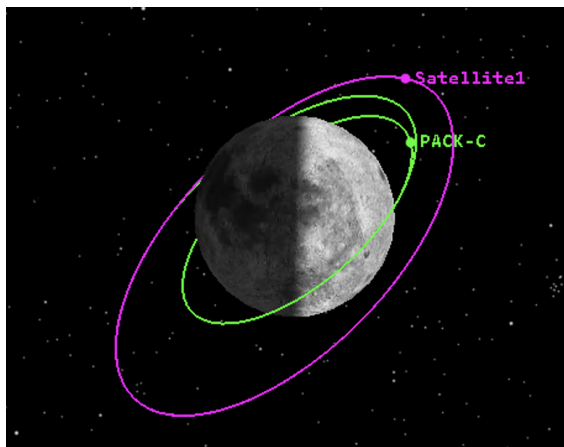
### 6.7.3 Conjunction Analysis

As part of the comprehensiveness of the ARGOS mission, the GNC team wanted to ensure that their chosen placement of the satellites would not infringe on the operations of other satellites and would not pose potential collision risks, especially with the increasing amount of space debris in the Cislunar domain. The GNC team used STK's Advanced Conjunction Analysis Tool (AdvCAT) to check for collisions and potential close approaches between ARGOS satellites and the Tier 1 Objects. A sphere of 10km in radius was put around every satellite and object to provide ample security and margin in the close approach analysis. Throughout the analysis (three years), there were no collisions and no close approaches. It was then taken to be generalized that there are no potential collisions over the operational lifetimes of the ARGOS satellites with each other or with the Tier 1 Objects. As such, the GNC team has successfully chosen "safe" orbits for the mission architecture that will pose no threats to each other, the Lunar Gateway, or the other tracked objects. The AdvCAT reports are in the GNC Appendix Section [A.4.4](#).

### 6.7.4 DeltaV Verification

The incorrect deployment orbit for PACK-E was calculated in the last GNC reports. The previous reports used a 505x2000km drop-off point, but the LV team recently clarified that the deployment orbit for PACK-E will be a 200x3495km orbit [15]. This is a smaller orbit that matches the apoapsis radius of PACK-E. Therefore, PACK-E will also be able to just perform a one burn maneuver into its desired orbit of 505x3495km. Using a Hohmann-like transfer for this burn, the new hand calculations reach 38.2 m/s instead of 96.4 m/s.

The GNC team also simulated these burns in STK to verify these values. The deployment orbit for PACK-C remained the same at a 505x2000km drop-off orbit [15], and as such, the satellite needed to perform a single burn to its 2000km altitude circular orbit. The insertion burn for PACK-C was 200 m/s, and the insertion burn for PACK-E was 51.5 m/s. These maneuver summaries are in the GNC Appendix Section [A.4.5](#). These values are higher than the 131 m/s and 38.2 m/s, respectively. This could be because STK accounts for more perturbation than the idealized Hohmann transfer. Also, STK may not be burning according to the optimal Hohmann transfer and may be using a less efficient maneuver instead of just hitting the target values within tolerance. Additionally, note that the STK simulation for PACK-C had difficulty converging. Instead, a very similar orbit to the one desired was targeted. However, since the 200 m/s value is so off from the hand calculations, the GNC team has deemed that STK was not a valid verification for PACK-C and will be taking the literature value instead. The STK simulation for PACK-E converged correctly, and the value is somewhat similar but higher than the hand calculations. With this, the GNC team will take an average of the values from the hand calculations and the STK simulations for PACK-E. This gives PACK-E a new insertion value of 44.85 m/s and a total deltaV of about 102 m/s. Figure [11](#) below shows the STK simulations of these two insertions.



(a) PACK-C Insertion



(b) PACK-E insertion

Figure 11: Insertion to PACK Orbits from Deployment Orbit

An insertion simulation for WOOF and HOWLL was also attempted. The launch vehicle for these satellites will launch to an orbit around the Earth with a 28.5 degree inclination and 200 km altitude [15]. It will then perform a Translunar Injection burn for a lunar flyby to the L2 point, and HOWLL and WOOF will be released upon completion of the burn [15]. Upon reaching the L2 point, WOOF will perform burns to insert itself into the desired L2 Southern Halo orbit, and HOWLL will maneuver to the L1 point and insert itself into its designated L1 Northern Halo Orbit. However, these simulations did not reach convergence. The GNC team also tried to loosen their constraints so that the simulation would converge, but these constraints were getting far too off from the desired point that the values were not really useful or reliable. As such, the GNC team will stick to their insertion values from the literature.

The End of Life plan is now optional to include for deltaV calculations. Still, the ARGOS GNC team will be accounting for these values. HOWLL and WOOF are expected to perform a year-long EOL cycle to use the least amount of deltaV. The plan is to perform small burns that perturb the orbit enough to reach a heliocentric orbit and exit the Cislunar space. This is the best disposal plan because it prevents the ARGOS satellites from populating the Cislunar environment, minimizing the risk of collision with operational satellites or missions and reducing space debris. A study is described in the GNC Subsystem PDR [12] [68] [69], where the HOWLL and WOOF values are studied and derived from literature, and they are 15 m/s and 20 m/s respectively.

On the other hand, the lunar orbiters PACK-C and PACK-E will perform a lunar impact for EOL, which was accurately simulated in STK. In the simulations, only one burn is performed to slow down the spacecraft to a crashing speed. For PACK-C, the circular orbit suggests that it does not matter where the maneuver is performed. For PACK-E, the calculations were performed with a burn at the elliptical orbit's apoapsis, when the spacecraft achieves its lowest speed, making it easy to perform a retrograde burn that slows it down just enough to crash onto the moon. Based on the STK simulations discussed in the GNC Subsystem PDR, the EOL values are 135 m/s and 45 m/s for PACK-C and PACK-E, respectively. Although lunar impacts can disrupt the lunar environment, potentially affecting scientific studies of the Moon's surface, and interrupting the state of the impacted region, it is the most efficient EOL plan for PACK that also accounts for the



sustainability of the Cislunar space.

The DeltaV total values for each satellite in the ARGOS architecture are described in Table 35, which includes insertion, station-keeping, and EOL. Additionally, because the Operations team has decided that in the case that HOWLL fails, WOOF will travel to the L1 point to replace HOWLL, the Propulsion team decided to make the propulsion needs for WOOF identical to HOWLL in the case that it needs to perform the extra L2 to L1 transfer. Unless discussed otherwise, most of these values are verified via STK simulations. The total DeltaV values comply with overall mission constraints and with other subsystems involved.

	Insertion	Station-Keeping	EOL	Total
PACK-C	131 m/s	~0 m/s	135 m/s	~266 m/s
PACK-E	45 m/s	0-3 m/s per year	45 m/s	~102 m/s
HOWLL	140 m/s	<5 m/s per year	15 m/s	~190 m/s
WOOF	20 m/s	<5 m/s per year	20 m/s	~75* m/s

Table 35: ARGOS Satellites DeltaV Requirements

The \* in the total deltaV value for WOOF is a note that this is the deltaV required just for WOOF operations. However, the actual tanks for WOOF will match that of HOWLL and be able to carry 190 m/s worth of fuel. Since the maneuver from L2 to L1 (140m/s) plus the WOOF deltaV total (75m/s) is greater than the 190m/s, if WOOF does end up having to move from L2 to L1, this will likely shorten the operational lifetime of the mission a bit. However, since the ARGOS team has designed everything with the 2037 timeline in mind, it will still meet the 2031 mission operations requirement if a few years from WOOF are docked. These total values for the deltaV fit within the tanks designed by the Propulsion team and will be able to fit and be carried in the satellite body designed by the Structures and Materials team.



## 7 Propulsion Design

It should be noted that all information presented in this section for the Propulsion Subsystem derives from previous design, analysis and writing carried out in Propulsion Subsystem Report 1 [70], Propulsion Subsystem Report 2 [71], and the Propulsion Preliminary Design Report (PDR) [72]. Wherever relevant, changes since the PDR will be indicated.

### 7.1 Subsystem Overview

The Propulsion (PROP) Subsystem is responsible for carrying out post-launch mission maneuvers for all ARGOS mission spacecraft, including HOWLL, WOOF, PACK-C and PACK-E. Quantitatively, an overview of the PROP subsystem's responsibilities is provided through consideration of the total delta-V requirement, which quantifies propulsive capability the subsystem must provide. Specifically, the subsystem is tasked with carrying out Delta-V maneuvers for four main purposes, including (1) **orbital insertion**, (2) **station-keeping**, (3) **ADCDS momentum dumping**, and (4) **end-of-life (EOL) spacecraft de-orbiting**. For orbital insertion, the PROP subsystem is tasked with providing the necessary delta-V to support the insertion of all ARGOS Mission spacecraft into their operational orbits, as determined by the GNC subsystem. These large, impulsive burns contribute the majority of the mission's delta-V needs [70]–[72]. In terms of station-keeping needs, the PROP subsystem must provide the necessary delta-V to sustain ARGOS Mission orbits through accommodating for gravitational perturbations, solar radiation pressure and the propagation of uncertainty in delta-V burn magnitude and pointing. The requirements for station-keeping delta-V are derived from the GNC subsystem's analysis [70]–[72]. With regard to the Attitude Determination and Control System (ADCDS), the PROP subsystem must provide sufficient delta-V and appropriate thrust levels to carry out momentum dumping [70]–[72]. Finally, the PROP subsystem must carry enough fuel to successfully execute EOL deorbiting maneuvers to ensure all ARGOS Mission spacecraft are disposed of in a safe and sustainable manner [70]–[72].

In order to accomplish this, the PROP subsystem carries out five vital operational functions. First, the PROP subsystem must allow for **thruster throttling**, or the capability to modulate thruster output in terms of both thrust and pulse duration to allow for applicability to both large maneuver burns and small positioning burns [70]–[72]. Next, the PROP subsystem must provide adequate **plume exhaust handling**, such that it does not disrupt the sensitive electronics and instruments operated by the Payload (PLD) and Communications (COMMS) subsystems [70]–[72]. Although this consideration falls mainly under the purview of the SM subsystem, the PROP subsystem's analysis informs relevant decisions by the SM subsystem with regard to thruster placement. Furthermore, the PROP subsystem must provide **propellant storage** that allows for safe spacecraft operation, propellant feeding, and combustion [70]–[72]. Additionally, the PROP subsystem must exhibit **environmental robustness** in the face of the harsh radiative, gravitational, vacuum, and thermal conditions of cislunar space [70]–[72]. Considered for the first time in this report is the operational need of a separate **pressurant storage and propellant feeding** system, to maximize the efficient use of space by the PROP subsystem, allow for reliable and controllable fuel delivery, and close the design loop for a complete propulsion system.



## 7.2 Subsystem Objectives

The major change to the subsystem objectives since the PDR consists of a clear decision to pursue only the Tier 1 and Tier 2 objectives from the RFP, which pertain to space object tracking and communications support, respectively [1]. At the mission level, consideration of the Tier 3 objective, which concerns autonomous proximity operation with space objects in the cislunar domain [1], was eliminated to allow for greater focus on meeting the primary and secondary mission-level objectives. The objectives of the PROP subsystem are nearly identical in terms of satisfying the primary and secondary mission-level objectives, have undergone no changes since the PDR design cycle, and are as follows:

1. Provide delta-V capabilities and carry out burns for (1) the insertion of HOWLL into an L1 Halo orbit, (2) the insertion of WOOF into an L2 Halo orbit, (3) the insertion of PACK-C into a 50° frozen circular lunar orbit, and (4) the insertion of PACK-E into a 135° frozen lunar orbit [70]–[72].
2. Provide delta-V capabilities and carry out burns related to station-keeping for the HOWLL, WOOF, PACK-C and PACK-E satellites in their respective orbits [70]–[72].
3. Provide delta-V supply for ADCS needs and execute momentum dumping burns for the HOWLL, WOOF, PACK-C and PACK-E spacecraft [70]–[72].
4. Provide the delta-V supply for all EOL needs and execute burns required to launch the PACK-C and PACK-E satellites onto long-term lunar impact trajectories at the conclusion of mission operations. Execute burns required to laundh HOWLL and WOOF into heliocentric graveyard orbits at the conclusion of mission operations [70]–[72].
5. Carry out all relevant mission operations without impeding the functionality of PLD or COMMS instrumentation, both of critical importance to the primary and secondary mission objectives [70]–[72].

## 7.3 Subsystem Requirements

There were no major changes to the subsystem requirements in this design cycle. Instead, a thorough inspection of every single requirement was conducted, with the purpose of finalising quantitative values and verifying consistency with mission-level requirements. Whilst no requirements were added or removed, a couple of minor changes were made. These are as follows, also summarised in Table 36, and the rest of the requirements can be accessed in the ARGOS Requirements Google Spreadsheet [6]:

1. Delta-V values of insertion, attitude control and end-of-life (EOL) disposal for HOWLL, WOOF, PACK-E and PACK-C were adjusted and finalised (PROP-F-003 to PROP-F-005).
2. Quantitative values for environmental requirements were adjusted and/or finalised upon confirmation from other subsystems (PROP-E-001 to PROP-E-017).



Table 36: Selected requirements for the propulsion subsystem [6]. The below requirements are for PACK, but the same edits with different quantitative values were made for HOWLL and WOOF as well.

Requirement ID	Requirement	Rationale	Verification, Validation Method
PROP-F-003	The propulsion system must carry out burns required for the mission architecture's end of life disposal plan [HOWLL Delta-V = 15 m/s, WOOF Delta-V = 20, PACK-C Delta-V = 135 m/s, PACK-E Delta-V = 45 m/s]	The RFP requires carefully planned end-of-life operations, emphasizing space sustainability. Such operations will require positional and attitudinal adjustments.	Analysis of propulsion system longevity and tank sizing
PROP-F-004	The propulsion system shall support the attitude control needs of all mission spacecraft [HOWLL Delta-V = 5 m/s, WOOF Delta-V = 5 m/s, PACK-C Delta-V = 0 m/s, PACK-E Delta-V = 0-3 m/s]	The ADCS subsystem has specified the need for thrusters to meet all mission ADCS requirements for all mission satellites.	Numerical analysis of propulsive gimbaling/torque capabilities
PROP-F-005	The propulsion system shall support the orbital insertion and stationkeeping needs of all mission spacecraft [HOWLL Delta-V = 140 m/s, WOOF Delta-V = 20 m/s, PACK-C Delta-V = 131 m/s, PACK-E Delta-V = 45 m/s]	The propulsion system must be able to provide orbital insertion capabilities to the PACK satellites to the extent that the LV subsystem cannot. Reliable and consistent positioning of PACK satellites is required for uninterrupted access and communication abilities with Cislunar spacecraft, both internal and external to the mission	Numerical analysis of propulsive high-thrust maneuver and station-keeping capabilities
PROP-E-001	The PACK propulsion system components must be capable of operating in the radiative environment of $10^8$ to $10^{20}$ eV/n for the duration of the mission	Survivability, longevity, and performance predictability of the propulsion subsystem in all possible radiative conditions	Simulation and Analysis
PROP-E-002	The PACK propulsion system must operate within the temperature range of 0 °C to 45 °C	Survivability, longevity, and performance predictability of the propulsion subsystem in all possible temperature conditions	Simulation and Analysis

*Continued on next page*



Table 36 – *Continued from previous page*

Requirement ID	Requirement	Rationale	Verification, Validation Method
PROP-E-003	All PACK propulsion system components must be capable of operating in the unstable and inconsistent gravitational environment for the duration of the mission	Survivability, longevity, and performance predictability of the propulsion subsystem in low gravity	Simulation and Analysis
PROP-E-004	All PACK propulsion system components must withstand the Launch Vehicle vibrational environment of $0.034 \text{ g}^2/\text{Hz}$ at 800-925Hz/5.13 GRMS during transit from Earth to the chosen orbit	Survivability, longevity, and performance predictability of the propulsion subsystem in all possible vibrational conditions	Simulation and Analysis
PROP-E-005	All PACK propulsion system components must withstand the Launch Vehicle load environment of axial -4 to 7 g and lateral $\pm 3.0 \text{ g}$ during transit from Earth to the chosen orbit	Survivability, longevity, and performance predictability of the propulsion subsystem after high-load launch conditions	Simulation and Analysis

## 7.4 Subsystem Constraints

There were no major changes to the subsystem constraints from the previous design iteration. The only changes made were the finalisation of numbers for the quantitative constraints. As such, there are no constraints to highlight in this report. The details of every constraint can be accessed in the ARGOS Requirements Google Spreadsheet [6].

## 7.5 Subsystem Drivers

There have been very few alterations to the PROP drivers since the previous design cycle. Importantly, pressure and temperature have been removed as drivers. During the FDR cycle, these important factors were re-categorized as design parameters, rather than drivers. This change was made to reflect the fact that the PROP subsystem had substantial freedom in selecting among a range of acceptable propellant and pressurant temperature and pressure storage conditions. The selected values thus reflected design decisions, rather than the drivers behind those decisions. Furthermore, the volume and space usage efficiency drivers have been combined for the purpose of succinctness. The updated and shortened list of the 5 PROP subsystem drivers is summarized as follows, in descending order in terms of their impact on PROP design decisions:

1. **Delta-V** [70]–[72]: The PROP subsystem must carry sufficient propellant to execute all post-launch delta-V needs of the ARGOS Mission.
2. **Mass** [70]–[72]: The design of the PROP subsystem must adhere to the subsystem mass

constraints imposed by the SM subsystem budgeting.

3. **Volume and Space Usage Efficiency** [70]–[72]: The PROP subsystem must occupy less than the total volume envelope budgeted by the SM subsystem. The PROP subsystem must utilize internal spacecraft volume as efficiently as possible to allow for a viable spacecraft layout and closure of the design loop.
4. **Complexity** [70]–[72]: The PROP subsystem must eliminate as many design complexities as possible to reduce points of failure for this mission-critical subsystem.
5. **Robustness to Environmental Conditions** [70]–[72]: All elements of the PROP subsystem must prove capable of reliable nominal operations in the harsh environment of cislunar space. The pressurized and volatile nature of PROP subsystem components makes this final driver particularly important for ensuring the safety of all ARGOS Mission subsystems, not only the PROP subsystem.

## 7.6 Subsystem Design Approach

In general, the Propulsion Subsystem design process relied on a combination of literature review, analysis, and inter-subsystem collaboration to arrive at a final design. In particular, Propulsion subsystem sizing requirements derived directly from the GNC, ADCS, and LV subsystems, as these subsystem designs dictated the quantity of delta-V necessary to carry onboard the mission spacecraft. Changes to delta-V requirements were ongoing over the course of the design process, meaning that iterative collaboration with the GNC, ADCS and LV subsystems was necessary up to and including the PDR design cycle. The literature was consulted for the purposes of (1) obtaining thruster and propellant specifications, (2) informing the tank sizing and feed system design analysis processes.

Since the previous report (PDR), the major updates to the design approach for the Propulsion subsystem have consisted of updates to the thruster layout, tank dimensioning and feed system design, as indicated by the pink boxes in the bottom right of the Design Approach Block Diagram provided in Figure 12 below. Previous iterations of the design for the first and second subsystem reports [70], [71], as well as the PDR design report [72], allowed for satisfaction of requirements relating to delta-V needs and ADCS momentum dumping capabilities. The most recent design updates were undertaken to satisfy requirements relating to mass and volume constraints, resulting in the selection of a regulated pressure feed system and heavy iterative collaboration with the SM subsystem to ensure that all subsystem design components fit successfully within the HOWLL, WOOF, PACK-C and PACK-E buses. Furthermore, the thruster layout was rearranged in collaboration with the Structures and Materials subsystem to improve on existing delta-V and momentum dumping capabilities according to feedback received during the presentations at the Final Design Review (FDR) and NASA Goddard.

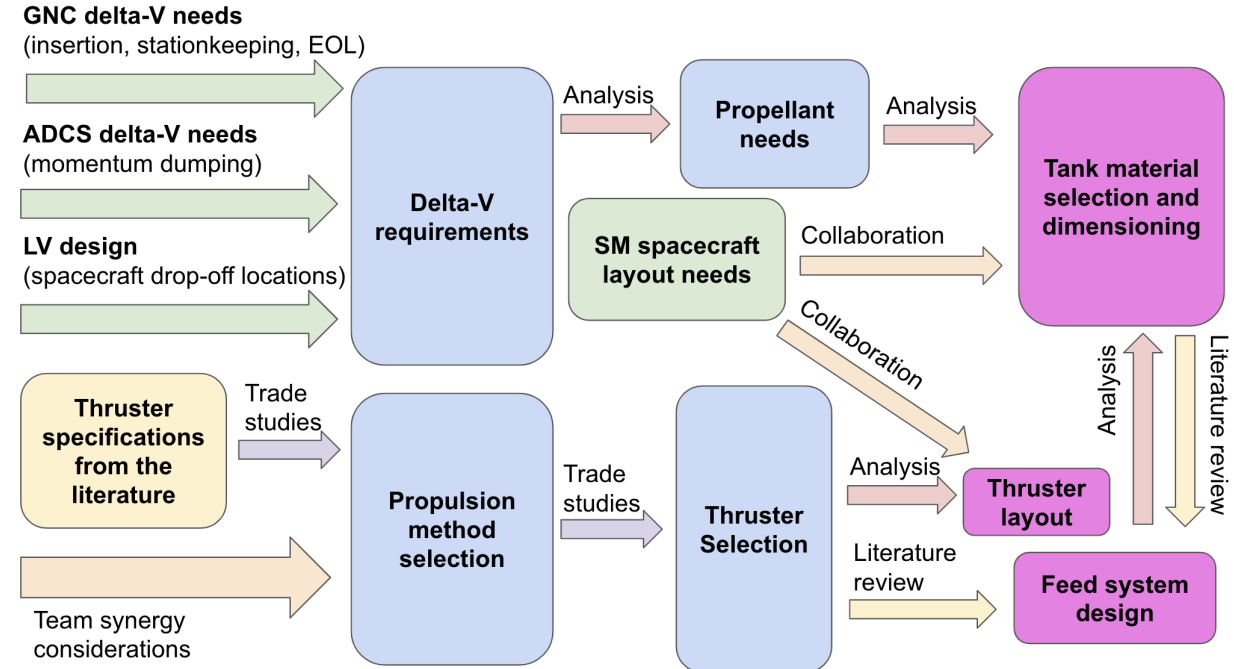


Figure 12: Propulsion Subsystem Design Approach Block Diagram

### 7.6.1 Thruster Selection, Operation and Layout

The thruster selection has remained the same since the previous iteration of the subsystem report, in the form of the Bradford Space High Performance Green Propellant (HPGP) 1N thrusters. The thruster uses a type of HPGP called LMP-103S, which is a non-toxic, drop-in replacement for hydrazine [73]. This is extremely desirable as it significantly lowers the costs and risks involved in propellant handling. In terms of propulsive performance, it is in fact equal to or better than conventional hydrazine [73]. Finally, the thruster is rated at a technology readiness level (TRL) of 9, with over 200 years of cumulative space heritage [73], justifying confidence in its reliable operation to fulfill mission requirements.

Each thruster is capable of outputting 1 N of thrust, which is more than sufficient for the propulsion of the 27U HOWLL and WOOF satellites, and any lighter cargo such as the 12U PACK satellites. There will be four thrusters installed on each of HOWLL, PACK-E, PACK-C and WOOF, angled outward symmetrically such that both translational and rotational motion can be achieved. Specifically, there is rotational control over all three body axes, as will be analysed in Section 7.7. This is another area inquired during the Preliminary Design Review (PDR) and FDR presentations, and therefore this report looks to demonstrate robust rotational control capabilities.

The thruster layout has been altered since the previous design iteration to allow for more a robust and efficient propulsion of the satellites. Whilst the previous design implemented the four thrusters in rather irregular arrangements, the new design allows for a regular rectangular arrangement with the centre of thrust through the satellite's centre of mass. This comparison is visualised for the 27U HOWLL in Figure 13.

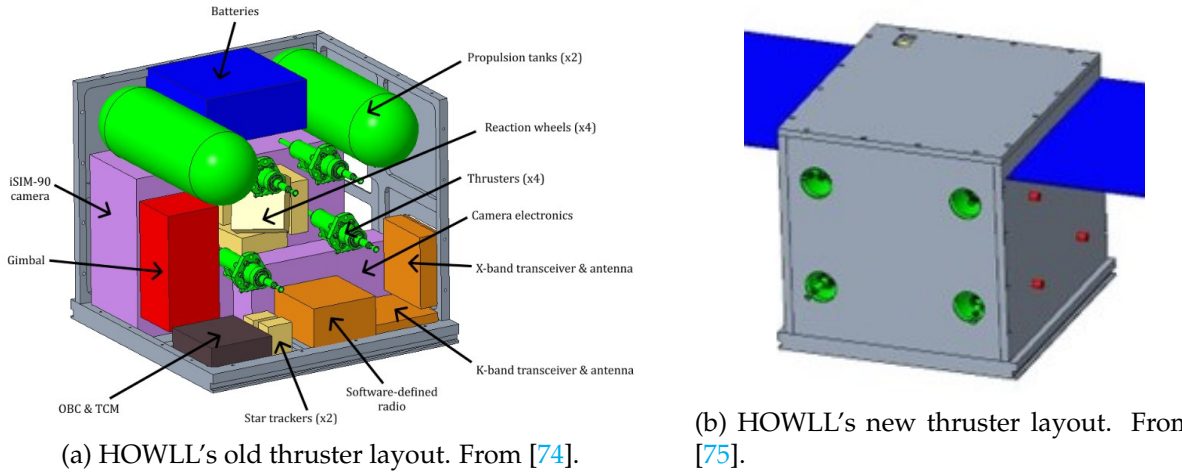


Figure 13: Improvement of the thruster layout for increased separation and adjustment of thrust centre to align with mass centre.

This was the high-level design approach during the selection of the Bradford Space HPGP 1N thruster, and quantitative analysis of the thruster will be conducted in Section 7.7 to ensure compliance with subsystem requirements.

### 7.6.2 Nozzles

The nozzle also remains the same from the previous design iteration. This is mainly due to the fact that the nozzle will come as a package with the Bradford Space HPGP 1N thrusters, as a commercial-off-the-shelf (COTS) component. The nozzle is of a simple conical geometry, and a computer-aided design (CAD) model of the Bradford Space HPGP 1N thruster is displayed in Figure 14.

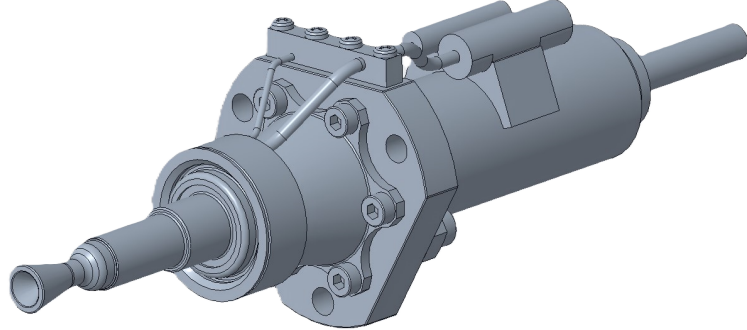


Figure 14: CAD model of the Bradford Space HPGP 1N thruster. Model obtained from [76].

However, there is scope for improvement from technical and cost budget perspectives. As such, work was carried out to characterise the nozzle geometry, followed by the chamber geometry, allowing for the calculation and verification of the nozzle performance. Furthermore, it has laid the foundation for any further optimisation of the nozzle design, which is a possibility considering the large cost budget margins currently available for the mission.



Furthermore, plume exhaust from the nozzle must be investigated to ensure no direct or indirect interference with other components on the satellites. For example, direct plume impingement may cause thermal or chemical damage, whilst the plume exhaust should also avoid interfering with the line of sight of payload components such as the camera and other tracking equipment.

### 7.6.3 Propellant Storage and Management

The propellant storage and management design process allowed for the satisfaction of delta-V requirements for all ARGOS mission spacecraft (i.e. PROP-F-001, PROP-F-004, PROP-F-005). Additionally, the design process allowed for the satisfaction of performance requirements related to propellant and pressurant storage conditions (i.e. PROP-P-014, PROP-P-022, PROP-P-031, PROP-P-026, PROP-P-028, PROP-P-030). Finally, the design process ensured that mass and volume constraints were successfully satisfied. The propellant storage and management process was iterative and continuous in nature, but can be understood fundamentally as consisting of two major components:

- **Tank Design:** This design process consisted of first determining acceptable storage conditions for the propellant and pressurant. These conditions could be combined with the total required delta-V for each ARGOS Mission spacecraft to determine the necessary volume of propellant and pressurant for each spacecraft. Following tank sizing, tank dimensions were selected so as to support spacecraft layout needs. After selection of the tank wall material, analysis of propellant and pressurant storage parameters allowed for the evaluation of necessary tank wall thickness and resulting mass and volume. This process will be presented in greater conceptual and numerical detail in the formal analysis section.
- **Propellant Management:** The design process for propellant management first involved the selection of a feeding system type. As pointed out in *Space Mission Analysis and Design*, Third Edition (SMAD), monopropellant feeding systems can be divided into pump-fed or pressure-fed systems [8]. Pressure-fed systems represent a more appropriate choice for smaller spacecraft such as those of the ARGOS Mission, due to (1) their increased simplicity relative to pump-fed systems, and (2) their decreased weight relative to pump-fed systems for small spacecraft [8].<sup>1</sup> Once a propellant management system was selected, there remained a choice between a regulated and blowdown pressure-fed system. The following schematic, pulled from Chapter 17 of SMAD, highlights the differences between these two system profiles.

<sup>1</sup>It should be noted that for “launch vehicles or large upper stages,” pump-fed systems represent the more weight-efficient choice [8].

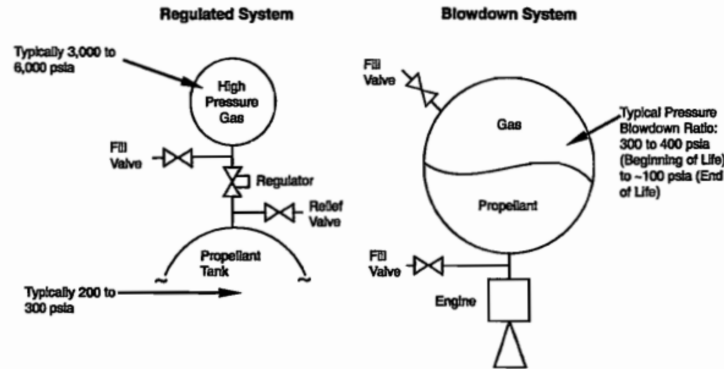


Figure 15: Figure from [8] contrasting regulated vs. blowdown pressure-regulated systems

A regulated system was selected over a blowdown system, motivated by the PROP subsystem driver “Volume and Space Usage Efficiency. As is shown in the above figure, regulated systems allow for storage of the pressurant gas in a separate tank from the propellant itself, whereas blowdown systems incorporate both fluids within the same tank, separated by a diaphragm. A separate pressurant tank allows for approximately 10 times greater pressurant storage pressure than a blowdown system, which for constant temperature, provides a ten-fold reduction in required pressurant storage volume. For all ARGOS mission satellites, but in particular the PACK-C satellite, volume constraints simply could not be satisfied with a blowdown system, whereas the regulated system allows for an acceptable fit and spacecraft layout, as determined by SM subsystem CAD modeling and analysis.

## 7.7 Formal Analysis

Formal analysis for thruster selection, thruster operation and layout, nozzle design, and propellant storage and management is now presented.

### 7.7.1 Thruster Selection

The formal analysis process for the thruster selection consisted of a comprehensive trade study of 22 thruster models representing a variety of propulsion methods, including monopropellant, hybrid, solid, electrospray, electrothermal, gridded-ion, Hall-effect, pulsed plasma and vacuum arc, ambipolar, and cold gas thrusters. In order to carry out this trade study, specifications for thrust  $T$  and specific impulse  $I_{sp}$  were gathered for each model under consideration; these values were sourced from NASA’s State-of-the-Art Small Spacecraft Technology report [77]. Thrust and specific impulse values were used in conjunction with a representative spacecraft mass to determine the burn time required to execute a given delta-V maneuver using Equation below.

$$t = \frac{m_0 \left( 1 - e^{\frac{-\Delta v}{I_{sp} g_0}} \right)}{\dot{m}} \quad (1)$$

Rocket Equation, solved for burn time [78]



As was expected, this analysis pointed out the vast discrepancy between the time required to carry out the necessary delta-V maneuvers with chemical versus electric propulsion methods. Both monopropellant/bipropellant chemical propulsion and propellant-less methods produced burn times ranging from a few seconds to approximately 40 minutes for a delta-V of 100 m/s by a 24-kg spacecraft, whereas electrical produced burn times on the order of days, weeks, or even months [79]. The aforementioned mass and delta-V values were selected so as to provide approximately representative figures for ARGOS mission spacecraft. Exact figures for the results of this trade study are included in Section A.5.1 in Figures 83 and 84. While the results of this analysis were not unexpected, they underscored the possible complexity of executing all ARGOS mission spacecraft maneuvers with low-thrust electric propulsion, especially in terms of the GNC subsystem's role.

In choosing a specific chemical propulsion method, monopropellant methods were prioritized over bipropellant methods to maximize design simplicity and reduce tank and feeding system mass. To determine which monopropellant thruster would be ultimately selected, an extensive trade study was again conducted with 32 individual monopropellant thruster models. Specifications were again pulled from [77]. Performance rankings in terms of time required to execute a 100 m/s delta-V maneuver for a 24 kg spacecraft. Numerical results of these trade studies can be viewed in Section A.5.2 in Figures 85, 86, and 87. Monopropellant thruster performance rankings were combined with rankings in terms of lowest power draw and lowest mass to generate a Merit Index value for each thruster that took into account performance and compatibility with mission constraints. Any thruster models incapable of executing the precise maneuvers required for attitude control were eliminated from consideration, which left the Bradford Space Systems 1N HPGP Thruster as the highest-ranked option.

Thus, as a result of this study as well as inter-subsystem meetings and conversations with the course staff, chemical propulsion with the Bradford Space Systems 1N HPGP Thruster was selected for all ARGOS Mission spacecraft. This decision was motivated in large part by the goal to promote team synergy and allow for closure of the ARGOS mission design loop within the time constraints of the project. However, as noted in Section 7.6.1, the extensive flight heritage of the selected thruster also provided strong motivation for its ultimate selection.

### 7.7.2 Thruster Operation and Layout

It is important to quantitatively analyse the overall operation and layout of the Bradford Space HPGP 1N thruster to ensure compliance with subsystem requirements.

#### Thruster Operation

The LMP-103S HPGP is of 1.3 times the density- $I_{sp}$  of conventional hydrazine [80]. Furthermore, the reduced handling costs due to the non-toxicity of the propellant can result in up to 72 % lower loading costs [80]. In addition to the TRL 9 rating and cumulative space heritage of over 200 years [73], the thruster is currently operating on 25 satellites [80]. From a broader perspective, these specifications instill confidence in equal or improved performance, cost and reliability of the Bradford Space HPGP 1N thruster relative to the mature technology of conventional hydrazine thrusters.

With regard to more specific operating parameters, the Bradford HPGP 1N thruster can officially throttle between 0.25 N and 1 N by varying the propellant feed pressure [80]. Thrusts just below



0.2 N have also been demonstrated [80], and even finer control is possible by pulsing the thruster at short intervals. Such pulses can be as short as 10 ms to as long as 60 min [80]. Whilst the official upper bound of the minimum impulse bit is 0.1 N s [80], by firing the thruster at 0.25 N for 10 ms pulses it is possible to achieve impulse bits as low as 2.5 mN s. As such, the thruster can fulfill high-thrust responsibilities such as primary propulsion, whilst also providing fine adjustments for attitude control purposes. It should be noted that, whilst attitude control is possible with these thrusters, such manoeuvres will primarily be performed using reaction wheels. The thrusters will, however, be used to conduct reaction wheel desaturation. In terms of overall performance, the Bradford Space 1N thruster has demonstrated specific impulses of up to 231 s [73], which is sufficient to maintain the propellant requirements for all of HOWLL, PACK-E, PACK-C and WOOF within mass and volume budgets.

### Thruster Layout

Furthermore, these operating parameters must be verified in combination with the thruster layout. The dimensions of the thruster layout are as shown in Figure 16. As mentioned earlier, there are two significant improvements to this design. First, the regular arrangement of the thrusters allow for the thrust centre to align with the mass centre. This is a significantly more propellant-efficient technique than having to apply off-centred thrust and continuously correct the attitude using reaction wheels, as that will increase the reaction wheel desaturation necessity. Second, more torque will be exerted during reaction wheel desaturation due to the increased separation of the thrusters from the torque axes. This will similarly increase propellant efficiency.

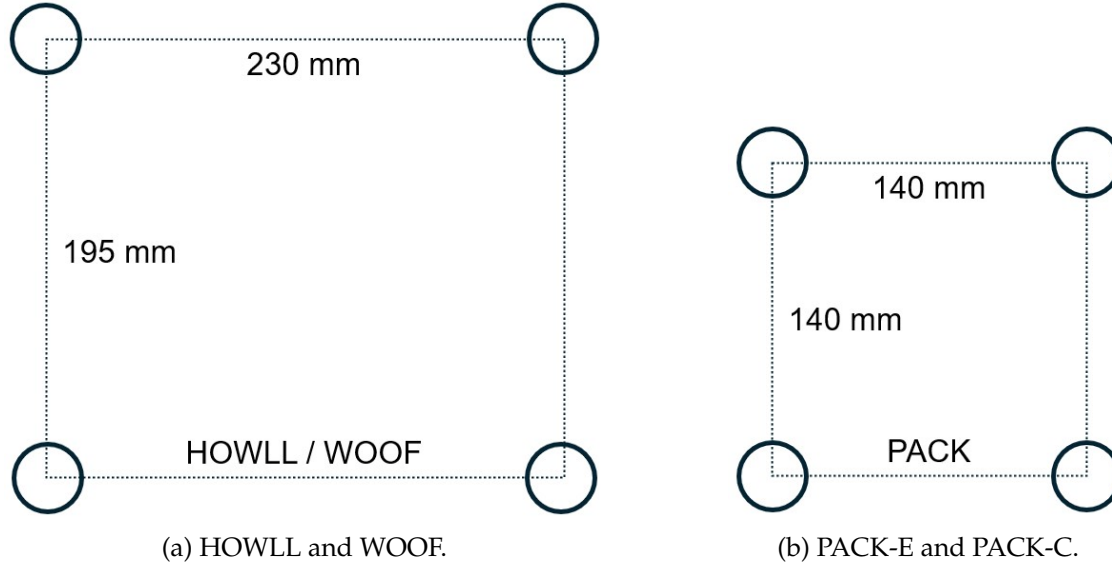


Figure 16: Thruster separations on all satellites.

This configuration has been studied in the literature as one capable of achieving rotational control over all three body axes, albeit with some translational motion. A 2015 study by Nehrenz and Sorgenfrei investigated thruster implementation strategies in nanosatellites, which refers to satellites of masses 14 kg or under [81]. This is comparable to the masses of all satellites involved in Project ARGOS. The paper compares two thruster implementation strategies: a four-nozzle cold gas thruster system (Fig. 17a) and an electrical thruster system with 12 individual thrusters (Fig.



17b). The latter is the more common configuration amongst satellites, whilst the former is the layout implement in Project ARGOS.

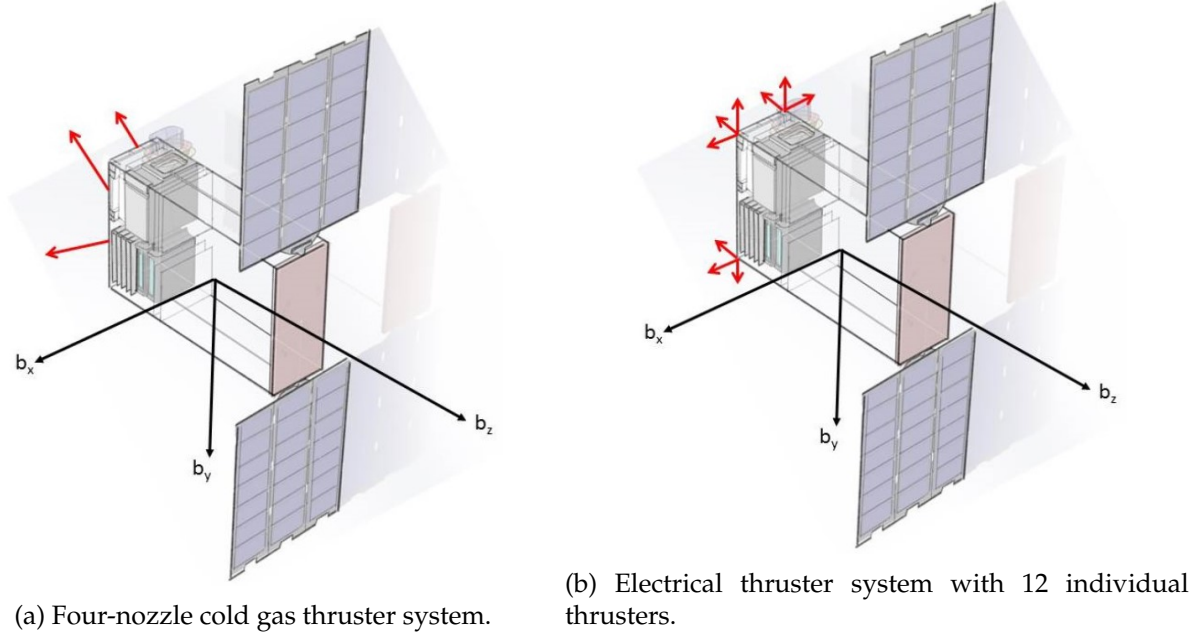


Figure 17: Thruster configurations studied by Nehrenz and Sorgenfrei [81].

The paper studies the configurations in Figure 17 for the purposes of pure translational motion, attitude control and momentum dumping. Specifically, it mentions pointing an antenna on the satellite towards Earth for communication, along with reaction wheel desaturation [81]. It should be noted that the cold gas thrusters in configuration 1 (Fig. 17a) are capable of thrusts of up to 40 mN, whilst the micro-electrospray propulsion (MEP) thrusters in configuration 2 are capable of thrust of up to 100  $\mu\text{N}$  [81]. A simulation is conducted in the study where the two thruster configurations are compared during a detumbling manoeuvre of the 14 kg satellite from an initial angular velocity about each body axes of  $5^\circ \text{ s}^{-1}$  to a complete rotational stop. The 14 kg mass is distributed uniformly throughout the entire 6U volume. The simulation finds that configuration 1, used in Project ARGOS, detumbles the spacecraft in under 5 seconds, whilst configuration 2 takes nearly 1200 seconds. The results are plotted in Figure 18. Whilst there must be consideration for the fact that the thrusters in configuration 1 can apply thrusts of two orders of magnitude larger, it is equally significant that the detumbling duration was over two orders of magnitude shorter. As such, the two configurations are comparable and the paper even suggests that configuration 1 may be more suitable for missions requiring impulsive translational burns [81].

Whilst the study implements the thrusters canted at  $45^\circ$  angles as the focus was on rotational motion [81], Project ARGOS will implement them at  $25^\circ$  to increase the propellant efficiency during purely translational motion. Optimisation can and should be performed in the future to find the optimal cant angle to finely balance the needs of primary propulsion and momentum dumping. There is confidence that  $25^\circ$  is sufficient to desaturate the reaction wheels, given that the Project ARGOS thrusters produce 25 times more thrust than the cold gas thruster in the study and yet the detumbling manoeuvre was completed in under 5 seconds [81].

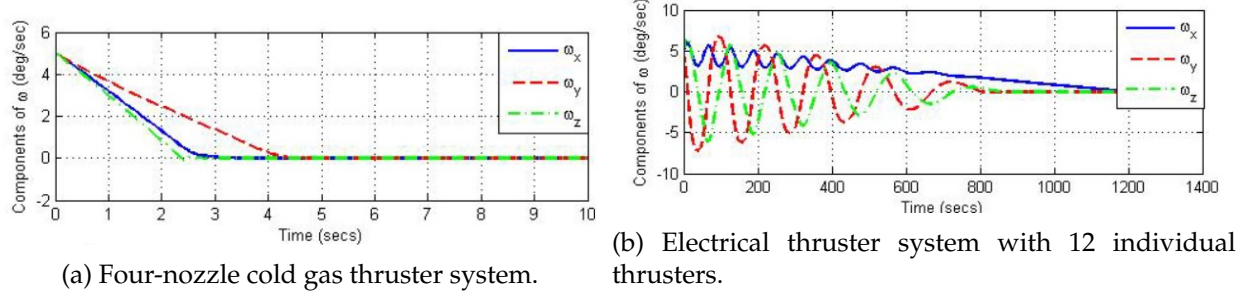


Figure 18: Detumbling time of two thruster configurations. From [81].

### 7.7.3 Nozzles

#### Nozzle Characteristics

The nozzle material remains as platinum from the previous design iteration, due to its ability to withstand high temperatures and its suitability for additive manufacturing [82]. With regard to the quantitative parametrisation of the nozzle characteristics, a high-level overview will be provided in this report. Details of the process are laid out thoroughly in the Propulsion Subsystem Preliminary Design Review (PDR) Report [83].

To begin the nozzle characterisation, the nozzle geometry was first obtained from a thesis by Stachowicz [82]. Specifically, the ratios between nozzle exit radius,  $R_e$ , nozzle throat radius,  $R_t$  and nozzle length,  $L$ , were measured. These ratios were combined with the actual nozzle length obtained from Bradford Space [84] to calculate the actual exit radius,  $R_e$ , and actual throat radius,  $R_t$ . Furthermore, the conical angle,  $\alpha$ , was calculated via trigonometry and the effective momentum ratio,  $\lambda$ , was obtained by  $\lambda = \frac{1+\cos\alpha}{2}$ .

Subsequently, the characteristic length of the chamber, unique to the propellant, was retrieved [85]. This value,  $L^*$  was used to calculate the chamber volume,  $V_c$ , and the chamber area,  $A_c$ :

$$V_c = A_t L^*, \quad (2)$$

$$A_c = A_t (8.0 d_t^{-0.6} [\text{cm}] + 1.25). \quad (3)$$

$d_t$  is the diameter of the throat, where  $d_t = 2R_t$ . Subsequently, the total chamber length,  $L_{tot}$ , was obtained from Bradford Space [84], which allowed for the calculations of  $L_1$  and  $L_c$  from Figure 20:

$$V_c = A_c L_1 + A_c L_c \left(1 + \sqrt{\frac{A_t}{A_e}} + \frac{A_t}{A_e}\right), \quad (4)$$

$$L_{tot} = L_1 + 3L_c. \quad (5)$$

$$L_c = \frac{L_{tot} - \frac{V_c}{A_c}}{2 - \sqrt{\frac{A_t}{A_c}} - \frac{A_t}{A_c}}, \quad (6)$$

$$L_1 = L_{tot} - 3L_c. \quad (7)$$

With the nozzle and chamber geometries determined, the nozzle performance could be calculated. The ratio of specific heat,  $\gamma$ , was obtained as 1.25 [88] and the chamber pressure was taken from

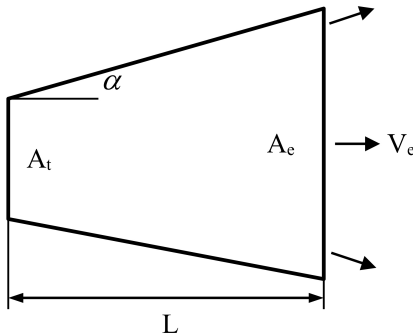


Figure 19: Nozzle geometry and its parameters. From [86].

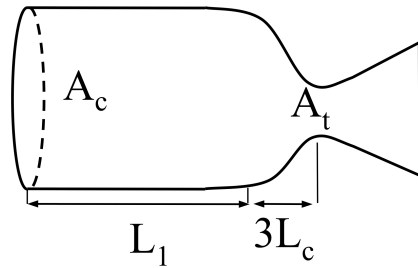


Figure 20: Chamber geometry and its parameters. From [87].

the Stachowicz thesis as  $p_c = 1.5 \times 10^6$  Pa [82]. Finally, the following set of equations were solved to calculate the remaining parameters:

$$\frac{A_e}{A_t} = \frac{1}{M_e} \left( \frac{2}{\gamma + 1} \right) \left( 1 + \frac{\gamma - 1}{2} M_e^2 \right)^{\frac{\gamma+1}{2(\gamma-1)}}, \quad (8)$$

$$p_e = p_t \left( \frac{1 + \frac{\gamma-1}{2}}{1 + \frac{\gamma-1}{2} M_e^2} \right)^{\frac{\gamma}{\gamma-1}}, \quad (9)$$

$$C_F = \lambda \sqrt{\frac{2\gamma^2}{\gamma-1} \left( \frac{2}{\gamma+1} \right)^{\frac{\gamma+1}{\gamma-1}} \left[ 1 - \left( \frac{p_e}{p_c} \right)^{\frac{\gamma-1}{\gamma}} \right]} + \left( \frac{p_e - p_a}{p_c} \right) \frac{A_e}{A_t}, \quad (10)$$

$$c^* = \frac{I_{sp} g_0}{C_F}. \quad (11)$$

The atmospheric pressure in space,  $p_a$ , was taken as zero, and the  $I_{sp}$  of 231 s was used [73]. The calculated parameters are summarised in Table 37, including beginning-of-life (BOL) and end-of-life (EOL) values. Overall, these calculations verify the sufficient propulsive performance of the Bradford Space HPGP 1N nozzle. However, if resources are available, these calculations have laid the foundations for further optimisation of the nozzle and chamber. The MATLAB script developed for this analysis can be used directly for parameter-varying optimisation, whilst the CAD model can be used to set up numerical simulations in software like ANSYS for higher fidelity optimisation. There exists sufficient margin in the cost budget to potentially invest in a custom-made nozzle, possibly through additive manufacturing.

### Plume Interference Mitigation

The plume exhaust has been studied thoroughly for the Bradford Space HPGP 1N thruster by Pokrupa et al. [89]. The results from the paper provides confidence that plume impingement will not pose an issue for Project ARGOS.

Firstly, the fundamental propulsion technique of the HPGP monopropellant thruster is chemical decomposition, which immediately eliminates any possibility of ion scattering and other electromagnetic effects. Often, these are significant concerns with electric propulsion. Furthermore, the exhaust species are safe and relatively inert in a vacuum environment. The mole composition is as follows: 50%  $\text{H}_2\text{O}$ , 23%  $\text{N}_2$ , 16%  $\text{H}_2$ , 6%  $\text{CO}$  and 5%  $\text{CO}_2$  [89].



Table 37: Nozzle and chamber parameter values

Parameter	Symbol	Value
Nozzle length	$L$	8.1 mm
Nozzle exit radius	$R_e$	2.36 mm
Nozzle throat radius	$R_t$	0.236 mm
Nozzle area ratio	$\frac{A_e}{A_t}$	100
Nozzle cone angle	$\alpha$	14.7°
Effective momentum ratio	$\lambda$	0.985
Chamber characteristic length (LMP-103S)	$L^*$	0.770 m
Chamber volume	$V_c$	0.135 cm³
Chamber area	$A_c$	0.0896 cm²
Chamber cylindrical length	$L_1$	10.9 mm
Chamber convergent length	$L_c$	3.52 mm
Ratio of specific heat (hydrazine)	$\gamma$	1.25
Chamber pressure	$p_c$	$1.5 \times 10^6$ Pa
Exit Mach number	$M_e$	5.32
Exit pressure	$p_e$	778.9 Pa
Thrust coefficient	$C_F$	1.86
Specific impulse (BOL)	$I_{sp\ BOL}$	231 s
Specific impulse (EOL)	$I_{sp\ EOL}$	204 s
Characteristic velocity (BOL)	$c_{BOL}^*$	$1.22 \text{ km s}^{-1}$
Characteristic velocity (EOL)	$c_{EOL}^*$	$1.08 \text{ km s}^{-1}$

A numerical simulation was also performed to model the plume exhaust into vacuum. This model was based on mature theory of flow from a nozzle into vacuum [89]. A simulation of the plume density upon exhaust from the nozzle in polar coordinates is conducted, and finds negligible interference outside of a 1 m radius and a 35° exhaust angle [89]. This result is visualised in Figure 21. The layout of the Project ARGOS thrusters ensure that all other components fall outside of this interference zone. Furthermore, since the last design iteration, the thrusters have been moved to the opposite side of the payload equipment to also ensure zero indirect interference with the line of sight of any tracking devices.

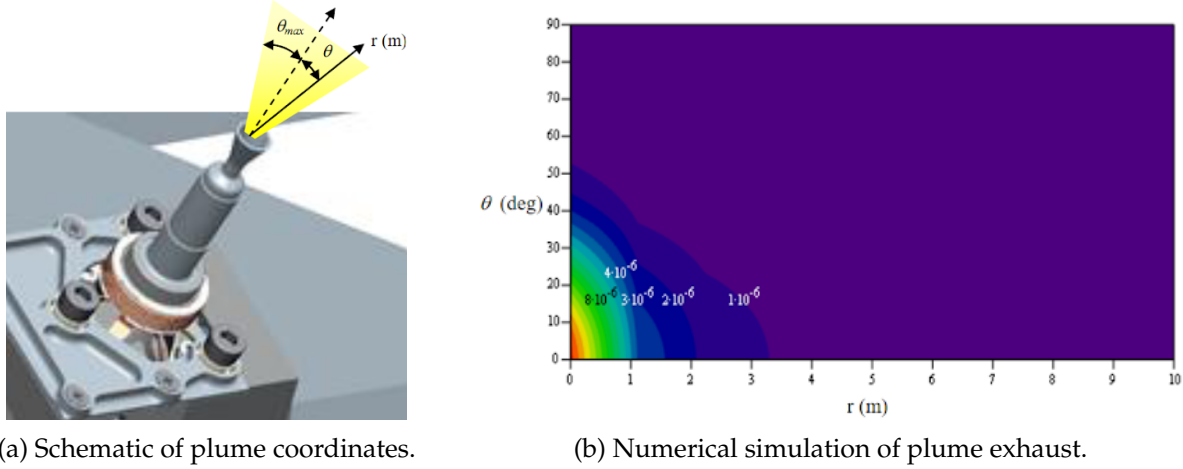


Figure 21: Plume exhaust analysis. From [89].

#### 7.7.4 Propellant Storage and Management

##### Tank Design

The first step in carrying out the design for propellant storage system (i.e. the tanks) lay in choosing the chemistry and storage conditions for the propellant and pressurant, as well as the tank material. The Bradford Space Systems Thruster was designed to operate with High-Performance Green Propellant, or LMP-103S [84]. A storage pressure of 18.5 bar and a storage temperature of 294.15 K were selected for the propellant based on the storage parameters used in both the SkySat and PRISMA missions, which also used the Bradford 1N HPGP Thruster for small spacecraft propulsion [71], [90], [91]. Based on the example of these two missions, Helium was selected as the pressurant for the ARGOS Mission spacecraft [71], [90], [91]. The storage parameters for the Helium pressurant were found by taking the median values of acceptable ranges provided in SMAD [8]. Finally, aluminum was selected for tank wall material for its light weight and strength, as well as its use in SMAD [8]; a value of 420 MPa was used to represent the maximum stress of aluminum [8]. A summary of propellant and pressurant storage parameters is provided below in Table 39.

	Chemistry	Phase	Initial Pressure [MPa]	Instantaneous Pressure [MPa]	Temperature [K]
Propellant	LMP-103s	Liquid	1.85	—	294.15
Pressurant	Helium	Gas	31.03	3.10	287.5

Table 38: Propellant and Pressurant Storage Parameters [8], [79]

After determining appropriate storage parameters, the next step in tank design lay in sizing the tanks appropriately for the delta-V values provided by the GNC and ADCS subsystems. The total delta-V values determined by these subsystems for HOWLL, WOOF, PACK-C, and PACK-E were 190 m/s, 190 m/s, 266 m/s, and 101.85 m/s, respectively. These figures include delta-V needs related to orbital insertion, station-keeping, attitude control, and EOL deorbiting. Once these delta-V values were obtained, a multi-step calculation process was conducted to completely

size the propulsion system. Due to the complexity of the analysis, a schematic is provided below in Figure 22 to assist in illustrating the calculation process. The entire tank design process was informed heavily by Chapter 17 of SMAD, with most of the equations presented in Figure 22 cited directly from the book [8]. Other equations used to convert between masses, volumes, and densities of propellant and pressurant, as well as the ideal gas law, and tank wall volume and mass formulas, derive from common knowledge. Specific figures and intermediate calculation steps from the calculations described in this section are included in Sections A.5.3, A.5.4, and A.5.5, in Figures 89, 90, 91, 92, 93, 94, 95, and 96.

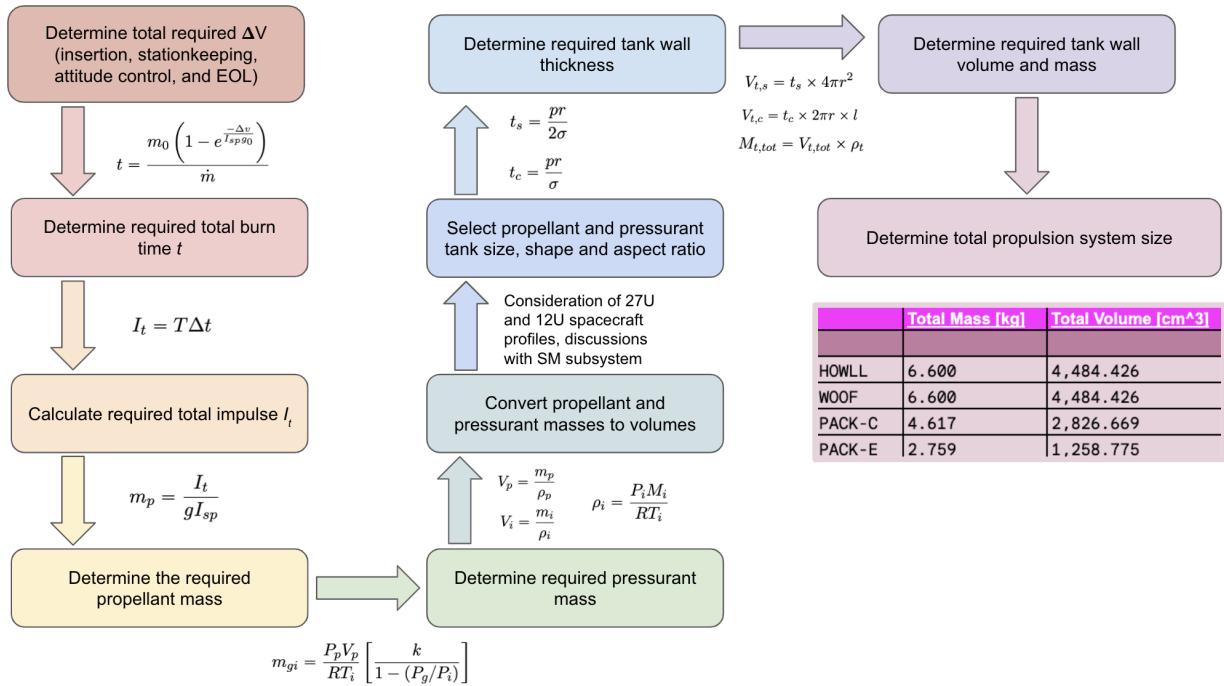


Figure 22: Propellant Tank Feed System Design, with time  $t$ , total spacecraft delta-V  $\Delta V$ , specific impulse  $I_{sp}$ , total impulse  $I_t$ , thrust  $T$ , acceleration of gravity  $g$ , mass  $m$  (with subscripts p and i for propellant and pressurant respectively), volume  $V$ , density  $\rho$ , tank material stress  $\sigma$ , pressure  $P$ , gas constant  $R$ , molar mass  $M$ , specific heat ratio  $k$ , tank radius  $r$ , tank length  $l$ , cylindrical tank wall thickness  $t_c$  and spherical tank wall thickness  $t_s$  [8]

As depicted by the above figure, the process began with determining the total burn time required to achieve the provided delta-V values with the selected Bradford Space Systems 1N HPGP Thruster and LMP-103s propellant chemistry, using a version of the rocket equation solved for time. Next, the total burn time combined with the thrust specification for the selected thruster could be combined to determine the total impulse required. This total impulse value allowed for the calculation of required propellant and pressurant masses, which were then converted to volumes. Next, close work with the SM subsystem allowed for the selection of tank dimensions which would be conducive to a successful spacecraft layout. Once tank dimensions were secured, required wall thicknesses could be calculated based on tank geometry, storage pressure, and tank wall material maximum stress. Finally, the masses and volumes of the tank wall material were calculated



and combined with the masses of the thrusters, feed system, propellant, and pressurant to size the overall propulsion system. More information on the feed system will be provided in the next section, entitled “**Propellant Management**.”

The dimensions for the cylindrical propellant tanks, as determined by the above analysis process, are summarized below in Table 39, while the dimensions for the spherical pressurant tanks are summarized in Table 40. The decisions to use a cylindrical tank for the propellant and a spherical tank for the pressurant were informed by their relative volumes, as well as a desire to reduce required tank wall material as much as possible. For the higher-pressure storage conditions of the pressurant gas, a choosing a spherical rather than cylindrical tank allowed for a substantial reduction of required tank wall material.

Spacecraft	Radius [cm]	Length [cm]	Volume [cm <sup>3</sup> ]	Quantity
HOWLL	4.56	29.30	1,711.89	2
WOOF	4.56	29.30	1,711.89	2
PACK-C	5.07	29.30	2,093.15	1
PACK-E	4.56	15.75	830.28	1

Table 39: Cylindrical Propellant Tank Dimensions [79]

Spacecraft	Radius [cm]	Volume [cm <sup>3</sup> ]	Quantity
HOWLL	4.49	378.10	1
WOOF	4.49	378.10	1
PACK-C	3.81	231.48	1
PACK-E	2.80	91.95	1

Table 40: Spherical Pressurant Tank Dimensions [79]

Ongoing and iterative conversations with the SM subsystem members confirmed that the above tank dimensions allowed for successful internal configurations in all four ARGOS Mission spacecraft as determined by CAD modeling, resulting in a successful closure of Propulsion Subsystem design loop.

## Propellant Management

As mentioned in Section 7.6.3, a regulated pressure feed system was selected over a blowdown pressure feed system. With this information, the propellant feed system was designed based heavily on examples in [8] and [92]. The design is presented in Figure 23.

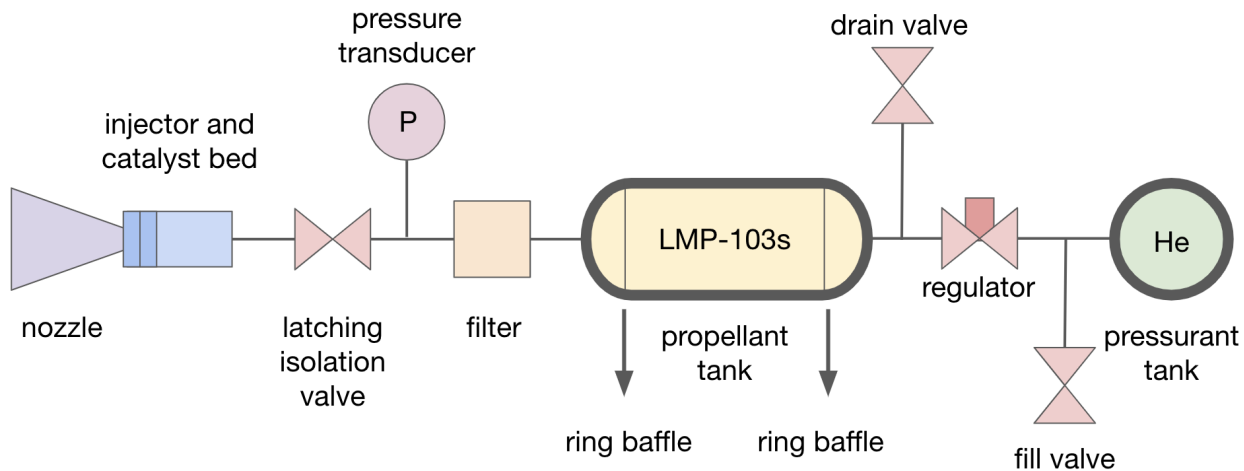


Figure 23: Propellant Tank Feed System Design [8], [92], [93]

The design includes fill and drain valves for the propellant tank, as well as a regulator between the pressurant tank and propellant tank. The pressure regulator serves to modulate the 31.03 MPa storage pressure of the Helium pressurant down to the 3.10 MPa instantaneous pressure necessary to feed the propellant to the thruster. A filter, pressure transducer, and latching isolation valve are included between the propellant tank and thruster to prepare and monitor the propellant influx to the thruster, while preventing backflow into the propellant tank. Based on figures provided in [8], [94], [95], it was determined that a reasonable mass estimate for the propellant feed system, including tubing, valves, filters, and pressure transducers, could be derived by taking 10% of the mass of the propellant for each spacecraft. Each thruster within each spacecraft is connected to the propellant tank through its own individual feed system, although only a single thruster is depicted in Figure 23 for maximum clarity and simplicity.

A detailed consideration of tank sloshing mitigation is beyond the scope of this course, since as revealed in conversations with the MAE 342 Course Staff, sloshing is not a well-understood problem and research into sloshing mitigation methods is ongoing. As a result, a simple and brief solution is presented for the ARGOS Mission Propulsion system in the form of ring baffles, included at either end of the propellant tank to mitigate sloshing in the liquid LMP-103s propellant after some of the propellant has been drained [93]. Ring baffles were selected as a first-order sloshing mitigation method due to their simplicity; they are mounted as flat disks at either end of a cylindrical tanks, as shown in Figure 24 below. Hartwig et al. also point out that ring baffles have been used successfully in previous missions, including but not limited to the British EUSTAR System, the Mars Global Surveyor (MGS), the Chandra x-ray telescope, and the DARPA Micro-satellite Technology Experiment (MiTEx) [93]. Thus, ring baffles provide a simple, low-risk and passive sloshing mitigation method for ARGOS Mission Spacecraft.



Figure 24: Image of a ring baffle within a propulsion tank. Reproduced from [93]

### Mass and Volume Budget Compliance

Given the above analysis for tank sizing and dimensioning as well as feed system design, the total mass and volume of the Propulsion subsystem for each ARGOS Mission Spacecraft can be determined. Summaries of ARGOS Mission spacecraft masses and volumes are provided in Tables 41 and 42, respectively. Positive margins remain for all spacecraft mass and volume figures, indicating that the PROP subsystem has successfully satisfied all mass and volume constraints in addition to its other requirements. This indicates a successful closing of the PROP Subsystem design loop.

Units [kg]	Tanks	Thrusters	Feed System	Total	Budget	Margin
HOWLL	4.65	1.52	0.43	6.60	7.7	14.3%
WOOF	4.65	1.52	0.43	6.60	7.7	14.3%
PACK-C	2.84	1.52	0.27	4.62	5.3	12.8%
PACK-E	1.14	1.52	0.16	2.82	5.3	47.9%

Table 41: Propulsion Subsystem Mass Budget Compliance [79]

Units [cm <sup>3</sup> ]	Tanks	Thrusters	Feed System	Total	Budget	Margin
HOWLL	3,921.34	221.32	341.76	4,484.43	5300	15.3%
WOOF	3,921.34	221.32	341.76	4,484.43	5300	15.3%
PACK-C	2,396.12	221.32	209.23	2,826.67	3300	14.3%
PACK-E	954.48	221.32	82.98	1,258.77	3300	61.9%

Table 42: Propulsion Subsystem Volume Budget Compliance [79]



## 8 ADCS Design

### 8.1 Subsystem Overview

The Attitude Determination and Control System (ADCS) subsystem maintains precise orientation and stability of the ARGOS satellites throughout the mission. It ensures the satellites remain stable by adjusting for external forces, torques, and drift, and it can alter their orientation when necessary to meet mission objectives or support other subsystems. The control and maneuverability of satellite attitudes are pivotal for achieving mission goals, as detailed in sections on objectives and constraints (8.2 & 8.4).

For the HOWLL, WOOF, and PACK satellite types, the ADCS subsystem closely interfaces with nearly all other subsystems. Stability, attitude determination, and control are vital for the success of many subsystems and the overall mission. This subsystem orients the satellites to establish specific communication links, accurately track other satellites, and enable other subsystems to meet their requirements. Moreover, satellite size, volume, mass, and power considerations must be coordinated with other subsystems due to satellite size, impacting sensor and control choices, power needs, and maneuverability.

Operational requirements for the ADCS subsystem include three-degree rotational capabilities, precise location and orientation to determine the mission's following adjustments, and adequate power and propellant for maneuvering and momentum dumping.

Close interaction between the ADCS subsystem and other subsystems, especially those with specific orientation needs, is essential to the mission's success. These primarily include the Payload for object tracking, Power for electricity generation, Communications for data relay, and GNC for orbit correction. Furthermore, collaboration with the Propulsion subsystem was integral for momentum dumping and Structures to determine the proper orientation of the attitude control and determination components onboard the spacecraft.

### 8.2 Subsystem Objectives

The ADCS objectives are outlined below and are aligned with each tier of the mission-level objectives outlined in the RFP [1] as follows:

**Tier 1 Mission Objective:** The related Tier 1 ADCS subsystem objectives are as follows:

- Ensure precise and reliable attitude determination using sensors, providing critical data for the control systems to make necessary adjustments.
- Efficiently manage attitude control to stabilize rotations, counteract external forces or torques, and adjust attitude according to mission requirements, including power, communication, object tracking, and rendezvous maneuvers.
- Continually maintain the satellite's attitude and orientation throughout the mission lifetime.
- Demonstrate reliable performance in various environments and under external influences to ensure mission success.

**Tier 2 Mission Objective:** The related Tier 2 ADCS subsystem objectives are as follows:



- Ensure proper satellite orientation to provide a secure and seamless communication network across Cislunar space.
- Foster effective collaboration with other subsystems and optimize utilization of space, mass, power, and budget to enhance the mission's success.

### 8.3 Subsystem Requirements

Few subsystem requirements have changed since the last design iteration. However, many of the requirement values have been confirmed and updated to accurately represent the numerical requirements for this mission. A comprehensive list of requirements can be accessed in the ADCS section of the "Requirements Spreadsheet" Google Sheet [6].

Functional requirements consider mission and tier-related requirements such as pointing, jitter, momentum, and control of each of the spacecraft. In the case of ADCS, these specifications define expected operational parameters and accuracy ranges, guiding decisions regarding sensor selection and momentum storage device implementation.

Performance requirements specify precise objectives for each function, detailing desired outcomes that can be tested and achieved. This includes tasks such as accuracy, frequency, and timing of each orientation change or correction through various maneuvers and attitude determination utilizing sensors and algorithms.

Table 43 gives selected examples of new and updated requirements on the performance and functionality of the ADCS subsystem.

Table 43: Selected requirements for the ADCS subsystem [6].

Requirement ID	Requirement	Rationale	Verification, Validation Method
ADCS-F-001	The ADCS subsystem must obtain a 1-sigma average pointing value of at least 0.5 deg for all satellites.	The capability to point the spacecraft in the desired direction with a certain accuracy is necessary to maintain the intended trajectories, communication channels, and object tracking ability.	Theoretical Analysis
ADCS-F-003	The ADCS subsystem shall have a minimum torque ability of 5 mNm.	This lower limit for the Reaction wheels ensures minimum operability to satisfy mission-level requirements.	Theoretical Analysis

*Continued on next page*



Table 43 – *Continued from previous page*

Requirement ID	Requirement	Rationale	Verification, Validation Method
ADCS-F-007	ADCS must be able to point all satellites towards each other for communication at least 1% of the operational time.	As part of the Tier 2 mission requirement, in order to provide a reliable and functioning communication network, the orientation of the satellites needs to be such that signals and information can be exchanged.	Literature
ADCS-F-010	The ADCS subsystem must align the satellites so they can generate maximum power for at least 90% of the time.	Due to the mass constraints on the satellites, our batteries are so small that they can only function the essential instruments during eclipse times. Otherwise the power must be generated via solar panels.	Theoretical Analysis
ADCS-F-011	The ADCS subsystem must be able to adjust for external disturbances via thrusters at a maximum of 5% of the time.	External disturbances will change the overall momentum of the satellite, which then requires a certain amount of momentum storage to be lost. This needs to be accounted for.	Analysis
ADCS-P-001	The ADCS subsystem shall perform slewing maneuvers outside of the resonance frequency bands of 5 deg/second.	Avoiding resonance frequency bands is necessary to reduce structural resonance, which could degrade the spacecraft integrity.	Theoretical Analysis
ADCS-P-005	The ADCS subsystem on all satellites shall be operational for at least 10 years.	It is known that the reaction wheels endure demanding missions. Therefore, it is important to ensure operational life for the mission lifetime to complete the mission.	Error Analysis

## 8.4 Subsystem Constraints

Within the framework of our mission, the ADCS subsystem operates within specific constraints and limitations shaped by mission design, inter-subsystem collaboration, and environmental conditions. These constraints persist from the previous reports and are reiterated here for clarity.

Mission-driven constraints encompass parameters such as mass (3.25kg for HOWLL, WOOF, and PACK satellites); volume (at most  $1250\text{ cm}^3$  for all satellites); average (at most 3W for all satellites) and peak power consumption (at most 20 W for all satellites); computational capabilities (at most 50 Mbps); and cost (at most \$25,641,000 for all satellites). These constraints vary be-



tween the different satellite types in our mission. For instance, the HOWL and WOOF satellites, crucial for object tracking and communication, necessitate high accuracy and precise controls. Conversely, the smaller PACK satellites require smaller-scale sensors and control systems. Additionally, budget considerations play a role in selecting ADCS subsystems, balancing precision with cost-effectiveness. Collaboration with other subsystems is ongoing to establish budgetary allocations for each satellite type's ADCS subsystem. Moreover, the ADCS subsystem's power and computational requirements must align with overall power constraints, prompting ongoing discussions with other subsystems to define acceptable ranges.

Environmental constraints, including gravitational fields, magnetic fields, radiative environments, temperature ranges, and launch conditions specific to Cislunar space, further influence ADCS subsystem design.

Refer to the Requirements Spreadsheet [6] for a comprehensive constraints overview.

## 8.5 Subsystem Drivers

For the ADCS preliminary design report, the drivers maintain more or less the same; they have been restructured here for a better understanding.

- **Safety and Reliability:** This is the main driver of the design approach. Just like any other subsystem, the safety and reliability of the ADCS operation is the highest priority. Otherwise, the mission would fail. Hence, design choices were made based on redundancy and probability of failure. A careful literature review was made, and systems were chosen with this driver in mind. This includes external as well as internal disturbances.
- **Mission-Level Requirements:** Meeting these requirements is another highly prioritized driver. They involve the trace-down requirements for other subsystems, especially for Payload and Communications. Special effort was made to design an ADCS that is agile, meaning that maneuvers are performed fast and with high precision.
- **Size, Mass, and Power:** To free up space for the other subsystems, especially for Power and Propulsion, who asked for mass and volume trades, attention was paid to picking actuators and sensors that reduce mass, size, and power. While there are no direct limits, ADCS aims to keep them as low as possible.
- **Cost:** Another driver that was considered was the cost. Although ADCS expects not to exceed their assigned budget (See Budgets Spreadsheet [96]), it is still important to remember, especially since the Launch Vehicle design has changed their approach drastically.

## 8.6 Subsystem Design Approach

Moving from the Preliminary Design Review (PDR) [13] to this final report, the control modes and requirements were finalized, enabling the ADCS subsystem to confirm their design choices and ensure the satisfaction of the subsystem's functionality. As part of this, and following a similar design approach as in the PDR, the following choices have been confirmed for the ADCS subsystem for the ARGOS missions.

As mentioned in previous design iterations, the ADCS subsystem will not be off-the-shelf due to the complexity of this mission and the unique conditions of Cislunar space. To be more precise,

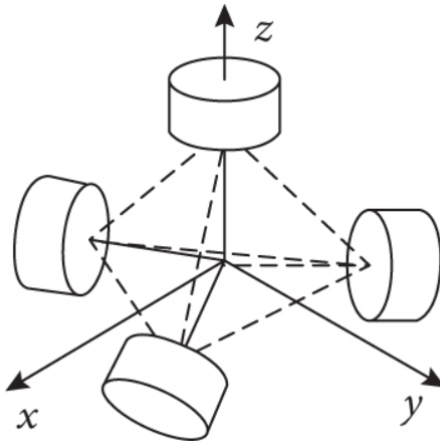


Figure 25: 4-RW Tetrahedral Structure [97].

the complex gravitational environment and lack of magnetic field make magnetometers infeasible, which are the basis for off-the-shelf ADCS systems. We will outline the design choices made here.

As part of our attitude control, the satellites will be controlled via zero-momentum three-axis stabilization as opposed to gravity-gradient or spin stabilization with the use of reaction wheels (RW) as our main actuators and cold gas thrusters to desaturate these wheels. We decided against control moment gyroscopes due to added complexity in the computation, singularity failures, and mass constraints (more than 3.5 kg). To compensate and ensure our mission safety, we will have a four reaction wheel configuration in a tetrahedral structure as seen in Fig.25. This enables the ADCS subsystem to be operational even if one RW fails. The RWs that were chosen for the mission are the AAC Clyde Space RW400 for the HOWLL and WOOF satellites and Blue Canyon RWP100 for both PACK satellites. The analysis will detail the satisfaction of all mission and subsystem requirements.

As for our attitude determination, we chose a combination of 6 sun sensors, 2 star trackers, and 1 inertial measurement unit (IMU). Each component individually would be enough to provide accurate information on satellite orientation; however, superposing multiple measurements ensures the maximum reliability, accuracy, and precision that we wanted for our system. These measurements will be superposed using a TRIAD algorithm with an extended Kalman filter to account for any non-linear errors and noise. We chose the CubeSpace Satellite Systems CubeStar GEN for our star tracker, the Cielo Inertial Solutions IMU 42-XP for our IMU, and the NewSpace Systems NCSS-SA05 for our sun sensor. Again, the formal analysis will provide details about these choices.

This design iteration we included the additional torque due to the solar panels, giving an even more in-depth analysis of the moment of inertia and torque requirements. Furthermore, we finalized our control modes in Table 44 to give a detailed plan of when and where to switch. As part of this a parametrized fuzzy-logic controller was selected over traditional controllers such as proportional integral and derivative (PID) or linear quadratic regulator (LQR). We also refined our external disturbances to give a more detailed approximation on momentum storage and momentum dumping capabilities. Following this, we defined the internal disturbances to ensure that the mechanical systems do not produce any disturbances that could impact the Payload measure-



ments, since the Payload camera is very sensitive. Finally, we went through budget compliance and failure analysis to ensure operability and compliance with the overarching mass, volume, power and costs budgets. For failure, HOWLL and PACK-C were considered to represent the worst-case scenario, hence if the ADCS system on those satellites is found operable, PACK-E and WOOF would also be.

## 8.7 Formal Analysis

### 8.7.1 Control Modes

The table below gives an overview of the different control modes the ADCS subsystem will operate in and switch between. These are directly related to the mission-tier objectives and the demands of the other subsystems. After extensive discussion with the other subsystems, all the values for the percentage in operation have been confirmed. These objectives drive our design, especially as part of our attitude control actuators' momentum storage and the ADCS subsystem's power requirements.

Control Mode	Duration Requirements	Percentage
Orbit Insertion	Until s/c is in desired orbit	100%
Object Tracking	Once every 10 min	13%
Communication	Once every 30 min	3.3%
Power	Remainder of available time	90%
Disturbance Correction	Once per s/c orbit	5%

Table 44: Different control modes needed for each spacecraft

It must be noted that these percentages overlap. To fulfill the requirements of other subsystems, the satellite will need to perform multiple tasks simultaneously, meaning it will be operating in multiple modes simultaneously.

As part of this, the ADCS subsystem has set an upper and lower boundary on the slewing capabilities. ADCS should be capable of performing a rotation of 180° within 60 seconds, which relates to a max. slew rate of 3 deg/sec. Any faster than this, the solar panels will move past their frequency limit and will rip off, meaning a satellite failure. Furthermore, as part of the thermal balancing defined by ADCS-F-016, the lower bound is a slew rate of 0.01 deg/sec. This was found to be adequate for maintaining the thermal balance. The torque requirement based on these requirements will be given later.

### 8.7.2 Disturbances

As outlined in the Design Approach, addressing external perturbations is crucial to ensuring the robust performance of the ADCS subteam within the demanding Cislunar environment for the entire mission duration. This section describes the calculations required to quantify the impact of external perturbations on the system and determine the control systems necessary for maintaining a stable attitude.

#### Gravity-Gradient Torques (GGT)



Modeling GGT involves considering it a constant torque exerted on the spacecraft due to gravitational forces, primarily influenced by its inertia and orbital altitude. The following equation is used to calculate the torque resulting from gravity-gradient forces [8]:

$$T_g = \frac{3\mu}{2R^2} |I_z - I_y| \sin(2\theta) \quad (12)$$

Here,  $T_g$  represents the maximum gravity torque,  $\mu$  denotes the Moon's gravity coefficient ( $4.91 \times 10^{12} \frac{m^3}{s^2}$ ),  $R$  stands for the orbit radius ( $1.74 \times 10^7 m$ ),  $\theta$  signifies the maximum deviation of the Z-axis from local vertical (assuming maximum deviation from axis), and  $I_z$  and  $I_y$  denote the moments of inertia about the z and y axes in  $kg * m^2$  [98].

With the above equation, we estimate that the effects of gravity-gradient torque on the HOWLL, WOOF, and PACK satellites could reach up to  $4.52 \times 10^{-8} Nm$ . While this value may initially appear small, its cumulative impact over the mission's duration and the satellites' operational lifespan of 10 years is significant, requiring careful consideration in mission planning and ADCS design.

### Solar Radiation Torques

To quantify the influence of Solar Radiation Pressure (SRP), the following equation can be applied [8]:

$$F = v \frac{F_s}{c} A_s (1 + q) \cos(I) (c_{ps} - c_g) \quad (13)$$

Here,  $F_s$  denotes the Solar constant ( $1367 W/m^2$ ),  $c$  represents the speed of light ( $3 \times 10^8 m/s$ ),  $A_s$  stands for the surface area,  $c_{ps}$  signifies the location of the center of solar pressure,  $c_g$  represents the center of gravity,  $q$  denotes the reflectance factor (0.8), and  $I$  stands for the angle of incidence of the sun srp.

Utilizing this equation, we estimate that the effects of SRP on the HOWL satellite and the PACK satellites (assuming equivalent maximum surface areas) could amount to approximately  $4.88 \times 10^{-7} Nm$ . Despite appearing minor, this force can significantly affect the drift and attitude of the satellites, thus necessitating careful consideration in satellite design and attitude regulation strategies.

The table below shows the calculated results and determines the values for total torque exerted on the spacecraft by external forces.

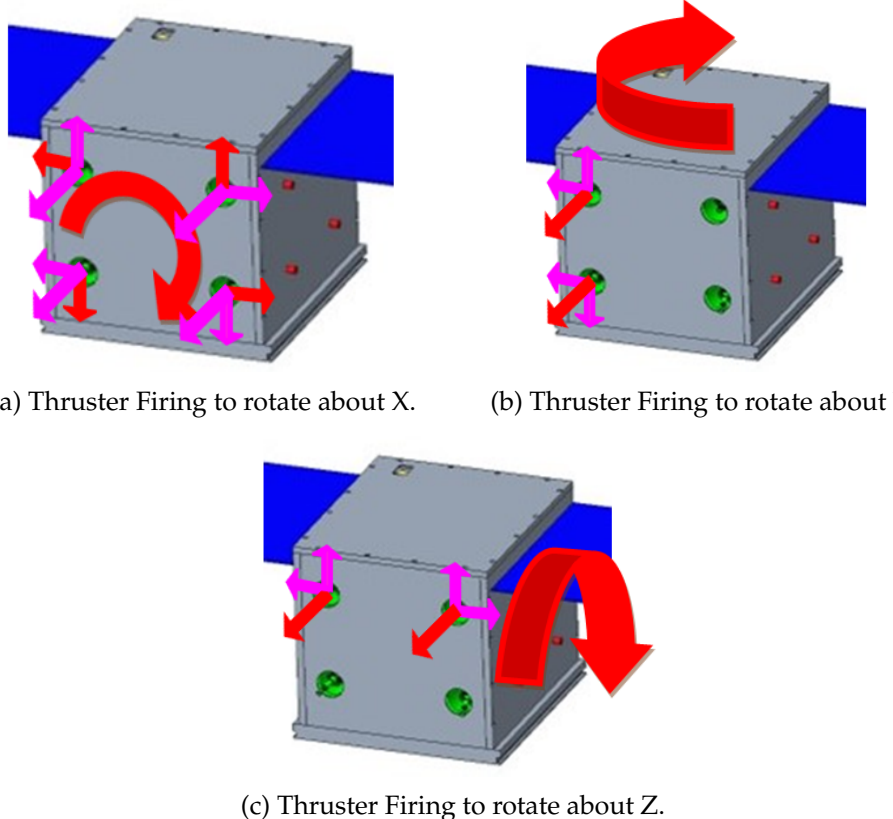
Satellite	Gravity-Gradient Torque (Nm)	Solar Radiation Torque (Nm)	Sum of Torques
HOWLL	$2.09 \times 10^{-7}$	$2.23 \times 10^{-5}$	$2.23 \times 10^{-5}$
PACK-C	$4.27 \times 10^{-7}$	$1.74 \times 10^{-5}$	$1.75 \times 10^{-5}$

Table 45: External perturbations acting on each satellite.

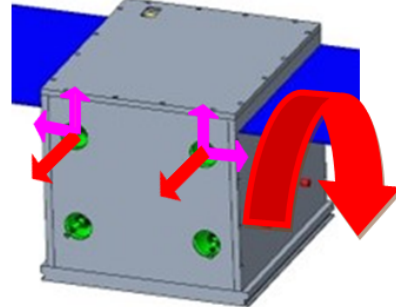
The table shows that the external forces impacting the spacecraft constitute only a small fraction of the total torque management and control necessary to ensure precise pointing and observation of



the target. Considering these external perturbations alongside internal system dynamics is crucial to developing effective strategies for maintaining mission objectives.



(a) Thruster Firing to rotate about X.      (b) Thruster Firing to rotate about Y.



(c) Thruster Firing to rotate about Z.

Figure 26: Firing of Thrusters for Momentum Dumping along each Axis.

The external disturbances, the time when ADCS can use the thrusters, and the amount of propellant ADCS can burn at once (both given by the Propulsion subsystem) will drive the momentum storage capabilities of our subsystem. Based on the Propulsion subsystem, ADCS expects to dump accumulated external disturbances every orbital period, preferably during eclipse times due to the shutdown of most other subsystems. Given the previous values for our torques and the different orbital periods, we determined the net momentum difference per period. The values for each satellite are given below:

- **HOWLL:**  $4.57 \times 10^{-1}$  Nms
- **WOOF:**  $4.42 \times 10^{-1}$  Nms
- **PACK-C:**  $7.81 \times 10^{-3}$  Nms
- **PACK-E:**  $7.54 \times 10^{-3}$  Nms

This gives the upper bound the momentum storage the ADCS subsystem needs for its design choice. To calculate the mass of propellant required for such dumping, we collaborated with the Propulsion and Structures subsystem to look at the thruster configuration. Fig. 26 is a schematic of using the cold-gas thrusters to momentum dump in each direction, where the thruster vector



is broken down into its three components. The red component indicates the main drive of the rotation, while the pink one indicates the additional thrust due to the placement and orientation of the nozzle. The angle between the nozzle and the normal plane of the satellite face is  $25^\circ$  as specified in the Propulsion section, and the angle the shadow of the nozzle makes with respect to the y-axis (up direction) is  $45^\circ$ . The distance is specified by Propulsion in Fig. 16. It is important to note that due to this configuration, rotating the satellite about the x-axis requires a certain firing logic, specified by a study from 2015 as mentioned by Prop in Section *Thruster Selection* [81].

Understanding this configuration, ADCS can calculate the time required for momentum dumping to ensure operation below the 5% defined by ADCS-F-012 in the Requirement Spreadsheet [6]. The results are given below:

Table 46: Satellite Operation Times

Satellite	Time_X (secs)	Time_Y (secs)	Time_Z (secs)	Operation Time (%)	Propellant Needs per Cycle (g)
HOWLL	$1.65 \times 10^2$	$2.37 \times 10^2$	$2.80 \times 10^2$	$9.53 \times 10^{-2}$	3.41
WOOF	$2.28 \times 10^2$	$3.27 \times 10^2$	$3.86 \times 10^2$	$9.55 \times 10^{-2}$	2.03
PACK-E	2.62	4.30	4.30	$1.09 \times 10^{-1}$	$5.61 \times 10^{-2}$
PACK-C	2.62	4.30	4.30	$1.09 \times 10^{-1}$	$5.61 \times 10^{-2}$

As seen in the Table 46, the operational times for momentum dumping for each period are well below the 5% margin given by the requirements, comfortably satisfying that requirement. Furthermore, this also frees up operational times for other modes, such as Payload or Power generation. Additionally, we are well within the limits of the propellant mass defined by the Propulsion subsystem.

### 8.7.3 Spacecraft Control

Given the stringent requirements for orienting the spacecraft from the Power, Payload, and Communications subsystems, enough torque was generated to quickly change orientation as desired. To properly account for these different control modes and ensure that all subsystems were able to meet their requirements, and given the pointing accuracy of the payload sensor, a slew rate of 10 deg/sec was used for the PACK satellites. A slew rate of 5 deg/sec was used for both the HOWLL and WOOF satellites. This is well within the limits of the 3 deg/sec requirement set previously; hence, for these torques requirements, we are well within the limits and redundant.

The following Moment of Inertia (MOI) was provided from a detailed analysis conducted by the structures team and incorporates all of the different mass components and placements within the satellites.

Satellite	Ix ( $kgm^2$ )	Iy ( $kgm^2$ )	Iz ( $kgm^2$ )
HOWLL	0.580	0.625	0.652
PACK-C	0.157	0.278	0.295

Table 47: Moment of Inertia for stowed configuration



Several different MOI calculations were considered, as both spacecraft would experience a significant change in MOI when the solar panels are deployed compared to when they are stowed. Both satellites will remain in their deployed state for most of the mission lifetime, as the solar panels must continuously generate power for the spacecraft.

Satellite	$I_x (kgm^2)$	$I_y (kgm^2)$	$I_z (kgm^2)$
HOWLL	0.634	0.699	0.724
PACK-C	0.215	0.292	0.343

Table 48: Moment of Inertia for deployed configuration

In addition to determining the MOI for each satellite in its stowed and deployed states, torque needs to be determined based on the MOI and the desired angular acceleration of the system. The torque calculations would further influence the decision-making regarding the hardware of these spacecraft and their ability to contribute to completing mission requirements. Given the requirements of the other subsystems, a desire to have the spacecraft rotate 180 deg in 60 seconds would adequately allow all other subsystems to be functional. Using the following equation, the torque was calculated:

$$T = \alpha * MOI$$

Where T is the torque,  $\alpha$  is the angular acceleration, and MOI is the moment of inertia.

The results are summarized in the Table below:

Satellite	$T_x$	$T_y$	$T_z$
HOWLL	0.0290	0.0313	0.0326
PACK-C	0.00785	0.0139	0.0148

Table 49: Torque for stowed configuration

As the MOI changes for the stowed and deployed configurations, so does the torque required for each spacecraft. Below are the torque values required for the deployed configuration of the HOWLL and PACK-C satellites.

Satellite	$T_x$	$T_y$	$T_z$
HOWLL	0.0317	0.0350	0.0362
PACK-C	0.0108	0.0146	0.0172

Table 50: Torque for deployed configuration

#### 8.7.4 Hardware Determination

Based on the calculated MOI and torques from the previous section, the selection of hardware for all the satellites is crucial for the mission's success and the spacecraft's functionality.



Considering that the ADCS system is comprised of attitude determination and control, several different hardware systems need to be integrated into the spacecraft to determine and control the spacecraft's orientation in the Cislunar environment.

To determine the satellites current orientation in space, it needs to be able to keep track of its change in orientation relative to itself, as such the use of an IMU is used to provide relative attitude determination for the spacecraft. The following table is a trade study conducted on several different viable IMU options with extensive space heritage. As one can see, the Cielo Inertial Solutions IMU 42-XP was selected for its dynamic range, low angular random walk, bias stability, low mass, and high data rate. All of these characteristics made this the ideal choice for the suitability of both the HOWLL, WOOF, and PACK satellites.

Provider	Name	Input Voltage	Power consumption (W)	Dynamic Range (deg/sec)	Angular Random walk (deg/vh)	Bias Stability (deg/hr)	Scale Factor Stability (ppm)	Mass (Kg)	Data Rate (Hz)
Northrup	LN-200S	5-15	12	1000	0.07	1	100	0.748	400
Tamagawa	TA7584Series	15-28	3.5	5-10		5			1.2
Airbus	ASTRIX120	22-50	6	10-140	0.0016	0.01	10-200	6.5	
Airbus	ASTRIX 200	22-50	5.5-7.5	5-15	0.0001	0.0005	15-200	12.7	
Cielo inertial solutions	IMU 42-CV	5-15	15	1000	0.07	1	100	0.84	100-4800
Cielo inertial solutions	IMU 42	5-15	15	2000	0.02	0.5	150	0.84	100-4800
Cielo inertial solutions	IMU 42-XP	5-15	15	1000	0.008	1	150	0.84	100-4800

Table 51: COTS IMU trade study [99]

The table below shows a trade study conducted on different star trackers to be used on these spacecraft. Each spacecraft in this mission is equipped with two star trackers to allow for redundancy within the system if either star trackers fail during the mission lifetime. Please refer to the structures and materials section 15.6.2 for the specific orientation of these star trackers onboard the spacecraft.

Shown in the table below, the CubeSpace Satellite Systems CubeStar GEN2 was determined to be the ideal star tracker due to its accuracy, wide field of view, and wide operating temperatures, satisfying the pointing accuracy and history requirements (ADCS-F-006, ADCS-F-001).

Provider	Name	Accuracy (arcsec)	Update Rate (Hz)	Slew Rate (deg/sec)	FOV (deg)	Power Consumption (W)	Size	Mass (g)	Operating Temperature
Kongsberg NanoAvionics	ST-1	1.5	5 hz	1.5 deg/sec		1.2		108	-30 to 40 C
AAC Clyde Space	ST200	30	5 hz	0.6 deg			29 x 29 x 38.1 mm	42	-20 to 40 C
ARCSEC	Sagitta Star Tracker	2	5 hz		40	1.3	95 x 50 x 45 mm		
Berlin Space Technologies	STAR TRACKER-ST200		5 hz	1 deg/sec		0.55 to 0.67	30 x 30 x 39 mm	40	-20 to 40 C
CubeSpace Satellite Systems	CubeStar GEN 2	0.02 to 0.06	1 hz	0.3	24 to 59.4	271 mW	35 x 49 x 24 mm	47	-35 to 80 C

Table 52: COTS Star Tracker trade study [99]

As previously mentioned, the star tracker is used in conjunction with sun sensors to provide accurate absolute attitude determination for the spacecraft. Each satellite would be equipped with six sun sensors, one on each face. These sun sensors take in the incident angle of the solar rays coming into the focal view of the sun sensor; the angle of the incoming light rays is used to determine the orientation of the sensor in relation to the sun. The six sun sensors allow for redundancy and accurate readings of the spacecraft's position in relation to the sun at different orientations.



The table below provides a trade study on the different sun sensors with adequate space heritage. As we can see, the NewSpace Systems NCSS-SA05 was chosen for its high accuracy, wide field of view, and quick update rate while also being able to optimize its mass.

Provider	Name	Accuracy (deg)	FOV (deg)	Update Rate (Hz)	Mass (g)	Supply Voltage
CubeSpace Satellite Systems	CUBESENSE	0.2	180	2	30	3
Antrix	4pi sun sensors	5			50	
NewSpace Systems	NCSS-SA05	0.5	114	10	5	5
NewSpace Systems	NFSS-411	0.1	140	5	35	5-50
Solar MEMS	nanoSSOC-D60	0.5	60		6.5	3.3-5
Space Micro	5MP		14-89		1000-2500	5
Solar MEMS	ACSS	1	60		40	15-30

Table 53: COTS Sun Sensor trade study [99]

After finalizing these attitude determination sensors, the use of a control board is essential to take all of these measurements and determine the amount of torque needed to be applied to the system to move the spacecraft from its current position to its desired position. The following table is a trade study on the different control boards with extensive space heritage.

As shown in the table, the CubeSpace Satellite Systems CUBEADCS Gen 1 was used for our specific mission due to its extensive capabilities and onboard equipment.

Provider	Name	Equipment	Mass (kg)	Size	Power Consumption (mW)	Thermal (Celcius)
CubeSatShop	MAI-400	3-axis MEMS accelerometer, 3-axis MEMS gyro, 3 sets of reaction wheels circuitry		8.6 x 8.8 cm		
Berlin Space Technologies	IADCS-100	reaction wheel, magnetorquer, star tracker, gyro, magnetometer, accelerometer	0.4	105 x 91 x 32 mm	1150	-20 to 40
CubeSpace Satellite Systems	CUBEADCS Gen 1	3-axis MEMS rate sensor, magnetometer, sun sensors, sun & earth sensors, magnetometer, star tracker	0.5	90 x 96 x 57 mm	570 to 2300	-10 to 60
Tensor Tech	ADCS10	magnetorquer, sun sensor, magnetometer	0.14	0.2U volume	1000	-20 to 60
AAC Clyde Space	iADCS200	Reaction wheel, magnetorquer, IMU	0.4	95 x 90 x 32 mm	1400	-45 to 85

Table 54: COTS Control Board trade study [99]

For the choice of reaction wheels, we performed the following trade study, given the torque and momentum requirements, while keeping reliability in mind. As seen in the table below, the AAC Clyde Space RW400 was used for the HOWLL and WOOF satellites, while the Blue Canyon RWP100 was used for both PACK satellites. These were chosen for their low mass and power consumption while also providing adequate torque and angular momentum for the spacecraft.



Provider	Name	Torque (mNm)	Angular Momentum (Nms)	Mass (kg)	Speed	Supply Voltage	Power Consumption (W)	Operating Temperature (C)
AAC Clyde Space	RW400	8-12	0.015-0.05	0.197-0.375	5000	2.3-5.25	0.075-15	-40 to 60
Tensor Tech	RS100	1	0.01	0.25		3.3-5	1	-20 to 60
Tensor Tech	RS 200	2	0.02	0.5		3.3-5	2	-20 to 60
Blue Canyon	RWP100	7	0.1	0.33		10-14	0.89	
VECTRONIC Aerospace GmbH	VRW-B-02	20	0.2	1	6000	9-36	45	-20 to 70
TAMAGAWA SEIKI	Reaction Wheel	20	0.3	1.1	5000	5	10	-10 to 50

Table 55: COTS Reaction Wheel trade study [99]

### 8.7.5 Control Algorithms

As mentioned throughout the report, the ADCS subsystem requires several different algorithms to manage the overall attitude of our Cubesats. We begin by outlining the various algorithms and their functions.

#### Control Mode Algorithm

To switch efficiently and effectively between the control modes of our satellite mission, we will be using Parameterized fuzzy-logic controllers as outlined by a comparative study by Bello et al. [100] as opposed to classical Proportional Integral and Derivative (PID) or Linear Quadratic Regulator (LQR) control theories. The study compares the fuzzy-logic controllers in a mission very similar to ours, with fast rotational requirements and high-accuracy Payload requirements. Their study found that the controller operates faster, more reliably, and with less computational costs than the classic PID controller.

It has to be mentioned that this controller used three reaction wheels instead of four, which requires altering the algorithm and optimizing it for four. This can be achieved using NASA guidance for the tetrahedral reaction wheel structure outlined below.

#### Attitude Determination

The critical component for attitude determination is taking the readings from the IMU, the Sun sensors, and the Star trackers and calculating the attitude in a certain reference frame. This requires the comparison between measurements as well as the filtering of any noisy signals coming from the sensor measurements. Literature suggests the application of the Tri-axial attitude determination algorithm (TRIAD) optimized by an Extended Kalman Filter (EKF) for non-linear optimization [101]. Although this increases computational time (25% increase), the mean error was significantly reduced. More specifically, the standard deviation was halved from  $0.6138^\circ$  to  $0.3245^\circ$ . Due to this algorithm choice, we are able to satisfy our ADCS-F-001, which defines the  $1-\sigma$  pointing accuracy requirement to be at most  $0.5^\circ$ .

#### Attitude Control

As mentioned, our Cubesats will use four reaction wheels in a tetrahedral structure to perform even if one of the RWs fails. However, this complicates the algorithm for controlling the space-craft's attitude. However, NASA has published a paper on the performance and changes to the algorithm for reaction wheel arrays [102]. The study finds the performance effectiveness of a 4-wheel setup compared to a 3-wheel one as  $\sqrt{8}/3 = 1.633$ . This means that due to the off-axis



alignment of the reaction wheels, the reaction wheels require 1.633 times the amount of just three reaction wheels. This applies to the momentum storage and the maximum torque. However, our design choices still satisfy the momentum storage requirements given by ADCS-F-004, which requires 0.1 Nms for HOWLL and WOOF and 0.05 Nms for PACK under normal configuration, so 0.163 Nms for HOWLL and WOOF and 0.08165 Nms for PACK with 4 RWs.

Furthermore, as reaction wheels are often the first point of failure for missions due to mechanical wear, it is often "undesirable to have multiple wheels running simultaneously" [102]. To avoid this, vectors in the (n-3)-dimensional null space will be used, which separates wheel speeds.

### 8.7.6 Mass and Volume Budget Compliance

As seen in Table 56, the design choices for the ADCS subsystem on all satellites satisfy the constraints set by mission-level requirements focused focus on the mass and costs budget since, in earlier design stages, there was a major mass that which was then solved through primary payload launches, requiring a significant cost.

Table 56: Compliance Requirements for Satellite Specifications

Compliance	Requirement ID	Budget	Estimation
Mass	ADCS-C-001	Max. Mass HOWLL: 3.25 kg, Max. Mass PACK: 3.25 kg	Total Mass HOWLL/WOOF: 2.28 kg, Total Mass PACK: 1.75 kg
Volume	ADCS-C-002	Max. Volume HOWLL: 1250 cm <sup>3</sup> , Max. Volume PACK: 1250 cm <sup>3</sup>	Total Volume HOWLL/WOOF: 1035 cm <sup>3</sup> , Total Volume PACK: 815 cm <sup>3</sup>
Power	ADCS-C-003	Peak Power: 20W	Max. Power HOWLL/WOOF: 19.4W, Max. Power PACK: 16.1W
Costs	ADCS-C-006	Max. Budget: \$25,641,000	Total Costs: \$700,000
Environmental	ADCS-E-X	Satisfy Launch, Radiation, Temp., and Gravity Environment	All instrumentation are able to withstand the environment at Launch and Cislunar space.
Mission Lifetime	ADCS-P-004 & ADCS-P-005	Satisfy the mission lifeimte requirements and risk analysis.	All instrumentation has excellent flight heritage and MTBF (Mean Time Between Fails) well beyond the scope of the mission.



## 9 Payload Design

### 9.1 Subsystem Overview

The Payload subsystem plays a crucial role in the success of the ARGOS mission by supporting the necessary equipment to meet the high-level mission objectives. Specifically, the Payload subsystem seeks to fulfill the Primary Objective of object tracking and orbit determination through the design and analysis of components [1]. In order to meet this objective, the Payload subsystem is responsible for capturing high-resolution imagery of the Mission Catalog Tier 1 space objects [103].

Payload interacts closely with several other subsystems on ARGOS. Payload relies on the GNC and ADCS subsystems to correctly position and orientation the satellite sensors for optimal data acquisition. Additionally, payload collaborates closely with C&DH for data management and orbit determination. Other subsystems, such as Power, Thermal, and Structure and Mechanisms, will provide the necessary corresponding support to enable the capabilities of the payload instruments.

### 9.2 Subsystem Objectives

The payload subsystem objective derives directly from the overall ARGOS mission objective by providing the necessary capabilities to accurately and frequently track space objects in the Cislunar regime. These capabilities are also important for navigation around space objects, debris mitigation, and communications from Lunar-based assets to Earth-based resources. The payload subsystem will outline the required onboard instruments integral to the success of ARGOS and analyze their capabilities in STK. The objectives are listed as:

1. Outline the required onboard instruments to capture high quality imagery of space objects for precise orbit determination, navigation, and debris mitigation.
2. Conduct research and trade studies to determine the equipment and vendors that are best suited for the ARGOS mission's tracking objective
3. Analyze selected sensors to ensure they meet the mission-level tracking requirements from the Tier 1 Catalog [103]

### 9.3 Subsystem Requirements

The requirements for the Payload subsystem fall into four categories: Functional, Operations, Constraint, and Environment. A full list of requirements is listed on the "Payload" tab of the "Requirements Spreadsheet" with the final values [6]. For the scope of this project, the requirements are focused on addressing precision tracking of the Tier 1 space objects from the Mission Catalog [103]. An example requirement for each category is listed in Table ....

Due to its critical importance in the success of ARGOS, the payload subsystem drives many requirements for other subsystems, such as Power, S&M, and ADCS. For example, the wattage of each sensor was given to Power to be included in their budget, rather than the Power team directing the wattage for each subsystem. Additionally, Payload provided a pointing requirement



in terms of field-of-view (FOV) half angle to the ADCS subsystem. This required close collaboration with dependant subsystems to ensure that Payload's design choices could successfully be supported by various components of the spacecraft bus.

## 9.4 Subsystem Constraints

The constraints for the Payload subsystem are listed as follows:

- Mass & Volume** - Each satellite must weigh no more and be no larger than its given role's allowable weight and size. Although the Payload subsystem drove the final quantitative values for the maximum weight and size, it still functioned to find instruments within the 12U (for PACK) and 27U (for HOWL/WOOF) CubeSat range.

Table 57: Mass and Volume Constraints by Satellite

Satellite	Mass (kg)	Vol (cm <sup>3</sup> )
PACK	1.5	2500
HOWLL	4	5000
WOOF	4	5000

- Power** - For successful operation at all times, each satellite's payload must not use more power consumption than is able to be supported. Although the Payload subsystem drove its exact power requirement through instrument selection, it communicated back and forth with Power to ensure this was feasible.
- Budget** - The entire mission must cost no more than 400 million dollars. Of that 400 million dollars, the payload must use no more than its allotted amount of \$58,275,000, of which it is expected to use about \$5,800,000 for a margin of over \$52 million.

## 9.5 Subsystem Drivers

The Payload subsystem is driven by producing high quality and efficiency data acquisition while remaining within the constraint requirements. Ranked by priority, the drivers are as follows:

- Mass & Volume** - While the payload subsystem has an allotted mass and volume budget, it should strive to use a minimal amount while still prioritizing data acquisition and transmission so that the mass and volume can be used elsewhere if necessary.
- Data acquisition** - While operating within the required mass and volume, the payload subsystem sought to produce the highest quality data possible using the most sophisticated commercial-off-the-shelf (COTS) hardware currently available.
- Reliability & Robustness** - The payload subsystem must be operational throughout the satellites' lifespan, so equipment must be robust enough to operate without severe hardware degradation or technical failures. Therefore, purchasing sensors with strong flight history from industry-leading vendors was prioritized.
- CubeSat Compatibility** - For simplicity in design and integration, it was advantageous to use equipment designed specifically for CubeSats in order not to complicate integration.



5. **Power** - While the payload subsystem has an allotted power consumption budget, it should strive to use a minimal amount (while still prioritizing data acquisition and transmission) so that the power can be used elsewhere if necessary.
6. **Budget** - While the payload subsystem has an allotted budget, it should strive to use as little as possible while prioritizing data acquisition and transmission so that the money can be used elsewhere if necessary.

## 9.6 Subsystem Design Approach

The approach to designing the Payload subsystem began with thorough research on the capabilities of different sensors for object tracking in space. This enabled us to allocate necessary instruments to each spacecraft based on their distance from the space objects. The Lunar satellites, PACK-C and PACK-E will each have one High-Resolution Camera (HRC) onboard. Such instruments are incredibly common on tracking satellites and are now commercial available from many vendors to better support simple design integration [104], [105]. An HRC has high spatial resolution (i.e. pixel identity), which enables accurate monitoring of small-sized objects [106]. Depending on the exact sensor chosen, HRCs can capture light in multiple spectral bands, enhancing object viewing capabilities. An HRC can remain effective even in challenging lighting conditions due to its sensitivity and high dynamic range [107]. An Infrared Sensor (IS) was chosen for the Lagrange satellites, HOWLL and WOOF, as they can provide better resolution in low-light conditions and across a farther range by detecting emitted thermal radiation [108], [109]. Based on our final GNC simulations, the HOWLL and WOOF satellites need to track objects up to 80,000 km away.

Once we outlined the required sensors and instruments for the ARGOS mission, we conducted on-line research on commercially available options. As described previously, our design was driven by finding COTS sensor that were developed specifically for CubeSats. After completing a sensor trade study, we selected the Kairospace 90mm Camera for our HRC on PACK and the Satlantis i-SIM (integrated Standard Imager for Microsatellites) 90 for our IS on HOWLL and WOOF [110], [111]. See Figure 27. The 90mm Camera offered the best resolution within 2kg and 2500 cm<sup>3</sup> constraints and Kairospace has over 20 years of expertise in developing onboard cameras for small satellite missions. The i-SIM 90 was selected due to its incredibly high resolution, though that came at the price of greater mass and volume. However, after communicating back and forth with S&M, we derived 4.5kg and 4000 cm<sup>3</sup> requirements for the Payload subsystem, which was met with the i-SIM 90. This sensor is a two-in-one IS and HRC due to its broad wavelength tracking capabilities, which can provide higher quality data to be processed and analyzed by C&DH. Satlantis is a leading US SmallSat products provider that offers flight proven optical imagers for CubeSats and MicroSats. Given the flight history of both Kairospace and Satlantis products, we felt confident in the reliability of our sensor choices. More details about our trade study is included in the Appendix.



(a) 90mm Sensor on PACK-C  
and PACK-E



(b) i-SIM 90 Sensor on HOWLL and WOOF

Figure 27: Sensors for ARGOS Satellites

## 9.7 Formal Analysis

After selecting on onboard instrumentation and receiving the final STK simulations from GNC, we conducted signal-to-noise ratio (SNR) analyses in STK using the EOIR capabilities. We inserted all of the Tier 1 space objects into the STK simulation and attached the corresponding sensor to each of our satellites. These sensors were outfitted with the specifications in Table 58. Using EOIR Pointing, we allocated certain space objects to each satellite and generated both a report and graph for SNR data for around 10 days. This is roughly the maximum amount of days a simulation can be run with the memory available on our computers, but can be extrapolated to data for 30 days of orbit to give us a good estimate of our SNR values across a month. Since the orbital periods of HOWLL and WOOF are approximately 10 days and PACK is 6 hours, it was deemed sufficient to extrapolate our data given our margins were over 30%. It is important to note here that all of our margins were over 40% and most were on magnitudes of 100% to 1000%.

Table 58: STK Sensor Specifications

Specification	90mm (PACK)	i-SIM 90 (HOWL/WOOF)
FOV Half Angle (deg)	0.75	0.9
Spectral Band Wavelengths (um)	0.4-1.4	0.4-1.7
Effective Focal Length (cm)	55	77.5
Effective Pupil Diameter (cm)	9	7.5

While each space object could potentially be tracked by all four of satellites, this approach would required each satellite to track eight objects at once. To simplify object tracking as much as possible while still maintaining redundancy due to these single points of failure, we split the tracking responsibilities by domain. This mean that PACK-C and PACK-E would be responsible for tracking the LLO and LG objectives, and HOWLL and WOOF would track the L1/L2 Halo and GTO



to L1/L2 Halo objects. As a result, each space object is being tracked simultaneously by two satellites, and each satellite is tracking four space objects at once. These allocations are outlined in Table 59.

We communicated closely with ADCS to finalize the nominal procedure for object tracking. After all our satellites reach their final orbits, they will start space object tracking by properly orienting themselves and capturing images of each responsible space object in sequence. The satellites will capture images of each space object once every 30 minutes. It is estimated that the time necessary to take pictures of all four space objects sequentially is 5 minutes at maximum. Rotating the satellite by 180 degrees (the maximum rotation required) takes around 60 seconds, according to ADCS.

Table 59: Space Object Tracking Allocation

Space Object	Tracked By
LLO 1-3	PACK-C, PACK-E
LG	PACK-C, PACK-E
L1 Halo	WOOF, HOWLL
L2 Halo	WOOF, HOWLL
GTO to L1 Halo	WOOF, HOWLL
GTO to L2 Halo	WOOF, HOWLL

Each STK simulation was ran with a noise profile of O(-18). Simulations were ran for 10 days, with a step size of an hour (3600 seconds) and beginning on August 3rd, 2027 at 00:00:00 UTC. Additional simulations were run for the GTO objects during their corresponding Low Thrust Spiral Phases (Feb 11-21 for GTO to L1 Halo and Feb 23-Jan 4 for GTO to L2 Halo). This allowed us to extrapolate 30 days of data from much shorter simulations.



### 9.7.1 PACK

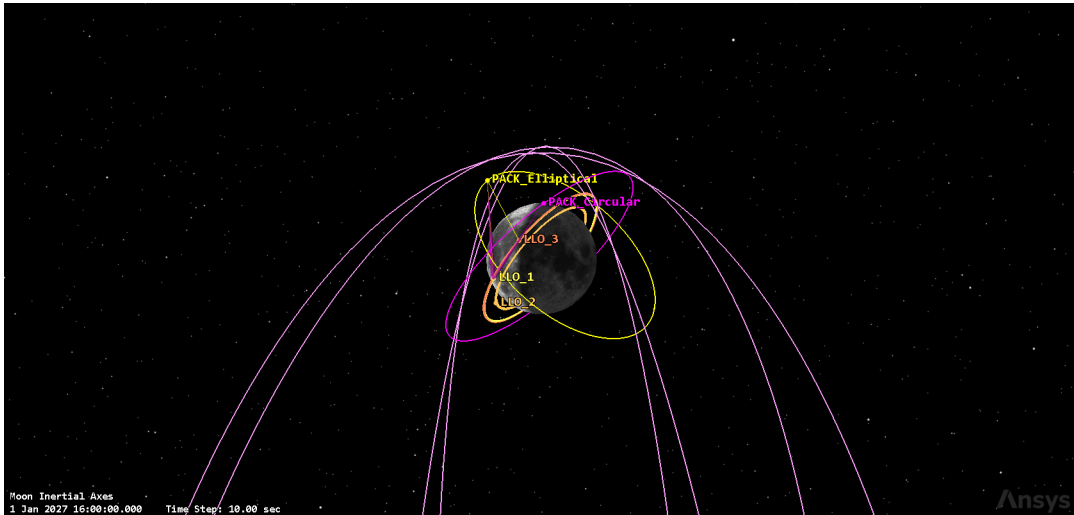


Figure 28: The signal-to-noise ratio of the from the circular orbit PACK satellite (black) and the elliptical orbit PACK satellite when targeting space object lunar gateway

As described above, PACK -C and PACK-E are outfitted with the Kairospace 90mm camera. Given their orbits around the moon, these satellites will be tracking the Low Lunar Orbit and Lunar Gateway objects. In order to ensure redundancy, each satellite will track all four space objects simultaneously. We will describe the STK SNR analysis organized by each space object below.

#### LLO-1

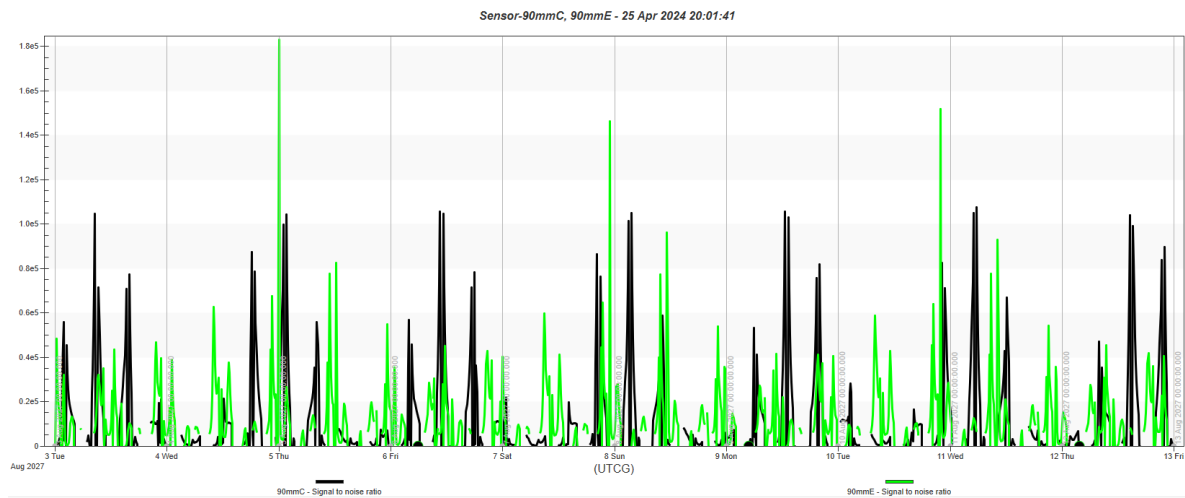


Figure 29: The signal-to-noise ratio of the 90mm Camera attached to our PACK-C and PACK-E satellite and pointed at the LLO-1 space object with a sample rate of 1 hour. The black line represents SNR from PACK-C, while the green line is from PACK-E.

The Low Lunar Orbit-1 space object is successfully tracked by PACK-C and PACK-E and our STK



analyses demonstrate that our requirements are met. Just by briefly observing this graph, we can clearly see we are meeting the requirements by several magnitudes. Our SNR peaks at 180000, which alone satisfies all three of our tracking requirements. Furthermore, the trend this graph follows clearly repeats, making it likely that the pattern will extend to 30 days and indicating that our extrapolation is valid. This also reflects the orbital periods of PACK-C and PACK-E, which are roughly 6 hours. As such, we can use the report version of this graph, which compiles the values at each point on this graph, to calculate the integrated SNR and ensure that the other requirements are met.

Table 60: Tracking requirements for LLO-1

Requirement	Result
Spacecraft must achieve a SNR $\geq 10$ at least once.	Yes
On average, spacecraft should maintain an SNR $\geq 5$ for at least 10 days per month.	Yes, $> 19$ days
Spacecraft should maintain an integrated SNR $\geq 300$ hours per month.	Yes, $> 9000000$

The first requirement was determined by simply finding one data point where the SNR surpasses 10. The second requirement was determined by counting all of the data points where the SNR surpasses 5. The step size is one hour, meaning that each data point can represent one hour of SNR, allowing us to calculate the total amount of time where SNR is greater than 5. For the last requirement, we could simply sum up the values of the data points, since the step size is one hour. For the second and third requirements, values were simply multiplied by three to extrapolate to 30 days. Thus, we can see that our sensor selection satisfies all of requirements for LLO-1.

## LLO-2

Thus, we can move onto LLO-2. By pointing both PACK-C and PACK-E at LLO-2 and generating a plot of SNR for 10 days, we get the following result.

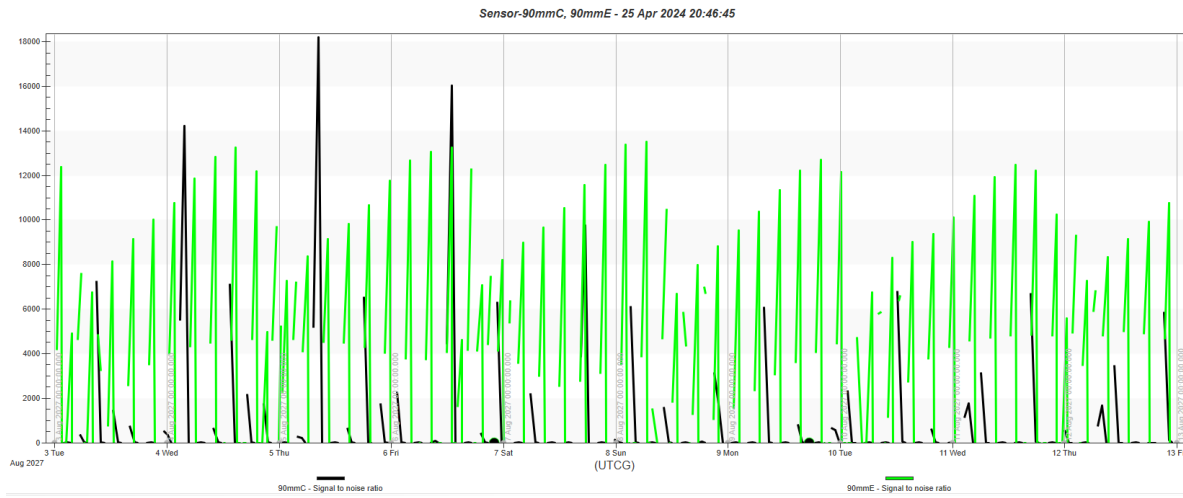


Figure 30: The signal-to-noise ratio of the 90mm Camera attached to our PACK-C and PACK-E satellite and pointed at the LLO-2 space object with a sample rate of 1 hour. The black line represents SNR from PACK-C, while the green line is from PACK-E.

Much like with LLO-2, we can quickly infer that the SNR graph indicates that we are meeting all three of our requirements for LLO-2. The SNR peaks at over 10000, again satisfying all three of our requirements. To guarantee this, however, we can complete calculation to determine specific values for each of these requirements:

Table 61: Tracking requirements for LLO-2

Requirement	Result
Spacecraft must achieve a SNR $\geq 10$ at least once.	Yes
On average, spacecraft should maintain an SNR $\geq 5$ for at least 10 days per month.	Yes, $> 13$ days
Spacecraft should maintain an integrated SNR $\geq 300$ hours per month.	Yes, $> 3000000$

The values for this table were determined using the same procedure for LLO-1. The slight difference in values relative to LLO-1 are likely due to the differences in distances to targets and orbit periods. Regardless of these differences, however, our results indicate that the resulting SNR from our sensor selection is more than satisfactory for LLO-2.

### LLO-3

With LLO-2 validated, we can now proceed with the analysis of SNR for LLO-3. Again, we simulate the SNR with the satellites pointed at the LLO-3 space object, and simulate 10 days of orbit propagation.

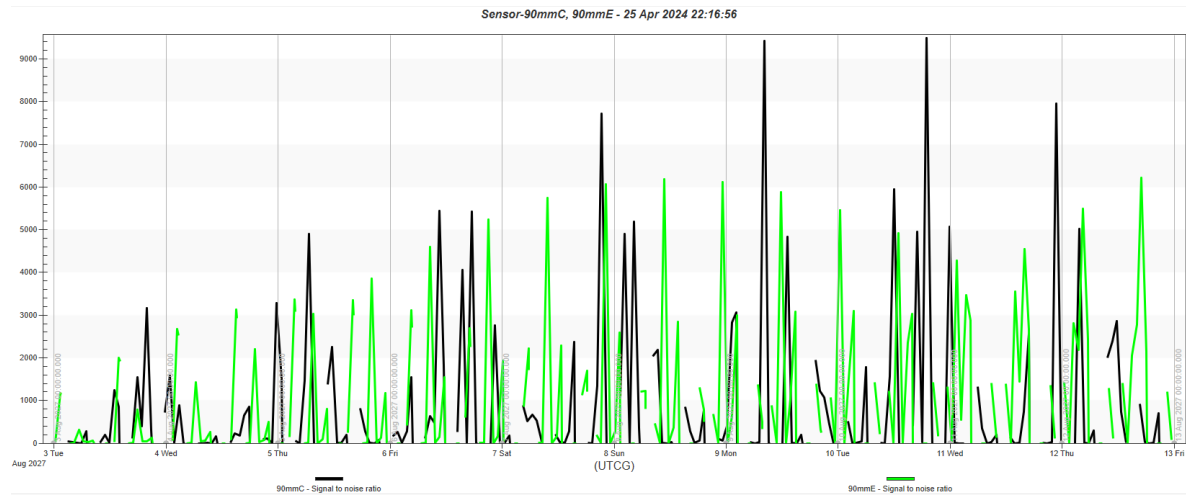


Figure 31: The signal-to-noise ratio of the 90mm Camera attached to our PACK-C and PACK-E satellite and pointed at the LLO-3 space object with a sample rate of 1 hour. The black line represents SNR from PACK-C, while the green line is from PACK-E.

In general, this simulation produced lower SNR values than any of the other LLO space objects. This is rather interesting since it propagates through an orbit that is nearly identical to LLO-1, but has an SNR that is  $\frac{1}{20}$ th of LLO-1's SNR peak. Even still, this SNR peak is over 9000, suggesting that all of the requirements will be met with ease. To confirm this, we can use the report to calculate the desired values for the tracking requirements.

Table 62: Tracking requirements for LLO-3

Requirement	Result
Spacecraft must achieve a SNR $\geq 10$ at least once.	Yes
On average, spacecraft should maintain an SNR $\geq 5$ for at least 10 days per month.	Yes, $> 16$ days
Spacecraft should maintain an integrated SNR $\geq 300$ hours per month.	Yes, $> 1000000$

## LG

As expected, the three LLO objects with similar orbits all meet their respective tracking requirements with relatively similar SNR values. We can now turn our focus to the lunar gateway object, which will likely have much more inconsistent results due to its more eccentric orbit with a perapsis that extends much further from the moon than any of the LLO space objects.

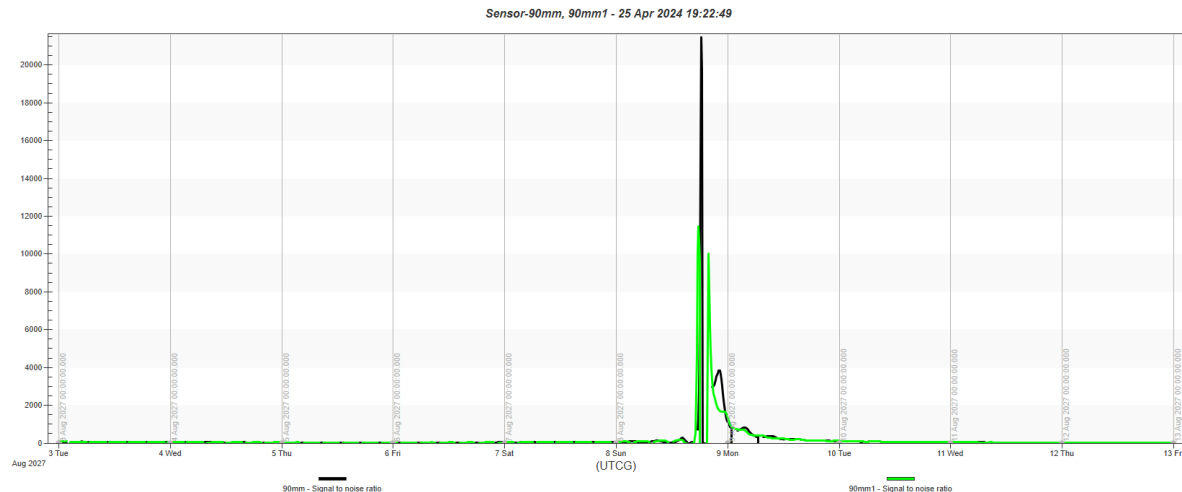


Figure 32: The signal-to-noise ratio of the 90mm Camera attached to our PACK-C and PACK-E satellite and pointed at the LG space object with a sample rate of 1 hour. The black line represents SNR from PACK-C, while the green line is from PACK-E.

These SNR results are quite different from the trends we have been observing in the LLO objects. Because the orbit period for the LG space object is much greater than the LLO objects, we only see one large spike rather than multiple repeating spikes within the ten days of simulation. Furthermore, the single SNR spike surpasses 20000. While there are several days which appear to have a steady SNR of 0, by checking the report we can see that the SNR does not dip lower than 30. We can continue referring to the report to determine to calculate the necessary values for our tracking requirements to validate that our sensors are meeting our requirements.

Table 63: Tracking requirements for LG

Requirement	Result
Spacecraft must achieve a SNR $\geq 10$ at least once.	Yes
On average, spacecraft should maintain an SNR $\geq 5$ for at least 10 days per month.	Yes, $> 16$ days
Spacecraft should maintain an integrated SNR $\geq 120$ hours per month.	Yes, $> 230000$

Based on our calculations, we can confirm that the 90mm camera meets the tracking requirements despite its more eccentric orbit. With all PACK satellites having demonstrated that their sensors output a satisfactory SNR for all four of its assigned space objects when equipped with this sensor, we are confident that the 90mm camera is a great choice for this mission. Because the SNR requirements were met with just the PACK satellites, the Payload team deemed this analysis sufficient for meeting the LG requirements, and as such, WOOF will simply act as a further form of redundancy to Gateway.



### 9.7.2 HOWLL and WOOF

#### L1 Halo

The L1 Halo object is tracked by both HOWLL and WOOF and the SNR simulation was run for ten days with a step time of one hour starting on August 3, 2027, as described above. A .csv file was exported in order to calculate the integrated SNR and number of days that requirements were met. A simple script was run to count the number of hours (i.e. step times) that were above the corresponding SNR value (i.e. 5 or 15), translate this into days, and extrapolate from 10 days to 30 days. As described above, we were unable to run the SNR simulations for more than 10 days due to the processing limits on our computers. However, extrapolating our values was a valid method since the orbital periods of HOWLL and WOOF are approximately 10 days and since our SNR values are meeting requirements by a significant margin. Had our margin been a lot smaller, we could have incrementally run SNR simulations for three sets of 10 days, but this was deemed unnecessary.

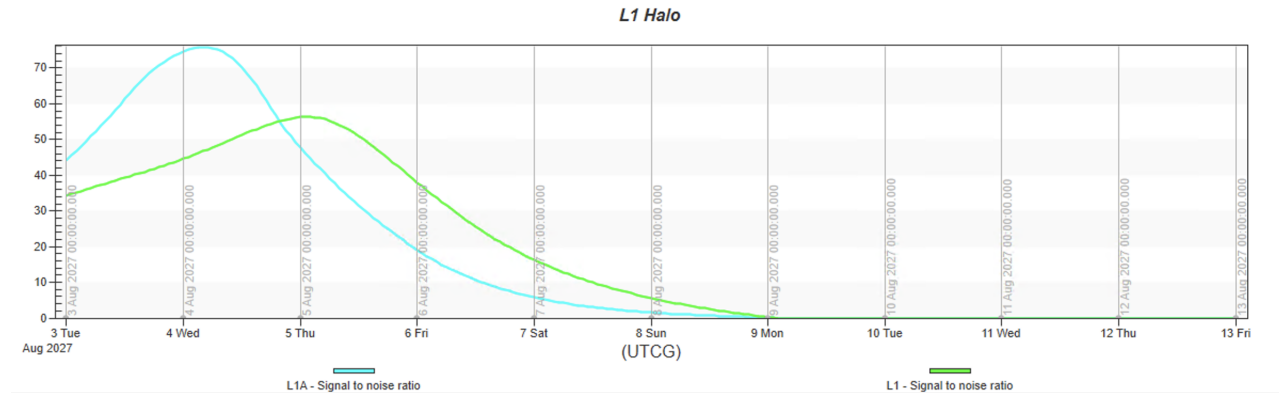


Figure 33: SNR of i-SIM 90 camera attached to HOWLL/WOOF pointing at L1 Halo. Note: Green corresponds to WOOF, and blue corresponds to HOWLL

Table 64 outlines the requirements for the L1 Halo object and our results. Given our significant positive margin in the SNR values, we are confident that the i-SIM 90 is a great choice for the HOWLL and WOOF objects.

Requirement	HOWLL	WOOF	Total	Margin
Spacecraft must achieve a SNR $\geq 15$ at least 7 days during the Low Thrust Spiral phase.	6.875 days	6.21 days	13.085 days	86.9%
On average, spacecraft should maintain an SNR $\geq 5$ for at least 7 days per month after insertion.	9.17 days	10.04 days	19.21 days	174.4%
Spacecraft should maintain an integrated SNR $\geq 150$ hours per month.	72,484 hours	45,455 hours	117,939 hours	785%

Table 64: SNR Requirements for L1 Halo

#### L2 Halo



Unfortunately, while conducting SNR analysis for the L2 Halo object, we achieved no results as our graphs and reports gave values of 0.0000 for all time. There are several possible reasons for this—two being our choice of sensor or orbits for HOWLL and WOOF. However, after replacing our i-SIM 90 with three alternative choices, we still got no values. Having L2 Halo tracked by PACK did not resolve the issue either. Increasing the sensitivity by a magnitude of 6 did not work. We also tried changing the reflectivity of the object, but still received 0.000.

Therefore, we strongly believe that it was not a product of our design choices, but likely a fatal error in the STK file itself. We are confident that our design is able to meet the SNR requirements, but due to the limited scope of this project, we were not able to investigate in enough depth to resolve the issue. Furthermore, we tested the i-SIM 90 camera's capabilities at a distance of 100,000 km in our second design cycle, which is 20% greater than the maximum distance between WOOF and L2 Halo. Furthermore, if our sensors were simply weak, we should expect slightly higher SNR values for WOOF than HOWLL since it is closer.

Future work should investigate the exact error in our STK file by communicating with field experts and re-developing the entire project in order to confirm that our design meets the requirements. However, as mentioned above, this investigation was outside the scope of this project.

### GTO to L1 Halo

SNR simulations were run for the GTO to L1 Halo object during the Low Thrust Spiral Phase, which begins on February 11, 2027, and after insertion into the L1 Halo orbit. To maintain consistency across all space objects, the "after insertion" analysis was run for ten days starting again on August 3, 2027. The SNR values were also exported to a .csv file to calculate the integrated SNR and number of days that met the SNR requirements. The graphical results are shown in Figures 34 and 35.

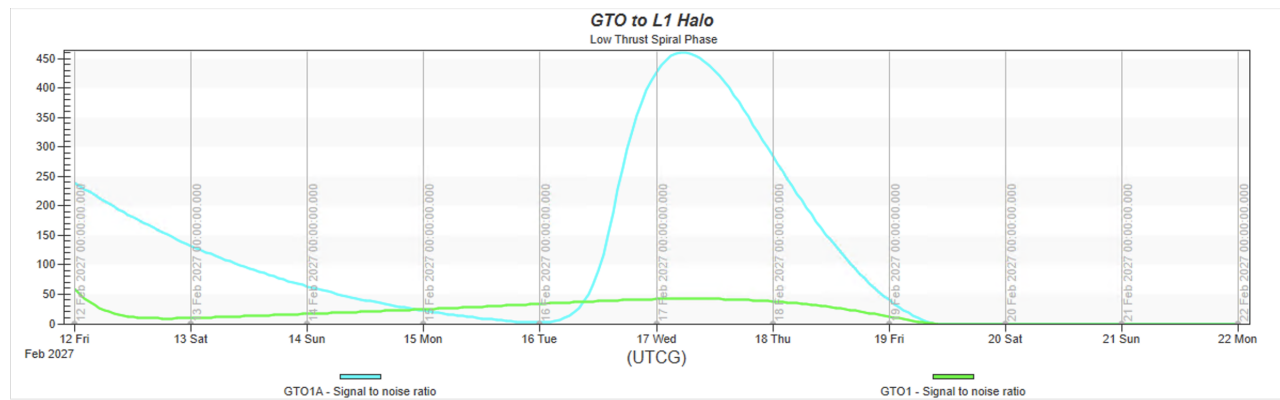


Figure 34: SNR of the i-SIM 90 camera attached to HOWLL/WOOF pointing at GTO to L1 Halo during the Low Thrust Spiral Phase. Note: Green corresponds to WOOF, and Blue corresponds to HOWLL

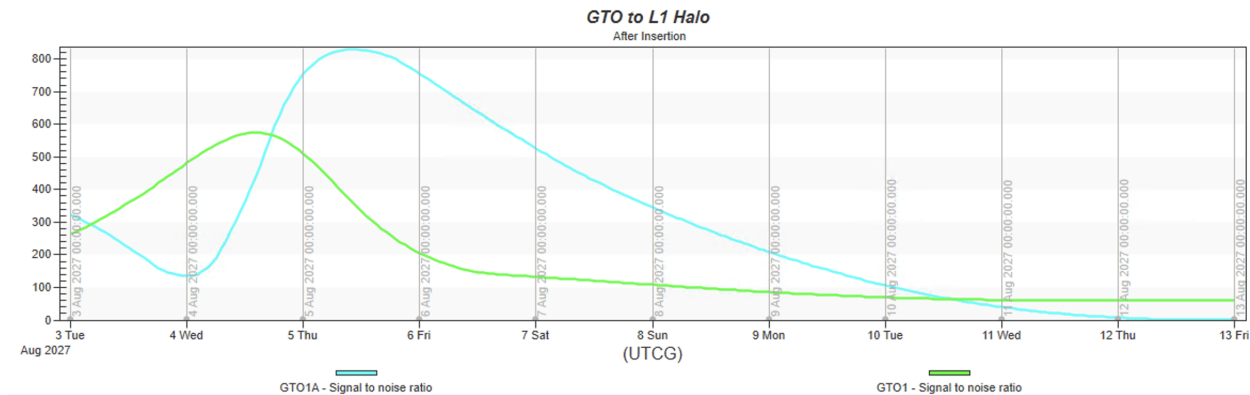


Figure 35: SNR of the i-SIM 90 camera attached to HOWLL/WOOF pointing at GTO to L1 Halo after insertion. Note: Green corresponds to WOOF, and blue corresponds to HOWLL

The SNR values are tabulated in the Table 65 below, demonstrating that the requirements are met. For the summed days SNR requirements, they may only be partially met by one satellite, but given that two satellites are tracking the GTO to L1 Halo object, it can be met when both of them are tracking.

Table 65: SNR Requirements for GTO to L1 Halo

Requirement	HOWLL	WOOF	Total	Margin
Spacecraft must achieve a SNR $\geq 15$ at least 7 days during the Low Thrust Spiral phase.	6.875 days	6.21 days	11.25 days	60.71%
On average, spacecraft should maintain an SNR $\geq 5$ for at least 7 days per month after insertion.	9.17 days	10.04 days	14.21 days	103%
Spacecraft should maintain an integrated SNR $\geq 150$ hours per month.	72,484 hours	45,455 hours	117,939 hours	78,526%

It is important to note that some of the requirements are not fully met by either HOWLL or WOOF alone. Therefore, we summed up the results for both to get the total SNR values and calculated the margin from this. For the requirements on the number of days, a simple script was run to confirm that these days did not significantly overlap between HOWLL and WOOF. The days that were overlapped were removed from the final results. Therefore, the final value represents the number of independent days that meet the SNR requirements.

### GTO to L2 Halo

SNR simulations were run for ten days the GTO to L2 Halo object during the Low Thrust Spiral Phase, which begins on February 23, 2027. As mentioned above, the step time was 1 hour or 3600 seconds. SNR simulations were also run after the GTO to L2 Halo object was inserted into the L2 Halo orbit. To maintain consistency with the other space objects, this simulation was run for ten days beginning on August 3, 2027. The SNR values were exported to a .csv file to calculate the integrated SNR and number of days that met the SNR requirements. The graphical results are shown in Figures 36 and 37.

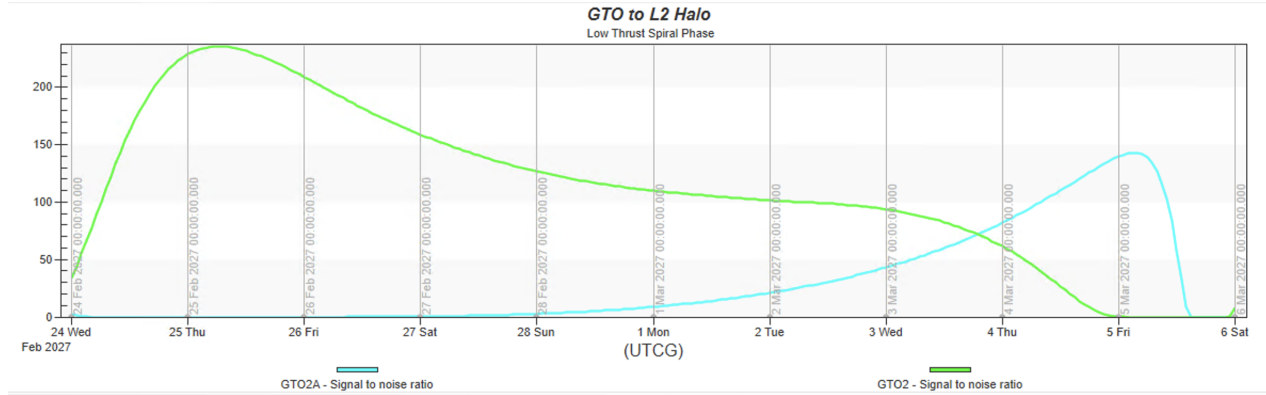


Figure 36: SNR of the i-SIM 90 camera attached to HOWLL/WOOF pointing at GTO to L2 Halo during the Low Thrust Spiral Phase. Note: Green corresponds to WOOF, and blue corresponds to HOWLL

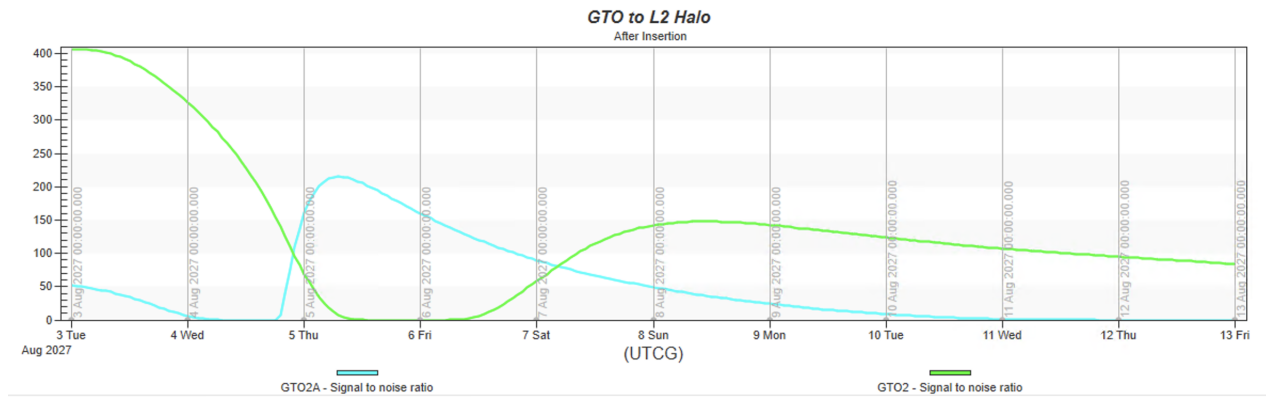


Figure 37: SNR of the i-SIM 90 camera attached to HOWLL/WOOF pointing at GTO to L2 Halo after insertion. Note: Green corresponds to WOOF, and blue corresponds to HOWLL

From these figures, we can see that SNR values on the magnitude of hundreds are frequently being met. However, to confirm that we are meeting these requirements, a simple script was ran on the .csv file to calculate the exact values. The results are depicted in Table 66.

Table 66: SNR Requirements for GTO to L2 Halo

Requirement	HOWLL	WOOF	Total	Margin
Spacecraft must achieve a SNR $\geq 15$ at least 7 days during the Low Thrust Spiral phase.	3.95 days	8.67 days	9.97 days	42.43%
On average, spacecraft should maintain an SNR $\geq 5$ for at least 7 days per month after insertion.	6.625 days	8.875 days	14.76	110.86%
Spacecraft should maintain an integrated SNR $\geq 150$ hours per month.	11,776 hours	31,830 hours	43,606 hours	28970.67%

Like the GTO to L1 Halo object, some of the SNR requirements for GTO to L2 Halo are not met by



HOWLL or WOOF alone. Therefore, the script was run again to calculate the number of individual days that meet the SNR requirements, which is reflected in the "Total" column in Table 66.



## 10 Communications Design

### 10.1 Subsystem Overview

The communications subsystem is responsible for sending and receiving data between mission architecture, ground stations, and cislunar space objects. Said signals carry spacecraft operational data, communication relays, and space object tracking information. These messages are critical to mission architecture operation and completing both primary and secondary mission objectives as outlined in the RFP [1].

Figure 38 outlines the roles of the Communications subsystem and its interaction with other subsystems. The communications subsystem relies on other subsystems for power, positioning, data processing, and hardware support. Other subsystems rely on the communication infrastructure to send and receive their produced or necessary data. These relationships are further discussed below.

Interactions with operational subsystems are represented in green in Figure 38. Communications relies on said subsystems to operate. The most critical needs for communication operations are power and appropriate pointing. All subsystems rely on Communications to transmit relevant spacecraft data and maintain mission architecture operations. These messages could include battery state of health, fuel levels, orbit information, and more. In addition to sending spacecraft status updates, the communication subsystem must receive operational commands. Said signals are processed by CDH before being used to direct spacecraft operations.

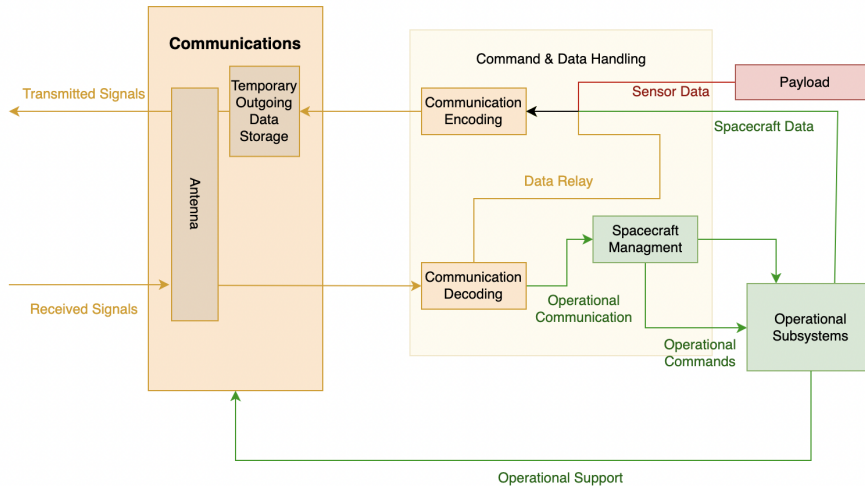


Figure 38: The block diagram for the Communications subsystem, showing its relationship to the other subsystems comprising the mission.

The payload system, shown in red, heavily relies on the communications subsystem. After sensor data is compressed by CDH, it is sent to the communications subsystem for temporary storage. It is then transmitted to a relay satellite or ground station.



Finally, the CDH subsystem works hand in hand with Communications, as shown in yellow in the figure. CDH is first responsible for processing signals upon being received and prior to transmission. It then determines the kind of message being sent and directs it accordingly. Data relay messages, like mission data or necessary relayed communication from other space objects, are sent directly back to communication encoding to be sent to their next location. Operational commands are processed and handled according to the process above.

## 10.2 Subsystem Objectives

The Communications subsystem objectives are divided into two categories—establishing reliable communication links and establishing high-performance communication links. Reliable links are necessary between mission architecture, earth, and external space objects. High-performance communication ensures that our tracking data can be efficiently transmitted while utilizing a minimum amount of power and time. Our objectives remained the same as the previous design cycle.

Our first set of objectives focuses on creating reliable communication pathways for our mission:

- **Reliable Ground Communications:** Ensure consistent and stable communication links between Earth and mission infrastructure.
- **Reliable Cislunar Communications:** Ensure consistent and stable communication links between mission architecture and space objects supported by the mission's communication network.

Our next objectives focus on achieving high performance and efficient communication. These objectives will be necessary to achieve the aforementioned reliability objectives.

- **Maximize Communication Bandwidth:** Maximize data rate and link availability to allow for high data throughput. This allows for the transmission of tracking information and communication messages while minimizing the required duty factor.
- **Minimize Communication Latency:** Minimize the delay in communication links to ensure the timely delivery of communication signals. This will ensure efficient and responsive operational communication and timely delivery of information through the supporting communication network.

## 10.3 Subsystem Requirements

The Communications subsystem has 13 requirements relevant to achieving the aforementioned objectives and mission success. As such the full list has been compressed into requirement categories. The first 4 categories are organized based on their relevance to achieving listed communications objectives. The final two requirement categories focus on communications reliability. Given that communications are a critical point of failure for each spacecraft, reliable operation was addressed in requirements to prevent catastrophic mission failure. All requirements can be traced up to higher-level mission requirements. A full list of requirements, their verification method, rationale, and trace-up requirements are available on the 'Comms' tab of the "Requirements Spreadsheet" Google sheet. [112]

All requirements have been satisfied as a result of our design process. The data rate category was satisfied through hardware analysis and data rate analysis. The signal strength category was



Table 67: COMMS Subsystem Requirements

Req. ID (COMM-####)	Description	Objective Category
P-004, P-005	The Communications subsystem shall provide an adequate data rate for inter-satellite communications and communications to Earth	Subsystem Data Rate
P-002, P-007, P-008	The Communications subsystem shall provide low noise and uninterrupted communications	Subsystem Signal Strength
F-002	The Communications subsystem shall allocate the distribution of communication periods among the different subsystems	Internal Data Handling
F-001, F-003, F-004, F-006, P-001, P-003	The communications subsystem shall provide communication capabilities between the mission components and external entities	Subsystem Encompassing
F-005	The Communications subsystem shall provide redundant systems that shall not render the system due to a single failure	Reliability

satisfied through technical analysis. The subsystem-encompassing category was satisfied through hardware analysis and selection. Finally, reliability concerns have been addressed through, hardware analysis, selection, and redundancy.

#### 10.4 Subsystem Constraints

The Communications subsystem is constrained by size, power consumption, and cost. A list of constraints for each of the satellites in our mission design is listed in Table 68. A full list of Communications constraints, their respective requirement IDs, trace-up requirements, and verification methods are outlined in the Communications tab on the "Requirements Spreadsheet" Google Sheet [6].

Table 68: Constraints for HOWLL, WOOF, and PACK Satellites

Constraint	HOWLL	PACK	WOOF
Mass (kg)	1.5	0.6	1.0
Volume (cm <sup>3</sup> )	1000	500	1000
Peak Power (W)	60	40	60
Nominal Power (W)	2.5	2	2

Size limitations, particularly regarding mass and volume, stem from the mass and volume allocations of the Structures and Materials subsystem. These allocations are determined by the overall scale of the mission architecture, such as the 27U, 54 kg setup of HOWLL and WOOF, and the 12U, 24 kg configuration of PACK, as elaborated in Section 15. Because HOWLL is our linkage between Earth and the other satellites, it was allocated more mass and power than PACK to meet the communications subsystem requirements. WOOF is designed to mirror HOWLL. In case of a HOWLL failure it can maneuver to the L1 point and take over Earth communications, thus it was given many of the same constraints as HOWLL. To accommodate the originally planned smaller satellites, our size constraints were extremely stringent. After deciding to increase total volume



and mass, however, our size constraints were loosened and our chosen design had a significant margin to utilize for the addition of redundancy.

Power constraints are derived from the capabilities of the Power subsystem. Both nominal and peak power are considered, given Communications will need to coordinate periods of heavy draw when communications are taking place with windows of low power draw from other subsystems. Power consumption is higher for HOWLL given that it will be communicating with the Earth, which is the most demanding communication task.

The cost constraint is not included in the table, given our subsystem has been allocated a cumulative cost. COMMS-C-013 dictates the cumulative cost of the communications subsystem shall not exceed \$48 million. This is derived from the total mission cost ceiling of \$400 million. Our estimated cost is much less than this value, making this our least stringent constraint.

## 10.5 Subsystem Drivers

The design of our communications subsystem is motivated by 5 predominant drivers. Our drivers enable the subsystem design to optimize performance while ensuring cohesion with mission architecture and reliable operations. Drivers and their descriptions are listed below.

- **Transmitter Power:** Transmitter power directly correlates to the strength of the signal propagated from the communications infrastructure. This is essential for ensuring communication signals can travel required distances while overcoming path losses. The most relevant constraint limiting this driver is available power.
- **Transmitter Gain:** Transmitter gain relates to the effectiveness of concentrating transmitter power in the desired direction. This improves the quality and effectiveness of the communication link. Transmitter antennas with high gain can be large and are thus constrained most stringently by mass and volume.
- **Receiver Gain:** Similar to transmitter gain, receiver gain relates to how well receivers can focus incoming transmissions. This allows communication hardware to detect weaker signals, improving link integrity. Receivers may also contain large hardware and are similarly constrained by mass and volume.
- **Data Rate:** Data rate specifies the amount of information that can be transmitted in a given amount of time. This will determine the resolution of tracking data and communication bandwidth. Data rates will be most stringently constrained by available power and the cost of sophisticated hardware.
- **Power Consumption:** The spacecraft's power usage is rigorously regulated due to limitations in mass, volume, and the requirement to maintain a normal orientation to the sun. Ensuring adequate power allocation for other pointing requirements is crucial, thus imposing strict constraints on the overall power consumption of the spacecraft. The communications subsystem plays a pivotal role in managing spacecraft power usage through careful selection of hardware and protocols. This involves opting for components with low nominal power consumption and efficient operation during transmission.



Table 69: The compliance table for the communication subsystem's various constraints.

	HOWLL Used	HOWLL Allocated	PACK Used	PACK Allocated	WOOF Used	WOOF Allocated	Total Used	Total Allocated
Mass	1.197 kg	1.5 kg	0.551 kg	0.6 kg	0.874 kg	1.0 kg		
Volume	757.009 cm <sup>3</sup>	1,000 cm <sup>3</sup>	258.925 cm <sup>3</sup>	500 cm <sup>3</sup>	507.967 cm <sup>3</sup>	1,000 cm <sup>3</sup>		
Peak Power Consumption	53 W	60 W	13 W	40 W	13 W	40 W		
Computational Consumption	0%	20%	0%	20%	0%	20%		
Cost							\$1,167,400	\$48,000,000

## 10.6 Subsystem Design Approach

In this design cycle, the communications team has focused on adding redundancies and relaxing assumptions made earlier in the design process. Due to this, there have been no major design changes. After the PDR, the subsystem had large margins remaining for cost, mass, and volume, and the primary goal of this final iteration was to take advantage of this leeway to establish redundancies in fulfillment of requirement F-005. With this remaining margin, we added a backup X-band communication system on HOWLL. Additionally, we introduced X-band communication capabilities on WOOF in the event of a worst-case scenario, described further in Section 10.7.5.

As of now, the communications subsystem satisfies all of its objectives, requirements, and constraints. Our link margins and access times to the various nodes demonstrate that the communications systems on the various satellites are both reliable and high-performance. Requirements F-001, F-003, F-004, and F-005 are satisfied through the formalization of conceptual architecture and physical hardware. F-002 and F-006 are satisfied by working in conjunction with the Operations and CDH subsystems to allocate subsystems' communication needs as well as choosing frequency bands that fit within the allocated ranges as per the FCC in SR2 [113]. Requirements P-001 through P-008 have all been satisfied through the selection of communications hardware to facilitate a robust link design. P-001 was satisfied by working with the Operations, GNC, and ADCS subsystems. P-007 and P-008's SNR requirements are addressed through the establishment of a satisfactory link margin.

The subsystem fulfills all environmental constraints as a result of the hardware being selected from NASA's State-of-the-Art Small Spacecraft Technologies Report [114].

Other physical constraints of the subsystem are satisfied as well, and a summary is available in Table 69.

## 10.7 Formal Analysis

### 10.7.1 Conceptual Architecture and Frequency Band Selection

The first step in our link design was selecting from where communications would be sent and received. At this stage, we chose how communications would be transmitted to and from Earth, as well as how they would be transmitted from HOWLL to the other satellites.

We chose to utilize NASA's Near-Space Network (NSN) of antennas to transmit and receive com-



Table 71: The preliminary link budget analysis for potential S-band communication systems.

System	Uplink margin (dB)	Downlink margin (dB)
Isispace S-Band Antenna and Transceiver [117]	-23.08	-29.82
Haigh-Farr S-Band Patch with Syrlinks Transceiver [118] [119]	-20.90	-24.58
IQ Spacecom S-Band High Gain Antenna and Transceiver [120]	-18.98	-22.10
EnduroSat Commercial S-Band Patch Antenna and Versatile Transceiver [121] [122]	-21.01	-24.88

munications on the Earth's surface due to its wide dispersal resulting in constant access time from Near-Earth space. [115] Additionally, after discussion with the GNC team, it was determined that HOWLL and WOOF will have constant access to each other, negating the need to route communications to the latter through the PACK satellites.

Table 70: Details of typical frequency bands as defined by the IEEE. [116]

Frequency Band	Frequency Range (GHz)	Typical Wavelength (cm)
UHF	0.3-1	100-30
L	1-2	30-15
S	2-4	15-7.5
C	4-8	7.5-3.75
X	8-12	3.75-2.5
Ku	12-18	2.5-1.67
K	18-27	1.67-1.11
Ka	27-40	1.11-0.75
V/W	40-110	0.75-0.273

The next step in our communications link design was selecting the frequency bands that each satellite would communicate with, with our options outlined in Table 70. Early in the design process, we conducted a trade study on various antennas and transmitters capable of communicating in both the S-band and the X-band due to their common usage for near-space communications. Through a preliminary link margin analysis, S-band communications were ruled out, largely due to the distance required for communication between HOWLL and the Earth. These values are summarized for a variety of S-band hardware systems in Table 71. As is seen in the table, each system analyzed had a link margin well below the +3 dB needed to fulfill our requirements. Therefore, we decided that HOWLL would communicate with Earth solely through the X-band.

Additionally, we chose to utilize K-band communications for all inter-satellite crosslinks. This was due to the K-band's capacity for higher transmission data rates. Though K-band systems typically have lower half-power beamwidths relative to lower frequencies and are therefore more susceptible to interference and require more accurate pointing, they are commonly used for inter-



satellite communication. [116]

### 10.7.2 X-Band and K-Band Hardware Selection

In the next design cycle, the hardware for the X-band and K-band communication systems was finalized through a trade study comparing their masses, volumes, power draws, and resultant link margins.

A link margin calculation relies on certain variables to be input and then iterated through. These variables are summarized in Table 72.

Table 72: Input variables for link margin calculations

Input	Units	How it's determined	Example values
Frequency	GHz	Transceiver/Antenna range, FCC allocations	8.2 (X-band)
Transmitter Power	W	Datasheets	1-4
Transmitter Line Loss	dB	SMAD recommendation	-1
Transmit Antenna Half-Power Beamwidth	deg	Datasheets	20 (X-band)
Transmit/Receive Antenna Pointing Offset	deg	Discussion with ADCS subsystem	0.5
Propagation Path Length	km	Average distance between source and receiver	320,000 (Earth-HOWLL)
Transmit/Receive Antenna Diameter	m	Datasheets	0.093
Data Rate	bps	Discussion with CDH and Payload subsystems	150,000,000
Bit Error Rate	N/A	SMAD Recommendation	0.00001
Implementation Loss	dB	SMAD recommendation	-1

These input values for a variety of different X-band systems were then used to calculate link margins through a process described. The equation below summarizes how to calculate the signal-to-noise ratio of a communications link by representing it as a normalized quantity  $\frac{E_b}{N_0}$ .

$$\frac{E_b}{N_0} = EIRP + L_r + L_s + L_p + G_{rt} + 228.6 - 10 \log T_s - 10 \log R$$

Once this value is known, the margin of a communication link can be determined from the following equation.

$$M = \frac{E_b}{N_0} - \frac{E_b}{N_0 \text{ desired}} + L_i$$

The specifics of the various terms in the previous two equations are detailed in Section 2.2 of the Communications PDR, as well as in Section A.7.1. In the PDR, hardware was chosen such that all communication links satisfy the margin and data requirements to fulfill the mission's objectives, as well as remain within the various constraints. The preliminary hardware choices and their specifications are summarized below in Table 73, as well as the strength of the communication links they complete in Table 74.



Table 73: The details of our selected communications hardware upon the conclusion of the FDR.

Company	Type	Band	Dimensions (cm x cm x cm)	Mass (g)	Power Usage (W)	Locations	Number Needed	Cost per Unit	Total Cost
EnduroSat [123]	4x4 Patch Antenna	X	9.8 x 8.3 x 0.3	53	N/A	HOWLL (x2), WOOF	3	\$8,700	\$26,100
EnduroSat [124]	4x4 Patch Antenna	K	6.5 x 6.5 x 0.9	76	N/A	HOWLL, PACK, WOOF	4	\$11,100	\$44,400
EnduroSat [125]	Transceiver	X	9 x 9.6 x 2.6	270	40	HOWLL (x2) WOOF	3	\$32,300	\$96,900
Paradigma [126]	Transceiver	K	9.4 x 9.4 x 2.5	475	13	HOWLL, PACK, WOOF	4	\$250,000	\$1,000,000

Table 74: The strength of the various communication links in the mission upon the conclusion of the FDR.

Communications Link	Communications System	Link Margin (dB)	Supported Data Rate (Mbps)
Earth-HOWLL Uplink	EnduroSat X-Band Antenna and Transceiver	3.55	25
Earth-HOWLL Downlink	EnduroSat X-Band Antenna and Transceiver	4.36	150
HOWLL-PACK Crosslink	EnduroSat K-Band Antenna with Paradigma Transmitter	18.04	1,000
HOWLL-WOOF Crosslink	EnduroSat K-Band Antenna with Paradigma Transmitter	12.02	1,000

### 10.7.3 Continuing Design Evolution

Upon the conclusion of the PDR, it was evident that the most pressing issue facing the design of ARGOS's communications systems was the lack of redundancy built into the mission architecture. The nature of HOWLL as a node through which all mission communications pass means that if the X-band system on board experiences failure, the mission's objectives would no longer be able to be completed. The contingency plan to mitigate these impacts is detailed below.

### 10.7.4 HOWLL Hardware Augmentation

Given the sizable margin remaining for both mass and volume on HOWLL for communications hardware, we have elected to install a duplicate X-band communications system on the satellite as a backup for if the primary transceiver or antenna fails. The mass and volume margin remaining is summarized in Table 75.

### 10.7.5 WOOF Hardware Augmentation

When the only communications hardware on WOOF was the K-band system, the mass and volume constraints for the mission provided significant margin, as seen in Table 76. However, due to the nature of WOOF as a 27U satellite with a layout similar to HOWLL, mission-level discussion



Table 75: Mass and volume budgets on HOWLL, before and after the addition of an additional X-band communication system to the satellite.

	Mass used (g)	Mass used (%)	Volume used (cm <sup>3</sup> )	Volume used (%)
Before	874	58.2	507.967	50.8
After	1,197	79.8	757.009	75.7

Table 76: Mass and volume budgets on WOOF, before and after the addition of an X-band communication system to the satellite.

	Mass used (g)	Mass used (%)	Volume used (cm <sup>3</sup> )	Volume used (%)
Before	551	55.1	258.925	25.9
After	874	87.4	507.967	50.8

prompted the team to consider adding extra components for redundancy. Because of this, the X-band system on HOWLL has been duplicated for use on WOOF. If HOWLL experiences a catastrophic failure, WOOF can maneuver to the L1 point to re-establish nominal operations, including HOWLL's communication capabilities.

#### 10.7.6 Summary After Adjustments

After adding these redundancies to the communications subsystem on HOWLL and WOOF, the finalized conceptual architecture resembles what is shown in Figure 39. The hardware and link summaries are still shown in Table 73 and Table 74.

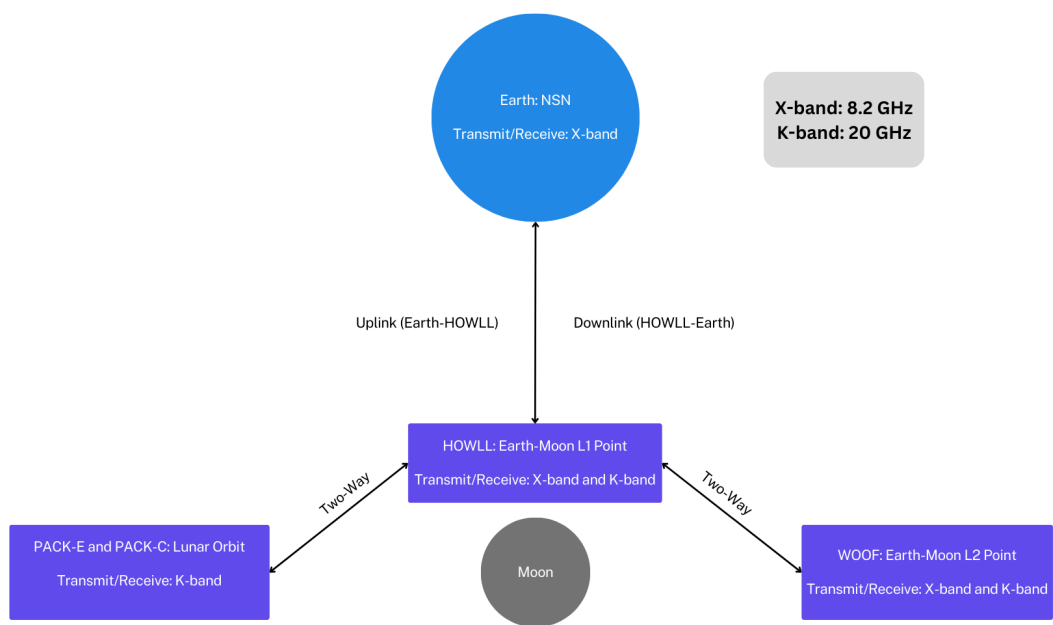


Figure 39: The finalized conceptual architecture diagram for the Communications subsystem, showing the links present in the mission design as well as the frequency bands able to be transmitted through.



## 11 Command and Data Handling Design

### 11.1 Subsystem Overview

C&DH subsystem handles all spacecraft data and performs required computation to achieve mission objectives. The C&DH subsystem is responsible for three main tasks:

- Managing Spacecraft Operations
- Enabling Spacecraft Communication
- Supporting Mission Data Collection

To manage spacecraft operations, the C&DH subsystem process information and issues commands. Operational subsystems including ADCS, GNC, Payload, Launch Vehicle, Power, Propulsion, Thermal, and Mechanisms send data to C&DH. Additionally external commands are received from the communications subsystem. Finally C&DH has access to stored hardware state data to inform spacecraft management. C&DH aggregated and processes all data streams. C&DH then directs relevant satellite state data to be stored on board for future use. After data processing C&DH also issues commands to other subsystems to facilitate nominal operations, data collection, and communication.

The second role of C&DH is supporting the Communication abilities of the spacecraft. Communication hardware receives transmitted information to be sent to C&DH for decoding. The C&DH subsystem identifies this information as either data relay or spacecraft commands. Commands are sent to be processed to manage spacecraft operations. Relay data is sent to be re-encoded in the appropriate frequency band to be transmitted by communication hardware.

The final role of C&DH is facilitating mission data collection. The payload subsystem collects object tracking data. C&DH uses compression algorithms to limit the necessary data transmission. This data is then encoded and packaged along with necessary communication relay data to be transmitted by communication hardware.

Figure 40 displays a system block diagram of C&DH accomplishing required tasks. In the figure managing satellite operations is color coded green, communications support in blue, and mission data collection in purple. Mission data is displayed in purple as it represents a combination of communication and sensor data.

As discussed the three tasks for which C&DH is responsible are critical for the functionality of the entire spacecraft. Almost all subsystems rely on successful C&DH operation. This subsystem is thus an important single point of failure for each satellite in our mission architecture. As such, ensuring adequate performance of the C&DH subsystem is as important as reliability.

### 11.2 Subsystem Objectives

The high level tasks of the C&DH subsystem are maintaining satellite operations and supporting successful achievement of mission level objectives.

As the metaphorical brain of the satellite C&DH coordinates with all other subsystems to manage nominal satellite operations. C&DH interconnects the roles of all other subsystems to ensure functional mission architecture. As mentioned this requires data handling and issuing subsystem

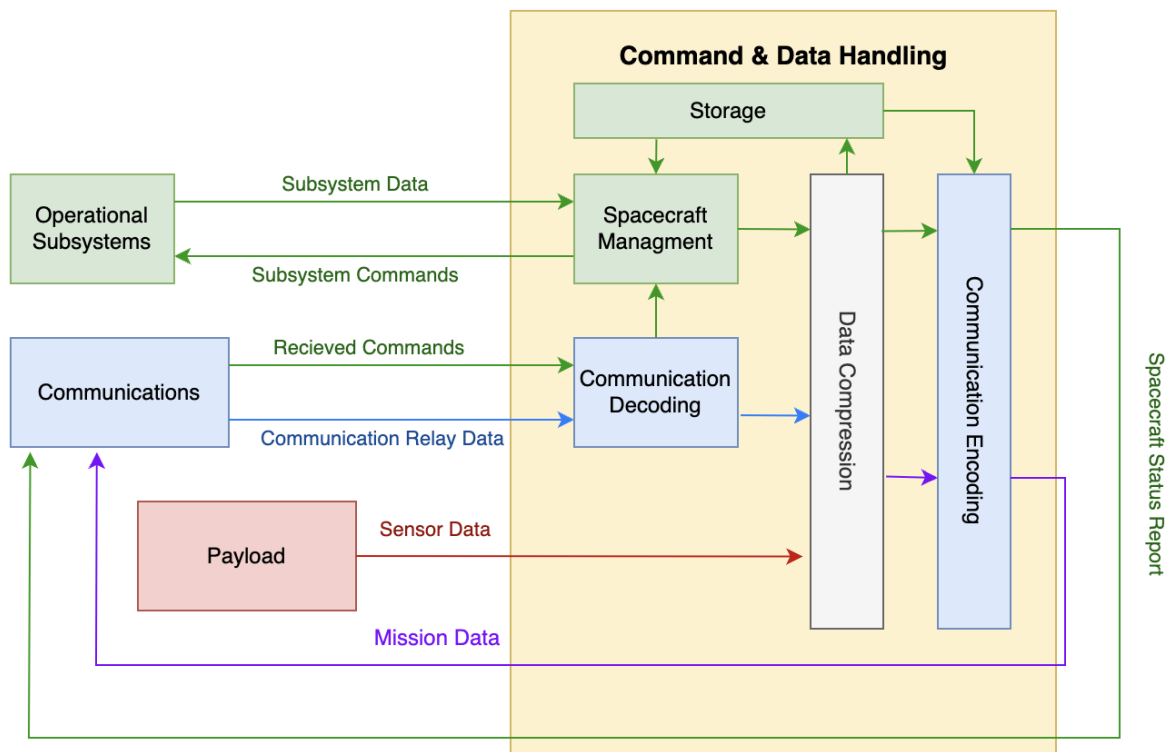


Figure 40: C&DH System Block Diagram



commands. The C&DH subsystem has the three following objectives related to ensuring successful satellite operation:

- **Subsystem Data Processing:** The C&DH subsystem must collect relevant data from all other subsystems, including but not limited to mission phase timing, attitude positioning, and power levels. After collecting this data C&DH must process it effectively to direct subsequent action.
- **Subsystem Data Storage:** The C&DH subsystem must store relevant spacecraft data including but not limited to propellant levels, attitude information, and subsystem state of health. This will allow spacecraft management to be informed by both current and historic subsystem data.
- **Command Management:** After collecting, processing, and storing relevant subsystem data, C&DH is responsible for issuing appropriate commands to control spacecraft operation. Effective command management will be crucial to ensuring the successful timing and execution of other subsystem's tasks, including those relevant to supporting mission objective accomplishment such as appropriate satellite pointing.

C&DH also plays a critical role in supporting the direct achievement of the object tracking and communication relay network mission objectives. Both tasks are heavily reliant on data processing. The two objectives of C&DH relevant to directly accomplishing mission objectives are as follows:

- **Process Tracking Data:** The C&DH subsystem is responsible for collecting and processing data from the Payload subsystem's sensors. This allows for the necessary objects outlined in the mission catalog to be tracked and for their orbital information to be efficiently communicated to other space objects and earth.
- **Communication Processing:** Process and interpret received signals. Direct information to spacecraft management command issuance or to be re-packaged and sent out by communication subsystem.

### 11.3 Subsystem Requirements

The C&DH subsystem has nearly 20 requirements relevant to achieving the aforementioned objectives and mission success. As such the full list has been compressed into requirement categories. The first 5 categories are organized based on their relevancy to achieving listed C&DH objectives. The final two requirement categories focus on C&DH reliability. Given C&DH is a critical point of failure for each spacecraft, reliable operation was addressed in requirements to prevent catastrophic mission failure. All requirements can be traced up to higher level mission requirements. A full list of requirements, their verification method, rationale, and trace up requirements are available on the C&DH tab of the "Requirements Spreadsheet" Google sheet [112].

Table 77 lists the 7 categories of requirements. The first column contains the requirement ID; all C&DH requirement ID's begin with "CDH-", thus this part of the ID was excluded for brevity. The next column aggregates content from the group of requirements to provide a high level description of the category's specifications. The final column contains the relevant objective the requirements intend to satisfy.



Table 77: C&DH Subsystem Requirements

Req. ID (CDH-####)	Description	Objective Category
F-001, P-001, P-003, P-004	The C&DH subsystem shall provide data storage of 32 GB for HOWLL, WOOF, and PACK	Subsystem Data Storage
F-002, F-003, F-006, F-009	The C&DH subsystem shall provide and allocate appropriate computational resources for mission architecture	Subsystem Data Processing
F-004	The C&DH subsystem shall facilitate command issuance and mission architecture control	Command Management
F-005	The C&DH subsystem shall facilitate data processing for communication	Communication Processing
F-011	The C&DH subsystem shall effectively and efficiently process collected mission data	Process Tracking Data
F-007, F-010, P-002, F-012	The C&DH subsystem shall operate reliably with redundancies and a failure rate of less than 0.1%	Reliability
E-001, E-002, E-003	The C&DH subsystem shall be able to survive in radiative, temperature, and gravitational environments of cis-lunar space	Reliability

All requirements have been satisfied as a result of our design process. The subsystem data storage and processing categories are satisfied through hardware analysis and finalization of a data budget. Command management, communication processing, and process tracking are satisfied with software analysis and data budget allocations. Finally, reliability concerns are mitigated through hardware analysis and selection.

#### 11.4 Subsystem Constraints

The C&DH subsystem is constrained by size, power consumption, and cost. A list of constraints for each of the satellites in our mission design is listed Table 78. A full list of C&DH constraints, their respective requirement IDs, trace up requirements, and verification methods are outlined in the C&DH tab on the "Requirements Spreadsheet" Google Sheet [6].

Table 78: Constraints for HOWLL, WOOF, and PACK Satellites

Constraint	HOWLL / WOOF	PACK
Mass (kg)	0.3	0.3
Volume (cm <sup>3</sup> )	1400	1400
Peak Power (W)	10	5
Avg. Power (W)	2.5	2

Size constraints, namely mass and volume are derived from the the Structures and Materials subsystem's mass and volume budgets. These budgets are based on the overall size of mission architecture, namely HOWLL and WOOF's 27U, 54 kg configuration and PACK's 12 U 24 kg configuration discussed further in Section 15. Despite the larger size of HOWLL and WOOF size constraints are the same across all satellites given our chosen C&DH hardware is equivalent. To accommodate the originally planned smaller satellites, size was extremely stringent. After deciding to increase total volume and mass however our size constraints were loosened and our chosen design had



significant margin.

Power constraints are derived from the capabilities of the Power subsystem. Both nominal and peak power is considered, given C&DH will need to coordinate its most heavy computational periods with windows of low power draw from other subsystems. Power consumption is higher for HOWLL and WOOF given they will be performing payload data compression, the most computationally demanding C&DH task.

The cost constraint is not included in the table, given our subsystem has been allocated a cumulative cost. CDH-C-013 dictates the cumulative cost of the C&DH subsystem shall not exceed \$24 million. This is derived from total mission cost ceiling of \$400 million. Our estimated cost is orders of magnitude less than this value, making this our least stringent constraint.

## 11.5 Subsystem Drivers

The design of our C&DH subsystem is motivated by 5 predominant drivers. Our drivers push the C&DH subsystem design to optimize performance ability while ensuring cohesion with mission architecture and reliable operations. Descriptions of each driver and their applicability to C&DH or mission operations is listed below:

- **Computation Capacity:** Computation capacity is essential for the satellites' ability to process operational and mission data. It influences input and output data bandwidth to other subsystems to perform operational tasks including trajectory and attitude adjustments, power management, mechanism deployment, and thermal monitoring. The power subsystem requires solar panels to point normal to the sun at an average of 90% of non-eclipse time. For effective tracking payload will require pointing to each space object for 1 minutes every 30 minutes. Strict pointing requirements will significantly constrain the time wherein satellites can up-link and down-link data. It will be necessary to compress data, perform independent satellite operations, and encode/decode communication as quickly and with the highest bandwidth as possible. This allow other subsystems to optimize the pointing of the spacecraft for their operation. Key limitations include managing heat generation, power use, cost, mass, and volume. Heat generation has been excluded from further analysis given assurances from the thermal subsystem that even the maximum power consumption worth of heat production (i.e. zero energy efficiency while consuming max power) can easily be dissipated away from the C&DH subsystem.
- **Limiting Latency:** Latency for the C&DH systems refers to the delay between internal command issuance, processing times, and execution. Limiting latency is critical for precision in mission and operational tasks. Temporal accuracy is critical for task such as orbital adjustments, emergency debris avoidance, communication coordination, and sensor pointing. Low latency is required particularly to meet the strict ADCS requirements for precision attitude control. Latency is most constrained by the sophistication of chosen hardware. It is thus primarily limited by reliability of modern systems given the single point of failure nature of C&DH and the higher risk associated with new, more advanced technology. Secondarily latency is constrained by cost, mass, and volume.
- **Data Storage Capacity:** Storage capacity on PACK, HOWLL, and WOOF will be critical for maintaining spacecraft operation data. The communications subsystem has significant data



storage capabilities allowing C&DH storage to prioritize operational data. C&DH storage capacity will determine the amount of historic information available on power levels, orbital elements, pointing directions, and hardware stress. Sufficient data storage will allow for appropriate and accurate spacecraft operational management. C&DH storage will still be constrained by the size of our chosen system and secondarily power for all volatile storage.

- **Limiting Power Consumption:** Power consumption on the spacecraft is stringently constrained by mass, volume, and ability to point normal to the sun. Overall power consumption of the spacecraft is critically constrained to allow for other pointing needs. The C&DH subsystem limits spacecraft power consumption through hardware and protocol choice. Namely, choosing components with low nominal power consumption, and performing optimized data compression. Data needs to be compressed by the C&DH subsystem to limit the transmission power needs of the communication subsystem. Compression of course consumes power within the C&DH subsystem, but requires less power use to transit lower data levels. Ability to limit power consumption is constrained by technology sophistication and the data resolution needs to determine orbital information for tracked objects.
- **Reliability:** Given our subsystem itself is a critical failure point ensuring reliable operation is a key system driver. As shown in Figure 40, spacecraft operations relies on data processing and command management from C&DH. Mission data also is processed by the C&DH subsystem. This makes reliable operation of the C&DH subsystem critical for the mission. Reliability is primarily limited by the desire to use more sophisticated technology. Improved performance often comes at the expense of less flight heritage adding mission risk.

## 11.6 Subsystem Design Approach

The design approach to determine the hardware for the C&DH subsystem relies on two major trades. The first trade deals with the architecture of the subsystem, which decides whether there is a centralized computer that handles the entire spacecraft, a decentralized network where individual computers handle specific tasks, or a semi-centralized architecture where a few computers share the workload amongst each one. Our analysis of CubeSat C&DH systems on other missions showed that a decentralized network is often more complicated than is needed and is able to fit within the small mass and volume of a CubeSat, so our analysis functioned primarily on the decision between a centralized and semi-centralized architecture. The benefits of a centralized architecture are that the architecture is simpler and more compact, which results in lower mass, volume, and fewer challenges from a layout standpoint when the SM subsystem needs to allocate space for the C&DH system. However, a semi-centralized architecture is more able to cater directly to the needs of a specific subsystem or group of subsystems, which is difficult in a centralized system where one computer must handle all of the workload.

The second trade involves selecting a commercial-of-the-shelf (COTS) component versus customizing a system to best suit the needs of our mission. Generally, COTS components will have lower risks involved due to flight heritage and extended testing, where designing a custom component may introduce additional points of failure to the design. However, when choosing a COTS component, the design is limited to components that have been designed for other missions, which means they may not suit the specific needs of our mission. Our design approach was to first try to find a set of COTS components that would satisfy the objectives and requirements for our

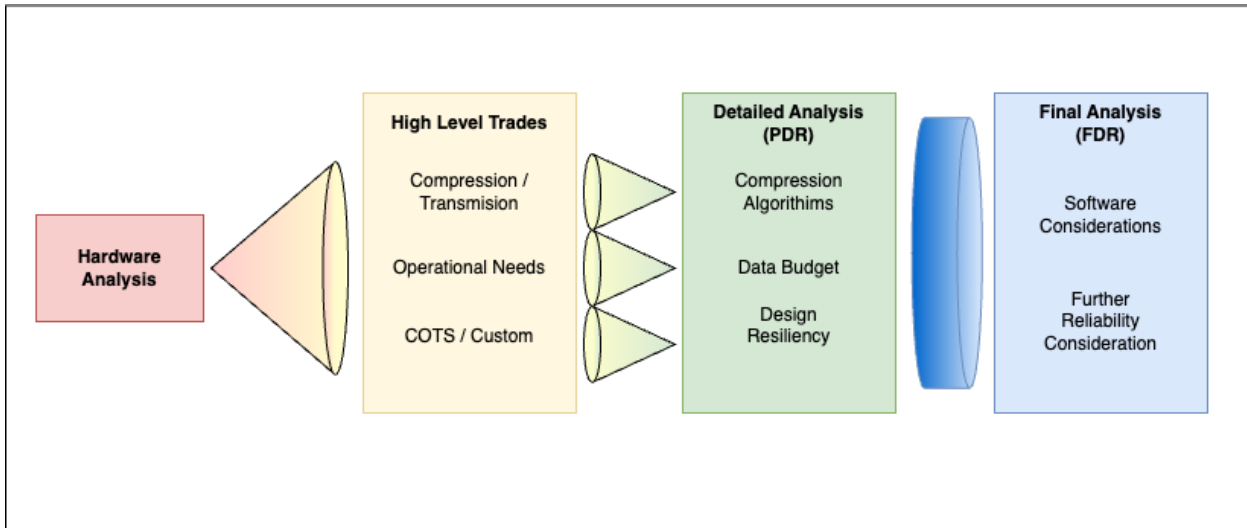


Figure 41: Overview of Design Approach through each Design Cycle

subsystem. If COTS components failed to be satisfactory, we would begin a design of custom components.

Our hardware design has stayed very similar to the design described in the PDR. A centralized Sirius OBC&TCM (onboard computer and telemetry and command module) supports the entire mission architecture by supplying commands from Earth to each subsystem and from subsystem to subsystem within the spacecraft. After the PDR, we made the decision to include the Sirius Development Kit (DevKit)[127], which envelopes our OBC&TCM system providing physical protection, radiation hardening, and allows for easier interfacing with other subsystems. The datasheet for the Sirius system is shown in Figure 97.

Data storage and transmission budgets have been designed and implemented by incorporating internal trades between compression and transmission as well as trades external to the C&DH subsystem. The external trades are primarily focused on the transmission abilities of the communications subsystem, which relies on the transmission budget to design for the correct data rate for all links both from satellite to satellite and from up-link and down-link with the Earth. This analysis is discussed in more detail in section 11.7.2

Payload data processing is used to limit the transmission needs for our mission through image compression. Our approach for analyzing these data processing options was to prioritize image compression methods designed for object tracking in space to ensure compatibility with our mission. We chose a streak detection processing and compression method, detailed in section 11.7.3.

An overview of our design approach through each design cycle and the main concepts examined is shown in Figure 41. Since the PDR, the main changes to the design have been through software considerations as well as in further reliability considerations, which includes the addition of the Sirius DevKit.



## 11.7 Formal Analysis

### 11.7.1 Hardware Analysis

Table 79: Performance Metrics of Top 3 Choices for On-Board Computers

	Argotec OBC FERMI[128]	Sirius OBC & TCM[129]	RC RadPCSBC-001[130]
<b>Previous Missions Flown</b>	Deep Space, Cislunar, LEO	LEO, Cislunar	LEO, Lunar (Planned 2024)
<b>Radiation Tolerance</b>	100 krad (Si)	20 krad TID	COTS w/ SEE protection
<b>Dimensions (L, W, H) [cm]</b>	(10.24, 10, 4.49)	(9.589, 9.107, 1.720)	(10, 10, x)
<b>Volume [cm<sup>3</sup>]</b>	459.78	148.72	100
<b>Area of Largest Side [cm<sup>2</sup>]</b>	102.4	86.46	100
<b>Average Power [W]</b>	5	1.3	1.5
<b>Non-Volatile Storage</b>	20 Mbit EEPROM, 16 GB ECC Core Corrected Memory	NVRAM 16 kB (post-EDAC), Nand Flash 2 GB (post-EDAC), Mass Memory Storage 32 GB (post-EDAC)	8k Program Memory
<b>Volatile Storage</b>	256 Mbyte SDRAM	SDRAM 64 MB (post-EDAC), Instruction Cache 8 kB, Data Cache 8 kB	2k Data Memory
<b>Processor</b>	32-bit LEON3FT (IEEE-1754 SPARC v8)	32-bit LEON3FT (IEEE-1754 SPARC v8)	RISC-V 32-Bit (AMD Artix 7)
<b>Computation speed</b>	200 MIPS	200 MIPS	50 MIPS
<b>Fault Tolerance</b>	LEON3FT fault-tolerant soft processor, compliant to IEEE 1754, fault-tolerant memory controller	LEON3FT fault-tolerant soft processor, compliant to IEEE 1754, triple redundancy	"redundant computing cores, proprietary recovery algorithms to automatically detect, recover, and repair faults"

Our analysis of hardware components began with 51 C&DH systems with flight heritage shown in the NASA State of the Art design handbook.[131] Our initial parameters for narrowing the choices were the following:

- The system was required to have flight heritage in cislunar space, which ensured the system could survive the environmental conditions of our mission.
- The system was required to have a lifespan of at least 5 years in cislunar space, which is the duration of our mission.
- The system was required to have fault-tolerant processing to ensure reliability.
- The system was required to fall within 2U (2000 cm<sup>3</sup>) volume, which was an initial upper bound on our volume budget.
- The system was required to have an area of largest side lower than 200 cm<sup>2</sup> to ensure layout placement within the 12U CubeSat was possible.
- The system must consume less than 10 W of power, which was our initial power allocation.
- The system must supply at least 50 Million Inputs per Second (MIPS) of computation speed, which was an initial lower bound for processing needs.



Table 79 shows the specifications for the three COTS OBC systems that met each of these requirements. All will have cislunar flight heritage as of 2027, with the Argotec and Sirius systems already having flight heritage, and the Radian system planned for a cislunar mission in 2024. The fault-tolerant processing parameter is satisfied by each of these systems. The Argotec and Sirius systems are certified to standards by the Institute of Electrical and Electronics Engineers (IEEE)[128][129]. The Radian Computing system contains redundancy in the most susceptible parts to failure, boasting a lunar reliability improvement of 337% for mean time between failures when compared a simplex system[130]. Given that simplex systems have been used successfully in cislunar missions[132], a 337% improvement from this system is a reasonable amount of fault tolerance. The Radian system is has much lower specifications in terms of processing power and storage, with 50 MIPS computational speed compared to 200 MIPS for Argotec and Sirius. The most drastic difference is in both volatile and non-volatile storage, with Argotec and Sirius possessing storage on the order of GB, while the Radian system has storage on the order of kB. The Radian system would be a good option in a semi-centralized system to handle simple tasks without a need for storage, but does not constitute a great option in terms of a centralized architecture. The Sirius system contains the same computational speed and fault tolerance as the Argotec system, but at a lower mass, volume, and power consumption. The main benefit to the Argotec system is increase RAM, but the analysis in section 11.7.3 shows that the increased RAM is not required for our mission.

Using the available systems, we analyzed the trade between a centralized and semi-centralized architecture. Generally for COTS C&DH systems, we found that data storage and computational capabilities did not scale linearly with mass and volume, but instead it was more efficient to bring all the computation into one device. For example using two of the components from our three possible systems, the Radian PCSBC[130] system possesses a 50 MIPS computational speed at a  $100 \text{ cm}^3$  volume, while the Sirius OBC&TCM[129] possesses a 200 MIPS computational speed at a  $148 \text{ cm}^3$  volume, giving a 300% increase in computational speed for a 50% increase in volume. The Radian system also requires about the same amount of power as the Sirius system, (1.5 W for Radian and 1.3 W for Sirius), which shows that the increased processing power does not necessarily impact the power required. This trend held in other systems, meaning choosing a COTS system which could handle all of the necessary processes in a centralized manner was the most efficient method in terms of mass, volume and power.

Our analysis of computational needs relies on the assumption that payload data processing constitutes the majority of computational needs for an object tracking mission. This assumption is based on literature and relies on the fact that sending and distributing commands requires minimal computation.[133] More information on the data processing computational needs is given in section 11.7.3.

If a centralized system was not able to meet our constraints and requirements, a semi-centralized system using different components would have been necessary, but upon further integration with other subsystems, we found that a single Sirius OBC&TCM could satisfy all of our computation and storage needs.

### 11.7.2 Data Budget

The data budget for this mission was designed by analyzing each subsystem's data needs and analyzing the trading of these needs with C&DH architecture. Data storage budgets are primar-



ily driven by the C&DH hardware storage values, while transmission budget values are driven by trades between the communications architecture, ADCS pointing availability, and individual subsystem transmission needs. Data transmission values are designed for down-link capabilities, which relies on the assumption that up-link requirements will be much lower than down-link requirements. This assumption is justified by the fact that the majority of our transmission requirements are to send housekeeping data and payload data, which are only sent down-link. Up-link transmission is primarily in the case of commands, which are orders of magnitude smaller in terms of data than the housekeeping and payload data. In this budget, housekeeping data is kept as a separate category from other subsystems, which means the subsystem allocations are simply for commands and data unique to each subsystem.

The data storage allowable storage was set at 32 GB for all satellites, which is the data storage value for the Sirius OBC&TCM hardware selected for our subsystem. Due to the inclusion of the TCM, our storage values have high margin within each subsystem. Each subsystem is allotted a baseline of 1 GB for their data storage needs, which is a generous allocation because data will only be stored briefly before being down-linked. Similar CubeSats allow for on the order of 100 Mb of storage for each subsystem,[134], but due to the availability of storage given by the TCM module, we have given each subsystem the freedom to store more data within the C&DH architecture if necessary.

Housekeeping Data is allotted 5 GB of storage, which is enough storage to store 55 hours of continuous housekeeping data at our defined rate of 200 kbps. Our maximum eclipse for any satellite defined by the GNC subsystem in Chapter 6 is 5 hours, so this gives plenty of margin to store housekeeping data and gives time in the event of unexpected communication impediments or a need to go into safe mode for extended periods of time.

The payload data is allotted 10 GB of storage, which allows for both the uncompressed and compressed images to be stored. The largest uncompressed images are 111 Mb on the cameras used on the PACK satellites, which allows for storage of up to 720 uncompressed images. Given that the payload procedures in Chapter 9 denote a nominal procedure in which 10 images are captured per transmission cycle and a worst case scenario of 100 images to scan for an unknown object, a storage of 720 images gives significant margin.

With the allocated data, there is still a 25% margin for all satellites in terms of data storage. Glenn Rakow from Goddard advised that it is common that the last portion of data storage is reserved for miscellaneous software,[135] which means it is essential to maintain some margin. However, we believe our actual margin is much larger due to the generous allocations to each subsystem.

The transmission budgets detail the amount of data from each subsystem that needs to be transmitted to Earth from each satellite. The budgets shown compile the amount of data to be transmitted during each nominal 30 minute cycle. The 30 minute cycle is driven by the payload procedure to track each object every 30 minutes, as detailed in Chapter 9. Due to this cycle, communication links are operated at the very least once every 30 minutes, which means it is useful for the communications subsystem to receive transmission needs as amount of data per 30 minute cycle. The maximum transmission capabilities are defined by the transmission rates designed for by the communications subsystem in Section 10.7 and the time allotted for communication in the operational procedures. These times give transmission budgets of 3000 Mb for HOWLL and 1000 Mb for WOOF and PACK per 30 minute cycle. HOWLL's purpose as a data relay satellite for PACK and



WOOF results in the higher transmission budget, which is accounted for in the communication subsystem designs.

As a baseline, each subsystem is given 10 Mb per cycle for transmission. This accounts for any data not covered in the housekeeping budget such as confirmation of commands and any key data from the instruments within the subsystem. Since these packages are relatively small, they should not exceed the 10 Mb per subsystem. The lone exception to this 10 Mb allocation is for the ADCS subsystem because of their more constant use in orienting the satellite, which will require more data on orientation to be sent.

The two most important elements from a transmission budget standpoint are housekeeping data and payload data. Housekeeping data slowly accumulates and must be transmitted to Earth for processing. This data includes temperatures, voltages, power draws, stresses, and any other information essential for evaluating the life of the spacecraft. Payload data accounts for the images taken by the payload cameras for object tracking purposes.

Automated processing of housekeeping data onboard the spacecraft was considered to lessen the transmission needs of each spacecraft. However, housekeeping data is more often than not useful to have at hand at the ground station in order to have a more sophisticated view of the status onboard each spacecraft. For example, a gradual increase in temperature at a specific temperature sensor may not trigger anything within autonomous operations, but could be a sign of something irregular occurring within the spacecraft. A survey of past CubeSat missions indicated that most CubeSat missions do not process housekeeping data onboard and instead send all of the data to Earth for processing on Earth.[\[136\]](#) Our transmission capabilities allow for sending the housekeeping data uncompressed to Earth, so we plan to follow past missions and process housekeeping data at a ground station instead of onboard. Our housekeeping data rate for each satellite is 200 kbps, which accounts for 360 Mb per 30 minute cycle. This data rate is taken from an upper bound from similarly sized satellites.[\[136\]](#)

Payload data is accumulated through the imaging of objects to be tracked by our mission. For this data, we analyzed a similar trade study as with the housekeeping data in terms of analyzing whether the data should be compressed onboard or transmitted without compression to be processed at a ground station. Since the payload data comes in the form of images, the data sizes are very large, with sizes of 111 Mb for the camera onboard PACK and 18 Mb for the camera onboard HOWLL and WOOF. At a rate of 10 images per cycle specified by the payload subsystem to meet the tracking requirements, this would account for 1110 Mb of data to be sent from PACK, and 180 Mb of data to be sent from WOOF and HOWLL. This amount of data would not fit within our data budgets, so sending uncompressed payload images would require a redesign of communications architecture. Therefore, the images needed to be compressed. Our proposed method for compression is described in section [11.7.3](#).

For HOWLL specifically, data relay from PACK and WOOF accounts for the majority of the transmission requirements. All of the data from PACK and WOOF is relayed through HOWLL on its way to Earth, as detailed in the Communications subsystem design (section [10](#)).

Overall, both our data storage and transmission budgets indicate that the current design satisfies the hardware constraints for our subsystem and the communications architecture. In terms of data storage, 24 of the 32 GB are allocated, leaving a 25% margin. In terms of transmission needs, each satellite has above 20% margin in the budget. HOWLL contains the smallest margin, but 20% is



Subsystem	HOWLL		PACK (ea.)		WOOF	
	Data (GB)	Transmission (Mb)	Data (GB)	Transmission (Mb)	Data (GB)	Transmission (Mb)
Housekeeping Data	5	360	5	360	5	360
Structures and Materials	0	0	0	0	0	0
Mechanisms	1	10	1	10	1	10
Thermal	1	10	1	10	1	10
LV	1	10	1	10	1	10
Power	1	10	1	10	1	10
Propulsion	1	10	1	10	1	10
GNC	1	10	1	10	1	10
ADCS	1	25	1	25	1	25
Payload	10	102	10	23	10	102
C&DH	1	10	1	1	1	10
Ops	1	50	1	50	1	50
Comms	0	5	0	40	0	5
Relay from PACK/WOOF	-	1730	-	-	-	-
<b>TOTAL</b>	<b>24</b>	<b>2342</b>	<b>24</b>	<b>559</b>	<b>24</b>	<b>612</b>
<b>MARGIN (%)</b>	<b>25.00%</b>	<b>21.93%</b>	<b>25.00%</b>	<b>44.10%</b>	<b>25.00%</b>	<b>38.80%</b>
<b>MAX ALLOWABLE</b>	<b>32</b>	<b>3000</b>	<b>32</b>	<b>1000</b>	<b>32</b>	<b>1000</b>

Figure 42: Data Budget for Storage and Transmission needs for Each Subsystem

still enough margin to feel comfortable with the design.

### 11.7.3 Image Processing

To process the images taken by the payload cameras, a compression method must be chosen to account for the large sizes of the images. In order to limit integration risks, the goal was to choose a compression method that has been designed for object tracking in space. Image compression onboard a small spacecraft has very different drivers than image compression in other fields because of the lower processing power and storage capabilities onboard a satellite, so looking at compression methods used in space improves the likelihood that the method is suitable for our needs.

Object tracking has been approached with a variety of different methods in past missions. The main approaches to tracking are either in static image object detection or motion-only object detection. Static image detection has primarily been used to track large objects such as planes and ships on Earth from LEO or GEO,[137] and therefore is not entirely suitable for our mission due to the small visual footprint of the satellites being tracked in this mission. Motion-only detection is achieved by taking multiple images in quick succession and then refining the data with background subtraction and frame differencing.[137] Any pixels that see little to no difference between images are defined as background and removed, leaving just the moving objects. By comparing the difference between frames, the motion of each object in the frame can be extracted out.

A more refined method of this motion-only detection has been pioneered by Airbus DS Government Solutions in Germany where a long exposure image is taken of the object to be tracked. The streaks in the image are processed out, which then gives information on position and velocity of the object being tracked.[138] In the specific case given by Airbus, an image is taken with an exposure time of 0.5 s, which was determined to be long enough for moving objects to be separated from stars or other inconsequential debris in the frame. Objects moving at a high relative velocity to our satellite, in this case the object being tracked, will leave a streak on the image due to the



exposure time. A boundary tensor algorithm is then used to define the boundaries of each streak. Kothe (2003) gives more specific information on the math behind the boundary tensor algorithm and refining of the parameters involved.[139]

An analysis of the computational power required by this algorithm shows that this method can be easily incorporated into the Siruis OBC& TCM architecture if additional RAM is given to the system. The original implementation of the streak observation method was implemented recommending 128 MB of RAM on an FPGA microchip for intermediate storage for a frame rate of one 2000 x 2000 pixel image per second.[137] The Siruis OBC&TCM contains an FPGA microchip with 64 MB of RAM, which would not be sufficient to process the information in the original implementation case. However, it is mentioned that RAM requirements can be drastically reduced by limiting the frame rate and processing one image at a time instead of processing images in parallel. The frame rate of one image per second requires parallel processing of images and is important for the Airbus mission specifically because of their desire to track small space debris in LEO, which is much more volatile in its orbit than planned satellites with station-keeping in cislunar space. The payload subsystem decision to track each object every 30 minutes means that we will only be taking on average 10 images every 30 minutes. This means there is not the same time crunch on processing the images, and each image can be processed in series.

The streak observation method using a boundary tensor algorithm to extract the streaks provides both a data collection and compression method at the same time. After the boundary tensor algorithm is completed, the data to be sent has been transformed from 14 bit in the case of PACK[110] and 12 bit in the case of HOWLL and WOOF[111] to 1 bit information, where each pixel is either contained in a streak or not contained in a streak. This compression converts the information from 18 Mb per image on PACK and 111 Mb per image on HOWLL and WOOF to 1.3 Mb to be sent per image on PACK and 9.25 Mb to be sent per image on HOWLL and WOOF. Accounting for 10 images per cycle, these values give the payload data transmission needs for each satellite. These data values are given more concisely in table 80.

Table 80: Image Sizing Summary

Satellite	Initial Image Size (Mb)	Compressed Image Size (Mb)	Total Data to be Transmitted (Mb)
HOWLL	111	9.25	92.5
WOOF	111	9.25	92.5
PACK	18	1.3	13

#### 11.7.4 Software Considerations

Throughout the majority of the design process, design of the mission operations software has been neglected. This decision was made both due to our team's lack of experience with operations software design and a priority to ensure the C&DH hardware met the needs of the mission. Glenn Rakow from NASA Goddard Space Flight Center suggested the NASA Core Flight System (cFS) software, which is a generic flight software architecture framework developed by that is commonly used on CubeSats.[140] The cFS software operates as a bundle of modules that can be added and removed to satisfy each individual C&DH system to control the receiving and execution of commands, processing of housekeeping data from all subsystem, thermal and attitude



management, and any other needs.[141] The software is freely available to any small mission looking for a default operations software, and according to Glenn Rakow is highly customizable and should easily meet the needs of our mission.[135] Our team's operating software experience and the design stage of this mission means it is difficult to verify that all of the requirements for the software will be met by cFS, but this software has been developed to be easily customizable, which means any needs not currently met by the software could be met with slight edits to the software. cFS is also compatible with the Sirius hardware chosen for this subsystem. This means that cFS is a suitable choice for our mission software.

### 11.7.5 Compliance

Our chosen design falls within our constraints with more than sufficient margin. A list of the SIRIUS OBC/TCM system specifications and the smallest margin across our mission architecture is shown in Table 81.

Table 81: Specifications and Margins for Sirius OBC/TCM

Constraint	Sirius OBC/TCM	Min. Margin
Mass (kg)	0.26	13.33%
Volume (cm <sup>3</sup> )	1319	5.79%
Avg. Power (W)	1.3	35.00%
Unit Cost	\$100,000	-
Data Storage (GB)	32	25%

Mass and volume constraints were originally very stringent, but loosened after opting for a larger satellite size; this allowed us to include the Development Kit (DevKit) in our hardware design. The DevKit is a mechanical casing to house the chosen C&DH system. The DevKit increases the radiation tolerance of the C&DH system making it more reliable. Given the C&DH subsystem is a critical point of failure, increased reliability significantly reduces mission risk. Additionally the DevKit facilitates simple integration to overall satellite hardware easing physical design and manufacturing. It increases the required mass and volume of our hardware selection, but this was not problematic given our chosen design falls within our size constraints with sufficient margin.

Power consumption also falls well within the constraints outlined above. Average power consumption has a minimum margin of 35%. Peak power consumption will be controlled by satellite operational protocols to also fall within the aforementioned constraints.

Our estimated cumulative subsystem cost falls well within our allocated budget of \$24 million. Each C&DH system will cost a maximum of \$100,000. For our 4 satellites this corresponds to an estimated spend of \$400,000. Our subsystem cost has an extreme margin of 98.3%. Extra budget can be used to purchase testing systems, develop software, or given to other subsystems. Of course, limiting budget as much as possible will make our design proposal more attractive, thus this significant margin is beneficial.

As mentioned in section 11.7.2, our 32 GB of storage given by the Sirius OBC&TCM system maintains 25% margin, which is more than enough for stable operation.



## 12 Power Design

### 12.1 Subsystem Overview

The Power subsystem is responsible for ensuring that every subsystem within the mission has the power that they need to operate at any given time. This subsystem is an integral part of the mission, interacting with every subsystem and crucial to their functioning. The main purpose of the Power subsystem can be summarized into three goals: generation, distribution, and storage of power. Satellite power systems have multiple different options for each of these needs. In order to meet size, mass, and mission duration requirements, our team has determined the optimal method for each goal. For power generation, solar panels will be employed to allow the satellites to sustain their power needs for the lifetime of the mission. Power storage capabilities are essential to supply power when the spacecraft is in transit and eclipse, since these are times when power cannot be generated. Lithium-ion batteries will be used on all spacecraft to fulfill this need. Finally, the Power subsystem also needs to be capable of managing and distributing this power to the necessary components, which will be done by a Commercial-Off-The-Shelf (COTS) Power Management and Distribution System (PMAD). All of the equipment utilized by the Power subsystem will need to be able to withstand the space environment, particularly with regard to radiation and temperature extremes. The following will detail the design of the ARGOS Power subsystem and outline how the design meets our three main goals while remaining within the constraints of our mission.

### 12.2 Subsystem Objectives

The following are the specific objectives of the Power subsystem and how they relate to the overall mission goals.

Trace up to 3 main mission objectives (object tracking, communication and data relay, and autonomous navigation):

1. Generate sufficient power to support necessary subsystems to be able to track space objects in the cislunar domain, communicate and relay data between the satellites and earth, and perform autonomous navigation of spacecraft.
2. Store sufficient power to support necessary subsystems to be able to track space objects in the cislunar domain, communicate and relay data between the satellites and earth, and perform autonomous navigation of spacecraft when the satellite cannot generate power in eclipse.
3. Effectively distribute power to necessary subsystems to be able to track space objects in the cislunar domain, communicate and relay data between the satellites and earth, and perform autonomous navigation of spacecraft.

General Objectives:

1. Store sufficient power to support necessary subsystems during transit and orbit insertion of spacecraft.
2. Generate sufficient power to support necessary subsystems during transit and orbit insertion of spacecraft.



3. Effectively distribute power to necessary subsystems during transit and orbit insertion of spacecraft.
4. Ensure that the equipment used can withstand the environmental conditions of cislunar space such as extreme temperatures, radiation, and vacuum throughout the entirety of the mission lifecycle.
5. Utilize efficient, lightweight equipment to minimize the space, weight, and cost required for the power subsystem.

### 12.3 Subsystem Requirements

The power subsystem requirements detail what must be fulfilled by the power system design in order for mission success. All requirements are traced directly to one or several mission-level requirements and the latter is not fulfilled without the fulfillment of the former. A comprehensive list of the power subsystem requirements can be found in the Power Tab of the [ARGOS Requirement Spreadsheet](#) [6]. Target values found in many of the requirements are updated to reflect the final design of the power system. Listed below are all requirements grouped by their relevance to broader objectives of the power system.

Table 82: Power Subsystem Requirements

Req. ID (POW-####)	Description	Objective Category
F-001, F-002, F-003, F-006, P-004 through P-007	The Power subsystem shall generate sufficient power for the mission's subsystems for the duration of the mission	Power Generation
F-001, F-004, F-005, F-006, F-017, F-018, F-020, F-021, P-004 through P-007	The Power subsystem shall be capable of storing sufficient power for the mission's subsystems for times of no power generation over the duration of the mission	Power Storage
F-001, F-008, F-009, F-010, P-002, P-003	The Power subsystem shall be capable of distributing power to all subsystems that need it for the duration of the mission	Power Distribution
F-007, F-008, F-009, F-011, F-012, F-013	The Power subsystem shall identify and implement methods and/or equipment to mitigate the opportunity for system failure	Failure Avoidance
E-001 through E-008	The Power subsystem shall be capable of operating within the environments of the mission	Space Environment Operation

### 12.4 Subsystem Constraints

The power subsystem design is constrained by the mass, volume and cost budgets of the ARGOS mission. Regarding mass, PACK and HOWLL/WOOF are budgeted 2 kg and 4 kg, respectively. Regarding volume, PACK and HOWLL/WOOF are allotted  $1000\text{ cm}^3$  and  $2000\text{ cm}^3$ , respectively. Total cost for the power systems across all satellites in the mission architecture is constrained to \$32,634,000 and is recommended to be under \$2,000,000. Finally, the battery type for PACK satellites is constrained to 18650 Lithium-ion due to NASA crewed mission safety guidelines [142].



## 12.5 Subsystem Drivers

The following drivers guide all design choices of the Power subsystem.

### 1. Timeline

The lifespan of the spacecraft, from beginning of operations to end of life, is the ultimate driver for the power subsystem. This will determine how much total power the subsystem needs to be capable of generating and storing across its lifetime. This will directly influence the choice of solar panels, batteries, and PMAD. We cannot have solar panels and batteries that degrade too quickly, or else the entire mission will be cut short since power is an essential component to all subsystems.

### 2. Power required by each subsystem

The second most important driver behind the capabilities of the power subsystem is the total power required to operate the spacecraft. The power requirements of each subsystem will determine the solar panel area, the battery storage capacity, and the sophistication of the PMAD needed to support all operations of the spacecraft in any condition (launch, eclipse, etc.).

### 3. Environment: Temperature, Radiation, and Vacuum

The solar panels, batteries, PMAD, and accessory equipment must be able to withstand the extreme cislunar environment. Vast temperature variations, radiation exposure, and a vacuum environment will all be factors affecting the performance of the equipment. The hardware that we choose must be able to endure this environment for the lifecycle of the mission.

### 4. Equipment redundancy and availability

The equipment used by the Power subsystem needs to have sufficient redundancies to operate reliably for the duration of the mission. The Power subsystem is too vital to the mission to not safeguard against the possibility of failure. This means that we may have to factor in backup equipment for certain functions and consider the additional implications that would have. Furthermore, we need to take into account the availability of different components necessary to the Power subsystem. Some equipment may have lead times that are outside the scope of the mission life span and thus cannot be used.

### 5. Mass and Volume

The final driver behind the choices of the power subsystem is the mass and size of the equipment. The size of our equipment is constrained by the launch condition in order to accompany any Artemis Program launch, which would save copious amounts of resources and funds. The size condition also necessitates lightweight equipment to reduce the load on other subsystems. As a result, the solar panels must be able to generate the necessary power, while still being lightweight and deployable. The batteries must have sufficient energy density to store the required power while being as light and small as possible. The PMAD must also be able to manage the power load that we will be supplying, with redundancies, while avoiding unnecessary features and complications to reduce size, weight, and error.



## 12.6 Subsystem Design Approach

The Power subsystem utilized a design approach that was presented in lecture, with modifications to fit our mission needs made along the way [10]. We began with determining the different modes of operation for each satellite, such as nominal orbit, transit, and safe mode. These modes were used to determine which subsystems would require power at different stages of the mission and for what duration of time during that stage. This information was obtained from each subsystem and the Power subsystem tailored our capabilities to meet the needs of all subsystems. Each subsystem pursued a design that would minimize power, mass, and volume usage, so we were confident that every subsystem was requesting the minimum amount of power necessary to support their design. A margin of 10% was built into the design of the power system. After determining the power draw of each operational mode, we created the battery packs to meet the storage needs of the most demanding mode. This is the safe mode for each satellite, which is in operation eclipses lasting significantly longer than nominal ones. The batteries of each satellite are sized to be able to meet the nominal power draw of the safe mode for the duration of the eclipse. They are also sized taking into account the depth of discharge and capacity fade of the batteries throughout the length of the mission. The solar panels were then sized based on the power draw of the operational modes and the battery pack capacity. The solar panels must have enough area to be capable of both recharging the batteries and powering the satellite during sun time. The sizing must also account for periods of indirect sunlight and solar cell degradation. Finally, we chose a COTS PMAD system that meets the power and size needs of our subsystem while providing redundancy and reliability. This process was iterated numerous times as the needs of the mission became more defined and the power usage of each subsystem became clearer.

This design approach allows the Power subsystem to accommodate the needs of the mission and meet the power requirements while still minimizing mass and volume usage. Explicitly defining each operational mode gives a more comprehensive idea of the demands imposed on the Power subsystem and avoids overdesigning.

## 12.7 Formal Analysis

### 12.7.1 Eclipse Analysis

Satellite time in eclipse serves as a jumping off point for electrical power system design as this drives battery sizing. Analysis of eclipse and sun times for each satellite was performed in STK using the GNC subteam's simulation. Results from this analysis are tabulated below.

Table 83: Eclipse and Sun Time Data for ARGOS Satellites

Satellite Class	Nominal Eclipse Time	Nominal Sun Time	Maximum Eclipse Time
PACK	~45 min	~5 hrs	~5 hrs
HOWLL/WOOF	0 hrs	1 week-several months	~5 hrs



### 12.7.2 Power Load and Operational Mode Determination

Tables 84 and 85 below detail the ARGOS mission power load and duty cycle analysis for PACK and HOWLL. Due to the mission architecture requiring for WOOF to be relocated to the L1 lagrange point in the event of an emergency with HOWLL, WOOF is assumed to require the need for handling the same power loads. Analysis is derived from the power needs of other subsystems' components and from the power subsystem's modes of operation which are as follows:

- **Nominal Orbit:** Encompasses the vast majority of the mission during which the satellite is in its final orbit and experiencing nominal eclipse, as per Table 83. The satellite is performing nominal operations during this time, which includes data processing, heating during eclipse, attitude sensing, solar array articulation, and periodic communications, payload sensing, and attitude adjustment.
- **Transit Prior to Solar Array Deployment:** Encompasses the maximum of two hours of operation following satellite deployment from the launch vehicle dispenser and before solar arrays are fully deployed. This includes attitude sensing, data processing, and solar array deployment mechanism operation.
- **Transit Post Solar Array Deployment:** Encompasses the two hours of operation following solar array deployment during which time the satellite is inserted into its nominal orbit. Propulsion is the primary recipient of power during this mode, which also includes attitude sensing and adjustment, solar array articulation, and intermittent communications.
- **Safe Mode:** Encompasses those times during which the satellite is experiencing longer than normal eclipse. In this mode, only the essential components, namely the attitude sensors, heater, and on-board computer, are drawing power to keep the necessary power storage, and thus the battery size, low.



Table 84: PACK Power Budget Matrix

Component Information			Component Duty Cycle				
	Component Quantity	Nominal Power Draw (W)	Nominal Orbit	Transit Prior to Solar Array Deployment	Transit Post Deployment	Solar Array	Safe Mode
<b>ADCS</b>							
Sun Sensor	6	0.037	1	1		1	1
Star Sensor	2	0.271	1	1		1	1
IMU	1	15	1	1		1	1
Reaction Wheels	4	0.89	0.2	0		0.2	0
<b>Payload</b>							
Camera	1	4.2	0.1	0		0	0
<b>Propulsion</b>							
Thruster	1	40	0.000966	0		1	0
<b>Mech</b>							
Frangibolts	8	9	0	0.00417		0	0
Hinges	4	25.6	0	0.025		0	0
SADA	2	1.25	1	0		1	0
<b>Thermal</b>							
Heater	1	30	0.15	0		0	1
<b>Comms</b>							
Comms transceiver	1	13	0.0333	0		0.0333	0
<b>C&amp;DH</b>							
Processing Unit	1	1.3	1	1		1	1
Power Draw (W)			25.67	19.91		60.71	47.06
Required Storage (Wh)			34.22	39.83		121.41	235.32



Table 85: HOWLL/WOOF Power Budget Matrix

Component Information			Component Duty Cycle						
	Component Quantity	Nominal Power Draw (W)	Nominal Orbit	Transit Array Deployment	Prior to Solar Deployment	Solar Deployment	Post Deployment	Solar Array	Safe Mode
<b>ADCS</b>									
Sun Sensor	6	0.037	1	1		1			1
Star Sensor	2	0.271	1	1		1			1
IMU	1	15	1	1		1			1
Reaction Wheels	4	0.89	0.2	0		0.2			0
<b>Payload</b>									
Camera	1	4.2	0.1	0		0			0
<b>Propulsion</b>									
Thruster	1	40	0.000966	0		1			0
<b>Mech</b>									
Frangibolts	8	9	0	0.00417		0			0
Hinges	2	25.6	0	0.025		0			0
SADA	2	1.25	1	0		1			0
<b>Thermal</b>									
Heater	1	56.5	0.015	0		0			1
<b>Comms</b>									
Comms transceiver	1	53	0.0333	0		0.0333			0
<b>C&amp;DH</b>									
Processing Unit	1	1.3	1	1		1			1
Power Draw (W)				25.46	18.64		62.04		73.56
Required Storage (Wh)				33.95	37.28		124.08		294.26



### 12.7.3 Power Storage

Lithium-ion batteries were chosen to be the power storage option to support each satellite when they are in eclipse. Lithium-ion batteries were selected primarily for their high energy density and extensive flight heritage [143]. The sizing of the battery packs for each satellite is driven by the eclipse time and informs the size of the solar arrays. The approach detailed in Joe Troutman's lecture was utilized to determine the optimal batteries and sizing of the battery packs for each satellite [10].

The power draw for each subsystem in different operational modes was determined above to directly inform the power that the battery is required to produce throughout eclipse, transit, or other modes where power generation is not possible. A 10% margin was included for each power draw estimation to provide redundancy and reliability. Another component that determined the battery configuration was the nominal voltage at which each spacecraft operates. Per standards found in literature and lecture, we chose an operating voltage of 28 V for all satellites in the mission architecture [10], [144]. The basic requirements of the battery are detailed in table 86, summarizing the flight specific information that informed the battery selection.

Table 86: ARGOS Power Storage Requirements

Satellite Class	Power (W)	Draw	Power With Margin (W)	Voltage (V)	Current (A)
PACK	47.06		51.77	28	1.85
HOWLL/WOOF	73.56		80.92	28	2.89

We also computed the number of charge/discharge cycles that our batteries would experience throughout the lifetime of the mission.

$$\text{cycles/day} = \frac{\text{Hours in a day}}{\text{Period}} \quad (14)$$

Using equation 14, we determined that the PACK satellites' batteries would experience approximately 4.2 cycles/day, or 10,768 cycles throughout the 7 year life of the mission. Since the eclipses for HOWLL and WOOF are more sporadic, we estimated that for an eclipse average of every 1.5 weeks, the satellites' batteries would experience 243 cycles throughout the 7 year life of the mission. Battery cycling information was important to understand the depth of discharge (DOD) that we could achieve with each charge/discharge cycle and which brands could support our needs.

We chose Molcel ICR-18650M lithium-ion batteries for each satellite. Per the battery requirements of the back-up Artemis launches, we had to choose an 18650 battery size [142]. The Molcel ICR-18650M batteries have a high energy density at 217 Wh/kg, which was prioritized to minimize the mass of the battery packs [145]. Additionally, there was more testing and information about the performance of these batteries at high charge/discharge cycling. We chose to use the same batteries for all satellites for simplicity and continuity.

The capacity and details of the battery packs for each satellite are detailed in table 87. The EOL battery capacity is determined by equation 15, where  $I = 1.85$  A for PACK and  $I = 2.89$  A for HOWLL/WOOF.



$$Capacity = I * \text{Eclipse Time} \quad (15)$$

As previously stated, all batteries are designed for the longest eclipses experienced by each satellite, which happens to be roughly 5 hours for all satellites in the mission architecture. The BOL capacity is then determined using the chosen DOD and capacity fade of the battery in equation 16. To accommodate the high charge/discharge cycles, we chose to operate at a 60% DOD for all batteries to lengthen the life of our batteries with assuming a conservative 12% capacity fade [10].

$$\text{BOL Capacity} = \frac{\text{EOL Capacity} * (1 + \text{Capacity Fade})}{\text{DOD}} \quad (16)$$

Table 87: ARGOS Battery Pack Specifications

Satellite Class	EOL Capacity (Ah)	Series Cells	BOL Capacity (Ah)	Parallel Strings	Total Batteries	Total Mass (kg)	Total Volume (cm <sup>3</sup> )
PACK	9.24	8	10.35	4	28	1.40	106.56
HOWLL/WOOF	14.45	8	26.97	10	73	3.65	277.61

A complete breakdown of each table cell and equation can be found in tables 98 and 99 in the Appendix.

#### 12.7.4 Power Generation

For the ARGOS mission, power generation via solar cells was selected for a number of reasons including its widely predominant use in missions of similar size, destination, and timeline [143]. A trade study was performed to determine the optimal solar cell for the power needs of the mission. NASA's recent Small Spacecraft Technology Report offers information on some of the best available solar cells on the market [143], and information regarding beginning- and end-of-life efficiency as well as flight heritage was taken into account in order to downselect for a solar cell. Rocket Lab's Z4J cell was ultimately selected due to its comparable BOL efficiency, high radiation hardening for maintaining high efficiency in EOL [146], and for its use on NASA's highly funded and researched Lunar Gateway station set to orbit in the cislunar space [147].

Solar array sizing analysis was performed per Joe Troutman's lecture regarding Satellite Electrical Power System Design [10]. The power load for each satellite class can be determined using the information in Tables 84 and 85. The total power that must be generated during a satellite's sun time is the EOL power drawn from the subsystems during this period summed with the power necessary to recharge the battery. The former is represented by the nominal orbit power draw in the budget tables. The latter can be derived using the following equation:

$$\text{Battery Recharge Power (W)} = \frac{\text{Battery Capacity (Ah)} * \text{DOD} (\%)}{\text{Sun Time per Period (hrs)} + 0.08 \text{ hr margin}} (\text{Nominal Bus Voltage (V)}) \quad (17)$$



where the sun time for each satellite is the nominal sun time from Table 83. A 2.5% harness drop and a 90% pointing frequency, per ADCS, is accounted for, and a 10% margin is applied to final power load values. Using the Z4J datasheet information [146], a max EOL cell voltage and current are determined which are 2.84 V and  $11.47 \text{ mA/cm}^2$ , respectively. Per advisory from Joe Troutman, a cell voltage of 2.79 V and an accompanying current of  $11.42 \text{ mA/cm}^2$ , below the max power point, were selected to avoid a severe drop off in power just beyond the max power point [10]. From here, the number of series cells is determined simply by dividing the nominal bus voltage by the cell voltage and the number of parallel cells is determined by dividing the power load by the power generated per cell. The latter is determined assuming a cell size of  $32\text{cm}^2$  and simply taking the product of the operating cell voltage and current. Table 88 below shows final values regarding power generation.

Table 88: ARGOS Power Generation Data

Satellite Class	Total Power Load (W)	Number of Series Cells	Number of Parallel Cells	Total Cell Number	Total Cell Area ( $\text{cm}^2$ )
PACK	42.03	12	4	48	1536
HOWLL/WOOF	29.38	12	3	36	1152

### 12.7.5 Power Distribution and Management

The Power subsystem chose to use a COTS PMAD system to distribute and regulate power for each satellite. Specifically, the Pumpkin Space Systems EPSM 1 was selected. The same COTS PMAD will be used for all satellites. As with the choice to use the same battery type on all satellites, using the same PMAD will allow for increased simplicity as well as interchangeability, if needed. The low mass and small volume of the Pumpkin Space Systems EPSM 1 allows this PMAD to be implemented on all of the satellites [148]. The peak power output of the Pumpkin Space Systems EPSM 1 is higher than the power loads experienced by our satellites, but the other qualities of the PMAD made it the optimal choice, despite what may seem like an unnecessarily high margin for peak power output. The specifications of the Pumpkin Space Systems EPSM 1 are summarized in table 89.

Table 89: Specifications of Pumpkin Space Systems EPSM 1 [143], [148]

Peak Power Output (W)	Mass (kg)	Volume ( $\text{cm}^3$ )	Efficiency	Technology Readiness Level
300	0.3	180	99%	9

In a small satellite that is severely constrained by mass and volume requirements, high efficiency is important in a PMAD. If the PMAD is inefficient, then there has to be excess battery storage and power generation capabilities to account for the power that the PMAD will waste. This comes at the price of increased mass and volume. At an efficiency of 99%, the Pumpkin Space Systems EPSM 1 will not waste power. In addition to being lightweight and compact itself, it will not necessitate that we increase the mass or volume of any of our other components.

Due to the small loads of each satellite and operating time of our mission, direct energy transfer



was also a viable option for power distribution and management [144]. The main advantage of this type of distribution is the sparse equipment that it requires, making it lightweight [144]. However, after an increase in the mass and volume budget of each satellite and refining the mass of the battery packs, each satellite had the margin for a COTS PMAD. Including 10% of the mass and volume budget of each spacecraft for electrical wiring and connections, the chosen PMAD still allows each satellite to comply with the constraints and requirements. Given this compliance and the added benefits, the Power subsystem proceeded with a COTS PMAD. The COTS PMAD allows for increased redundancy and reliability. The EPSM 1 has an integrated shunt system, protecting the power system from overloading and failures.



## 13 Mechanisms Design

### 13.1 Subsystem Overview

The mechanisms subsystem is tasked with ensuring the functionality of all spacecraft components that have relative motion within the body frame. The first role of the mechanisms subsystem is to dispense the satellites from the launch vehicle. The subsystem relies on communication with the LV team, as the dispenser must be compatible with the vehicle chosen to launch each satellite. Mechanisms also communicates with the SM team to ensure the dispenser interfaces properly with the satellite frame. After the satellite has been separated from the launch vehicle, mechanisms is responsible for releasing solar arrays from their stowed position and deploying them to their operational position. The deployment may cause a torque to be exerted on the spacecraft, so the ADCS team must be consulted. Additionally, release and deployment cause shocks within the spacecraft, so mechanisms must collaborate with the SM team to ensure the shocks do not damage any other components. Throughout the remainder of the operation of the mission, the mechanisms subsystem is responsible for articulating the solar arrays towards the sun. Solar articulation is intricately involved with the Power and ADCS teams.

### 13.2 Subsystem Objectives

The mechanisms subsystem will ensure that all dynamic components of the spacecraft are high-functioning and robust. The satellites need to be separated from the launch vehicle once it has reached the appropriate point in its trajectory, and a mechanism must be used to reliably deploy the satellites to begin their own mission.

Solar panels must be stowed and then deployed on each satellite in order to provide the required power to the satellites to allow for all mission-level operations that require power (tracking, communications, etc).

All of these objectives will aid in the mission-level objective to create a robust communications and data relay network in the cis-lunar space. The mechanisms will be sufficiently robust such that one minor failure will not create a sequence of cascading failures, but the mechanisms simultaneously aim to be as budget-efficient as possible.

### 13.3 Subsystem Requirements

The Mechanisms subsystem has thirty requirements which set out to define what the subsystem must achieve. The requirements are split into four categories: functional requirements define the need for a subsystem to complete a task, performance requirements define the standard to which those tasks must be completed, constraints define limits for parameters such as mass and power draw, and environmental requirements define the external factors that the subsystem must operate within. Since the Preliminary Design Review, many numerical values were refined from their previous TBC or TBR values. Additionally, some requirements were added to reflect roles that the subsystem was performing that lacked requirements previously. Table 90 provides an overview of the requirements, while a comprehensive list and description of them can be found in the "Mech" tab of the "Requirements Spreadsheet" Google Sheet [6].



Table 90: Mechanisms Subsystem Requirements

Req. ID (MECH-#-##)	Description	Objective Category
F-001, F-002, P-005	The Mechanisms subsystem shall constrain, release and deploy solar arrays on each satellite	Solar Array Deployment
F-003, P-006 through P-009	The Mechanisms subsystem shall provide a method for precisely articulating the solar arrays while maintaining the ability to transfer power back to the satellite body	Solar Array Articulation
F-005, F-011 through F-013	The Mechanisms subsystem shall provide a method for dispensing each satellite from the launch vehicle.	Satellite Dispensing
C-001 through C-006	The Mechanisms subsystem shall operate within all imposed budgets of mass, volume, and power	Budget Compliance
F-006, F-012, P-001	The Mechanisms subsystem shall operate reliably with redundancies and a failure rate of less than 1%	Reliability
F-007, F-008, E-001 through E-003	The Mechanisms subsystem shall be able to survive in the radiative, temperature, and gravitational environments of cislunar space, as well as all modes and loads required by the mission	Reliability

### 13.4 Subsystem Constraints

The mechanisms subsystem must operate within many of the same constraints that encompass the entire mission. The primary trade-off for the mechanisms is to ensure they can operate robustly while not requiring an excessive mass, cost, or power budget. The mechanism subsystem masses are constrained to 2.25 kg for each satellite, while the volumes are constrained to 1000 cm<sup>3</sup> on the 27U satellites and 1600 cm<sup>3</sup> on the 12U satellites. The mechanisms power budget is 2.5W for nominal draw on all satellites, 72W for peak draw on 27U satellites, and 102.4W for peak draw on 12U satellites. The thermal constraint is that each mechanism must be stable within a range of -50°C to 70°C. The design approaches in this report aim to stay within these constraints.

### 13.5 Subsystem Drivers

The Mechanisms subsystem has a variety of considerations which drive our subsystem design, some of which relate to budgets and are derived from the overall mission drivers, and others that arise from environmental concerns and margins specific to mechanisms.

- Mass:** The mass limitations of the spacecraft will directly influence the amount and type of mechanisms that can be included. Design choices may favor mechanisms that weigh less.
- Volume:** Similar to mass, the volume budget will influence the complexity of mechanisms that can be used, so design choices may favor mechanisms that have a smaller volume.
- Power:** The power budget will influence the amount of power the mechanisms can be used, so design choices may favor mechanisms that use less power.
- Timeline:** The timeline for the beginning of operations and lifespan of the spacecrafts is a driving factor that will influence mechanism design. Mechanisms must be developed and tested prior to launch, which encourages the use of components which have an extensive flight heritage.



5. **Vacuum/Low Gravity Tolerance:** The system chosen for our spacecraft must also function effectively in vacuum and low-gravity. The necessity to operate successfully in these conditions may drive mechanism decisions, as well as create the need to design smaller mechanisms to prevent these valve and pump issues.
6. **Thermal Considerations:** As the parts of the satellite contract and expand with varying temperatures, mechanisms must keep in mind thermal considerations, primarily operating temperatures.
7. **Vibrational Considerations:** Selected mechanisms must be tested under vibration to ensure that they remain secure.
8. **Radiation and Debris Tolerance:** Many aspects of space systems contain delicate electrical components, actuators and circuits. It is necessary to select mechanical components that are radiation hardened and robust enough to withstand impacts from particulate matter.
9. **Failure Rate:** If any of the mechanisms fail, the mission will not meet its objectives, so it is important to choose designs with a low failure rate for each mechanical component.
10. **Mean Time to Failure:** Mean time to failure will measure how long a mechanism can continue functioning until it needs to be replaced. A longer mean time to failure is more favorable, as it will ensure that the mission can stay operational as long as is required.
11. **Built in Redundancy:** Any mechanism that is put in place should have a built in redundancy measure to ensure that, if the mechanism fails, there is a backup in place that can complete the same task.
12. **Force and Torque Margin:** Designing around high force and torque margins will ensure that the mechanisms can perform their role correctly with the necessary actuation capabilities.

## 13.6 Subsystem Design Approach

Four primary mechanisms were investigated to carry out the mechanisms subsystem objectives: a satellite dispenser, and solar array release, deployment and articulation mechanisms. In our designs, the main drivers were mass and volume constraints, as well as ensuring that the components we chose could withstand the various environmental challenges (e.g., vacuum, vibrations, temperature, etc.), and had low failure rates and high force and torque margins. The majority of Mechanisms' design did not focus on timeline, but we did aim to choose readily available commercial off-the-shelf (COTS) components to ensure that the manufacturing and testing process would be timely and efficient. Additionally, the selection of COTS products automatically leads to the verification of requirements surrounding survival in the space environment.

### 13.6.1 Satellite Dispenser

The satellite dispensing mechanism will be used to eject the satellite from the launch vehicle once it has reached its predetermined drop-off location. The design of satellite dispenser depended on a variety of factors, such as actuation redundancy, allowable internal volume, and compatibility with the necessary launch vehicles. The final selected launches are all compatible with CubeSat dispensers, so the downselection process (outlined in Section 13.7.1) involves a trade study between various types of dispensers. The dispenser that was selected, Canisterized Satellite



Dispenser, meets the subsystem requirements for redundancy, failure rate internal volume, and compatibility with all the launch vehicles, which will be further described in Section 13.7.1.

### 13.6.2 Solar Array Release

As previously described in Section 12, each spacecraft will use solar arrays to generate power, and more surface area of panels is needed than can be provided by the exterior of the spacecraft alone. Thus, the solar arrays must be folded up during launch and released when the satellite is separated from the launch vehicle. The constraint and mechanism and its method of release is crucial, as deployables are a common source of CubeSat failure [149]. Many different methods exist for releasing solar arrays, so an in depth trade study was performed to investigate the merits of each. Several factors were considered, first, the constraint force must be sufficient for the solar arrays not to release prematurely. This is a crucial characteristic, but given that more points of contact could be added, it was not an extremely strong driver of the decision. Reliability and simplicity were also considered. A reliable system with redundancies is required, as failures in solar deployment would be catastrophic to the overall mission, and an overly complex system with moving parts provides many possible failures modes. Redundancy was the largest driver of the decision on solar array release mechanism. Actuation time is also considered, as it is sometimes important for components to be deployed simultaneously. Shock is an important factor in solar deployment, as quick movements can create large shocks in the spacecraft, which must be avoided or mitigated to ensure other systems are not damaged [150]. Lastly, of course, mass, volume, power, and cost were considered to ensure the mechanisms subsystem stays within its budget for those core mission elements.

### 13.6.3 Solar Array Deployment

After the solar panels are released from their stowed position, they must be unfurled to maximize power generation. Many different methods exist and several configurations of solar panels are possible, but for simplicity, and due to its flight heritage on similar scale spacecraft, a unidirectional panel alignment was chosen. Torque is the most important factor for hinges, as the panels must be able to deploy. Reliability is also crucial, as if the panels fail to unfurl, mission operations will be severely hindered by the lack of power. An additional consideration was shock, as if the hinges open too rapidly, there will be a shock upon reaching the fully deployed position. Once the fully deployed position is reached, the hinges should be able to lock in place to ensure the panels maintain their deployed position throughout the remainder of the mission. Lastly, the hinges must stay within the mechanisms subsystem budgets for mass, volume, power, and cost. Research was performed to identify hinges that had been used on previous missions, but few COTS components were found. Thus, some level of custom hinge design would have to occur. Different types of hinges were investigated before selecting and designing a hinge for the satellites.

### 13.6.4 Solar Array Articulation

In order to maximize power generation, the solar panels should be pointed normal to incoming sunlight. Adjusting the attitude of the satellite to fully face the sun would be taxing both in terms of propellant and for the time it would require, as other systems onboard the spacecraft also require pointing, including communications antennae and payload sensors. Thus, the ability to independently articulate the solar panels is quite important to the success of the mission. Research



into similar missions showed that the vast majority of spacecraft that articulate their solar panels employ a Solar Array Drive Assembly (SADA), and many such products exist on the market.

A trade study was performed on different SADAs in order to determine the best product. Bi-axial articulation was investigated, but such products are costly and heavy, so only single-axis SADAs were included in the trade study. Many characteristics of the SADAs were compared. Torque is the most obvious requirement, as the SADA must be able to move the arrays at a reasonable speed. Torque values are calculated in Section 13.7.4. The SADA must be capable of full and precise rotation in order to successfully complete its objective. Additionally, because the SADA serves as the link between the solar panels and the rest of the spacecraft, power must be transmitted across it. Extra complexity is created due to the rotating joint, but all analyzed components are capable of transmitting power, most often using a slip-ring mechanism to do so. As with all mission components, operation within the standard constraints and within the cislunar environment was also considered and highly valued.

### 13.6.5 Other Considered Mechanisms

The inclusion of several other mechanisms was discussed, including sensor covers and pointing mechanisms. However, after consultation with other subsystems (primarily LV, Payload, and ADCS) it was determined that they are not necessary—it is possible to ensure the sensors are sufficiently protected without covers, and eliminating the covers both reduces risk and decreases the subsystem's toll on several different budgets. Including a sensor cover is a single point of mission failure: if the cover fails to open, the mission cannot meet its primary object tracking objectives. While redundancy can be implemented in the method of releasing the sensor, there are inherent risks in developing our own system to protect the satellites. This was a risk that did not outweigh the reward of having extra safety for the sensors. In fact, our analysis showed that there is a higher risk of failure due to sensors not deploying than there is risk of damage during testing and launch.

The pointing mechanism, specifically the gimbal we had considered, was also determined to be unnecessary. If we were to include it, it would cause too complex of a design, since we would also need to design a "hold down and release" mechanism to keep the sensor from moving during launch. In addition, the large size of the sensor would have been difficult to mount to a gimbal and the entire setup would likely exceed volume requirements. In the end, ADCS determined that they should instead take over the responsibility of pointing the sensor towards the objects. In the ADCS team's analysis, they determined that they could use their reaction wheels to rotate the satellite, thereby eliminating the need for the extra mass that the gimbal would have.

Although we did not include these two mechanisms, our subsystem requirements are still being met. The sensor protection requirement is met by our plan to place temporary covers over the sensors during testing and integration, which will be removed before launch. Further, the selected launch vehicles have fairings which are ISO Clean Room 8, and, after consultation with the Payload subsystem, we determined that sufficient dust would not accumulate on the sensors during launch to necessitate an actuated cover [55]. The pointing requirement has been passed off to ADCS, who will use other methods to ensure the mission-level tracking requirements are met.



## 13.7 Formal Analysis

### 13.7.1 Satellite Dispenser

The selection of dispenser went through many iterations, as the launch vehicles changed multiple times. In addition, through the design process, it became clear that the dispenser must be able to have a payload volume of at least 12U, and then later at least 27U.

Table 124 in Appendix A.10 contains a summary of the trade study conducted to select a satellite dispenser.

In earlier stages of our analysis, when we were considering only dispensers compatible with the Photon fairing, the two possible dispensing options were the Canisterized Satellite Dispenser (CSD) and the Maxwell Satellite Dispenser.

We considered the CSD to be beneficial for its low cost, 99.6% chance of success (or a 0.4% failure rate) with a 97.5% confidence level, as well as its extensive flight heritage [151]. In addition, it has two independent circuits and a triple redundant commutator to ensure deployment, and it allows for payloads with 15% more volume and 1 inch longer than standard CubeSats [151]. Finally, it is the only dispenser that was considered which had a tab interface design (as opposed to rails) to reduce vibrations.

On the other hand, the Maxwell was beneficial for its lightness, dual separation switches, one-way clutch bearing, in-door hinge to restrict door bounce back, low spin-rate reliable deployment [152]. It has a maximum payload mass of 5.5kg/U (although they still recommend 2kg), and promises a reduced lead time, arriving 4 weeks after ordering [153]. However, it is not available above 6U, so we selected the CSD as our dispenser. The rest of the launches were chosen to also use CSD in order to maintain consistency in design and lower testing and integration costs.

After further design iterations, the LV subsystem has determined that PACK-C will launch on the Firefly Aerospace Blue Ghost [34] for deployment to Low Lunar Orbit (LLO), and PACK-E will be launched on the Artemis IV [154]. The 27U HOWLL and WOOF satellites will be launched as primary payloads on SpaceX's Falcon 9. We decided to maintain our choice of using CSD, as it continued to meet all the requirements and is said to have a lower cost than most other dispensers [155].

One caveat with using a 27U design for our mission was that there are no readily available commercial off-the-shelf 27U dispensers. However, Rocket Lab states that their CSD is scale-able up to 27U in a 3U x 3U x 3U layout [151][156]. In order to maintain consistency in dispenser between all the satellites, mechanisms will design a version of the CSD scaled up from 12U to 27U. The following chart shows key dimensions for the scaled-up 27U dispenser, with exact dimensions determined in consultation with the SM subsystem.

Table 91: Dimensions of Scaled 27U CSD

Product	s (kg)	Height, +Y dimension (mm)	Width, ±X dimension (mm)	Depth, +Z dimension (mm)
12U CSD [151]	5.65	270.51	263.28	454.3
Scaled 27U [156]	15.1	470	470	470



To summarize the CSD's compliance with the Mechanisms requirements: it has redundant actuation, a failure rate of 0.4% (less than the required 1%), it fulfills the volume requirements for 12U and 27U, and it is compatible with all the launch vehicles. In addition, it uses a tab interface to reduce vibrations. Figure 43 shows the CSD and an example of what it might look like dispensing a satellite.

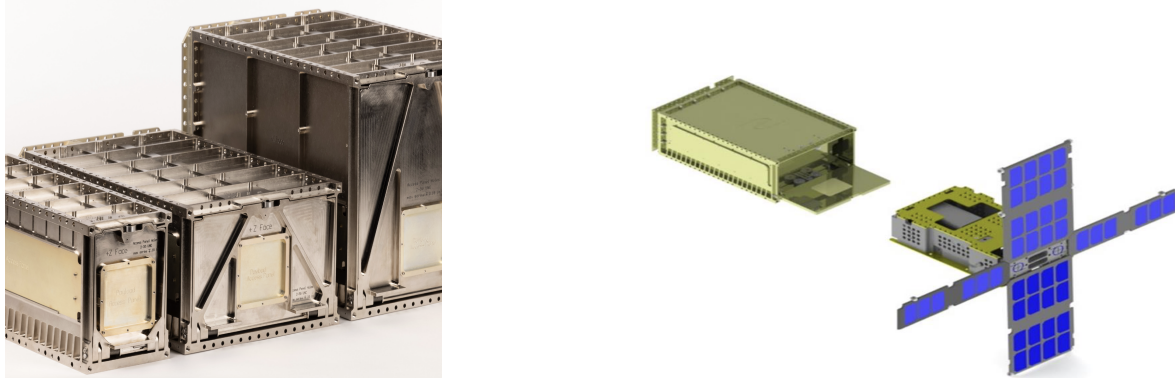


Figure 43: Rocket Lab CSD and Example of Dispensing [151]

### 13.7.2 Solar Array Release

As a result of the trade study found in Appendix A.10 (Figure 101), Frangibolts were selected as the constraint and release mechanism for solar arrays. This choice stemmed primarily from their redundancy and simplicity. The Shape Memory Alloy (SMA) material fractures at a certain temperature as a result of its material properties, and the mechanism contains two redundant heaters to activate the bolt. The Frangibolts have a longer release time than other methods, but due to the controlled method of deployment which will be described in Section 13.7.3, simultaneity was not required. Any small differences between actuation of each Frangibolt will not create a significant torque on the spacecraft, as one panel releasing before another would not lead to a rapid deployment of the panels and asymmetry of the satellite. Ensign-Bickford Aerospace and Defense (EBAD) is the industry leader of Frangibolts, and they offer a wide array of sizes. Mass, power, and volume decrease along size, so the only characteristic that we wanted to be large is constraint force.

In order to determine the required constraint force, the SM team performed an analysis in CREO. They placed four Frangibolts on each stack of panels (one in each corner to prevent flapping), and they determined that the maximum stress in the Frangibolts is 42 MPa for any spacecraft. The smallest Frangibolt that EBAD manufactures provides 667 N of load support, and the bolt has an area of  $6.8 \text{ mm}^2$ , leading to a maximum stress of 97.8 MPa [157]. Thus, each Frangibolt has a stress margin of at least 0.16 with a safety factor of 2, using the following equation [158]

$$\text{Stress margin} = \frac{\text{strength of material}}{\text{maximum von Mises stress} \cdot \text{safety factor}} - 1 = 97.8/(42 * 2) - 1 = +0.16 \quad (18)$$

Thus, the smallest size can be chosen. The Frangibolts do have a comparatively high power draw (9 W each), for a total of 72 W (four frangibolts each on two stacks of panels), but their deployment only takes around 35 seconds, and after that, no power is required. The Power subsystem

determined that this high but short power draw would not be an issue. All four Frangibolts must activate to release the solar panels, but they have built-in redundancies and no documented in-space failures were found, so we are confident in the reliability of this mechanism.

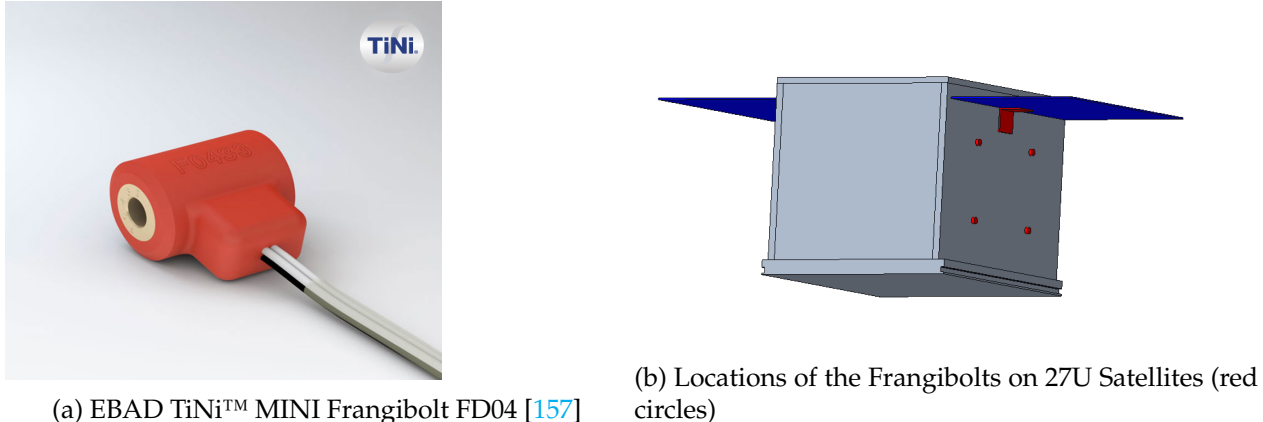


Figure 44: Frangibolt and Locations

### 13.7.3 Solar Array Deployment

Before designing and analyzing a hinge for solar deployment, the torque required to unfurl them must be identified. In order to find the torque, the size and number of solar panels was determined in conjunction with the Power and SM subsystems. To increase symmetry, which assists the ADCS subsystem, the same number and size of solar panels will be on two opposing faces of each satellite. We will thus have two sets of panels on each satellite, which will henceforth be referred to as a "stack." For the 27U satellites, there will be one solar panel per stack, measuring 350mm x 230mm x 2.5mm, and it weighs 624g. For the 12U satellites, there will be two solar panels per stack, measuring 350mm x 150mm x 2.5mm, for a total weight of 809g. These sizes are further explained in Sections 15.7.5 and 15.7.6.

The torque required for each hinge derives from the size of the solar panels. The maximum possible torque required would be if every panel unfurls before the first hinge does so. That would lead to a maximum length for both of 280mm for 27U and 300mm for 12U (allowing 50mm for the base hinge and 100mm for the second hinge). We will approximate the solar arrays as a rectangular prism of constant density. The moment of inertia of a rectangular prism about a point not through the center is given by

$$I = \frac{1}{12}m(h^2 + w^2) + md^2 \quad (19)$$

where  $d$  is half of  $w$  because of the parallel axis theorem. Because the width is much larger than the thickness, we can ignore the thickness term ( $h^2$ ). Thus, for PACK

$$I_{PACK} = \frac{1}{12}(0.809)(.3^2) + 0.809 \times 0.15^2 = 0.024\text{kg} \cdot \text{m}^2 \quad (20)$$

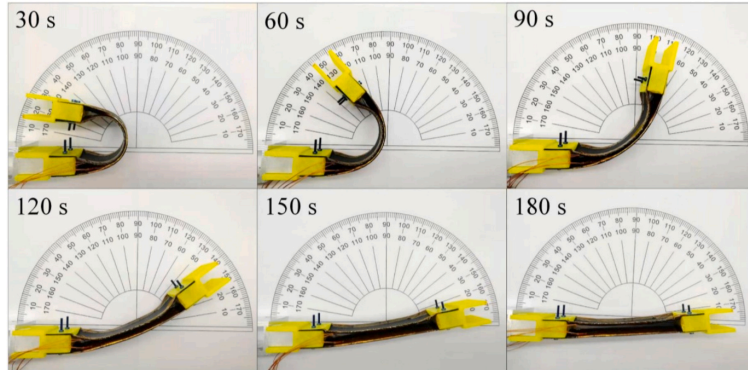


Figure 45: Recovery Process of SMPC Smart Hinge [159]

and for HOWLL and WOOF

$$I_{HOWLL/WOOF} = \frac{1}{12}(0.624)(0.28^2) + 0.624 \times 0.14^2 = 0.016 \text{ kg} \cdot \text{m}^2 \quad (21)$$

If we assume a maximum angular acceleration of  $0.5 \text{ rad/s}^2$ , which is exaggerated (per standard rotation rates [150]), we get torques of

$$\tau_{PACK} = I_{PACK} * \alpha = 0.012 \text{ Nm} \quad (22)$$

$$\tau_{HOWLL/WOOF} = I_{HOWLL/WOOF} * \alpha = 0.008 \text{ Nm} \quad (23)$$

These required torques are quite small, which means that the torque requirement should be achievable for any hinge. Many types of hinges and springs for deployables exist [150]. On the passive side, there torsion springs, constant force springs, gas springs, and tape hinges, among others. For an actively controlled hinge, stepper motors can be used. Inherently, passive control is more reliable than active, as there are no mechanical issues or component failures that could prevent the hinge from rotating. Each of the aforementioned spring types functions in a slightly different way, leading to differences in torque, mass, and predictability. One commonality between the passive hinges, though, is that their deployment is not controlled. With the incredibly small moments of inertia shown above, if the torque is too high, the panels will accelerate incredibly fast, leading to large shocks at the end of their motion. A damper could be added to the hinge to slow it down, but this would add mass and complexity. Thus, an alternative solution was sought out, where shock could be minimized without overtaxing our mass budget.

A shape memory polymer composite (SMPC) smart hinge has been developed by researchers for the very purpose of deployable space structures [159]. The material properties of this hinge allow it to be pre-bent, and upon heating, it will slowly unfurl itself. In the research paper describing the qualities of the hinge, a resistive film was placed on the material, and when power was sent through it, it heated up [159]. The hinge then unfurled from bent to 180 degrees over the course of three minutes. Upon reaching full extension, the SMPC is "self-locking" and stiffens [159]. Thus, there is no risk of the hinge returning to its bent position or flexing to interfere with other parts of the spacecraft. Figure 45 shows the SMPC hinge as it unfurls over time.

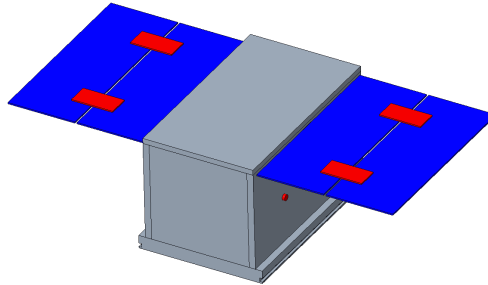


Figure 46: CAD of the Solar Array on PACK satellites (solar arrays in blue, hinge brackets in red)

Some elements of the hinge will be slightly changed to enhance its utility for the ARGOS mission. First, a redundant heating method will be employed, so if one heater fails, the hinge will still be able to unfurl. Second, the hinge at the base of the stack will only rotate 90 degrees, as the orientation of the stack relative to the satellite itself only necessitates 90 degrees. This mechanism is still under development, which does create some risks, but the slow deployment and low weight of the SMPC hinge outweighs that risk, especially when considering the redundant heating that can be implemented and the fact that the hinge relies on chemistry to deploy, not a mechanical component. Further, no hinges were found with a high TRL, so selecting this hinge with TRL 4 or 5 is no worse than any other option. Obviously, hinges for this purpose do exist, but no COTS hinges could be identified, so it seems likely that satellites typically have custom hinges built.

The SMPC hinge can provide 1.1 Nm of torque at full compression, which is over 100x the requirement as described above. This amount of torque leads to an angular acceleration of

$$\alpha_{PACK} = \frac{\tau}{I_{PACK}} = 45.3 \text{ rad/s}^2 \quad (24)$$

$$\alpha_{HOWLL/WOOF} = \frac{\tau}{I_{HOWLL/WOOF}} = 67.5 \text{ rad/s}^2 \quad (25)$$

These accelerations are far higher than would ever be needed. Fortunately, while they appear to be so excessive that they would cause damage to the spacecraft, the material properties of the SMPC prevent it from reaching such speeds. The hinges take 180s to fully deploy, so the average angular velocity will be 1 degree per second, leading to much smaller accelerations.

In addition to the SMPC hinge, aluminum brackets will be placed at the base of the solar panels and at the joints to increase stability. These brackets will be custom built, as they are simple components that seek to provide more than one contact point (or strengthen the one contact point) between solar panels. Figure 46 shows the two hinge brackets in red, while Figure 44 shows the 90 degree bracket on the underside. The SMPC hinge would lie between the two hinge brackets at the panel interface and along the hinge bracket at the base of the array.

#### 13.7.4 Solar Array Articulation

With the solar panel sizes as previously stated, torque calculations were performed for solar articulation. Rotation is about the axis normal to the satellite, so the "length" for the moment calculation



is 350mm for each spacecraft. We can again disregard the thickness term because it is incredibly small, and when squared it only becomes smaller.

$$I = \frac{1}{12}m * (h^2 + l^2) \quad (26)$$

$$I_{PACK} = \frac{1}{12} * 0.809 * (0.35^2) = 0.0082 \text{ kg} \cdot \text{m}^2 \quad (27)$$

$$I_{HOWLL/WOOF} = \frac{1}{12} * 0.624 * (0.35^2) = 0.0064 \text{ kg} \cdot \text{m}^2 \quad (28)$$

If we assume an angular acceleration of  $0.5 \text{ rad/s}^2$ , we get torque requirements of

$$\tau_{PACK} = I_{PACK} * \alpha = 0.0041 \text{ Nm} \quad (29)$$

$$\tau_{HOWLL/WOOF} = I_{HOWLL/WOOF} * \alpha = 0.0032 \text{ Nm} \quad (30)$$

All power generated by the solar panels must be transmitted across the SADA as well, and Section 12.7.4 shows that under 40W needs to be transmitted to the satellite. Thus, from each solar array, only 20W must be transmitted.

Every SADA that was analyzed in the trade study shown in Table 127 in Appendix A.10 meets both the torque and power transmission requirements [160][161][162][163][164][165][166]. Thus, the decision between SDAs was based on other factors. Principally, the availability of specifications was important, as without data on the component, it would be difficult to determine our budget compliance. Also, the ability to interface with both the 27U and 12U satellites was an important factor, as some SDAs, such as the MicroSADA from DHV Technology, are not made for 27U satellites [165]. Thus, the SADA made by HoneyBee Robotics was selected, as sufficient information was available about it and it is one-sided so it is compatible with any CubeSat size. As is, the HoneyBee product has extremely high torque and power transmission margins. Thus, the ARGOS mission will employ a custom, scaled-down version of their COTS component. The SADA is scaled down by a factor of 4, and all values except precision and range are scaled by the same factor. While some specifications may not change linearly, plenty of margin remains within our budgets and for the requirements to account for discrepancies. The specifications for the original and scaled down versions of the SADA are shown in table 92.

Table 92: Scaled down HoneyBee Robotics SADA

Product	Torque	Mass (g)	Power (W)	Precision (deg)	Range (deg)	Power Transmission (W)
Original Product [163]	0.75 Nm	900	5	+/- 1.8	+/- 180	450
Scaled down (1/4)	0.1875 Nm	225	1.25	+/- 1.8	+/- 180	112.5

The SADA can provide 0.1875 Nm of torque, which can accelerate the 27U array at  $29.3 \text{ radians/s}^2$  and the 12U array at  $22.9 \text{ radians/s}^2$ , both of which are excessive given the listed rotation rate of 1 degree (0.017 radians) per second [163]. The torque margin is thus far higher than 200%, as even half of those angular accelerations would not be necessary.



### 13.7.5 Budget Compliance

In this section we provide a brief summary of budget compliance, to ensure that our subsystem not only meets the objectives and requirements, but also remains within the constraints for budgets.

#### Cost

Although we used all COTS components, the costs for all mechanisms were very difficult to find. Course staff advised us not to contact companies directly to inquire about prices, and since many products do not have prices listed, determining the price required estimation. Thus, the method we used to obtain costs was researching past missions that used similar components and estimating our costs based on this research. Table 93 is a breakdown of estimated cost for the mechanisms subsystem.

For the shape memory polymer composite smart hinge, we use an estimate that shape memory polymer costs approximately \$11 per pound [167]. Multiplied by approximately 0.01 kg or 0.022 pounds per hinge, this yields a unit cost of 24 cents per hinge. To account for other materials in the hinge, such as epoxy resin and twill fabric [159], we estimate a cost of \$1 per hinge. Similarly, we estimate the brackets to cost at most \$10 per unit, since they will be manufactured by us and made of aluminum.

Our cost for the scaled-down Honeybee SADA is based on two estimates. The first was obtained from speaking to Mr. Galvin, one of the course instructors with years of experience in industry, who informed us that, since Honeybee does high-end work (for Mars missions, etc.), the cost of such a device would be on the order of \$50,000-100,000 [168]. The second estimate is that our SADAs would cost on the similar order as a cryovaccum-compatible stepper motor from Phytron, which is approximately \$10,000-20,000 [169]. Our final estimate, then, is an average of these values, considering that the SADAs will be scaled down from the standard Honeybee size, but will still require development and testing costs.

Table 93: Estimated Costs for Mechanisms

Component	Cost per Unit (\$)	Units per Satellite	Total units	Estimated Total (\$)	Source(s) for estimate
Rocket Lab CSD [151]	150,000 for 27U (includes cost to scale up), 40,000 for 12U	1	2 27U, 2 12U	380,000	[170]
EBAD TiNi™ MINI Frangibolt FD04 [171]	100	8	64	6,400	[172]
Shape Memory Polymer Composite Smart Hinge [159]	1	4 for each PACK + 2 for HOWLL/WOOF	12	12	[167] [159]
Aluminum Stabilizing Hinge Bracket	10	6 for each PACK + 2 for HOWLL/WOOF	16	160	Mech subsystem estimate
Honeybee Robotics Micro-Sat SADA[163]	45,000	2	8	360000	[168] [169]
<b>Total (\$)</b>				<b>746,572</b>	
<b>Budget (\$)</b>				<b>20,000,000</b>	
<b>Margin</b>				<b>96%</b>	



## Mass, Volume and Power

Tables 94, 95, and 96 show the mass, volume, and power used by each component, and that Mechanisms is within compliance for all our allocated budgets.

The dispenser is excluded from this analysis since it will be left behind on the launch vehicle and not part of the actual satellites. However, we have ensured that the CSD is compatible with the launch vehicles, so it is within compliance. The power margin is 0% because the mechanisms subsystem provided the power subsystem with what our power draw values would be, and they derived the power generation and allocation (with overall margins) accordingly. See Section 12 for more details.

Table 94: Mechanisms Mass Compliance

Component	PACK Mass (kg)	HOWLL/WOOF Mass (kg)
EBAD TiNi™ MINI Frangi-bolt FD04 [171]	$8 \times 0.01 = 0.08$	0.08
Shape Memory Polymer Composite Smart Hinge [159]	$4 \times 0.01 = 0.04$	$2 \times 0.01 = 0.02$
Aluminum Stabilizing Hinge Bracket	$6 \times 0.2 = 1.2$	$2 \times 0.2 = 0.4$
Honeybee Robotics Micro-Sat SADA[163]	$2 \times 0.225 = 0.45$	$2 \times 0.225 = 0.45$
<b>Total (kg)</b>	1.77	0.95
<b>Budget (kg)</b>	2.25	2.25
<b>Margin</b>	21%	58%

Table 95: Mechanisms Volume Compliance

Component	PACK Volume (cm <sup>3</sup> )	HOWL/WOOF Volume (cm <sup>3</sup> )
EBAD TiNi™ MINI Frangi-bolt FD04 [171]	$8 \times 1.65 = 13.2$	$8 \times 1.65 = 13.2$
Shape Memory Polymer Composite Smart Hinge [159]	$3.48 \times 4 = 13.92$	$3.48 \times 2 = 6.96$
Aluminum Stabilizing Hinge Bracket	$6 \times 214.8 = 1288.8$	$2 \times 214.8 = 429.6$
Honeybee Robotics Micro-Sat SADA[163]	$2 \times 105.3 = 210.6$	$2 \times 105.3 = 210.6$
<b>Total (cm<sup>3</sup>)</b>	1527	661
<b>Budget (cm<sup>3</sup>)</b>	1,600	1,000
<b>Margin</b>	4.6%	34%



Table 96: Mechanisms Power Compliance

Component	PACK Nominal Power (W)	PACK Peak Power (W)	HOWL/WOOF Nominal Power (W)	HOWL/WOOF Peak Power (W)
EBAD TiNi™ MINI Frangibolt FD04 [171]	0 (power used only at deployment)	72	0 (power used only at deployment)	72
Shape Memory Polymer Composite Smart Hinge [159]	0 (power used only at deployment)	$25.6 \times 4 = 102.4$	0 (power used only at deployment)	$25.6 \times 2 = 51.2$
Honeybee Robotics Micro-Sat SADA[163]	$2 \times 1.25 = 2.5$	2.5	$2 \times 1.25 = 2.5$	2.5
<b>Total (W)</b>	2.5	102.4 (no peaks are simultaneous)	2.5	72 (no peaks are simultaneous)
<b>Budget (W)</b>	2.5	102.4	2.5	72
<b>Margin</b>	0%	0%	0%	0%



## 14 Thermal Design

### 14.1 Subsystem Overview

The thermal subsystem supplies each satellite of the ARGOS mission with the ability to maintain heat dissipation and heat retention so that the satellites remain within operating temperatures. Outside of these temperatures, components that are sensitive to temperature may fail if the temperature is outside of their individual survival temperature range. This heat management capability will be accomplished mainly through passive thermal coatings and a passive louver and partially through active heating. The thermal subsystem must meet all requirements and help accomplish mission objectives.

The thermal subsystem interacts broadly with all subsystems as thermal capabilities ensure the survival of spacecraft components in the space environment. However, this subsystem works closely with the Structures & Materials team due to the integration of outer coatings on the outside of the satellite bus. The propulsion and power subsystems in particular had strict thermal considerations that the thermal subsystem had to adhere to. The GNC subsystem determined the heating conditions that the satellites will experience. In general, subsystems that involve hardware will also be addressed by the thermal subsystem, which includes Payload, Comms, C&DH, Power, and Mechanisms.

### 14.2 Subsystem Objectives

The most up-to-date list of thermal subsystem objectives are as follows; the overall objectives have not changed, but there have been minor edits for extra clarity and specificity.

- Characterize all thermal environments that the mission satellites will be exposed to over their lifetime such that satellite temperature extremes can be derived for each environment
- Characterize extremes of thermal flux in the cislunar environment, including through the course of transfer orbit
- Maintain, over the course of the mission, heat retention and dissipation for spacecraft components both external (antennas, thrusters, etc.) and internal (batteries, CPU, etc.) such that they remain in operating and survival temperature ranges
- Provide sufficient redundancy for spacecraft thermal control over the mission lifetime
- Sense temperatures of spacecraft components and detect abnormal thermal situations

### 14.3 Subsystem Requirements

The requirements for thermal subsystem design define the minimum performance of each component of the thermal design. Table 1 contains a shortened list of key requirements, and a full list of requirements for the thermal subsystem can be found on the "Thermal" section of the Team ARGOS "Requirements Spreadsheet" [6]. The requirements are split into technical requirements, constraint requirements, and environment requirements. All values have been changed from TBC to final values.



Table 97: Subsystem Requirements

Requirement ID	Requirement	Rationale	Verification Method
THM-F-006	The thermal subsystem shall characterize the steady state thermal behaviour of the mission architecture	The thermal behaviour of the mission architecture in its nominal operating environment impacts the successful completion of mission operations	Analysis
THM-P-001B	The thermal subsystem shall maintain a minimum temperature of at least 0 degrees Celsius for the power battery subsystem	The spacecraft has a lower end of the operating temperature range	Analysis
THM-P-002B	The thermal subsystem shall maintain a maximum temperature of at most 45 degrees Celsius for the power battery system	The spacecraft has a higher end of the operating temperature range	Analysis
THM-C-001	The thermal subsystem shall have a cumulative mass of at most 1.5 kg for the HOWLL satellite	Compliance with the mission architecture mass budget	Subsystem mass budget
THM-E-002	All thermal subsystem components must be operational within the radiative environment of the maximum heat flux conditions from the Sun and albedo of the Moon, and the minimum heat flux conditions when the satellite is eclipsed for the duration of the mission	The thermal system must be adequately prepared for operation in all environments, otherwise other systems may be impeded	Analysis



## 14.4 Subsystem Constraints

The thermal subsystem faces a mass constraint. For the two 27U satellites (HOWLL and WOOF), the thermal subsystem may not contribute more than 1.5 kilograms of mass, and for the two 12U satellites (PACK-C and PACK-E), the subsystem is limited to 750 grams of mass. Similarly, there is a volume constraint that limits the space taken up by thermal components to 2,000 cm<sup>3</sup> for the 27U class satellites and 1,250 cm<sup>3</sup> for the 12U class satellites. These mass and volume budgets were initially assigned and consistently managed by the Structures and Materials subsystem.

Other subsystems impose, on the thermal subsystem, temperature ranges for which a certain component must stay within. There are two different kinds of temperature ranges; operating and survival. Within operational temperatures, the component or subsystem should function as intended with no temperature-dependent harm or hindrance. The survival temperature range, which envelops the operating range, describes the range within which the component or subsystem is expected to survive and be operational after. Since operational temperature ranges were the limiting condition, they were the main consideration for thermal design. For satellite components, the minimum and maximum operating temperatures both came from the Power subsystem, whose batteries would have an ideal charging operating temperature from 0 to 45 degrees Celsius [173].

There is also a financial constraint placed upon the subsystem, which are that the cost of the thermal subsystem, from manufacturing to operation, cannot exceed \$2,797,200. This was the result of a higher-level operations decision on the division of financial budget throughout the various subsystems.

The space environment poses multiple constraints on the thermal subsystem. First, the harsh environment of space poses a potential radiation hazard on the spacecraft, which is common to all subsystems. More specific to the thermal subsystem is the fact that the satellites are subject to different thermal loading environments that vary per time and per satellite class.

Namely, the orbits that the satellites are placed in expose the satellites to different thermal environments. For instance, the HOWLL and WOOF satellites situated around L1 and L2 face largely consistent thermal fluxes throughout the year except for a 5-hour eclipse once every year or so. However, the PACK satellites in frozen lunar orbits face eclipses much more frequently, on the order of a 45-minute eclipse once every 5 hours. During an eclipse, direct solar radiation no longer acts on the satellite, so the thermal flux decreases significantly.

Lastly, the power budget constrains the thermal subsystem (although in some way, the budget is self-imposed and then reported to the power subteam). The budgets, respectively, are a peak draw of 56.5 Watts and 30 Watts for the 27U and 12U classes, and the nominal draws are 0 Watts for both.

Details and sources for the numerical figures discussed in this subsection can be found under the ARGOS budgets spreadsheet [96].

## 14.5 Subsystem Drivers

**Mass and volume:** Since the thermal subsystem has a tighter mass and volume budget than most other subsystems, selecting components within the budget is a challenge. This is a driver in calculations of the radiator and louver and component selection. This rules out most active components



with fluid heat transfer cycles and limits the amount of louver area on the satellite.

**Space environment:** Any protective shielding on the satellite must withstand the environment of space which can have harsh extremes of temperature and radiation especially when crossing the Van Allen belt. The thermal subsystem must also resist degradation from the radiative environment to ensure a long operational lifetime. Also, thermal protection systems must work in the vacuum of space, which involves selecting materials with low out gassing properties.

**Duration:** The duration of the mission influences the reliability of the thermal management systems. For example, a mission that is expected to operate over a year may pose different standards of reliability than a mission expected to remain operational for ten years since elements such as fatigue and degradation collect over time.

**Reliability:** Reliability is primarily dependent on the likelihood of failure. Comparisons of likelihood of failure can be made from the idea that more moving parts and degrees of control breed more opportunities for failure. A non-controlled, static, passive thermal regulator is less likely to fail than an active regulator, etc.

**Operational temperatures:** The component selection of the other subsystems directly impacts the operational temperature range that the thermal subsystem must design around. This poses certain challenges regarding the external coatings that the thermal subsystem applies to the spacecraft. A change in operational temperature can change the type of external coating on the spacecraft.

**Efficiency:** If a device is more capable of achieving thermal regulation, there may be a trade-off with how reliable the system is. For example, a mechanism to change the emissivity of the spacecraft by transforming its external cover may do a great job of changing the equilibrium temperature and returning the satellite to equilibrium rather quickly, but the added complexity of the moving parts can decrease the reliability of that mechanism.

## 14.6 Subsystem Design Approach

### 14.6.1 Thermal Environments and Extremes

The very first step in the design approach follows two of the stated objectives of the thermal subsystem, which are to characterize the steady state thermal environments that will affect the satellites throughout their lifetime and to identify their extremes. First, it is stated that due to the distance and view factor from the Earth, the Earth albedo and infrared radiation has been ignored since fluctuations in other heating conditions are much more significant than the amount of flux from the Earth.

The first two states are exclusive to the 27U class satellites at the Lagrange points. When these satellites undergo solar eclipses, the thermal flux is  $0 \text{ W/m}^2$  because not only does it lack solar thermal flux, there is also a negligible lunar infrared radiation at that distance. This is believed to give the thermal subsystem design since leaning the thermal environment colder (at zero flux) is a conservative choice. When the two satellites are not in eclipse, then they face the thermal flux consisting of the solar constant of roughly  $1361 \text{ W/m}^2$  although it varies around 6 percent throughout the year due to the Earth's perihelion and aphelion [7].

The next two states are exclusive to the 12U class satellites which lie in frozen orbit, and they are more complex in their various sources. When these satellites are in eclipse, they face lunar infrared



Table 98: Environmental Heating Conditions

Condition	HOWLL/WOOF		PACK		Both
	Eclipse	Nominal	Eclipse	Nominal	Transit
Flux (W/m <sup>2</sup> )	0	1361	303.1	1800	2009

radiation (the black-body radiation of the Moon) that is significant enough to be considered for thermal loads; the lower end of the environmental thermal flux (for the apolune or "lunar apoapsis" condition), therefore, becomes 303.11 W/m<sup>2</sup> per calculations performed in the PDR with the blackbody radiation equation which have remained the same. For nominal operations, the satellites are subject to lunar albedo (reflection of sunlight by the Moon), lunar infrared radiation, as well as solar flux. This value is 1,800 W/m<sup>2</sup>. This is the peak case, accounting for the PACK-E (elliptical) satellite's perilune (periapsis in lunar orbit).

There is an additional fifth thermal environmental state during satellite transit and deployment; at its peak, it was calculated to be 2,009 W/m<sup>2</sup> environmental thermal flux due to the Earth albedo and solar flux. However, since the PDR, this environmental state has been jettisoned for several reasons. First, conversations with the various subteams (such as GNC, Ops, and LV) have revealed that the amount of time exposed to this peak environmental thermal flux is on the order of less than an hour, which while being the same length as the PACK eclipses, occurs once in its lifetime. In addition, the satellite will already be exposed to the thermal environment of the transit condition since it resides in the quasi-equilibrium temperature of the transit environment during its pre-deployment containment within the launch vehicle fairing. This is an environment that is out of control of the thermal subsystem. Lastly, if the satellite does not assume full operations immediately (i.e. solar panel deployment), then the satellite does not yet have thermal flux coming onto its solar panels, neither does it have the power necessary to manage and regulate not just the thermal subsystem, but other subsystems such as C&DH and ADCS which are more critical at the beginning of its trajectory. A table of summarized heating conditions is shown.

In this report, a passively actuated louver is also established as a method to switch between an insulating and radiative mode in the satellite. A certain portion of the spacecraft surface is covered by the louver which has a material on the top with a high  $\alpha\text{-}\epsilon$  ratio (the ratio of absorptivity to emissivity, which is an important characteristic in thermal considerations), this louver covers a radiative material under it that will have a low  $\alpha\text{-}\epsilon$ . Whenever the springs in the louver experience more heat entering the system, they expand the louver so that the radiative material is revealed. The fully expanded or closed louver conditions are enough to keep the equilibrium temperature within the desired ranges. Although the various coatings are situated in different locations of the satellite surface, the direction to which the satellite faces does not effect the theoretically equilibrium temperature because the average  $\alpha\text{-}\epsilon$  ratio and thermal flux (two contributing elements in the temperature equation) are both independent of its orientation.

#### 14.6.2 Subsystem Temperature Requirements

Since the PDR, the operating temperature ranges of various other subsystems have been refined from further clarifications and down-selection. The ranges are shown in the following table.

The temperatures are most narrowly restricted by the Power subsystem's batteries, which have an



Table 99: Temperature Requirements for ARGOS Satellite Components

Components	Operational Temperature Range (deg C)
Solar panels (Power subsystem)	-150 to +100
Structures subsystem	-80 to +200
Mechanisms subsystem	-50 to +70
Kairospace 90mm camera (Payload subsystem)	-40 to +60
Bradford Space HPGP Monopropellant Thruster	-5 to +60
IQ Combined System Antenna	-30 to +60
Combined Endurosat System Antenna	-40 to +80
Batteries (Power subsystem)	0 to +45

ideal charging temperature of 0 to 45 degrees Celsius. However, their power draw temperature is more relaxed, from -30 to 60 degrees Celsius.

#### 14.6.3 Minor Underlying Assumptions

It is assumed that the energy dissipation from mechanical work being performed by mobile mechanisms from various subsystems and electromagnetic wave emissions performed by communications relays are negligible to the outgoing heat flux conditions of the spacecraft. This assumption is justified due to the fact that the duty ratio of communications by the Comms subsystem is on the order of a minute once every half hour, and the power required is not a negligible yet minor contribution to the nominal power dissipation as heat [96]. In addition, solar flares, while they may interrupt communication, do not contribute a significant intensity to the spacecraft for considering incoming energy dissipated as heat. In fact, even strong solar flares present an intensity on the order of a milliwatt per square meter [174].

### 14.7 Formal Analysis

The biggest changes from the previous report is the change from the thermally insulated multi node analysis to a 3-node analysis with the spacecraft main body as one node and the solar panels as 2 nodes. We have decided to no longer go with the approach of having individual components be their own thermally isolated nodes.

The methodology for determining the temperature remains largely the same as the first two subsystem reports. By using the steady state heat fluxes provided by the Stefan-Boltzmann equation, it can be plugged into a relationship between temperature and a heat flux, with absorptivity and emissivity as the two variables that the thermal team can determine.

This equation details the total heat flux an object in space receives due to albedo and infrared radiation.

$$\dot{Q}_{in} = R * S + \dot{Q}_{IR} \quad (31)$$

This equation gives the IR radiation for the heat flux equation radiated from a body, including



celestial bodies and the spacecraft.

$$\dot{Q}_{IR} = \sigma * T^4 \quad (32)$$

With the relations in mind from above, the temperature of a single node can be found. (All heat fluxes—Q dot—are in units of Watts per square meter.)

$$Q_{in} = Q_{out} \quad (33)$$

$$\dot{Q}_{in} * A_{in} * \alpha = \epsilon * \sigma * T^4 * A_{out} \quad (34)$$

$$T = \sqrt[4]{(\alpha/\epsilon) * (1/\sigma) * (\dot{Q}_{in})} \quad (35)$$

These equations were used to find temperature ranges at different heat flux conditions based on the absorptivity ( $\alpha$ ) and emissivity ( $\epsilon$ ) of a suitable materials for the external coating of the spacecraft. As well as the necessary ratio of louver to coating on the outside of the spacecraft. The calculation for temperature was performed on each of the three nodes we were considering. For the panels on the side of the spacecraft, a view factor of 1/4 was decided based on literature we found [175]. For the solar panels, the view factor was 1/2 since the solar panels have one side always facing the sun and 2 sides radiating constantly.

Table 100: Temperature Regulation Calculations for PACK Body

a/e louver closed	ECLIPSE Q: IR, Power, + Heater (30W)	Temp at Eclipse (C)
2.25	593.11	3.96
a/e louver open	NONECLIPSE Q: Albedo, IR, Solar Flux + Power	Temp at Non-Eclipse (C)
1.396	1969.375	51.430

Table 101: Temperature Regulation Calculations for HOWLL/WOOF Body

a/e louver closed	ECLIPSE Q: Power + Heater (41.5 W)	Temp at Eclipse (C)
2.25	140.23	0.12
a/e louver open	NONECLIPSE Q: Solar Flux + Power	Temp at Non-Eclipse (C)
1.396	1530.375	38.530

Table 102: Temperature Regulation Calcs for Solar Panel Nodes

PACK Solar Panel		HOWLL/WOOF Solar Panel		
a/e:	ECLIPSE Q: IR + Heater	Temp at Eclipse (C)	ECLIPSE Q: Heater	Temp at Eclipse (C)
0.6	303.1	-72.9	35.5	-133.8
NONECLIPSE Q: Albedo, IR, Flux	Temp at Non-Eclipse (C)	NOMINAL Q: Solar Flux	Temp at Non-Eclipse (C)	
1630.6	31.8	1191.6	8.8	



The basis of the temperature calculations were on the coldest heat flux case, where the absorptivity ( $\alpha$ ) - emissivity ( $\epsilon$ ) ratio was determined to make the low end of the temperature within range. However, this  $\alpha\text{-}\epsilon$  ratio could not be too "insulating" based on the equation, as although an increase in  $\alpha\text{-}\epsilon$  is beneficial when  $\dot{Q}_{in}$  is low, when it is high, the temperature also begins to get out of range. Thus a lower  $\alpha\text{-}\epsilon$  was chosen, with heaters making up for the out of range temperature in the low heat case and the louver opening on the satellite body to make up for the high heat case for both HOWLL/WOOF and PACK. The addition of the heater affected the heat flux values going into the entire spacecraft system while the radiator impacted the  $\alpha\text{-}\epsilon$  ratio of the external surface. By tweaking these values in an iterative process, we were able to get values of the spacecraft that kept the spacecraft within temperature range. First, an  $\alpha\text{-}\epsilon$  was selected, then the wattage for the heater was calculated, then the area of spacecraft covered by the louver and  $\alpha\text{-}\epsilon$  ratio under the louver was calculated. It was important in this process to get realistic values for each parameter, for example it was unrealistic to have a  $\alpha\text{-}\epsilon$  ratio of 0.01 to get very low heater wattage values since materials with that ratio most likely do not exist for spacecraft usage. With these values, the specific components that meet these parameters were able to be considered and down selected through trade studies.

Execution of formulas and more specific details behind the temperature steady-state calculations can be found under the "Active Use Thermal Calcs" tab of the "Thermal Regulation Calcs" spreadsheet, as is cited in the references [176]. It is worth mentioning that although the PACK satellite temperature in non-eclipse conditions goes above 45 degrees C, the new temperature is still within nominal power draw operating temperature ranges, and battery charging can take place during the time when the PACK satellites are farther away from the Moon (for the elliptical PACK case, since the circular PACK satellites are already farther than the elliptical periapsis). The tables of trade studies can also found under the "Trade Studies" tab of the same spreadsheet, where decision matrices were used to assess and rank the components. Reference links to components that were compared can also be found on the spreadsheet, so individual citations have not been made. The next several sections will give some commentary on the trade studies and justify the selections.

#### 14.7.1 External Coating

The external cover of the spacecraft is one which experiences foremost thermal interaction with the space environment. Therefore, it is important to choose a cover that helps meet the goal of thermal maintenance. In the case of our analysis, we wanted the external coatings of when the louver was closed to be an insulating case, built specifically to retain heat. We found that an  $\alpha\text{-}\epsilon$  ratio of 2.25 provided a realistic balance with the capabilities of the other heat management mechanisms through our thermal regulation analysis. Thus, our goal was to find a material that fit the insulating ratio of 2.25 we found in our analysis.

This need for insulation rules out OSRs which are for radiating heat. Although it would be possible to have a OSR outer coating and increase insulation with the louver, we decided to have a insulating case when the louver is closed to reduce heater loads as much as possible. This is less cumbersome on the power subteam than our previous design that was focused on reflecting heat with an OSR outer coating.

Thus, there are three viable candidates for the selection of the external cover. The first is multi-layer insulation (MLI), which consists of many thin reflective films typically made from polyimide



or polyester that are assembled together and coated with aluminum [177]. The second is an external coating that is either painted or vapor deposited on to the aluminum shell of the spacecraft and can be made of various materials such as plastic or metal. The third is various tapes made of polyimide or kapton that adheres to the spacecraft through usually an acrylic adhesive.

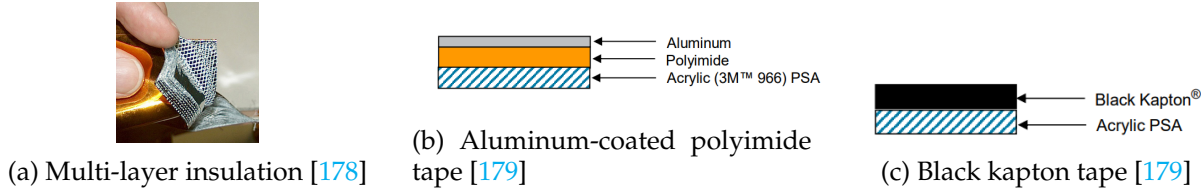


Figure 47: Various external coating options

Each of these three options can be configured to have a low emissivity and high absorptivity to ensure that the most heat possible is absorbed and retained. In terms of characteristics of all three possible coatings, MLI is possibly the most effective in capability. It has very little degradation due to its multiple layers, the increase of layers also provides thermal conductive resistance to the spacecraft, and it is very versatile due to the customization of its inner layers [8]. However, although it is the most capable, there are many design challenges to implementing it on a CubeSAT due to the MLI getting caught on the launcher when the CubeSAT is deployed and due to the difficulty in securing the MLI to a small surface area.[180] In addition, MLI at small scales on cubesats exhibits a different effective emissivity due to mechanically attached joints acting as conduction hot spots. This effectively only leaves applied coatings and tapes in consideration for the external coating on the spacecraft.

The main drivers in this component type selection process were the environment, duration, and capability of the types of coatings in the spacecraft. The capability for both the applied coatings and polyimide/kapton tape is generally similar as the wide range of each type of component ensures there is an  $\alpha\text{-}\epsilon$  ratio that fits the criteria of the mission. The harsh radiative environment degrades all materials, however, some materials degrade at a faster rate than others. Applied coatings generally degrade faster and lead to a lower alpha value for the outside of the spacecraft. This is why polyimide and kapton tapes were selected for the outside of the spacecraft with the louver closed. However, it was difficult to find a tape with the exact  $\alpha\text{-}\epsilon$  ratio needed. Thus, it was determined a combination of coatings was needed and a weighted average  $\alpha\text{-}\epsilon$  around the exterior of the spacecraft would give the correct number for the analysis. First, we needed to determine which specific tapes to use, so we conducted a trade study in the thermal regulation calcs spreadsheet [176]. Degradation and reliability over time are taken into account in the trade study.

After selecting the materials and getting their  $\alpha\text{-}\epsilon$  ratio, it was determined that 40% of the spacecraft would have a  $\alpha\text{-}\epsilon$  ratio of 5 and 60% of the spacecraft would have a  $\alpha\text{-}\epsilon$  of 1.09 on the exterior. This equation below outlines the weighted average based on area, AE represents the  $\alpha\text{-}\epsilon$  ratio.

$$AE_{average} = (A_{mat1}/A_{tot}) * AE_{mat1} + (A_{mat2}/A_{tot}) * AE_{mat2} \quad (36)$$

This gave us a weighted average  $\alpha\text{-}\epsilon$  of 2.25, which met our requirement from our thermal analysis. So when the louver is closed, the spacecraft exterior has 40% First Surface Aluminum Coated



Polyimide Tape with Acrylic 3M™966 Adhesive and 60% Black Kapton Tape with Acrylic Adhesive. Then when the louver is open, the 40% of Aluminum Coated Polyimide Tape is lifted up and no longer insulates the spacecraft, instead making the radiator under the louvers part of the weighted average  $\alpha\text{-}\epsilon$ .

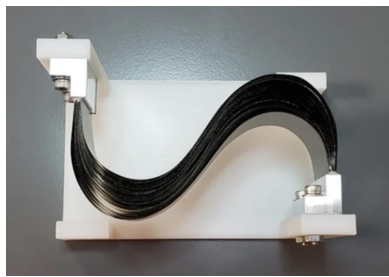
#### 14.7.2 Conductive Elements

In the space environment, the dominant form of heat transfer for disconnected bodies is radiation. This is because of the very low density of molecules in cislunar (and deep) space that makes conduction or convection between two separated bodies impossible. Therefore, the latter two modes of heat transfer can be neglected [181].

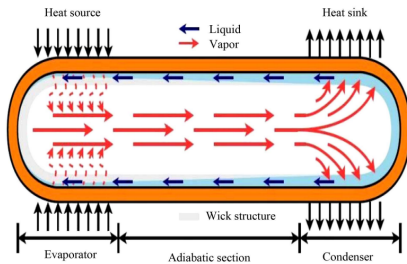
However, for the satellite body, it is in the best interest of the thermal subsystem to design connected pathways between components such that there is heat transfer not just by means of radiation, but by conduction. This is because if physically adjacent components are allowed to be in thermal contact with one another, there can be an offloading of heat from a heat source that dissipates lots of heat (i.e. power consumption, data handling and other computational processes, thruster, etc.) onto a heat sink that will produce less heat and/or vents heat (i.e. passive components, radiator).

Therefore, there need to be conductive elements between components to regulate the temperatures of components and justify the satellite body's treatment as a single thermal node in which there is a homogeneity of temperature within and throughout itself in steady state conditions.

For small spacecraft such as the ARGOS CubeSats, thermal straps and heat pipes are the main two technologies for internal heat conduction. Thermal straps are (often flexible and malleable) conductive links formed into cables and elongated panels made out of conductive materials such as copper, aluminum, or graphite which latch onto the heat sink and heat source surfaces [182]. Heat pipes are more sophisticated devices that use capillary action to carry a working fluid which delivers heat to other parts of the satellite in the form of a vaporized gas which quickly travels and condenses into a liquid at heat sinks [183]. Both are passive devices that do not require any actuation, control, or power to use.



(a) Technology Applications Inc. Thermal Straps [184]



(b) Mechanism of a heat pipe [185]

Figure 48: Various conductive elements options

In the PDR, it was stated in the primary justification that the mode of heat conduction would be heat pipes due to the greater conductivity of a typical heat pipe compared to that of a typical



thermal strap. The ranges are around several hundred W/m-K for thermal straps, and tens of thousands of W/m-K of effective conductivity for heat pipes [184] [186] [187].

However, upon further discussion with Seth Abramczyk, Thermal Engineer at NASA Goddard Space Flight Center, and Michael Galvin, it was discovered that traditional heat pipes that rely on capillary action have historically been generally unpopular for small scale spacecraft application. In the same discussion with Seth Abramczyk, we learned that there are some new interesting developments in the industry for 2D heat pipes and oscillating heat pipes, but none have been established enough to have good reliability and flight heritage due to their lack of historical use. Therefore, thermal straps have been selected for ARGOS satellite usage.

Despite their lower conductivity, thermal straps are mechanically very simple and easily formed into various shapes unlike heat pipes which involve more complex geometries to allow for wick-like capillary action and fluid transportation which place limits on its geometric variability. Because there are no moving components, and no working fluid, thermal straps' reliability trumps that of the regulation capability of the heat pipe.

Thermal straps by Technology Applications, Inc. (TAI) were chosen as a result of this down selection. TAI presents many options for flexible thermal straps which are very important for the maneuverability of the straps between various ARGOS satellite components. Notably, the PyroFlex graphite sheet straps have low stiffnesses on the order of a few mN/mm. In addition, TAI can produce very favorable minimum thicknesses. TAI also boasts a much more impressive heritage for their straps which have been used in multiple NASA, ESA missions as well as private space programs [188].

Because straps are mechanically attached and passively functional, there would be little room for failure other than a mechanical imperfection causing separation and detachment on one connection (e.g. CPU to structure frame). In case of such an event, other thermal straps and the general proximity of components to each other should maintain relative thermal homogeneity in the body. In addition, according to TAI, the straps have a Technology Readiness Level of 9 and have flight heritage, so the chance of failure occurring is low.

#### 14.7.3 Heater

For small satellites, the means of heat generation in cases of low power consumption by electrical components dissipated as heat or cases of blocked solar radiation is somewhat straightforward. In our case, heaters are only necessary where the satellite is in eclipse. There are two main types of heaters that can be considered for the small CubeSats: cartridge heaters and kapton electrical resistance heaters [189] [8]. Both of these types of heaters have downsides and benefits that need to be considered. However, the necessary capability for the heater needs to be established.

As stated earlier, the heater in effect increases the amount of heat flux entering into the system, so by tweaking the values in the spreadsheet to get the component within range and then noting the difference in heat flux, a heater requirement can be obtained. For the PACK satellite, the original heat flux value entering into the satellite during the eclipse is 303.11 W/m<sup>2</sup>, in order to get the satellite within temperature range of 0 C at an  $\alpha\text{-}\epsilon$  ratio of 2.25 using Equation (35), an additional heat flux of 290 W/m<sup>2</sup> is required. In safe mode during the eclipse, the satellite has a power draw of 62.8 W that also produces heat into the satellite, this heat divided across the surface area of the CubeSAT, which is around 0.32 m<sup>2</sup>, corresponds to a heat flux of approximately 196.25 W/m<sup>2</sup>.



The leftover heat flux of  $93.75 \text{ W/m}^2$  multiplied by the spacecraft surface area is 30 W, which is the heater capability requirement for PACK. If this process is repeated for the HOWLL/WOOF solar panels and body, we get a value of 41.5 W required for the body heater and 15 W for the solar panel heaters. Each of the heaters listed below had the capability for that heat.

A potential cartridge heater is the Vulcan Electric C2010A model [190]. The two potential kapton heaters are the Omega KHLVA model and the Tempco SHK model. The thermal subsystem's drivers present a trade-off between reliability and capacity, but in this case, there is a priority on simplicity since the capacity of the cartridge heater is outweighed by its complexity, thus making it more unreliable than it is capable. In addition, the kapton heaters use less mass, satisfying the mass driver. As for down selecting between each kapton heater, both of them have similar margins in terms of wattage. However, Tempco's kapton heater has a much wider margin of operating temperature which gives it the slight edge in terms of advantages.



(a) Vulcan Electric heater [190]

(b) Tempco SHK heater [191]

Figure 49: Various heater options

#### 14.7.4 Internal Heat Radiator

The material under the louver that is exposed when satellite experiences the high heat flux cases needs to be weighted with the black kapton tape to give the body an average  $\alpha\text{-}\epsilon$  ratio of 1.396. Similar to the process conducted in the external cover section, this requires an  $\alpha\text{-}\epsilon$  ratio of around 0.115 for the radiative material that will be exposed underneath the louvers. There are a few materials that can fulfill this requirement. The choice of materials are once again external tapes and applied coatings, but this time, optical solar reflectors (OSR) are also an option because of the need to radiate heat. As mentioned earlier in this report, applied coatings are not suitable due to their degradation. This leads to a trade off between OSRs and the external tapes which both have the necessary resistance to degradation and capability. We conducted a trade study with Silver FEP tape, which have a suitable  $\alpha\text{-}\epsilon$  ratio, and OSRs. [176]

Two notable vendors were examined for OSR: Excelitas Technologies and SQUID3 Space. The down selection of the OSR concluded with the choice of the Excelitas Technologies OSR due to its flight heritage; Excelitas' "space coverglass" has been proven to perform well by over three thousand applications of their OSR since 1970[192], whereas SQUID3 Space was only founded in 2023.[193] In addition, although the SQ-2 OSR had a lower density of  $2.00 \text{ g/cm}^3$  as opposed to the Excelitas'  $2.54 \text{ g/cm}^3$ , its solar absorptance (0.15) and emittance ( $>0.8$ ) were comparatively worse than that of the Excelitas OSR (0.085 and 0.87).[194] This aids in performing the goal of reflecting and emitting radiation away from the satellite while not compromising too much on the

mass budget. The Excelitas OSR also allows for a thinner (0.050 mm minimum) placement than the SQ-2 OSR (0.1mm).



(a) Excelitas Technologies OSR [192]



(b) SQUID3 SQ-2 OSR [194]

Figure 50: Various internal heat radiator options

#### 14.7.5 Temperature Sensor

In order for the thermal subsystem to function properly, there must be a constant monitoring of the satellite's components, namely the spacecraft body and the panels (which are the nodes for consideration). Although the satellite's cooling capabilities are entirely passive (i.e. heat dissipation by radiation and temperature-responsive self-actuation of louvers to allow for greater emission), the heating requires an "active" (although upon discussion with Seth Abramczyk, it was discovered that heaters are only nominally considered active) component to generate heat via power usage. In order for the satellite to use the heater only when necessary, and not when the temperature is warm enough, temperature sensing is necessary to tell the heater when to trigger.

Infrared (IR) sensors work by analyzing the black-body radiation spectrum of an object to deduce its temperature, but this complicated and more computationally intensive process may be an over-design for the scope of this project due to the fact that it is simply not the only necessary option for getting the temperature of the components. In addition, IR sensors in cislunar space are prone to error due to Earth and Moon radiation effects [195]. In addition, without rotating actuators or many infrared sensors, there would be no way to monitor the temperature of multiple sections of the spacecraft body, and designing such mechanisms is not only unnecessary, but not feasible at this stage of the design process. Therefore, IR sensors were not chosen for their complexity and mass and volume needed to operate.



(a) Infrared temperature sensor  
[196]



(b) Typical thermocouple [197]



(c) Typical thermistor [198]

Figure 51: Various temperature sensing options

Instead, there are two simpler options for temperature management: thermocouples and thermistors. A thermocouple has two different conjoined metals that create an electric potential that

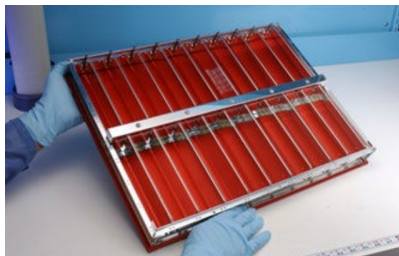


changes based on temperature, taking use of the Seebeck effect [199]. A thermistor, which derives its name from "thermal resistor", works by measuring resistance which is temperature-dependent [198]. Both thermocouples and thermistors are uncomplicated and present very easy burdens to mass and volume constraints, but the thermistor excels in providing more accurate measurements.

The following discussion especially varies from the PDR. Thermistors only have a sensible range of -50 to +150 degrees Celsius, and since the solar panels are expected to dip below the minimum temperature, thermocouples, which have the encompassing range, will be used for the solar panel heat sensing. It is also acceptable to use the thermocouples for solar panel temperature sensing because thermocouples sacrifice precision for range; however, given that the satellite body has the more temperature-sensitive components, very precise measurements of solar panel temperatures are not needed. So, thermistors that have a tenth of a degree Celsius sensitivity will be used for the satellite body. Discussions with NASA Goddard's Seth Abramczyk revealed that thermocouples, while they can be used in-flight, are more appropriate for ground testing which is why the more temperature-sensitive spacecraft main body will use thermistors instead.

#### 14.7.6 Louver

The selection of the louver, another differentiating choice from the PDR, comes from limited options, as there are not many commercial vendors for satellite louvers. This was confirmed in conversation with Seth Abramczyk, who told us that there is a monopoly in louver supply in the industry. In fact, we could only arrive at one searching on from online databases, which is the Sierra Nevada Corporation (SNC) [200]. Indeed, being the only vendor, SNC has great flight heritage for its louvers, but there is no flight heritage information on its louvers being used for cubesats and other small scale spacecraft. Thus, it makes sense that the minimum thickness is on the order of several inches, which is suitable for large satellites but presents great volume challenges for cubesats.



(a) Sierra Nevada Corporation passive louver  
[200]

Figure 52: Commercial OSR to be modified

An option would be to research, develop, and manufacture an in-house created passive louver, but given the launch timeline constraints of the ARGOS mission, in-house production would encroach on the strict timing. Delays with suppliers, lack of expertise, and other production difficulties could challenge our ability to deliver a passive louver.

Therefore, a hybrid option was taken since SNC provides an option to customers for custom sizing. The dimensions of the SNC louvers would be modified to fit within the dimensional con-



straints of the spacecraft. Since the outer surface of the spacecraft frame, according to Structures and Materials, leaves 10 mm of "free" thickness, the louvers will be modified to fit within such geometry. This means that the louver panels, while using the same principles (temperature-dependent movement of spring) as the original louvers, will be resized and reassembled.

In addition, the SNC louvers are able to be tuned to actuate at certain positions at specified temperatures, which makes them ideal for passive changes in a/e ratio.

Experimental adjustments in the absorptivity/emissivity ratio accounting for 5% of louver panel failures from thermal fatigue showed that the equilibrium temperature incurs a steady-state change on the order of a few degrees Celsius, which means there is enough margins in the design of the louvers.

#### 14.7.7 Budget Analyses

For this design, mass, volume, cost, and power usages were checked for compliance with the respective budgets. The spreadsheet titled "ARGOS Thermal Subsystem Budget Calculations" includes the expanded details and calculation steps for the mass and volume budgets [201]. The budgets are well satisfied, and a summary of the budget compliance is as follows.

Notably, the cost margins are very high, since a minimal amount of the financial budget of 8.94% is used for the entire mission architecture. The power budget was not included in this table because our budgets are self-assigned based on how much heating we need and communicated to the Power subsystem. To reiterate from earlier in this report, the Power budgets are 56.5 W at peak for HOWLL/WOOF and 30 W at peak for PACK.

Table 103: Mass, Volume, Cost Budget Analysis

	27U (HOWLL, WOOF)		12U (PACK)		Whole 4-Satellite Architecture
	Mass	Volume	Mass	Volume	Cost (USD)
<b>Consumed Budget</b>	1,080.4g	1,890.1cm <sup>3</sup>	570.4g	1,085.2cm <sup>3</sup>	250,000
<b>Allocated Budget</b>	1,500g	2,000cm <sup>3</sup>	750g	1,250cm <sup>3</sup>	2,797,200
<b>Margin</b>	38.8%	5.8%	31.5%	15.2%	1,119%



## 15 Structures and Materials Design

### 15.1 Subsystem Overview

The Structures and Materials (SM) subsystem is responsible for designing the structures of the spacecraft buses to house the components of the HOWLL, WOOF, and PACK satellites. The structure must be able to withstand the vibrational and gravitational loads imparted by the launch vehicle. The spacecraft bus structures must also protect the components from the harsh cislunar space environment.

In addition, the SM subsystem is responsible for the material design of this spacecraft chassis. The chosen materials must meet the strength, radiation, temperature range, and outgassing requirements outlined in the mission level requirements. The SM subsystem also chooses the material of the solar panel array. The environmental verification tests will also be outlined by the SM subsystem.

Finally, the SM subsystem is responsible for the mass and volume budgets for the entire team. We make sure that each subsystem has a sufficient amount of space allotted in order to fulfill their purposes. The SM subsystem also is in charge of configuring the layout of the entire spacecraft bus, ensuring that all components can fit, with sufficient clearance .

### 15.2 Subsystem Objectives

The SM subsystem has several objectives that must be satisfied. These objectives are listed below.

1. The SM subsystem will design a spacecraft bus that can fit all of the components of the other subsystems throughout the mission lifetime.
2. The SM subsystem will design a spacecraft bus that can withstand the flight environment loads for the chosen launch vehicle.
3. The SM subsystem will choose materials that will satisfy its environmental requirements.
4. The SM subsystem will prioritize the location of the payload sensors when finalizing the satellite layout in order to meet the mission level objective of object tracking.
5. The SM subsystem will also prioritize the locations of the communication network in order to meet the mission level objective of providing a communications and data relay network.
6. The SM subsystem will provide radiation shielding for sensitive electronic components of other subsystems.
7. The SM subsystem will outline tests required for verification of environmental conditions.

### 15.3 Subsystem Requirements

The requirements of the SM subsystem are broken down into 3 main categories: technical (which includes functional and performance), constraints, and environmental. Table 104 shows some of the technical requirements placed on the SM subsystem. One additional requirement pertaining to the environmental conditions verification test has been added. This addition is also shown in

Table 104. A list of all requirements along with trace-up and trace-down requirements can be found in the "SM" tab of the "Requirements Spreadsheet" Google Sheet [6].

Table 104: Selected SM requirements.

Requirement ID	Requirement	Rationale	Verification Method
SM-F-004	The SM subsystem shall configure the placement of components from other subsystems in within the spacecraft bus	Some subsystems may need to be placed in certain locations for thermal profiles, minimization of wiring needed, or for sensor performance. The definition of configurations with the spacecraft bus accommodates these needs, and defines a volume budget for each subsystem	Analysis and modelling
SM-P-001	A yield safety factor of 2 shall be applied for static load analyses	The spacecraft bus must have sufficient margin to accommodate for changes in the weight of the mission architecture components. Derived from NASA GEVS.	Analysis
SM-C-001	The HOWLL SM subsystem shall have a cumulative mass of at most 10.75 kg	Compliance with the mission architecture mass budget	Subsystem mass budget
SM-E-005	All SM subsystem components must withstand the LV vibrational environment as defined in the Falcon 9 User's Guide and the SLS Mission Planner's Guide during transit from Earth to the desired orbit.	Withstanding the expected vibrations within the launch vehicle is necessary for the SM components to be functional upon arrival to orbit	Analysis of expected vibrations

## 15.4 Subsystem Constraints

The constraints for the SM subsystem are given below.

1. The total maximum volume budget of the HOWLL spacecraft bus shall not exceed 27U.
2. The total maximum volume budget of the WOOF spacecraft bus shall not exceed 27U.
3. The total maximum volume budget of the PACK spacecraft bus shall not exceed 12U.
4. The total maximum mass budget of the HOWLL spacecraft bus shall not exceed 54 kg.
5. The total maximum mass budget of the WOOF spacecraft bus shall not exceed 54 kg.
6. The total maximum mass budget of the PACK spacecraft bus shall not exceed 24 kg.
7. The materials chosen for each of the spacecraft buses must be able to survive under the changing radiation and temperature in the space environment.
8. The structures of the spacecraft buses must be able to withstand the forces during launch vehicle transit.



9. The manufacturing and assembly of all spacecraft buses must be completed by March 2025.
10. The total SM subsystem cost budget for all satellites must be under \$2,940,000.

## 15.5 Subsystem Drivers

The SM subsystem drivers are listed as follows. The drivers are listed in order of greatest importance.

1. **Mass and Volume Budgets:** The mass and volume budgets of the spacecraft buses are limited by the allowable budgets set by the launch provider. In addition, the mass is limited by the maximum spacecraft mass that is safe to launch under the launch vibrational and gravitational loads.
2. **Timeline:** The tight timeline defined in the mission RFP states that the planned operational date must be in 2027. In order to meet this deadline, all pre-launch activities, such as design, manufacturing, and assembly, must be completed by 2025 or earlier as indicated by the Operations team.
3. **Space Environment:** The spacecraft buses must be able to withstand the harsh cislunar space environments including harsh temperatures, radiation, and vacuum conditions. One of the objectives of the SM subsystem are to protect the other subsystems from these environments. Therefore, the choice of materials for the design of the spacecraft bus will play a crucial role.

## 15.6 Subsystem Design Approach

A high-level overview of our general design approach is shown in Figure 53. We have now moved into the detailed design stage.

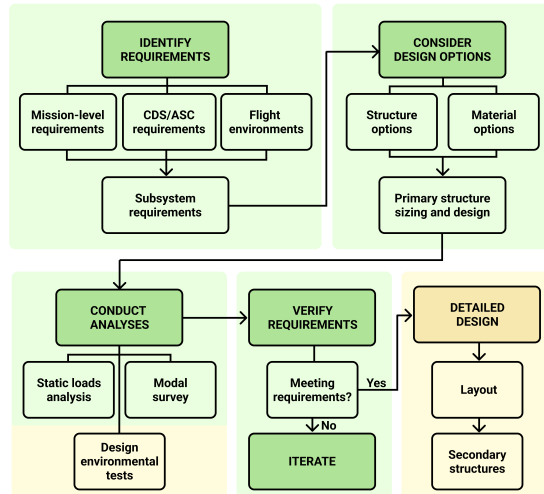


Figure 53: SM design approach. Green designates stages completed for PDR, and yellow designates stages completed for FDR.



### 15.6.1 Materials

As outlined in the CubeSat Development Specification (CDS), CubeSat structures are normally made of an aluminum alloy. After doing a trade study on various aluminum alloys, the SM subsystem has made the decision to use Aluminum 6061 as the material for the CubeSats. Furthermore, in order to add extra spot shielding for more sensitive areas, the SM subsystem has chosen to use Z-graded shielding using AlTiTa. In addition, the SM subsystem has found that the best material for the solar panel array is a printed circuit board (PCB) material reinforced with PCB stiffeners and viscoelastic acrylic tape.

### 15.6.2 Structures

In previous design iterations, we created primary structures for the upsized 27U and 12U spacecraft, modeled the stowed configuration of the solar arrays, created mass and volume models of internal components, and conducted static load and modal analyses.

During this final design iteration, we created higher-fidelity models of the HOWLL and PACK-C satellites. We chose to focus on these two because they each represent one satellite class (27U and 12U, respectively) and have more constraints on their design and internal layout than the other two satellites (WOOF and PACK-E), mostly due to their increased communication and propulsion requirements. We focused on incorporating mass and volume models of internal components into the spacecraft layouts and re-running static load analyses and modal surveys to ensure we still met requirements with the mass models included. In particular, we expanded our static load envelope to a 20g load in two axes. This provides a conservative envelope of the Falcon 9 Rideshare expected load environment. We also re-sized the solar arrays based on updated information from the Power subsystem, modeled the deployed configuration of the arrays, and found their vibrational modes. The purpose of the modal analysis for the deployed configuration analysis is not to satisfy a Falcon 9 requirement; rather, since the solar arrays have a low effective stiffness, we need to find their rigid modes and avoid any resonance issues with other components (e.g. the solar array drive assemblies or thrusters). Resonance could amplify the loads on the solar panels. At this design stage, we do not have data on the frequencies of other components; however, we can conduct a preliminary analysis of the solar array rigid modes and avoid these frequencies for other components.

One of the major elements of this design cycle was the internal layout of each spacecraft bus. Based on feedback from the preliminary design review and final design review presentations, we decided to move the payload cutout to the opposite side of the thrusters to avoid debris collection on the payload camera. We also rearranged the four thrusters to optimize for momentum dumping. Finally, we moved the patch antenna cutouts to the same side of the spacecraft for operational consistency and the star trackers to opposite sides of the spacecraft for redundancy. We made an effort to keep subsystems grouped together and keep components with changing mass (e.g. the propulsion tanks) near the center of mass of each spacecraft.

We did not design secondary structures (e.g. brackets and mounts) for the majority of internal components. This is because we do not have accurate CAD models for most of our components (and it would be out of the scope of this class to model each internal component given only pictures and basic dimensions), without which we cannot design attachment points. Since most secondary structures would be fastened to the satellite frames, we placed the mass models of each



component adjacent to the panel it would be fastened to.

As discussed in Section 15.7.8, we have met the vast majority of our objectives and requirements, and the few requirements that we were only able to partially meet would require information or work that is out of the scope of this class.

## 15.7 Formal Analysis

### 15.7.1 Materials Selection

The most common materials used in CubeSat structures are aluminum alloys, especially Aluminum 6061 and 7075 [26]. For this reason, these were the two main materials that the material trade study focused on. Relevant properties of each alloy are shown in the table below.

Table 105: Properties of aluminum 6061, aluminum 7075, and carbon fiber [202] [203]

Property	Aluminum 6061	Aluminum 7075
Density [g/cm <sup>3</sup> ]	2.7	2.81
Elasticity [GPa]	68.9	71.7
Coefficient of Thermal Expansion [K <sup>-1</sup> ]	$2.36 \times 10^{-5}$	$2.36 \times 10^{-5}$
Melting Point [°C]	582 - 652	477 - 635
Ultimate Tensile Strength [MPa]	310	572
Easy to Machine?	Yes	No

As seen in Table 105, Aluminum 6061 and 7075 are similar in value in terms of density, elasticity, and coefficient of thermal expansion. It is also seen that the ultimate tensile strength of Aluminum 7075 is much larger than that of 6061 [204]. However, both strengths are sufficient enough to withstand the loads required of the structure as shown in our static load analysis. Furthermore, Aluminum 7075 is also more expensive and harder to machine than 6061. For this reason, the SM subsystem has identified Aluminum 6061 as the best candidate for the material for the CubeSat structure.

Additionally, the SM subsystem analyzed the behavior of Aluminum 6061 in various temperatures as it must be able to withstand changing temperature environment, without facing a degradation in its structural abilities. The mechanical properties of Aluminum 6061 in varying temperature conditions is shown in Table 106.

Table 106: Mechanical properties of aluminum 6061 at elevated temperatures [205]

Property	100°C	200°C	300°C
Thermal Expansion [mm/mm]	0.001	0.003	0.0057
Yield Strength [MPa]	300	280	100
Ultimate Tensile Strength [MPa]	310	290	100



The data in Table 106 shows that Aluminum 6061 is able to withstand the temperature conditions up until 200°C. This is a sufficient margin for the temperature conditions the material will face during the mission, meaning that it meets its requirements. This further reinforces our decision to use Aluminum 6061 for the CubeSat structure.

### 15.7.2 Radiation Shielding

One of the objectives of the SM subsystem is to provide radiation shielding for the other subsystem components. The main sources of radiation in cislunar space are solar winds, solar particle events, and galactic cosmic rays [131]. Typical CubeSats use 2mm thick aluminum for radiation shielding. This typical thickness results in a yearly trapped dose of 1383 rad/year, with an additional 750 rad from solar particle events [131]. A rad is a unit that measures the absorbed radiation dose. This method of shielding involves using a single layer of sheet metal. The SM subsystem has decided to use this standard 2mm thick Aluminum 6061 for the CubeSats.

More sensitive components, such as the payload sensor and the communications transceiver, require additional radiation protection. For component-level shielding, the SM subsystem has decided to employ the use of Z-grade shielding. Z-grade shielding is a method of layering materials of different Z numbers. The Z number of a material is its number of protons [206]. In this method, a material of a high Z number is sandwiched in between two other materials of lower Z numbers. The method of Z-shielding increases the incorporation of flexible materials in the creation of radiation-shielding material. This makes it easy to place spot shields in places where traditional single sheet shielding would be difficult [207]. Figure 54, taken from NASA's State of the Art of Small Satellite Technology report shows the results of an experiment in which the radiation shielding of Z-shielding were tested and compared to single sheet shielding.

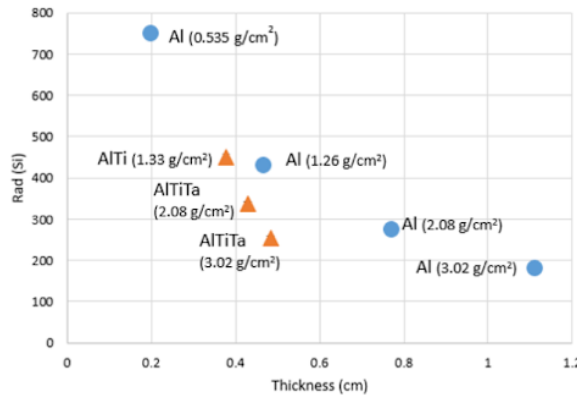


Figure 54: Radiation shielding thicknesses for various materials [208].

As seen in Figure 54, AlTiTa, composed of aluminum, titanium, and tantalum, is much more effective at radiation shielding than plain Al. For this reason, the SM subsystem has chosen to use 3.02 g/cm<sup>2</sup> of AlTiTa at a thickness of around 4mm. This translates to a mass of approximately 0.48g. This is because this thickness reduces the most radiation as shown in Figure 54.

The components that the SM subsystem has identified as needing additional shielding are the



payload camera, payload camera electronics, and the transceiver. We have no data from the manufacturers of these component about how much shielding is currently in place. As a result, the SM subsystem is unable to specify exactly how thick the radiation shielding is.

### 15.7.3 Solar Panel Array Material

In order to provide enough power for the mission, deployable solar panel arrays must be used. It is typical for solar panel arrays for CubeSats to be made of a PCB based material [209]. These deployable solar panels will need to withstand severe launch vibration environments imparted by the launch vehicle. Improper solar panel reinforcement could lead to cracks or fractures in the solar cells as a result of the launch vibrations. In order to minimize deflections, the stiffness of solar panels is increased through the use of various stiffeners. Some examples of stiffeners are aluminum, carbon fiber reinforced plastic, and fiberglass laminate [210]. However, the most cost and mass effective stiffener is PCB stiffeners, reinforced with viscoelastic tape.

In this case, the solar panel array will consist of a PCB panel, thin PCB stiffeners, and several layers of viscoelastic acrylic tape. The stiffeners and solar cells are integrated onto the PCB panel. The stiffeners are attached to the rear surface of the PCB panel with double sided tape. Figure 55 shows a visual of how the solar panel is joined together.

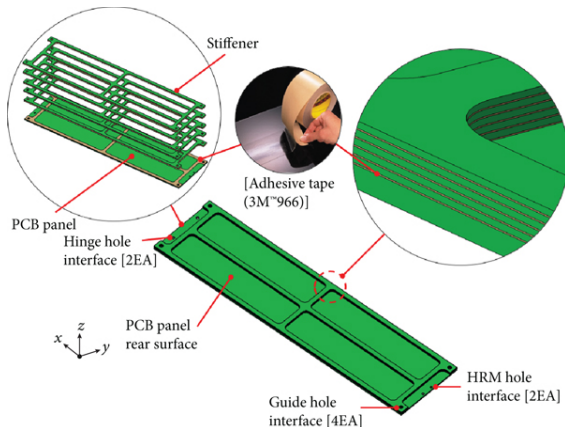


Figure 55: Stiffener Diagram [210].

The use of the viscoelastic tape in this method has demonstrated exceptionally high damping, which will decrease the oscillations induced by attitude maneuvering and position changes. Free-vibration tests have shown that the dynamic displacement of the panels reduces significantly when viscoelastic tape is used [210]. Figure 56 shows results from an experiment testing the dynamic displacement of the solar panel for a 3U CubeSat.

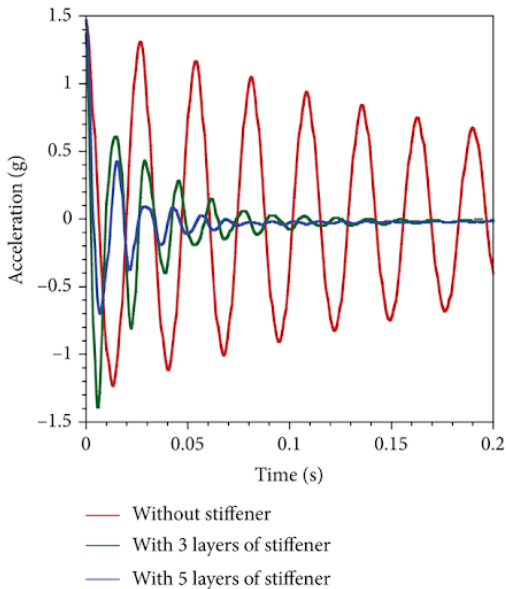


Figure 56: Free-vibration test results [210].

As seen in Figure 56, the greatest reduction in the dynamic displacement occurred when using 5 layers of tape. Each layer of tape is 0.06mm, making the total thickness for 5 layers to be 0.3mm [210]. Since these results were from a 3U CubeSat, it is likely that our 12U and 27 CubeSat will need more layers of tape. However, it was difficult to find information regarding whether the layers of tape scaled directly with the size of the CubeSat. As a result, the SM subsystem has decided to move forward with using 5-8 layers of tape. Each layer of tape weighs approximately 0.6g, so 5-8 layers would weigh 3-4.8g [210]. The tape would be attached to the solar cells in a similar layout as in Figure 55.

#### 15.7.4 Material Outgassing

In order to confirm that the aforementioned materials were the best candidates, the SM subsystem verified that they met the outgassing requirements specified in the SM requirements spreadsheet [6]. Outgassing refers to the process during which volatile molecules are released from the surface of the material in the form of gas. The total mass loss (TML) and the collected volatile condensable material (CVCM) of the PCB material and the viscoelastic tape were analyzed. The TML value demonstrates the amount of the material that is lost during outgassing. The CVCM value shows how much of the loss material condenses. Table 107 shows the properties of PCB and the tape and compares them to the SM outgassing requirements.



Table 107: Outgassing Properties of PCB and Viscoelastic Tape [211] [210]

Material	TML (%)	CVCM (%)
PCB	0.26	0.0
Viscoelastic Tape	0.93	0.1
Requirement	1.0	0.1

As seen in Table 107, both materials meet the outgassing requirements, further confirming that the SM subsystem will be moving forward with using a PCB material reinforced with PCB stiffeners and viscoelastic tape for the solar panel array.

It is important to note that the reason why the SM subsystem didn't include Al 6061 in our material outgassing analysis is because metals exhibit a negligible amount of outgassing and it is not necessary to take the effects into consideration. In addition, it was difficult for the SM subsystem to verify the outgassing requirements of other components from the rest of the subsystem, because it was difficult to find the exact materials that these components were made from. If we had this information from the manufacturers, we would have been able to verify other components as well.

### 15.7.5 HOWLL Structural Design and Analysis

#### Primary Structure Design

As mentioned in Section 15.6.2, we will create a detailed design and conduct analysis on HOWLL instead of both HOWLL and WOOF. HOWLL and WOOF are the same size (27U) and are almost identical with the exception of an additional redundant X-band antenna on HOWLL.

The design of the primary structure has not changed from the previous design cycle, with the exception of a few cutout windows provided for payload and ADCS sensors. As described in previous reports, the primary structure is composed of six aluminum panels and is constrained by the maximum dimensions provided in the Advanced Standard for CubeSats (see Figure 102), shown in Table 108.

Table 108: Maximum dimensions of a 27U CubeSat according to the Advanced Standard for CubeSats [156].

X-direction (mm)	Y-direction (mm)	Z-direction (mm)
331.8	350.7	365.9

As mentioned in previous reports, this monocoque construction has several advantages: it provides radiation shielding for internal components in the harsh radiation environment of cislunar space, provides additional mounting points for internal components, maximizes internal volume, and is easy to manufacture [212].

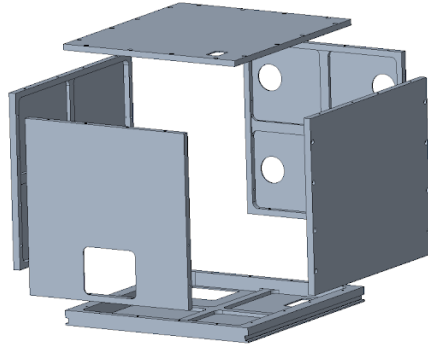


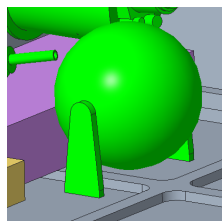
Figure 57: Exploded view of 27U primary structure.

HOWLL and WOOF will have the same primary structures, with the exception of an additional cutout window for the redundant X-band antenna on HOWLL. This will help reduce manufacturing costs and assembly time.

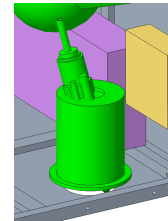
### Secondary Structures

Secondary structures include mounting brackets and fasteners. As mentioned in Section 15.6.2, we designed rough models of some of the secondary structures. We were not able to design all secondary structures because of a lack of high-fidelity CAD models for all internal components.

We designed bolted interfaces for the primary structure as well as rough models of mounting brackets for the propulsion tanks and thrusters, shown in Figure 58. We assume all other components will also be bolted to the frame panels. All brackets will be Aluminum 6061 and all fasteners will be 304 Stainless Steel.



(a) Pressurant tank mount.



(b) Thruster mount.

Figure 58: Models of secondary structures.

### Solar Array Sizing

We sized the solar arrays based on the Power subsystem's required solar cell areas. HOWLL and WOOF both require  $1423 \text{ cm}^2$  of solar cells. This is a large decrease from the area required in the previous design iteration; now, we only require two solar panels that are each 35 by 23 cm. This provides a total available area of  $2(35 \times 23) = 1610 \text{ cm}^2$ .

We estimate the mass of the solar arrays by adding the mass of the PCB substrate to the mass of the solar cells and a conservative estimate mass of wiring and other components. The PCB mass is  $1400 \text{ cm} \times 0.16 \text{ cm} \times 1.85 \text{ g/cm}^3 = 414.4 \text{ g}$  since typical PCBs are 1.6 mm thick and PCB material (FR-4, or "flame retardant 4") has a density of  $1.85 \text{ g/cm}^3$ . The solar cells have a mass of 110



grams, and we will add 100 grams for wiring. This yields a total mass of 624.4 grams, or about 317.2 grams per panel.

The solar arrays are either stowed (during launch and transit) or deployed (during on-orbit operations). These two configurations are shown in Figure 59.

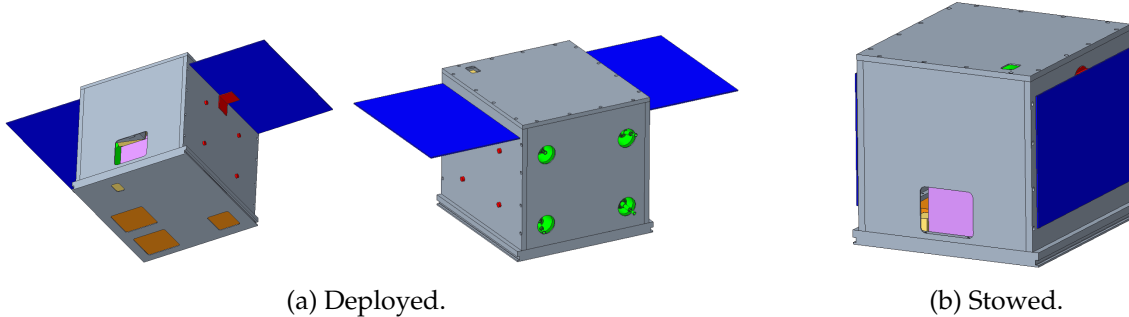


Figure 59: HOWLL solar array configurations. Solar arrays are shown in blue, and hinge brackets and Frangibolts in red.

## Layout

Figure 60 shows the internal layout of HOWLL. WOOF and HOWLL have the same internal layout except HOWLL has an additional X-band and transceiver. Some key features of this layout are as follows. Unless otherwise specified, these apply to all four satellites.

- *Propulsion thrusters:* The thrusters are placed at the four corners of the back face of the satellite. Each of the thrusters is angled outwards at 25° from each axis to provide adequate control for momentum dumping, and the net thrust vector passes through the center of mass of the satellite (roughly at its geometric center). This positioning was requested by the Propulsion team. Note that no other sensor cutouts are on the same face as the thruster cutouts to prevent propellant debris from affecting sensor measurements.
- *Propellant and pressurant tanks:* These tanks are placed as close to the center of mass as possible (while still maintaining attachment points for their secondary structures) since they will have changing mass values over the course of the mission. Positioning these tanks near the center of mass helps the ADCS subsystem effectively mitigate the effects of a shifting center of mass as the tanks empty.
- *Payload camera:* The camera cutout window is on the opposite face of the thrusters to avoid as much debris as possible. There are no obstructions to the camera's field of view.
- *Reaction wheels:* Three of the four reaction wheels are aligned with the X, Y, and Z axes of the satellite. The fourth redundant reaction wheel is tilted off-axis.
- *Star trackers and sun sensors:* The two star trackers are on different faces of the satellite for redundancy. We did not model the sun sensors due to time constraints, but these are very small components and there is more than enough room for them in the satellite. One sun sensor would be placed on each face of the satellite.
- *Antennas:* The patch antennas (three for HOWLL, two for WOOF, and one for each PACK



satellite) are placed adjacent to the frame panels and have cutout windows sized to the respective antennas.

- *Solar arrays:* The stowed solar arrays fit within the allotted launch volume for each satellite (27U for HOWLL/WOOF and 12U for PACK-C and PACK-E as defined by the Advanced Standard for CubeSats).
- *Wire harnesses:* Wire harnesses were not included in the CAD model as modeling and positioning them would be out of the scope of this class. However, we have adequate overall mass and volume margin to include additional wire harnesses in a future design phase, and there is enough space between components to place wire harnesses where necessary.

The EPSM1 (the power management and distribution unit) is located under the OBC (it is included in the CAD model but cannot be seen in the image). We have not included any thermal components since they are either very small or integrated directly into the panel frames. We also have not included the sun sensors since they are very small and there is more than enough room for them on the frame panels.

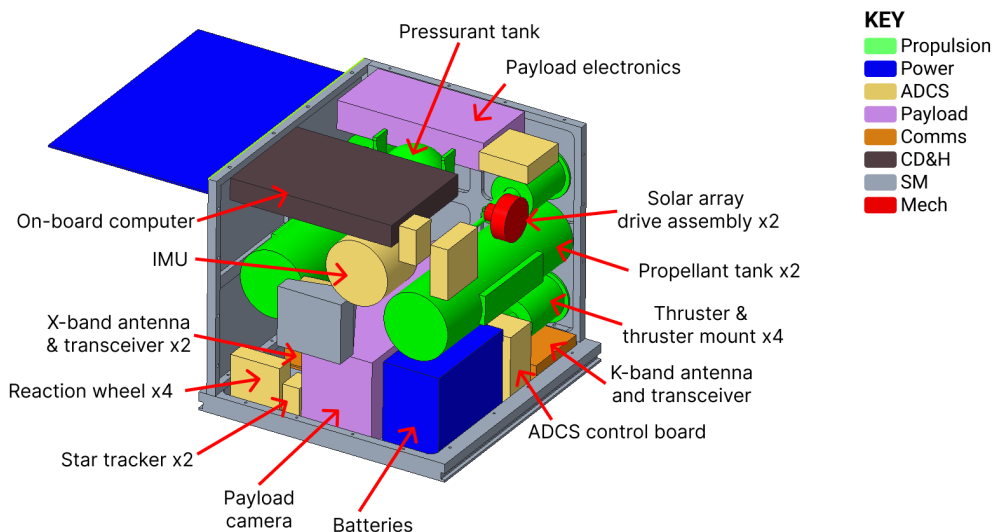


Figure 60: HOWLL internal layout.

### Static Load Analysis

For the preliminary design report, we conducted a static load analysis on only the primary structure by scaling the Falcon 9 launch load by the ratio of the maximum mass of HOWLL to the mass of the primary structure; this essentially simulated the effective launch load but with an inaccurate mass distribution. Now that the internal layout is finalized and (rough) mass and volume models of each components have been added, we can re-run the static load analysis with higher-fidelity mass properties.

### Simulation Setup

Creo Simulate calculates the mass of each component based upon its given volume and density. Since the model of each component envelops the entire component (e.g. a box-like component is modeled as a rectangular prism) and components are not uniform materials, we cannot simply



assign a typical material (e.g. Al-6061, which has a density of  $2.7 \text{ g/cm}^3$ ) to each component. Instead, we calculate the density of each component based on its enveloped volume and given mass (typically from datasheets). We then create custom materials with the correct densities and assign each component to a material accordingly.

Note that we are not concerned with the effects of launch loads on individual components; the vast majority of internal components have significant flight heritage and should be able to withstand launch loads, and we also would not be able to calculate the stresses with any degree of certainty without designing all the secondary structures and bolted interfaces to support the internal components (which, as previously mentioned, is out of the scope of this class). Thus, we are primarily concerned with the stresses on the primary structure, and we re-run the static load analysis with mass/volume models to discern if our particular mass distribution overloads the primary structure.

As with our previous static load analysis, all frame components except the solar panel stacks are assigned to the Al-6061 material. The solar panel stacks are FR-4 (PCB) material. The material properties are listed in Table 109.

Table 109: Material properties of Al-6061 and FR-4 [202], [213].

Material	Poisson Ratio	Young's Modulus (GPa)	Yield Strength (MPa)
Al-6061	0.3	69	276
FR-4	0.12	21	241

For our static load analysis, we impose the load on the spacecraft in its stowed configuration (before solar array deployment) as it will be during launch. At this stage of analysis, we are not concerned about loads on the spacecraft in its deployed configuration since this will only occur in the low gravitational environment of cislunar space. The primary loads on the deployed solar panels will result from impulsive loads from the propulsive thrusters; however, given that each thruster produces a maximum of 1N and there are only four thrusters, these impulsive maneuvers will produce only negligible loads on the solar panels.

As in the last design report, we simplified the finite element model by suppressing curved features such as bolt holes. We did not suppress frame cutouts. We use the same constraints as in the previous report, constraining the tabbed interfaces where the satellite touches the dispenser. The simplified model is shown in Figure 61.

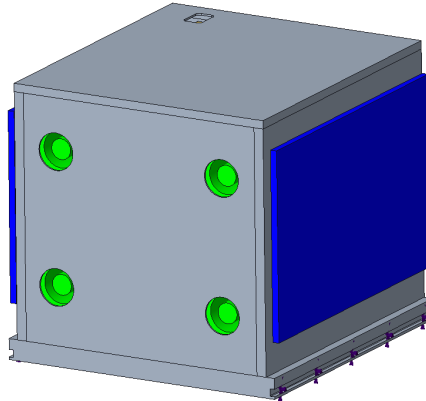


Figure 61: Simplified model of HOWLL for analysis.

Both HOWLL and WOOF will be launched as the primary payload on the Falcon 9 Rideshare launch vehicle. The maximum axial and lateral quasi-static loads are 10g and 16g, respectively [214]. Since we are not sure which direction the spacecraft buses will be oriented, we will simulate the 16g load in two directions.

At the time of analysis, not all internal components had been finalized, which means that the satellite mass was not final. At this point, the CAD model had a total mass of 32.3 kg. To account for potential changes in the total mass, we added a conservative factor of safety of 25% to the total mass (and, effectively, to the launch load; this brings the simulated load up to 20 g. (Note that this is separate from the analysis factor of safety, which will be applied later.)

We now have three load cases:

Table 110: Static load cases for analysis.

Load Case	Load in X	Load in Y	Load in Z
XY	20g	20g	0
YZ	0	20g	20g
XZ	20g	0	20g

These load cases form a conservative envelope of the loads that the satellite will experience on the Falcon 9. Since the primary structure is mostly symmetrical across axes, we do not need to simulate loads in the negative direction. If we find positive stress margins for these load cases, we can be confident that the satellite will survive the loads in the envelope provided by Falcon 9.

#### *Simulation Results*

The resulting stress values are shown in Table 111 below.



Table 111: Results from static load analysis.

Load Case	Max. Von Mises Stress (MPa)	Max. Displacement (mm)
XY	24.8	0.36
YZ	35.6	0.35
XZ	20.4	0.32

We use a safety factor of 2 as recommended by the NASA General Environmental Verification Standard (GEVS) for spacecraft structural analyses [215].

The formula we use to calculate the margin is [158]

$$\text{Stress margin} = \frac{\text{strength of material}}{\text{maximum von Mises stress} \cdot \text{safety factor}} - 1. \quad (37)$$

The highest stress in any direction is 35.6 MPa, which yields a margin of +3.70 for the lowest-strength material (FR-4) from Table 109.

Stress and displacement visualizations for the second load case are provided in Figure 62. Visualizations for the other load cases look very similar and are provided in Appendix A.11.

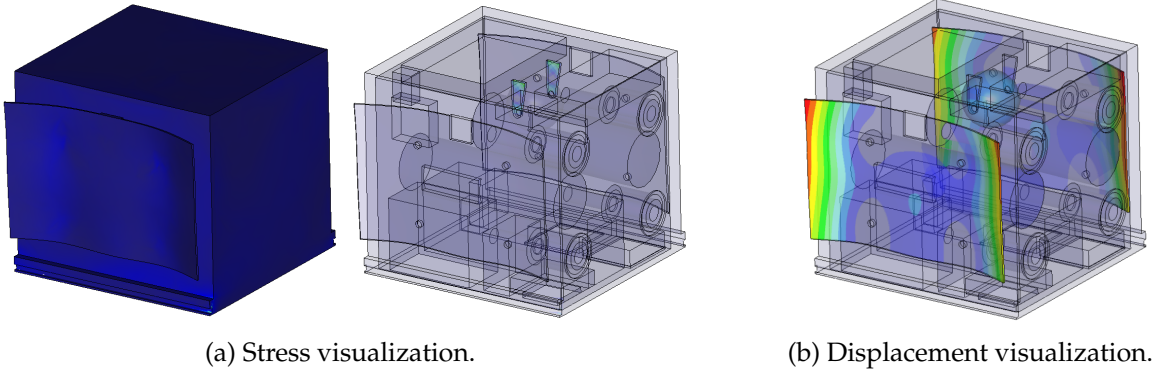


Figure 62: HOWLL static load analysis results for YZ load case.

Note that the greatest stress is actually on the mounting bracket for the pressurant tank, not the primary structure. This suggests that the stress margins for the primary structure are actually higher than calculated. The margin on the pressurant tank brackets still meets requirements, but future engineers can redesign the bracket if necessary.

#### Modal Survey: Stowed Configuration

In the previous design report, we conducted a modal survey of the spacecraft in its stowed configuration to determine if it met the minimum fundamental frequency requirement of the Falcon 9. Since the primary structure has not changed since the previous design report (except for a few additional cutout windows), we do not expect that the stiffness of the structure has changed appreciably. In addition, since we are not modeling the bolted interfaces of internal components, there is no point in determining their modes. Thus, we did not re-run the modal survey of the



stowed configuration for this report, and instead focused on the modal survey of the deployed configuration. For completeness, we include the results from the previous report in Table 112.

Table 112: Fundamental frequencies and corresponding effective masses of 27U bus in stowed configuration.

Frequency (Hz)	Greatest Effective Mass (%)	Direction of Greatest Effective Mass
189	13.1	Y translation
194	17.2	Y translation
211	4.1	X rotation
213	7.0	X rotation

The first mode is well above the 40 Hz requirement, which means we have satisfied this requirement from the Falcon 9 User’s Guide.

### Modal Survey: Deployed Configuration

For this design cycle, we also conducted a modal survey for the spacecraft in its deployed configuration (i.e. the solar arrays have been deployed). In cislunar space, the spacecraft will not be constrained to anything (unlike when it is in the dispenser). Thus, to find the solar array modes, we run an unconstrained modal survey in Creo Simulate. We instruct Creo to find the first ten modes. The first six modes will be the “rigid body modes” (three translational, three rotational) and should be very close to 0. The last four modes represent the first four vibrational modes of the spacecraft, where the spacecraft would have internal deformation. These modes are listed in Table 113.

Table 113: Vibrational modes of 27U bus in deployed configuration.

Frequency (Hz)
25.6
27.2
30.1
30.6

The first two modes describe a “flapping” motion of the solar arrays, and the second two describe a “twisting” motion. These combined give the mode shape seen in Figure 63.

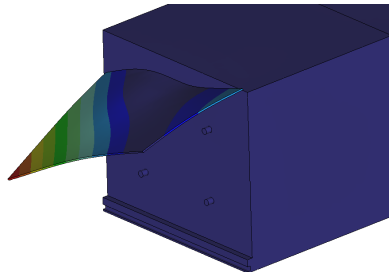


Figure 63: Visualization of HOWLL low-frequency vibrational modes.



Now that we have characterized these modes, engineers can avoid resonances at these frequencies in future design cycles. Depictions of these modes are included in Appendix A.11.

### 15.7.6 PACK-C Structure Design and Analysis

#### Primary Structure Design

As discussed in Section 15.6.2, we will design and analyze PACK-C instead of both PACK-C and PACK-E. These two satellites are very similar, with the exception of slightly smaller propellant and pressurant tanks on PACK-E. For this reason, PACK-C has the more constrained design and thus we choose to design PACK-C.

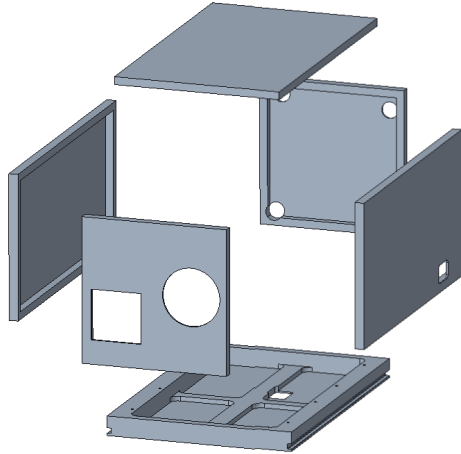
Like HOWLL, the design of the primary structure has not changed since the last design cycle with the exception of sensor and thruster cutouts. The primary structure is composed of six aluminum panels. The maximum dimensions of a 12U CubeSat are shown in Table 114.

Table 114: Maximum dimensions of a 12U CubeSat according to the Advanced Standard for CubeSats [156].

X-direction (mm)	Y-direction (mm)	Z-direction (mm)
219.1	238.0	365.9

An exploded view of the primary structure is shown in Figure 64.

Figure 64: Exploded view of PACK-C primary structure.



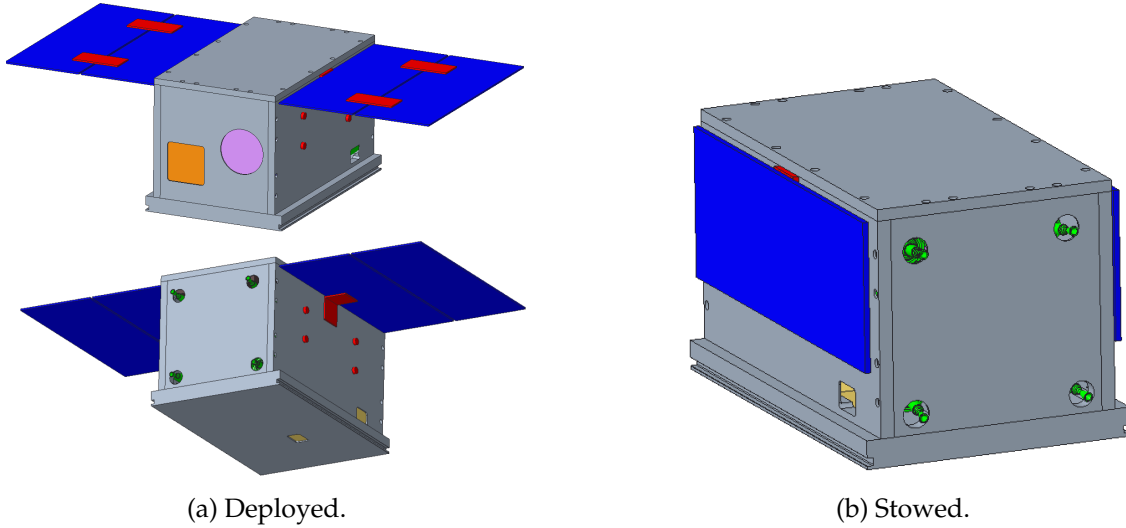
#### Solar Array Sizing

The Power subsystem requires  $1897 \text{ cm}^2$  of solar cell area for both PACK-C and PACK-E. We will satisfy this with four panels, each of size 35 by 15 cm. This yields a total area of  $4(35 \times 15) = 2100 \text{ cm}^2$ . The mass of these panels, calculated the same way as we did for HOWLL, is 809 grams.

The PACK solar arrays also have stowed and deployed configurations, shown in Figure 65 below.



Figure 65: PACK solar array configurations. Solar arrays are shown in blue, and hinge brackets and Frangibolts in red.



## Layout

Refer to the previous Layout section for rationale for the PACK layout. Note that PACK has a lower internal volume margin and thus its layout is more constrained than HOWLL's. That being said, we were able to position all components as desired by the respective subsystems without interference issues. The only exception is that we were unable to fit the previously-designed thruster mounts into the satellite. However, these mounts are low-fidelity models and are very likely overdesigned. There is enough empty volume around the thrusters for future engineers to design mounts for these thrusters.

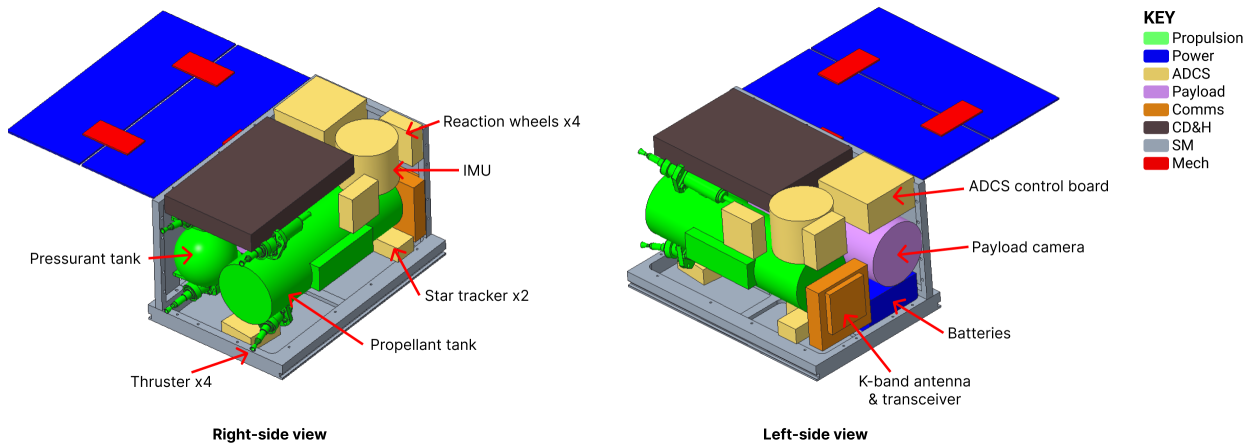


Figure 66: PACK-C internal layout.

As with HOWLL, the EPSM1 (the power management and distribution unit) is located under the OBC. We have not included any thermal components since they are either very small or integrated



directly into the panel frames.

### Static Load Analysis

The process for the static load analysis for PACK-C is the same as for HOWLL. As with the previous analysis, we have the three load cases described in Table 110. The resulting stresses are shown in Table 115 below.

Table 115: Results from static load analysis.

Load Case	Max. Von Mises Stress (MPa)	Max. Displacement (mm)
XY	42.0	0.56
YZ	38.8	0.52
XZ	35.2	0.50

The largest stress is 42 MPa, and the resulting margin is +1.87 for the FR-4 material.

### Modal Survey: Stowed Configuration

As with HOWLL, we did not re-run the modal survey for PACK-C in its stowed configuration because there were no major changes to the primary structure. The results of the modal survey from the previous design report are shown in Table 116.

Table 116: Fundamental frequencies and corresponding effective masses of 12U bus.

Frequency (Hz)	Greatest Effective Mass (%)	Direction of Greatest Effective Mass
469	8.9	Y translation
486	4.2	Y translation
511	17.9	Y translation
519	3.8	Y translation

### Modal Survey: Deployed Configuration

We conducted the same modal survey for PACK-C in its deployed configuration as we did for HOWLL. The first four vibrational modes are listed in Table 117.

Table 117: Vibrational modes of 27U bus in deployed configuration.

Frequency (Hz)
25.6
27.2
30.1
30.6

### 15.7.7 Verification Tests

The Falcon 9 Rideshare Payload User's Guide was used to determine the verification tests that would be needed. This guide was used because we are launching on a Falcon 9 launch vehicle, so



it is important that we perform the necessary tests. Table 118 shows the verification tests the SM subsystem has identified as necessary for our mission.

Table 118: Verification Tests [214]

Test	Unit Not Flown	Protoflight Qualification
Shock	6 dB above MPE, 3 times	3 dB above MPE, 2 times
Random Vibration	3 dB above acceptance for 2 minutes	In the MPE spectrum for 1 minute
Electromagnetic Compatibility	6 dB EMISM by test or 12 dB EMISM by analysis	6 dB EMISM by test or 12 dB EMISM by analysis
Combined Thermal Vacuum and Thermal Cycle	$\pm 10^\circ\text{C}$ beyond acceptance for 27 cycles total	$\pm 5^\circ\text{C}$ beyond acceptance for 20 cycles total
Sine Vibration	1.25 times the limit load, sweep rate of 2 octaves per minute	1.25 times the time load, sweep rate of 4 octaves per minute
Pressure System	Minimum 2 times MEOP	Minimum 2 times MEOP
System-level Pressure Leak Test	Not required	Full pressure system MEOP leak test
Pressure Vessel Leak Test	Not required	Pressure vessel level MEOP leak test

The abbreviations shown in Table 118 are as follows.

- **MPE:** Maximum predicted environment
- **EMISM:** Electromagnetic interference safety margin
- **MEOP:** Maximum expected operating pressure

These values are shown in future detail in the appendix in Section A.11. In Table 118, the highlighted tests are ones that are required by the launch provider. The tests that aren't highlighted aren't required, but are heavily advised by the the launch provider. Since they were heavily advised, the SM subsystem determined that it was important for our mission.

### 15.7.8 Compliance with Subsystem Objectives, Requirements, and Constraints

#### Objectives Compliance

We have satisfied all six objectives as defined in Section 15.2. Justification for each objective is as follows:

1. Supporting the mass and volume of all subsystems: We have created mass and volume budgets that encompass all subsystems with positive margins.
2. Withstanding flight environments: We have conducted static load and modal analyses, which suggest we can survive the load and vibration environments. Further testing (out of the scope of this class) would be completed to verify that we can survive the shock and acoustic environments.

3. Choosing materials: We have conducted load analyses and material outgassing analyses, which suggest that we are satisfying material requirements.
4. Prioritizing location of payload sensors: The payload camera is placed next to frame panels is provided with a cutout for external access in all four satellites.
5. Prioritizing location of communications equipment: Patch antennas are placed next to space-craft walls and have external access via cutouts in all satellites.
6. Protecting components from radiation: We have chosen materials and designed protection for internal components from radiation. We will confirm our design choices with other subsystems during the next design cycle.
7. Budget: The SM subsystem was able to meet their goal of keeping the cost of the total subsystem under \$200,000 by having a total cost of \$191,180 for the structures of all 4 satellites. A more detailed cost breakdown of all of the SM subsystem components can be found in Tables 137, 138, and 139.

### Verification of Requirements

Tables 134-136 in the Appendix verify and justify our requirements and constraints. See the “SM” tab in the Requirements Spreadsheet for a list of requirements [6].

We have met all but two of our functional and performance requirements. The two requirements that we have only partially met are designing secondary structures and characterizing resonant modes for the solar arrays. We are not able to complete these requirements using publicly available information for all components; doing so would be out of the scope of this class.

We have met all constraints. We have met all but two of our environmental requirements. The last two requirements, which are partially met, deal with the outgassing properties of all components. Again, due to lack of publicly available information, we are not able to complete this requirement at this time.



## 16 References

- [1] Ryne Beeson. *Princeton University MAE 342 Space System Design Course: Request for Proposal*. Tech. rep. Jan. 2024 (cit. on pp. 0, 1, 4, 56, 75, 94, 108, 123).
- [2] John F. Connolly. *The Moon as a Stepping Stone to Human Mars Missions*. Tech. rep. July 2018 (cit. on p. 0).
- [3] Shawn Willis. *To the Moon: Strategic Competition in the Cislunar Region*. Tech. rep. Nov. 2023 (cit. on p. 0).
- [4] MAE 342 Course Instructors. *Tier 1 Catalog*. Private communication. Feb. 24, 2024. URL: <https://drive.google.com/drive/folders/12ShG0cqzWwYJYH9-vv6yMc-Z-rcKRDo> (cit. on pp. 0, 63).
- [5] Team ARGOS. *Requirements Spreadsheet*. en. Mar. 2024. URL: [https://docs.google.com/spreadsheets/d/1Yf23XOx3rhpDRWjGT\\_SDC0ncHitQTD5iuh1EGGfD330/edit?usp=embed\\_facebook](https://docs.google.com/spreadsheets/d/1Yf23XOx3rhpDRWjGT_SDC0ncHitQTD5iuh1EGGfD330/edit?usp=embed_facebook) (visited on 03/02/2024) (cit. on p. 2).
- [6] MAE 342 Team 2. *Requirements Spreadsheet*. Private communication. Feb. 16, 2024. URL: [https://docs.google.com/spreadsheets/d/1Yf23XOx3rhpDRWjGT\\_SDC0ncHitQTD5iuh1EGGfD330/edit?usp=sharing](https://docs.google.com/spreadsheets/d/1Yf23XOx3rhpDRWjGT_SDC0ncHitQTD5iuh1EGGfD330/edit?usp=sharing) (cit. on pp. 2, 11, 64, 75–77, 95, 97, 102, 108, 125, 136, 148, 158, 172, 188, 194, 207).
- [7] Jerry Jon Sellers. *4.1.2 The Space Environment*. 2005. URL: [https://www.faa.gov/sites/faa.gov/files/about/office\\_org/headquarters\\_offices/avs/III.4.1.2\\_The\\_Space\\_Environment.pdf](https://www.faa.gov/sites/faa.gov/files/about/office_org/headquarters_offices/avs/III.4.1.2_The_Space_Environment.pdf) (cit. on pp. 5, 175).
- [8] James R. Wertz and Wiley J. Larson. *Space Mission Analysis and Design, Third Edition*. El Segundo, CA: Microcosm Press, 1999 (cit. on pp. 20, 21, 30, 48, 81, 82, 89–92, 100, 180, 182).
- [9] R. Amini, G. Aalbers, R. Hamann, et al. “New generations of spacecraft data handling systems: Less harness , more reliability”. In: 10 (Jan. 2006) (cit. on p. 23).
- [10] Joe Troutman. *Satellite Electrical Power System Design*. Forge Nano. Princeton University, Mar. 2024 (cit. on pp. 25, 150, 154–156).
- [11] MAE 342 Team 2. *Requirements Spreadsheet*. Private communication. Feb. 2024. URL: [https://docs.google.com/spreadsheets/d/1Yf23XOx3rhpDRWjGT\\_SDC0ncHitQTD5iuh1EGGfD330/edit?usp=sharing](https://docs.google.com/spreadsheets/d/1Yf23XOx3rhpDRWjGT_SDC0ncHitQTD5iuh1EGGfD330/edit?usp=sharing) (cit. on pp. 28, 51).
- [12] Sidney Bae and Sabrina Nicacio. *Preliminary Design Review*, GNC. 2024 (cit. on pp. 29, 30, 63, 72).
- [13] Albert Kreutzer and Ariana Rausch. *Preliminary Design Review*, ADCS. 2024 (cit. on pp. 29, 30, 40, 97).
- [14] Patrick Kozak and Isabel Kim. *Preliminary Design Review, Payload*. 2024 (cit. on pp. 29, 30).
- [15] Mori Ono and Julia Hutto. *Preliminary Design Review*, LV. 2024 (cit. on pp. 29, 71, 72).
- [16] Kazuki Tojo and Sarah Fry. *Preliminary Design Review*, Propulsion. 2024 (cit. on p. 29).
- [17] Raphael Vogeley and Pia Dicenzo. *Preliminary Design Review*, Power. 2024 (cit. on pp. 29, 30, 39).
- [18] Candace Do and Manali Badwe. *Preliminary Design Review*, SM. 2024 (cit. on p. 29).
- [19] Evan Alfandre and Anna Solzhenitsyn. *Preliminary Design Review*, Mech. 2024 (cit. on pp. 29, 30).
- [20] Rihan Sajid and Ben Kim. *Preliminary Design Review*, Thermal. 2024 (cit. on pp. 29, 30).



- [21] Jack Amen and Andrew Robbins. *Preliminary Design Review, Communications*. 2024 (cit. on pp. 29, 30, 43).
- [22] Charlie Rogers and Max Kreidl. *Preliminary Design Review, CDH*. 2024 (cit. on pp. 29, 30).
- [23] Space Exploration Technologies Corp. (SpaceX). “Rideshare Payload User’s Guide”. In: (Oct. 2022). URL: <https://forum.nasaspacesflight.com/index.php?action=dlattach;topic=59324.0;attach=2203594> (cit. on p. 30).
- [24] *ESPA User’s Guide: The EELV Secondary Payload Adapter*. MOOG Space and Defense Group. URL: <https://www.moog.com/content/dam/moog/literature/sdg/space/structures/moog-espa-users-guide-datasheet.pdf> (cit. on pp. 30, 59).
- [25] *CubeSat 101 - Basic Concepts and Processes for First-Time CubeSat Developers*. Tech. rep. National Aeronautics and Space Administration (NASA), 2017. URL: [https://www.nasa.gov/wp-content/uploads/2017/03/nasa\\_csls\\_cubesat\\_101\\_508.pdf](https://www.nasa.gov/wp-content/uploads/2017/03/nasa_csls_cubesat_101_508.pdf) (cit. on p. 30).
- [26] California Polytechnic State University. *6U CubeSat Design Specification*. URL: [https://explorers.larc.nasa.gov/APMIDEX2016/MO/pdf\\_files/12-6U\\_CDS\\_2016-05-19\\_Provisional.pdf](https://explorers.larc.nasa.gov/APMIDEX2016/MO/pdf_files/12-6U_CDS_2016-05-19_Provisional.pdf) (cit. on pp. 30, 191).
- [27] et al. William A. Hoey. *Towards Predictive Models of Launch Ascent Depressurization and Induces Particle Redistribution*. Tech. rep. Sept. 2021. URL: [https://ccmpp.gsfc.nasa.gov/2021-presentations/09%20\\_Hoey.pdf](https://ccmpp.gsfc.nasa.gov/2021-presentations/09%20_Hoey.pdf) (cit. on p. 52).
- [28] William Russel. *Lunar Landing Plans Are Progressing, but Challenges Remain*. Tech. rep. Jan. 2024. URL: <https://www.gao.gov/assets/d24107249.pdf> (cit. on pp. 54, 56).
- [29] Aria Alamalhodaei. *Firefly’s Blue Ghost lander represents a big bet on a future lunar economy*. Nov. 2023. URL: <https://techcrunch.com/2023/11/06/fireflys-blue-ghost-lander-represents-a-big-bet-on-a-future-lunar-economy/> (cit. on p. 54).
- [30] Next Spaceflight. URL: <https://nextspaceflight.com/> (cit. on pp. 55, 58, 59).
- [31] Michael Sheets. *SpaceX raises prices for rocket launches and Starlink satellite internet as inflation hits raw materials*. Mar. 2022. URL: <https://www.cnbc.com/2022/03/23/spacex-raises-prices-for-launches-and-starlink-due-to-inflation.html> (cit. on pp. 55, 58).
- [32] Jeffrey S. Parker and Rodney L. Anderson. *Transfers to Low Lunar Orbits*. Tech. rep. July 2013. URL: <https://descanso.jpl.nasa.gov/monograph/series12/LunarTraj--05Chapter4TransfersToLowLunarOrbits.pdf> (cit. on p. 56).
- [33] Condon et. al. *Libration Point Mission Design Consideration*. Tech. rep. Aug. 2019. URL: <https://core.ac.uk/download/pdf/84914463.pdf> (cit. on pp. 56, 62).
- [34] Firefly Aerospace. *Firefly Aerospace Blue Ghost Lunar Lander Condensed Payload User’s Guide*. Tech. rep. Feb. 2021. URL: [https://satcatalog.s3.amazonaws.com/components/1105/SatCatalog--Firefly\\_Aerospace--Blue\\_Ghost--Datasheet.pdf?lastmod=20210720030037](https://satcatalog.s3.amazonaws.com/components/1105/SatCatalog--Firefly_Aerospace--Blue_Ghost--Datasheet.pdf?lastmod=20210720030037) (cit. on pp. 56, 61, 163, 228).
- [35] Firefly Aerospace. *Blue Ghost Mission 2 to the Moon*. URL: <https://fireflyspace.com/missions/blue-ghost-mission-2/> (cit. on pp. 56, 59).
- [36] Ramy Kozman and Alex da Silva Curiel. *Commercial Data Relay Services in the Cis-Lunar Environment with SSTL’s Lunar Pathfinder*. Tech. rep. July 2023. URL: <https://digitalcommons.usu.edu/cgi/viewcontent.cgi?article=5633&context=smallsat> (cit. on pp. 56, 59).



- [37] NASA. *FY 2025 Budget Request*. <https://payloadspace.com/wp-content/uploads/2024/03/nasa-fiscal-year-2025-budget-summary-1.pdf>. Mar. 2024 (cit. on pp. 57, 59, 60).
- [38] NASA. *Artemis 2 Secondary Payloads 6U & 12U Potential Cubesat Accommodations*. Tech. rep. Aug. 2019. URL: [https://www.nasa.gov/wp-content/uploads/2019/09/sls\\_artemis-2\\_6u-12u-accommodations\\_8\\_1\\_19\\_0.pdf](https://www.nasa.gov/wp-content/uploads/2019/09/sls_artemis-2_6u-12u-accommodations_8_1_19_0.pdf) (cit. on p. 57).
- [39] SpaceX. *Starship User's Guide Revision 1.0*. Tech. rep. Mar. 2020. URL: [https://www.spacex.com/media/starship\\_users\\_guide\\_v1.pdf](https://www.spacex.com/media/starship_users_guide_v1.pdf) (cit. on pp. 57, 228).
- [40] Kathryn Hambleton and Catherine E. Williams. *NASA's Artemis IV: Building First Lunar Space Station*. Mar. 2024. URL: <https://www.nasa.gov/general/nasas-artemis-iv-building-first-lunar-space-station/> (cit. on p. 57).
- [41] Andrew Jones. *Russia's war on Ukraine has caused lasting damage to international spaceflight cooperation*. Mar. 2023. URL: <https://www.space.com/russia-war-ukraine-damage-international-spaceflight-cooperation> (cit. on p. 57).
- [42] NOAA Office of Space Commerce. *New Russian Sanctions Include Commercial Space Launch Activities*. Mar. 2021. URL: <https://www.space.com/new-russian-sanctions-include-commercial-space-launch-activities/> (cit. on p. 57).
- [43] Peter B. de Selding. *U.S. ITAR satellite export regime's effects still strong in Europe*. Apr. 2016. URL: <https://spacenews.com/u-s-itar-satellite-export-regimes-effects-still-strong-in-europe/> (cit. on pp. 57, 58).
- [44] Federal Aviation Administration (FAA). *Frequently Asked Questions (FAQs)*. URL: [https://www.faa.gov/space/additional\\_information/faq](https://www.faa.gov/space/additional_information/faq) (cit. on p. 57).
- [45] Mitsubishi Heavy Industries. *MHI LAUNCH SERVICES: LAUNCH VEHICLES*. URL: [https://www.mhi.com/products/space/launch\\_srv\\_lineup.html#pdi3](https://www.mhi.com/products/space/launch_srv_lineup.html#pdi3) (cit. on p. 57).
- [46] Audrey Decker. *ULA's new rocket took off. But can it challenge SpaceX?* Jan. 2024. URL: <https://www.defenseone.com/business/2024/01/ula-ready-launch-its-new-rocket-will-it-be-able-challenge-spacex/393175/> (cit. on p. 57).
- [47] John Schilling. *Launch Vehicle Performance Calculator*. URL: <https://silverbirdastronautics.com/LVperform.html> (cit. on pp. 58, 60).
- [48] SpaceX. *Falcon User's Guide*. Tech. rep. Sept. 2021. URL: <https://www.spacex.com/media/falcon-users-guide-2021-09.pdf%7D> (cit. on p. 58).
- [49] S Ramakrishnan. *Polar Satellite Launch Vehicle User's Manual*. Tech. rep. Mar. 2005. URL: <https://web.archive.org/web/20221228035248/https://www.mach5lowdown.com/wp-content/uploads/PUG/PSLV-Users-Manual-issue4-1999-12.pdf> (cit. on p. 58).
- [50] Rocket Lab. *Electron Payload User's Guide Version 7.0*. Tech. rep. Nov. 2022. URL: <https://www.rocketlabusa.com/assets/Uploads/Electron-Payload-User-Guide-7.0.pdf> (cit. on p. 58).
- [51] Rocket Lab. *Lunar Photon: Rocket Lab's Mission to the Moon*. Tech. rep. 2022. URL: [https://www.rocketlabusa.com/assets/Uploads/EXC22\\_017%20-%20Photon%20Doc\\_%C6%92%20\[Web\].pdf](https://www.rocketlabusa.com/assets/Uploads/EXC22_017%20-%20Photon%20Doc_%C6%92%20[Web].pdf) (cit. on p. 58).
- [52] Gina Anderson, Clare Skelly, Tracy Young. *NASA Awards Contract to Launch CubeSat to Moon from Virginia*. Feb. 2020. URL: <https://www.nasa.gov/news-release/nasa-awards-contract-to-launch-cubesat-to-moon-from-virginia/> (cit. on p. 58).



- [53] Bureau of Labor Statistics. *CPI Inflation Calculator*. URL: <https://data.bls.gov/cgi-bin/cpicalc.pl> (cit. on p. 58).
- [54] Jeff Foust. *Lunar landing restored for Artemis 4 mission*. Oct. 2022. URL: <https://spacenews.com/lunar-landing-restored-for-artemis-4-mission/> (cit. on p. 59).
- [55] SpaceX. *Rideshare Payload User's Guide*. Tech. rep. Dec. 2023. URL: [https://storage.googleapis.com/rideshare-static/Rideshare\\_Payload\\_Users\\_Guide.pdf%7D](https://storage.googleapis.com/rideshare-static/Rideshare_Payload_Users_Guide.pdf%7D) (cit. on pp. 59, 62, 162, 228).
- [56] SpaceX. *Smallsat Rideshare Program*. URL: <https://www.spacex.com/rideshare/> (cit. on p. 60).
- [57] Juan I. Morales Volosín. *Transporter-10—Falcon 9 Block 5*. Mar. 2024. URL: <https://everydayastronaut.com/transporter-10-falcon-9-block-5/> (cit. on p. 60).
- [58] Astrobotic. *Astrobotic Lunar Landers Payload User's Guide*. Tech. rep. Aug. 2021. URL: [https://www.astrobotic.com/wp-content/uploads/2022/01/PUG\\_Landers\\_011222.pdf](https://www.astrobotic.com/wp-content/uploads/2022/01/PUG_Landers_011222.pdf) (cit. on pp. 60–62).
- [59] Intuitive Machines. *Intuitive Machines Lunar Access Services User's Guide V.1.4*. Tech. rep. Nov. 2022. URL: [https://www.intuitivemachines.com/\\_files/ugd/7c27f7\\_458cf85ba6e94ba18f33702dc2c326af.pdf](https://www.intuitivemachines.com/_files/ugd/7c27f7_458cf85ba6e94ba18f33702dc2c326af.pdf) (cit. on pp. 60, 61).
- [60] Jeff Foust. *Japanese lunar lander, with NASA rideshare, to launch this month*. Nov. 2022. URL: <https://spacenews.com/japanese-lunar-lander-with-nasa-rideshare-to-launch-this-month/> (cit. on p. 60).
- [61] NASA. *Draper Lunar Lander*. URL: <https://nssdc.gsfc.nasa.gov/nmc/display.action?id=DRAPER> (cit. on p. 61).
- [62] National Aeronautics and Space Administration. *Commercial Lunar Payload Services*. URL: <https://www.nasa.gov/commercial-lunar-payload-services/> (cit. on p. 61).
- [63] Peterson and Schriever Space Force Base. *18th Space Defense Squadron*. Jan. 2023. URL: <https://www.petersonschriever.spaceforce.mil/About-Us/Fact-Sheets/Display/Article/3016228/18th-space-defense-squadron/> (cit. on p. 62).
- [64] Ryne Beeson. *DyLAN NASA SBIR Phase II Contract 80NSSC19C0140*. Tech. rep. CU Aerospace L.L.C., 2020. URL: <https://sbir.nasa.gov/SBIR/abstracts/18/sbir/phase2/SBIR-18-2-H9.03-5452.html> (cit. on pp. 67, 68).
- [65] Ryne Beeson, Amlan Sinha, Bindu Jagannatha, et al. “Dynamically Leveraged Automated Multibody (N) Trajectory Optimization”. In: *AAS/AIAA Space Flight Mechanics Conference*. American Astronautical Society. Charlotte, NC, Aug. 2022 (cit. on pp. 67, 68).
- [66] Ryan Whitley and Roland Martinez. “Options for Staging Orbits in Cis-Lunar Space”. In: (Oct. 2015). URL: <https://ntrs.nasa.gov/api/citations/20150019648/downloads/20150019648.pdf> (cit. on p. 70).
- [67] Deepak Gaur and Mani Shankar Prasad. “Communication relay Satellites constellation assessment for future Lunar missions”. In: *2020 8th International Conference on Reliability, Infocom Technologies and Optimization (Trends and Future Directions)(ICRITO)*. IEEE. 2020, pp. 1195–1200 (cit. on p. 70).
- [68] Roberto Armellin, Pierluigi Di Lizia, M Rasotto, et al. “Disposal strategies for spacecraft in lagrangian point orbits”. In: *The 24th AAS/AIAA Space Flight Mechanics Meeting*. 2014, pp. 26–30 (cit. on p. 72).
- [69] Paolo Guardabasso, Stéphanie Lizy-Destrez, and Marie Ansart. “Lunar orbital debris mitigation: Characterisation of the environment and identification of disposal strategies”. In: *8th European Conference on Space Debris*. Vol. 8. 2021 (cit. on p. 72).



- [70] Sarah Fry, Kazuki Tojo, Pia Dicenzo, et al. *Propulsion Subsystem Report 1*. Submission to MAE 342 Space Systems Design via Gradescope. 2024 (cit. on pp. 74, 75, 77, 78).
- [71] Sarah Fry, Kazuki Tojo, Pia Dicenzo, et al. *Propulsion Subsystem Report 2*. Submission to MAE 342 Space Systems Design via Gradescope. 2024 (cit. on pp. 74, 75, 77, 78, 89).
- [72] Sarah Fry, Kazuki Tojo, Pia Dicenzo, et al. *Propulsion Subsystem Preliminary Design Report*. Submission to MAE 342 Space Systems Design via Gradescope. 2024 (cit. on pp. 74, 75, 77, 78).
- [73] satsearch. *A guide to adopting thrusters for small satellite missions - a webinar by satsearch*. June 2021. URL: <https://www.youtube.com/watch?v=lMJPQs5pe1E> (visited on 02/24/2024) (cit. on pp. 79, 83, 84, 87).
- [74] Candace Do, Manali Badwe, Evan Alfandre, et al. *MAE 342 Team ARGOS Subsystem PDR: Structures and Materials*. Apr. 2024. (Visited on 05/07/2024) (cit. on p. 80).
- [75] Team ARGOS. *MAE 342 Team ARGOS NASA Goddard Presentation*. May 2024. (Visited on 05/07/2024) (cit. on p. 80).
- [76] satsearch. *1N HPGP Thruster — satsearch*. en. 2024. URL: <https://satsearch.co/products/ecaps-1n-hpgp-thruster> (visited on 05/07/2024) (cit. on p. 80).
- [77] Sonja Caldwell. *4.0 In-Space Propulsion*. Feb. 2024. URL: [https://www.nasa.gov/smallsat-institute/sst-soa/in-space-propulsion/#:~:text=In%2Dspace%20small%20spacecraft%20propulsion,\(iii\)%20propellant%2Dless](https://www.nasa.gov/smallsat-institute/sst-soa/in-space-propulsion/#:~:text=In%2Dspace%20small%20spacecraft%20propulsion,(iii)%20propellant%2Dless). (cit. on pp. 82, 83).
- [78] Ritvij Singh. *Explained: SpaceX and the Rocket Equation (for beginners)*. May 2020. URL: <https://medium.com/swlh/explained-spacex-and-the-rocket-equation-for-beginners-aa427c091f97> (cit. on p. 82).
- [79] Sarah Fry. *Argos Propulsion Trade Study*. Feb. 2024. URL: [https://docs.google.com/spreadsheets/d/1Am62Ztfp7LccnM\\_eMKpogFZdRluO3hGYxG0FBmIRww4/edit#gid=699650431](https://docs.google.com/spreadsheets/d/1Am62Ztfp7LccnM_eMKpogFZdRluO3hGYxG0FBmIRww4/edit#gid=699650431) (cit. on pp. 83, 89, 91, 93, 277).
- [80] ECAPS. *1N HPGP Thruster Datasheet*. 2024. (Visited on 05/06/2024) (cit. on pp. 83, 84).
- [81] Matt Nehrenz and Matt Sorgenfrei. “A Comparison of Thruster Implementation Strategies for a Deep Space Nanosatellite”. en. In: *AIAA Guidance, Navigation, and Control Conference*. Kissimmee, Florida: American Institute of Aeronautics and Astronautics, Jan. 2015. ISBN: 978-1-62410-339-1. DOI: [10.2514/6.2015-0866](https://doi.org/10.2514/6.2015-0866). (Visited on 02/23/2024) (cit. on pp. 84–86, 102).
- [82] Jessie Stachowicz. “Optimization and Additive Manufacturing for HPGP Rocket Engines”. en. In: (2022) (cit. on pp. 86, 87).
- [83] Kazuki Tojo, Sarah Fry, Pia Dicenzo, et al. *MAE 342 Team ARGOS Subsystem PDR: Propulsion*. Apr. 2024. (Visited on 05/07/2024) (cit. on p. 86).
- [84] Bradford Ecaps. *Flight-proven High Performance Green Propulsion*. 2017. URL: [https://static1.squarespace.com/static/603ed12be884730013401d7a/t/6054f44e4f133f08e2dd1ed1/1616180305816/Bradford\\_ECAPS\\_Folder\\_2017.pdf](https://static1.squarespace.com/static/603ed12be884730013401d7a/t/6054f44e4f133f08e2dd1ed1/1616180305816/Bradford_ECAPS_Folder_2017.pdf) (visited on 02/24/2024) (cit. on pp. 86, 89).
- [85] Kimberly Marie Hogge. “Quantifying the Characteristic Length of a Combustor for an Ionic Liquid Monopropellant Thruster”. en. In: (Jan. 2017) (cit. on p. 86).
- [86] Yiguang Ju. *MAE 426 Lecture Note 6: Nozzle Characteristics*. 2024 (cit. on p. 87).
- [87] Yiguang Ju. *MAE 426 Lecture Slide 9: Bipropellant Rockets*. 2024 (cit. on p. 87).



- [88] Astronautix. *N2O4/Hydrazine*. 2019. URL: <http://www.astronautix.com/n/n2o4hydrazine.html> (visited on 04/02/2024) (cit. on p. 86).
- [89] Nils Pokrupa, Kjell Anflo, and Oskar Svensson. "Spacecraft System Level Design with Regards to Incorporation of a New Green Propulsion System". In: *47th AIAA/ASME/SAE/ASEE Joint Propulsion Conference & Exhibit*. Joint Propulsion Conferences. American Institute of Aeronautics and Astronautics, July 2011. DOI: [10.2514/6.2011-6129](https://doi.org/10.2514/6.2011-6129). (Visited on 04/27/2024) (cit. on pp. 87–89).
- [90] Aaron Dinardi and Mathias Persson. "High Performance Green Propulsion (HPGP): A Flight-Proven Capability and Cost Game-Changer for Small and Secondary Satellites". In: (2012). URL: <https://digitalcommons.usu.edu/cgi/viewcontent.cgi?article=1033&context=smallsat> (cit. on p. 89).
- [91] Aaron Dinardj, Kjell Anflo, and Pete Friedhoff. "On-Orbit Commissioning of High Performance Green Propulsion (HPGP) in the SkySat Constellation". In: *31st Annual AIAA/USU Conference on Small Satellites* (2017). URL: <https://digitalcommons.usu.edu/smallsat/2017/all2017/139/> (cit. on p. 89).
- [92] UC Berkeley Space Technologies and Rocketry. *Feed System Types*. URL: <https://rocketry.gitbook.io/public/tutorials/propulsion/feed-system-types> (cit. on pp. 91, 92).
- [93] Jason W. Hartwig. "A Detailed Historical Review of Propellant Management Devices for Low Gravity Propellant Acquisition". In: *52nd AIAA/SAE/ASEE Joint Propulsion Conference*. DOI: [10.2514/6.2016-4772](https://doi.org/10.2514/6.2016-4772) (cit. on pp. 92, 93).
- [94] Donald Platt. "A Propulsion System Tailored to Cubesat Applications". In: 2007. URL: <https://api.semanticscholar.org/CorpusID:107524846> (cit. on p. 92).
- [95] H.E. Tacca, P. Rachov, and Diego Lentini. "Electric Feed Systems for Liquid Propellant Rocket Engines". In: (Dec. 2010). DOI: [10.13140/2.1.4431.9042](https://doi.org/10.13140/2.1.4431.9042) (cit. on p. 92).
- [96] MAE 342 Team 2. *Budgets Spreadsheet*. Private communication. Feb. 16, 2024. URL: [https://docs.google.com/spreadsheets/d/1AUlvS4XVfT65vEK6KG5z\\_SD355k4TbhXtIC5eigyL-o/edit?usp=sharing](https://docs.google.com/spreadsheets/d/1AUlvS4XVfT65vEK6KG5z_SD355k4TbhXtIC5eigyL-o/edit?usp=sharing) (cit. on pp. 97, 174, 177).
- [97] Thomas Krogstad and Jan Gravdahl. "6-DOF mutual synchronization of formation flying spacecraft". In: Jan. 2007, pp. 5706–5711. DOI: [10.1109/CDC.2006.376725](https://doi.org/10.1109/CDC.2006.376725) (cit. on p. 98).
- [98] URL: <https://nssdc.gsfc.nasa.gov/planetary/factsheet/moonfact.html> (cit. on p. 100).
- [99] URL: <https://www.satnow.com/search/sun-sensors> (cit. on pp. 104–106).
- [100] Álvaro Bello, Ástor del Castañedo, Karl Stephan Olfe, et al. "Parameterized fuzzy-logic controllers for the attitude control of nanosatellites in low earth orbits. A comparative studio with PID controllers". In: *Expert Systems with Applications* 174 (2021), p. 114679. ISSN: 0957-4174. DOI: <https://doi.org/10.1016/j.eswa.2021.114679> (cit. on p. 106).
- [101] Xiaoning Zhu, Ming Ma, Defu Cheng, et al. "An Optimized TRIAD Algorithm for Attitude Determination". In: *Artifical Satellites* 52 (2017). DOI: [10.1515/arsa-2017-0005](https://doi.org/10.1515/arsa-2017-0005) (cit. on p. 106).
- [102] F. Landis Markley, Reid G. Reynolds, Frank X. Liu, et al. "Maximum Torque and Momentum Envelopes for Reaction Wheel Arrays". In: NASA (2009) (cit. on pp. 106, 107).
- [103] Princeton University MAE 342 Instructional Staff. *MAE 342 Space System Design: Mission Catalog*. Feb. 2024. URL: <https://drive.google.com/drive/u/1/folders/12ShG0cqzWwYJYH9-vv6yMc-Z-rcKRD0> (cit. on p. 108).



- [104] *High-resolution satellite imagery*. URL: <https://eos.com/products/high-resolution-images/> (cit. on p. 110).
- [105] Chris Formeller. *Introducing 15 cm HD: The Highest Clarity From Commercial Satellite Imagery*. URL: <https://blog.maxar.com/earth-intelligence/2020/introducing-15-cm-hd-the-highest-clarity-from-commercial-satellite-imagery> (cit. on p. 110).
- [106] *Clarity and Confidence*. URL: <https://explore.maxar.com/Imagery-Leadership-Spatial-Resolution#:~:text=Monitoring%20activity%3A%20national%20security&text=In%20matters%20of%20national%20security,identify%20people%20on%20the%20ground> (cit. on p. 110).
- [107] *High-Resolution Imaging*. URL: <https://www.flir.com/discover/iis/machine-vision/high-resolution-imaging/#:~:text=Dynamic%20range%20is%20the%20difference,produce%20shadows%20and%20bright%20highlights>. (cit. on p. 110).
- [108] Steve Miller. *New Satellite Sensor Sees Earth at Night Almost as If It Were Day*. 2015. URL: <https://www.scientificamerican.com/article/new-satellite-sensor-sees-earth-at-night-almost-as-if-it-were-day/> (cit. on p. 110).
- [109] *Infrared Sensor - IR Sensor*. URL: [https://www.infratec-infrared.com/sensor-division/service-support/glossary/infrared-sensor/#:~:text=An%20infrared%20sensor%20\(IR%20sensor,systems%20to%20detect%20unwelcome%20guests](https://www.infratec-infrared.com/sensor-division/service-support/glossary/infrared-sensor/#:~:text=An%20infrared%20sensor%20(IR%20sensor,systems%20to%20detect%20unwelcome%20guests). (cit. on p. 110).
- [110] *Kairospace - 90mm Camera*. Accessed: 2024-02-24. URL: <https://satsearch.co/products/kairospace-90mm-camera> (cit. on pp. 110, 145, 257).
- [111] *Satlantis - iSIM 90*. Accessed 2024-02-24. URL: <https://satsearch.co/products/satlantis-isim-90> (cit. on pp. 110, 145, 257).
- [112] MAE 342 Team 2. *Requirements Spreadsheet*. Private communication. Feb. 16, 2024. URL: [https://docs.google.com/spreadsheets/d/1Yf23XOx3rhPDRWJGT\\_SDCOnCHitQTD5iuh1EGGfD330/edit?usp=sharing](https://docs.google.com/spreadsheets/d/1Yf23XOx3rhPDRWJGT_SDCOnCHitQTD5iuh1EGGfD330/edit?usp=sharing) (cit. on pp. 124, 135).
- [113] *Radio Spectrum Allocation — Federal Communications Commission*. URL: <https://www.fcc.gov/engineering-technology/policy-and-rules-division/general/radio-spectrum-allocation> (visited on 03/10/2024) (cit. on p. 127).
- [114] Feb. 2024. URL: <https://www.nasa.gov/smallsat-institute/sst-soa/soa-communications/> (cit. on p. 127).
- [115] *Near Space Network - NASA*. URL: <https://www.nasa.gov/communicating-with-missions/nsn/> (visited on 03/10/2024) (cit. on p. 128).
- [116] en. URL: <https://standards.ieee.org> (cit. on pp. 128, 129).
- [117] *S-Band High Data Rate Transmitter*. ISISPACE. URL: <https://www.isispace.nl/product/isis-txs-s-band-transmitter/> (visited on 03/10/2024) (cit. on p. 128).
- [118] *Conformal Antennas — Haigh Farr*. URL: <https://www.haigh-farr.com/products/antennas/conformal> (visited on 03/10/2024) (cit. on p. 128).
- [119] *syrlinks - S/S Band Transponder for nanosatellites & cubesatellites*. URL: <https://www.syrlinks.com/en/space/nano-satellite/s-band-transponder-ewc31> (visited on 03/10/2024) (cit. on p. 128).
- [120] *Antennas*. URL: [https://www.iq-spacecom.com/products/antennas#s-band\\_high\\_gain](https://www.iq-spacecom.com/products/antennas#s-band_high_gain) (visited on 03/10/2024) (cit. on p. 128).
- [121] *Commercial S-Band Patch Antenna*. CubeSat by EnduroSat. URL: <https://www.endurosat.com/cubesat-store/cubesat-antennas/s-band-antenna-commercial/> (visited on 03/10/2024) (cit. on p. 128).



- [122] Versatile Wideband Software Defined Radio (SDR) — EnduroSat. CubeSat by EnduroSat. URL: <https://endurosat.com/cubesat-store/cubesat-communication-modules/versatile-wideband-sdr/> (visited on 03/10/2024) (cit. on p. 128).
- [123] URL: <https://www.endurosat.com/cubesat-store/cubesat-antennas/x-band-patch-antenna/> (cit. on p. 130).
- [124] en-US. URL: <https://www.endurosat.com/cubesat-store/cubesat-antennas/k-band-4x4-patch-array-antenna/> (cit. on p. 130).
- [125] URL: <https://www.endurosat.com/cubesat-store/cubesat-communication-modules/x-band-transmitter/> (cit. on p. 130).
- [126] en-US. URL: <https://paradigma-tech.com/k-band-transmitter/> (cit. on p. 130).
- [127] Sirius OBC&TCM Development Kit. URL: <https://www.aac-clyde.space/what-we-do/space-products-components/command-data-handling/sirius-tcm-leon3ft-development-kit> (cit. on p. 139).
- [128] FERMI OBC - On-Board Computer — SatCatalog. <https://www.satcatalog.com/component/fermi-obc/>. Accessed: 2024-02-23 (cit. on pp. 140, 141).
- [129] SIRIUS-TCM-LEON3FT - Satellite Command & Data Handling — AAC Clyde Space. <https://www.aac-clyde.space/what-we-do/space-products-components/command-data-handling/sirius-tcm-leon3ft>. Accessed: 2024-02-21 (cit. on pp. 140, 141).
- [130] Single-Board Computer (RADPC-SBC-001). [https://img1.wsimg.com/blobby/go/edf1766a-2e03-4be0-a36f-8527e4310348/downloads/RadPC-SBC-001\\_Product\\_Overview\\_PRELIM\\_Dec2022.pdf?ver=1687376606611](https://img1.wsimg.com/blobby/go/edf1766a-2e03-4be0-a36f-8527e4310348/downloads/RadPC-SBC-001_Product_Overview_PRELIM_Dec2022.pdf?ver=1687376606611). Accessed: 2024-02-23 (cit. on pp. 140, 141).
- [131] Bruce Yost and Sasha Weston. *State-of-the-art small spacecraft technology*. Tech. rep. 2024 (cit. on pp. 140, 192).
- [132] Roberto et al. Furfaro. "Tracking Objects in Cislunar Space: The Chang'e 5 Case". In: *Advanced Maui Optical and Space Surveillance Technologies Conference (AMOS)* (2021) (cit. on p. 141).
- [133] "Communications". In: *Space Mission Analysis and Design*. Third. El Segundo, California: Microcosm Press, 2005, pp. 533–587. ISBN: 1-881883-10-8. URL: [https://drive.google.com/drive/u/1/folders/1-pOZs\\_NlVBqcuPBw8ARhcviePKCk9bOT](https://drive.google.com/drive/u/1/folders/1-pOZs_NlVBqcuPBw8ARhcviePKCk9bOT) (cit. on p. 141).
- [134] Toshinori Kuwahara. *Introduction to CubeSat Command and Data Handling System. "Presentation"*. URL: [https://www.unoosa.org/documents/pdf/psa/access2space4all/KiboCUBE/AcademySeason2/On-demand\\_Pre-recorded\\_Lectures/KiboCUBE\\_Academy\\_2021\\_OPL10.pdf](https://www.unoosa.org/documents/pdf/psa/access2space4all/KiboCUBE/AcademySeason2/On-demand_Pre-recorded_Lectures/KiboCUBE_Academy_2021_OPL10.pdf) (cit. on p. 142).
- [135] Conversation with Glenn Rakow, Electrical Engineer at Goddard Space Flight Center. personal communication. May 2, 2024 (cit. on pp. 142, 146).
- [136] Vision Space. *Satellite Housekeeping Data*. 2022. URL: <https://www.blog.visionspace.com/blog/2022/4/21/satellite-housekeeping-data#:~:text=The%20data%20bandwidth%20requirement%20typically,andservices%2C%20please%20contact%20us!> (cit. on p. 143).
- [137] Zerubia Josiane Aguilar Camilo Ortner Mathias. "Small Object Detection and Tracking in Satellite Videos With Motion Informed-CNN and GM-PHD Filter". In: *Frontiers in Signal Processing* (2022). URL: <https://www.frontiersin.org/articles/10.3389/frsip.2022.827160> (cit. on pp. 144, 145).
- [138] G. et al. Vives Vallduriola. "The use of streak observations to detect space debris". In: *International Journal of Remote Sensing* (2018) (cit. on p. 144).



- [139] Kothe. "Integrated edge and junction detection with the boundary tensor". In: *Proceedings Ninth IEEE International Conference on Computer Vision*. IEEE. 2003, pp. 424–431 (cit. on p. 145).
- [140] NASA Space Mission Design Tools. NASA. URL: <https://www.nasa.gov/smallsat-institute/space-mission-design-tools/> (cit. on p. 145).
- [141] Core Flight Systems Github Repository. NASA. URL: <https://github.com/nasa/cFS> (cit. on p. 146).
- [142] Judith A. Jeevarajan and Eric C. Darcy. *Crewed Space Vehicle Battery Safety Requirements*. NTRS Author Affiliations: NASA Johnson Space Center NTRS Report/Patent Number: JSC-CN-35260 NTRS Document ID: 20160003504 NTRS Research Center: Johnson Space Center (JSC). Jan. 2014. URL: <https://ntrs.nasa.gov/citations/20160003504> (visited on 03/10/2024) (cit. on pp. 148, 154).
- [143] State-of-the-Art Small Spacecraft Technology. 2017. URL: <https://www.nasa.gov/smallsat-institute/sst-soa/integration-launch-and-deployment/#10.4.1> (cit. on pp. 154–156).
- [144] Wiley J. Larson and James R. Wertz. *Space Mission Analysis and Design* (3rd Edition). 1999. URL: [https://drive.google.com/file/d/1vbiTBEYeeewWpnx\\_sEr4DO9aoILXMGY2/view?usp=embed\\_facebook](https://drive.google.com/file/d/1vbiTBEYeeewWpnx_sEr4DO9aoILXMGY2/view?usp=embed_facebook) (visited on 03/10/2024) (cit. on pp. 154, 157).
- [145] Molcel. PRODUCT DATA SHEET LITHIUM-ION RECHARGEABLE BATTERY MODEL ICR-18650M. URL: [https://www.molicel.com/wp-content/uploads/DM\\_ICR18650M-V3-80072.pdf](https://www.molicel.com/wp-content/uploads/DM_ICR18650M-V3-80072.pdf) (cit. on p. 154).
- [146] SOLAERO by ROCKET LAB. Z4J Space Solar Cell 4-Junction Solar Cell for Space Applications. URL: <https://www.rocketlabusa.com/assets/Uploads/RL-SolAero-Data-Sheet-Z4J.pdf> (cit. on pp. 155, 156).
- [147] NASA. Rocket Lab Delivers Final Solar Panels for NASA Gateway's Power and Propulsion Element. en. URL: <https://www.rocketlabusa.com/updates/rocket-lab-delivers-final-solar-panels-for-nasa-gateway-power-and-propulsion-element/> (visited on 03/10/2024) (cit. on p. 155).
- [148] High-power Multi-channel Electrical Power System Module (EPSM1). en. URL: [http://www.pumpkinspace.com/store/p216/High-power\\_Multi-channel\\_Electrical\\_Power\\_System\\_Module\\_%28EPSM1%29.html](http://www.pumpkinspace.com/store/p216/High-power_Multi-channel_Electrical_Power_System_Module_%28EPSM1%29.html) (visited on 04/29/2024) (cit. on p. 156).
- [149] Alphonso Stewart Alejandro Rivera. "STUDY OF SPACECRAFT DEPLOYABLES FAILURES". In: NASA GSFC (2021) (cit. on p. 161).
- [150] Joe Munder. *Design of Mechanisms: William Pierson Field Lecture*. Mar. 15, 2024 (cit. on pp. 161, 166).
- [151] Canisterized Satellite Dispenser. Tech. rep. Rocket Lab. URL: <https://www.rocketlabusa.com/assets/Uploads/2002337G-CSD-Data-Sheet-compressed.pdf#page38> (cit. on pp. 163, 164, 169, 262).
- [152] Payload User's Guide. Tech. rep. Rocket Lab USA. URL: [https://www.rocketlabusa.com/assets/Uploads/EXC22\\_017%20-%20Photon%20Doc\\_%C6%92%20%5BWeb%5D.pdf](https://www.rocketlabusa.com/assets/Uploads/EXC22_017%20-%20Photon%20Doc_%C6%92%20%5BWeb%5D.pdf) (cit. on p. 163).
- [153] Rocket Lab Rideshare CubeSat Launch in Maxwell. URL: <http://mstl.atl.calpoly.edu/~workshop/archive/2018/Spring/Day203/Session203/DanielGillies.pdf> (cit. on pp. 163, 262).
- [154] Cubesats On Nasa's Space Launch System. Tech. rep. National Aeronautics and Space Administration Goddard Space Flight Center. URL: [https://www.nasa.gov/wp-content/uploads/2018/02/0364\\_secondary\\_payloads\\_brochure\\_07282020\\_508\\_single\\_pages\\_for\\_web.pdf](https://www.nasa.gov/wp-content/uploads/2018/02/0364_secondary_payloads_brochure_07282020_508_single_pages_for_web.pdf) (cit. on p. 163).



- [155] *CubeSat Design Specification*. Tech. rep. Cal Poly – San Luis Obispo, CA. URL: [https://static1.squarespace.com/static/5418c831e4b0fa4ecac1bacd/t/62193b7fc9e72e0053f00910/1645820809779/CDS+REV14\\_1+2022-02-09.pdf](https://static1.squarespace.com/static/5418c831e4b0fa4ecac1bacd/t/62193b7fc9e72e0053f00910/1645820809779/CDS+REV14_1+2022-02-09.pdf) (cit. on p. 163).
- [156] Ryan Hevner, Walter Holemans, Jordi Puig-Suari, et al. *An Advanced Standard for CubeSats*. 2011. URL: <https://digitalcommons.usu.edu/cgi/viewcontent.cgi?article=1111&context=smallsat> (cit. on pp. 163, 195, 203, 273).
- [157] *EBAD TiNi™ Frangibolt® Actuator*. URL: <https://www.ebad.com/tini-frangibolt/#1562267018138-ae149058-3c03d991-d474> (cit. on pp. 164, 165, 263).
- [158] NASA. *Structural Stress Analysis*. URL: <https://llis.nasa.gov/lesson/819> (cit. on pp. 164, 201).
- [159] Xin Lang et al. Zhengxian Liu. “Design, material properties and performances of a smart hinge based on shape memory polymer composites”. In: *Composites Part B: Engineering* (2020). DOI: <https://doi.org/10.1016/j.compositesb.2020.108056> (cit. on pp. 166, 169–171).
- [160] *TYPE 1 SOLAR ARRAY DRIVE ASSEMBLY (SADA)*. URL: <https://www.moog.com/content/dam/moog/literature/sdg/space/actuationmechanisms/moog-Solar-Array-Drive-Assembly-SADA-Datasheet.pdf> (cit. on pp. 168, 264).
- [161] *Deployable Articulated Solar Array (DASA) User Manual*. URL: [https://www.pumpkininc.com/space/manual/UM-33\\_Pumpkin\\_DASA.pdf](https://www.pumpkininc.com/space/manual/UM-33_Pumpkin_DASA.pdf) (cit. on pp. 168, 264).
- [162] *SEPTA36 Datasheet*. URL: [https://www.beyondgravity.com/sites/default/files/media\\_document/2023-11/SEPTA36-Datasheet.pdf](https://www.beyondgravity.com/sites/default/files/media_document/2023-11/SEPTA36-Datasheet.pdf) (cit. on pp. 168, 264).
- [163] *HoneyBee Robotics*. URL: <https://www.honeybeerobotics.com/products/solar-array-drive-assemblies/#1562267018138-ae149058-3c0374f5-d928> (cit. on pp. 168–171, 264).
- [164] *COMAT SADM*. URL: <https://satsearch.co/products/comat-sadm-400-solar-array-drive-mechanism> (cit. on pp. 168, 264).
- [165] *DHV SADA*. URL: <https://satsearch.co/products/dhv-technology-micro-sada-10> (cit. on pp. 168, 264).
- [166] *Revolv SADA*. URL: <https://satsearch.co/products/revolv-space-sara-solar-array-drive-mechanism> (cit. on pp. 168, 264).
- [167] American Chemical Society. *High-Energy Shape-Memory Polymer Could Someday Help Robots Flex Their Muscles*. Online. Accessed: 2024-05-07. 2021. URL: <https://www.acs.org/pressroom/newsreleases/2021/september/high-energy-shape-memory-polymer-could-someday-help-robots-flex-their-muscles.html#:~:text=In%20addition%20to%20its%20record,to%20make%2C%20the%20researchers%20say> (cit. on p. 169).
- [168] Michael Galvin. *Personal communication*. Conversation. Discussion on cost estimation. May 2024 (cit. on p. 169).
- [169] *Product: Vacuum Stepper Motors VSS 43.200.1.2-HV*. 2024. URL: [https://www.e-motionsupply.com/product\\_p/vss-43.200.1.2-hv.htm](https://www.e-motionsupply.com/product_p/vss-43.200.1.2-hv.htm) (cit. on p. 169).
- [170] Daniel Gillies. *A Brief History of Time*. 2018. URL: <http://mstl.atl.calpoly.edu/~workshop/archive/2018/Spring/Day%203/Session%203/DanielGillies.pdf> (cit. on p. 169).
- [171] *EBAD TiNi™ Mini Frangibolt® Actuator*. URL: [https://www.ebad.com/wp-content/uploads/2021/03/TiNi-Mini\\_Frangibolt\\_released\\_12-8-21.pdf](https://www.ebad.com/wp-content/uploads/2021/03/TiNi-Mini_Frangibolt_released_12-8-21.pdf) (cit. on pp. 169–171, 263).



- [172] National Aeronautics and Space Administration. *Mars Sample Return Earth Entry Vehicle design overview*. Tech. rep. NASA, 1995. URL: <https://ntrs.nasa.gov/api/citations/19950020847/downloads/19950020847.pdf> (cit. on p. 169).
- [173] Lithium-Ion Rechargeable Battery Model ICR-18650M. Molicel. URL: [https://www.molicel.com/wp-content/uploads/DM\\_ICR18650M-V3-80072.pdf](https://www.molicel.com/wp-content/uploads/DM_ICR18650M-V3-80072.pdf) (cit. on p. 174).
- [174] Space Weather Prediction Center. *Solar Flares (Radio Blackouts)*. 2024. URL: <https://www.swpc.noaa.gov/phenomena/solar-flares-radio-blackouts#:~:text=Solar%20flare%20intensities%20cover%20a,8%20W%2Fm2> (cit. on p. 177).
- [175] Average area of the shadow of a convex shape. Online forum. May 2019. URL: <https://math.stackexchange.com/questions/3222317/average-area-of-the-shadow-of-a-convex-shape> (cit. on p. 178).
- [176] ARGOS Thermal Subsystem. *Thermal Regulation Calcs and Trade Studies*. Private communication. May 7, 2024. URL: <https://docs.google.com/spreadsheets/d/1HbUxjRE4eUUFLgqNBKCKupTlQRx0P2VagtqNjs/edit?usp=sharing> (cit. on pp. 179, 180, 183).
- [177] NOAA. As Good As Gold: Are Satellites Covered in Gold Foil? 2016. URL: <https://www.nesdis.noaa.gov/news/good-gold-are-satellites-covered-gold-foil#:~:text=These%20layers%20are%20usually%20made,it%20will%20be%20exposed%20to.> (cit. on p. 180).
- [178] Wikipedia Commons. Closeup of Multi-layer insulation from a satellite. 2006. URL: [https://en.wikipedia.org/wiki/Multi-layer\\_insulation#/media/File:MultiLayerInsulationCloseup.jpg](https://en.wikipedia.org/wiki/Multi-layer_insulation#/media/File:MultiLayerInsulationCloseup.jpg) (cit. on p. 180).
- [179] Inc. Sheldahl Flexible Technologies. *The Red Book*. 2020. URL: <https://sheldahl.com/wp-content/uploads/2023/07/RedBook.pdf> (cit. on p. 180).
- [180] NASA. 7.2.1 Sprayable Thermal Control Coatings, Tapes and MLI. 2024. URL: <https://www.nasa.gov/smallsat-institute/sst-soa/thermal-control/#7.2.1> (cit. on p. 180).
- [181] ISS JAXA. *Space-Extreme of Cold and Hot Temperature*. 2003. URL: <https://iss.jaxa.jp/kids/en/space/401.html#:~:text=Heat%20conduction%20and%20convection%20do,a%20vacuum%2C%20only%20by%20radiation.&text=While%20cooking%20a%20BBQ%2C%20the,for%20just%20a%20brief%20second.> (cit. on p. 181).
- [182] NASA. 7.2.2 Thermal Straps. 2024. URL: <https://www.nasa.gov/smallsat-institute/sst-soa/thermal-control/#7.2.2> (cit. on p. 181).
- [183] NASA. 7.2.8 Heat Pipes. 2024. URL: <https://www.nasa.gov/smallsat-institute/sst-soa/thermal-control/#7.2.8> (cit. on p. 181).
- [184] Technology Applications Incorporated. *THERMAL STRAPS*. URL: <https://www.techapps.com/thermal-straps> (cit. on pp. 181, 182).
- [185] K. N. Shukla. "Heat Pipe for Aerospace Applications—An Overview". In: *Journal of Electronics Cooling and Thermal Control* (2015) (cit. on p. 181).
- [186] Celsia. *Heat Pipe Thermal Conductivity*. 2024. URL: <https://celsiainc.com/heat-sink-blog/heat-pipe-thermal-conductivity> (cit. on p. 182).
- [187] Electronics Cooling. *Design Considerations When Using Heat Pipes*. 2024. URL: <https://www.electronics-cooling.com/2016/08/design-considerations-when-using-heat-pipes/> (cit. on p. 182).
- [188] Inc Technology Applications. *Copper Cable Flexible Thermal Links*. 2024. URL: <https://www.techapps.com/copper-thermal-strap-assemblies#> (cit. on p. 182).



- [189] NASA. 7.3.1 Heaters. 2024. URL: <https://www.nasa.gov/smallsat-institute/sst-soa/thermal-control/#7.3.1> (cit. on p. 182).
- [190] "Vulcan Electric". Cartridge Heaters. URL: <https://www.nasa.gov/smallsat-institute/sst-soa/thermal-control/#7.3.1> (cit. on p. 183).
- [191] Tempco. Flexible Heaters. URL: <https://www.tempco.com/Tempco/Resources/09-Flexible-Resources/KaptonCatalogPages.pdf> (cit. on p. 183).
- [192] Excelitas Technologies. Optical Solar Reflectors. 2024. URL: <https://www.excelitas.com/product/optical-solar-reflectors> (cit. on pp. 183, 184).
- [193] SQUID3 Space. Redefining Spacecraft Thermal Control. 2024. URL: <https://www.squid3.space/> (cit. on p. 183).
- [194] SQUID3 Space. SQ-1 Optical Solar Reflectors. 2024. URL: <https://www.satcatalog.com/component/sq-1-optical-solar-reflectors/> (cit. on pp. 183, 184).
- [195] European Space Agency. Flying Thermometers. 2012. URL: [https://www.esa.int/Applications/Observing\\_the\\_Earth/Space\\_for\\_our\\_climate/Flying\\_thermometers](https://www.esa.int/Applications/Observing_the_Earth/Space_for_our_climate/Flying_thermometers) (cit. on p. 184).
- [196] Solutions Direct. Hi-Temp Infrared Temperature Sensor with 30m Cable, -40 to 1112 F — RAYMI310LTHCB30. 2024. URL: <https://www.solutionsdirectonline.com/raytek-hi-temp-infrared-temperature-sensor-with-30m-cable-40-to-1112-f-raymi310lthcb30> (cit. on p. 184).
- [197] Minnesota Measurement Instruments. K-Type Thermocouple Wire High Temperature Sensor PK-1. 2024. URL: <https://www.meter-depot.com/k-type-thermocouple-wire-high-temperature-sensor-pk-1/> (cit. on p. 184).
- [198] Omega. What Is A Thermistor And How Does It Work? URL: <https://www.omega.com/en-us/resources/thermistor> (cit. on pp. 184, 185).
- [199] Encyclopaedia Britannica. Seebeck Effect. 2024. URL: <https://www.britannica.com/science/Seebeck-effect> (cit. on p. 185).
- [200] SatSearch. Sierra Nevada Corporation Passive Thermal Louvers. URL: <https://satsearch.co/products/sierra-nevada-corporation-passive-thermal-louvers> (cit. on p. 185).
- [201] ARGOS Thermal. ARGOS Thermal Subsystem Budget Calculations. Private document. Apr. 10, 2024. URL: <https://docs.google.com/spreadsheets/d/1DdgAQ7OyzldtkiWRwpfHbP3Rf5vRCQpuNvsDLuF9tQ/edit?usp=sharing> (cit. on p. 186).
- [202] Aluminum 6061-T6. 2024. URL: <https://asm.matweb.com/search/SpecificMaterial.asp?bassnum=ma6061t6> (cit. on pp. 191, 199, 266).
- [203] Aluminum 7075-T6. 2024. URL: <https://asm.matweb.com/search/SpecificMaterial.asp?bassnum=ma7075t6> (cit. on p. 191).
- [204] 7075 Aluminium vs 6061 Aluminium. URL: <https://www.thyssenkrupp-materials.co.uk/> (cit. on p. 191).
- [205] Patrick T Summers and et. al. "Overview of aluminum alloy mechanical properties during and after fires". In: *Fire Science Reviews* 4 (3 Apr. 2015). DOI: [10.1186/s40038-015-0007-5](https://doi.org/10.1186/s40038-015-0007-5) (cit. on p. 191).
- [206] NASA Technology Transfer Program. Atomic Number (Z)-Grade Radiation Shields from Fiber Metal Laminates. URL: <https://technology.nasa.gov> (cit. on p. 192).



- [207] Donald Laurence and et al. "Methods of Making Z-Shielding". In: *United States Patent* (2011) (cit. on p. 192).
- [208] *State-of-the-Art Small Spacecraft Technology*. Tech. rep. 2023. URL: <https://www.nasa.gov/wp-content/uploads/2024/02/soa-report-2023.pdf?emrc=4c0199> (cit. on p. 192).
- [209] Vanni Lugh Emanuele A. Slejko Anna Gregorio. *Material selection for a CubeSat structural bus complying with debris mitigation*. Tech. rep. 2021. URL: <https://www.sciencedirect.com/science/article/pii/S0273117720308383> (cit. on p. 193).
- [210] Shankar Bhattacharai, Hongrae Kim, and Hyun-Ung Oh. "CubeSat's Deployable Solar Panel with Viscoelastic Multilayered Stiffener for Launch Vibration Attenuation". In: *International Journal of Aerospace Engineering* (2020). DOI: <10.1155/2020/8820619> (cit. on pp. 193–195).
- [211] NASA. *Outgassing Data for Selecting Spacecraft Materials*. URL: <https://outgassing.nasa.gov/Home> (cit. on p. 195).
- [212] NASA. *NASA Small Satellite State of the Art Chapter 6: Structures, Materials, and Mechanisms*. URL: [https://www.nasa.gov/wp-content/uploads/2021/10/6.soa\\_structures\\_2021.pdf](https://www.nasa.gov/wp-content/uploads/2021/10/6.soa_structures_2021.pdf) (cit. on p. 195).
- [213] *Glass Epoxy (G10, FR4) Characteristics*. Dielectric Manufacturing. URL: <https://dielectricmfg.com/resources/knowledge-base/glass-epoxy/> (cit. on p. 199).
- [214] *Rideshare Payload User's Guide*. SpaceX. 2023. URL: [https://storage.googleapis.com/rideshare-static/Rideshare\\_Payload\\_Users\\_Guide.pdf](https://storage.googleapis.com/rideshare-static/Rideshare_Payload_Users_Guide.pdf) (cit. on pp. 200, 206, 267, 268).
- [215] *General Environmental Verification Standard (GEVS) for GSFC Flight Programs and Projects*. NASA Goddard Space Flight Center. 2021. URL: [https://standards.nasa.gov/sites/default/files/standards/GSFC/B/0/gsfc-std-7000b\\_signature\\_cycle\\_04\\_28\\_2021\\_fixed\\_links.pdf](https://standards.nasa.gov/sites/default/files/standards/GSFC/B/0/gsfc-std-7000b_signature_cycle_04_28_2021_fixed_links.pdf) (cit. on p. 201).
- [216] S.V. Vadawale et. al. *Radiation Environment in Earth-Moon Space: Results from Random Experiment Onboard Chandrayaan-1*. Tech. rep. Dec. 2010. URL: <https://arxiv.org/ftp/arxiv/papers/1012/1012.2014.pdf> (cit. on p. 228).
- [217] Kozak et al. Kim. *Payload Subsystem Report 1*. Tech. rep. Feb. 2024 (cit. on p. 257).
- [218] *Dragonfly Aerospace - Caiman Imager*. Accessed: 2024-02-24. URL: <https://satsearch.co/products/dragonfly-aerospace-caiman-imager> (cit. on p. 257).
- [219] URL: <https://satsearch.co/products/kairospace-90mm-camera> (cit. on p. 257).
- [220] URL: <https://satsearch.co/products/simera-sense-hyperscape100> (cit. on p. 257).
- [221] *Poly Picosatellite Orbital Deployer*. Tech. rep. Cal Poly - San Luis Obispo, CA. URL: [https://static1.squarespace.com/static/5418c831e4b0fa4ecac1bacd/t/5806854d6b8f5b8eb57b83bd/1476822350599/P-POD-MkIIIRevE-UserGuide\\_CPPPODUG-1.0-1\\_Rev1.pdf](https://static1.squarespace.com/static/5418c831e4b0fa4ecac1bacd/t/5806854d6b8f5b8eb57b83bd/1476822350599/P-POD-MkIIIRevE-UserGuide_CPPPODUG-1.0-1_Rev1.pdf) (cit. on p. 262).
- [222] *Nanoracks External CubeSat Deployer*. Tech. rep. Nanoracks, 2018. URL: <https://nanoracks.com/wp-content/uploads/Nanoracks-External-Cygnus-Deployer-E-NRCSID-IDD.pdf> (cit. on p. 262).
- [223] *ISIS CubeSat Deployers*. Tech. rep. ISIS - Innovative Solutions In Space. URL: <https://www.isispace.nl/wp-content/uploads/2016/02/ISIS-CubeSat-Deployers-Brochure-v1.pdf> (cit. on p. 262).
- [224] *RAMI - Reliable and Advanced Mission Injector*. Tech. rep. UARX Space. URL: [https://www.uarx.com/resources/UARX-Q-CRE-0051-C-RAMI\\_QuickSpecs-November2021.pdf](https://www.uarx.com/resources/UARX-Q-CRE-0051-C-RAMI_QuickSpecs-November2021.pdf) (cit. on p. 262).
- [225] *Internally Isolated 12U Rail CubeSat Dispenser with Analyzable Boundary Conditions*. Tech. rep. Tyvak Nano-Satellite Systems, Inc. URL: <https://digitalcommons.usu.edu/cgi/viewcontent.cgi?article=4123&context=smallsat> (cit. on p. 262).



- 
- [226] EBAD TiNi™ Pin Puller. URL: <https://www.ebad.com/tini-pin-puller/#advantages8008-dfac> (cit. on p. 263).
  - [227] Adam Thurn et al. A Nichrome Burn Wire Release Mechanism for CubeSats. Tech. rep. Naval Research Laboratory, 2012 (cit. on p. 263).
  - [228] PACSCI EMC Pyrotechnic Cable Cutter. URL: <https://psemc.com/products/pyrotechnic-cable-cutter/> (cit. on p. 263).
  - [229] EBAD NEA® Hold Down + Release Mechanisms (HDRM). URL: <https://www.ebad.com/nea-hold-down-release-mechanisms-hdrm/#1562267018138-ae149058-3c03b4fc-1b51c> (cit. on p. 263).



## A Appendix

This appendix is organized by section and includes supplemental information to accompany the report.



## A.1 General Mission Information



## A.2 Compliance

Subsystem	Component	HOWLL				WOOF				PACK-C				PACK-E			
		Unit Mass (kg)	Quantity	Total Mass (kg)	Unit Mass (kg)	Quantity	Total Mass (kg)	Unit Mass (kg)	Quantity	Total Mass (kg)	Unit Mass (kg)	Quantity	Total Mass (kg)	Unit Mass (kg)	Quantity	Total Mass (kg)	
ADCS	Control board	0.5	1	0.5	0.5	1	0.5	0.5	1	0.5	0.5	1	0.5	0.5	1	0.5	
ADCS	Star trackers	0.047	2	0.094	0.047	2	0.094	0.047	2	0.094	0.047	2	0.094	0.047	2	0.094	
ADCS	Sun sensors	0.005	6	0.03	0.005	6	0.03	0.005	6	0.03	0.005	6	0.03	0.005	6	0.03	
ADCS	IMU	0.84	1	0.84	0.84	1	0.84	0.84	1	0.84	0.84	1	0.84	0.84	1	0.84	
ADCS	Reaction wheels	0.375	4	1.5	0.33	4	1.32	0.33	4	1.32	0.33	4	1.32	0.33	4	1.32	
CD&H	OBC/TCM	0.3	1	0.3	0.3	1	0.3	0.3	1	0.3	0.3	1	0.3	0.3	1	0.3	
Comms	X-band antenna	0.053	2	0.106	0.053	1	0.053	0.053	0	0	0.053	0	0	0.053	0	0	
Comms	X-band transceiver	0.27	2	0.54	0.27	1	0.27	0.27	0	0	0.27	0	0	0.27	0	0	
Comms	K-band antenna	0.076	1	0.076	0.076	1	0.076	0.076	1	0.076	0.076	1	0.076	0.076	1	0.076	
Comms	K-band transceiver	0.475	1	0.475	0.475	1	0.475	0.475	1	0.475	0.475	1	0.475	0.475	1	0.475	
Mechanisms	Solar array drive asm	0.225	2	0.45	0.225	2	0.45	0.225	2	0.45	0.225	2	0.45	0.225	2	0.45	
Mechanisms	Frangibots	0.01	8	0.08	0.01	8	0.08	0.01	8	0.08	0.01	8	0.08	0.01	8	0.08	
Mechanisms	Hinge brackets	0.2	2	0.4	0.2	2	0.4	0.2	6	1.2	0.2	6	0.2	6	1.2		
Mechanisms	SMPC hinges	0.01	2	0.02	0.01	2	0.02	0.01	4	0.04	0.01	4	0.04	0.01	4	0.04	
Payload	Camera	3	1	3	3	1	3	1.4	1	1.4	1.4	1	1.4	1.4	1	1.4	
Payload	Camera electronics	1	1	1	1	1	1	0	1	0	0	1	0	0	1	0	
Power	Batteries	3.65	1	3.65	3.65	1	3.65	1.4	1	1.4	1.4	1	1.4	1.4	1	1.4	
Power	PMADD	0.23	1	0.23	0.23	1	0.23	0.23	1	0.23	0.23	1	0.23	0.23	1	0.23	
Propulsion	Thrusters	0.38	4	1.52	0.38	4	1.52	0.38	4	1.52	0.38	4	1.52	0.38	4	1.52	
Propulsion	Tanks	4.65	1	4.65	4.65	1	4.65	2.84	1	2.84	1.14	1	1.14	1.14	1	1.14	
Propulsion	Feed system	0.43	1	0.43	0.42	1	0.42	0.27	1	0.27	0.16	1	0.16	0.16	1	0.16	
Thermal	OSR	0.05	1	0.05	0.05	1	0.05	0.028	1	0.028	0.028	1	0.028	0.028	1	0.028	
Thermal	Louvres	0.189	1	0.189	0.189	1	0.189	0.105	1	0.105	0.105	1	0.105	0.105	1	0.105	
Thermal	Black kapton	0.025	1	0.025	0.025	1	0.025	0.014	1	0.014	0.014	1	0.014	0.014	1	0.014	
Thermal	Thermocouples	0.045	1	0.045	0.045	1	0.045	0.045	1	0.045	0.045	1	0.045	0.045	1	0.045	
Thermal	Heaters	0.032	1	0.032	0.032	1	0.032	0.032	1	0.032	0.032	1	0.032	0.032	1	0.032	
Thermal	Thermal straps	0.715	1	0.715	0.715	1	0.715	0.321	1	0.321	0.321	1	0.321	0.321	1	0.321	
Thermal	MISC	0.025	1	0.025	0.025	1	0.025	0.025	1	0.025	0.025	1	0.025	0.025	1	0.025	
Structures	X+ panel	1.114	1	1.114	1.114	1	1.114	0.654	1	0.654	0.654	1	0.654	0.654	1	0.654	
Structures	X- panel	2.128	1	2.128	2.128	1	2.128	1.994	1	1.994	1.994	1	1.994	1.994	1	1.994	
Structures	Y+ panel	1.078	1	1.078	1.078	1	1.078	0.64	1	0.64	0.64	1	0.64	0.64	1	0.64	
Structures	Y- panel	1.078	1	1.078	1.078	1	1.078	0.64	1	0.64	0.64	1	0.64	0.64	1	0.64	
Structures	Z+ panel	0.918	1	0.918	0.918	1	0.918	0.335	1	0.335	0.335	1	0.335	0.335	1	0.335	
Structures	Z0 panel	0.887	1	0.887	0.887	1	0.887	0.35	1	0.35	0.35	1	0.35	0.35	1	0.35	
Structures	Solar panels	0.68	1	0.68	0.68	1	0.68	0.68	1	0.68	0.68	1	0.68	0.68	1	0.68	
Structures	thruster bracket	0.28	4	1.12	0.28	4	1.12	0.28	0	0	0.28	0	0	0.28	0	0	
Structures	pressurant bracket	0.32	1	0.32	0.32	1	0.32	0.32	1	0.32	0.32	1	0.32	0.32	1	0.32	
Structures	propellant bracket	0.18	1	0.18	0.18	1	0.18	0.18	1	0.18	0.18	1	0.18	0.18	1	0.18	
Total				30.48			29.96			19.14			17.33				

Figure 67: Mass stackup for all subsystem components for each satellite.

Subsystem	Component	Unit Volume (g/cm³)				Quantity				Total Volume (g/cm³)				Unit Volume (g/cm³)				Quantity			
		Unit Volume (g/cm³)	Quantity	Total Volume (g/cm³)	Unit Volume (g/cm³)	Quantity	Total Volume (g/cm³)	Unit Volume (g/cm³)	Quantity	Total Volume (g/cm³)	Unit Volume (g/cm³)	Quantity	Total Volume (g/cm³)	Unit Volume (g/cm³)	Quantity	Total Volume (g/cm³)	Unit Volume (g/cm³)	Quantity	Total Volume (g/cm³)		
ADCS	Control board	414.72	1	414.72	414.72	1	414.72	414.72	1	414.72	414.72	1	414.72	414.72	1	414.72	414.72	1	414.72		
ADCS	Star trackers	41.16	2	82.32	41.16	2	82.32	41.16	2	82.32	41.16	2	82.32	41.16	2	82.32	41.16	2	82.32		
ADCS	Sun sensors	27.2	6	163.2	27.2	6	163.2	27.2	6	163.2	27.2	6	163.2	27.2	6	163.2	27.2	6	163.2		
ADCS	IMU	559.27	1	559.27	559.27	1	559.27	559.27	1	559.27	559.27	1	559.27	559.27	1	559.27	559.27	1	559.27		
ADCS	Reaction wheels	122.5	4	490	122.5	4	490	84.1	4	336.4	84.1	4	336.4	84.1	4	336.4	84.1	4	336.4		
CD&H	OBC/TCM	1319.05	1	1319.05	1319.05	1	1319.05	1319.05	1	1319.05	1319.05	1	1319.05	1319.05	1	1319.05	1319.05	1	1319.05		
Comms	X-band antenna	38.025	2	76.05	38.025	1	38.025	0	0	0	0	0	0	0	0	0	0	0	0		
Comms	X-band transceiver	224.64	2	449.28	224.64	1	224.64	0	0	0	0	0	0	0	0	0	0	0	0		
Comms	K-band antenna	220.9	1	220.9	220.9	1	220.9	380.25	1	380.25	380.25	1	380.25	380.25	1	380.25	380.25	1	380.25		
Comms	K-band transceiver	24.402	1	24.402	24.402	1	24.402	220.9	1	220.9	220.9	1	220.9	220.9	1	220.9	220.9	1	220.9		
Mechanisms	Solar array drive asm	105.63	2	211.26	105.63	2	211.26	105.63	2	211.26	105.63	2	211.26	105.63	2	211.26	105.63	2	211.26		
Mechanisms	Frangibots	1.65	8	13.2	1.65	8	13.2	1.65	8	13.2	1.65	8	13.2	1.65	8	13.2	1.65	8	13.2		
Mechanisms	Hinge brackets	214.812	2	429.624	214.812	2	429.624	214.812	6	1288.872	214.812	6	1288.872	214.812	6	1288.872	214.812	6	1288.872		
Mechanisms	SMPC hinges	3.48	2	6.96	3.48	2	6.96	3.48	4	13.92	3.48	4	13.92	3.48	4	13.92	3.48	4	13.92		
Payload	Camera	3511.2	1	3511.2	3511.2	1	3511.2	1948.88	1	1948.88	1948.88	1	1948.88	1948.88	1	1948.88	1948.88	1	1948.88		
Payload	Camera electronics	922.94	1	922.94	922.94	1	922.94	922.94	1	922.94	922.94	1	922.94	922.94	1	922.94	922.94	1	922.94		
Power	Batteries	1423.76	1	1423.76	1423.76	1	1423.76	143.76	1	143.76	143.76	1	143.76	143.76	1	143.76	143.76	1	143.76		
Power	PMADD	0	1	0	0	1	0	0	1	0	0	1	0	0	1	0	0	1	0		
Propulsion	Thrusters	223.68	4	894.72	223.68	4	894.72	223.68	4	894.72	223.68	4	894.72	223.68	4	894.72	223.68	4	894.72		
Propulsion	Tanks	3921.34	1	3921.34	3921.34	1	3921.34	3921.34	1	3921.34	3921.34	1	3921.34	3921.34	1	3921.34	3921.34	1	3921.34		
Propulsion	Feed system	341.76	1	341.76	341.76	1	341.76	209.23	1	209.23	209.23	1	209.23	209.23	1	209.23	209.23	1	209.23		
Thermal	OSR	23.02	1	23.02	23.02	1	23.02	12.82	1	12.82	12.82	1	12.82	12.82	1	12.82	12.82	1	12.82		
Thermal	Louvres	1473.28	1	1473.28	1473.28	1	1473.28	82.48	1	82.48	82.48	1	82.48	82.48	1	82.48	82.48	1	82.48		
Thermal	Black kapton	22																			



### A.3 Launch Vehicle

ARGOS Launch and Transfer Vehicle Core Criteria							
NAME	SLS Block 1 ICPS	SLS Block 1B EUS	SLS with Orion Deployment	Falcon Heavy with Gateway PPE/HALO	Starship HLS	Firefly Blue Ghost with Elytra on Falcon 9	RocketLab Electron with Blue Moon HLS on New Glenn Photon
<b>Mass</b>	12 kg (6U) 20 kg (12U)	14 kg (6U) 20.29 kg (12U)	Unknown [Use SLS Block 1 ICPS Assumption]	Unknown [Use SLS Block 1 ICPS Assumption]	Unknown [Use SLS Block 1 ICPS Assumption]	50 kg (Including Deployment Mechanism)	Unknown [Use SLS Block 1 ICPS Assumption]
<b>Volume</b>	20 cm x 30 cm x 10 cm (6U) 20 cm x 30 cm x 20 cm (12 U)	23.9 cm x 36.6 cm x 11.3 cm (6U) 23.8 cm x 36.6 cm x 22.6 cm (12 U)	Unknown [Use SLS Block 1 ICPS Assumption]	Unknown [Use SLS Block 1 ICPS Assumption]	Unknown [Use SLS Block 1 ICPS Assumption]	69 x 45 x 65 cm (Including Deployment Mechanism)	Unknown [Use SLS Block 1 ICPS Assumption]
<b>Resonant Frequency/Coupled Loads</b>	No Specific Regulation	No Specific Regulation	No Specific Regulation	Primary lateral frequency > 10 Hz Primary axial frequency > 25 Hz Secondary payloads: > 35 Hz	No Specific Regulation	Primary lateral frequency > 10 Hz Primary axial frequency > 25 Hz Secondary payloads: > 35 Hz	Primary lateral frequency > 6 Hz Primary axial frequency > 15 Hz Secondary payloads: > 35 Hz
<b>Peak g-Load</b>	Axial: -4.1 to 0.6 g Lateral: ± 3.0 g	Axial: -4.1 to 0.6 g Lateral: ± 3.0 g	Axial: -4.1 to 0.6 g Lateral: ± 3.0 g	-2, 6 g axial; -2, 2 g lateral	Axial: -2, 6 g Lateral: ± 3.5 g	Heavy payload: -2, 6 g axial; -2, 2 g lateral <4000 lb payload: -4, 8.5 g axial, +/-3.5 g lateral	Axial: -2, 6 g Lateral: ± 2.0 g
<b>Peak Shock</b>	4.000 g at 10,000 Hz	4.000 g at 10,000 Hz	4.000 g at 10,000 Hz	1000 g at 1000-10000 Hz	1000 g at 1000-10000 Hz	1000 g at 1000-10000 Hz	1000 g at 1000-10000 Hz
<b>Integration</b>	Payload charging only before vehicle stacking (<180 days before launch) for Lithium Ion 18650 batteries	Payload charging only before vehicle stacking (<180 days before launch) for Lithium Ion 18650 batteries	Payload charging only before vehicle stacking (<180 days before launch) for Lithium Ion 18650 batteries	Not designed to integrate secondary payload	Unknown [Use SLS Assumption]	Nominal power: 170 W pre-launch, 10 W launch, 270 W orbit Telecommunication: 2kbps downlink during transit	Unknown [Use SLS Assumption]
<b>Deployment Mechanism</b>	"SLS-Specified COTS Dispenser"	"SLS-Specified COTS Dispenser"	Custom Option, needs own dispenser	Custom Option, needs own dispenser	Custom Option, needs own dispenser	Able to integrate proprietary deployment mechanism and standard industry options	Custom Option, needs own dispenser
<b>Thermal</b>	Pre-Launch: -8 to 55 C Ascent: -16 to 32 C TLI to TLI + 24 hours: -74 to 100 C Separation: -69 to 32 C Orbit: -100 to 100 C USO: -77 to 30 C (Within dispenser)	Pre-Launch: -1 to 40 C Ascent to Orbit: -16 to 32 C Separation: -69 to 32 C Orbit: -100 to 100 C USO: -77 to 30 C (Within dispenser)	Assume Same Figures as SLS with Margin and Standard Cislunar Transit Temperatures	21 C pre-launch, Peak of 84 C during launch insitu fairing	No Information for Launch Standard Cislunar Transit Temperatures	7 to 29 C pre-launch 1000 W/m² free molecular heating flux from fairing	Controlled environment within fairing 115 W/m² free molecular heating at deployment
<b>Depressurization</b>	-1.034 kPa/sec avg. -3.45 kPa/sec peak	-2.07 kPa/sec peak for crew config payloads	Dependent on use of SLS Block 1 or 1B	2.8 kPa/sec, -4.5 kPa/sec for up to 5 sec periods	Unavailable Information	-2.8 kPa/sec, -4.5 kPa/sec for up to 5 sec periods	-2.4 kPa/sec, -4.1 kPa/sec at peak -2.0 kPa/sec, -3.7 kPa/sec at peak
<b>Radiation</b>	Exposure for Standard TLI	Exposure for Standard TLI	Exposure for Standard TLI	Exposure for Low-Thrust SEP Transfer (383 days, 153 days in van Allen belt)	Exposure for Standard TLI	Level expected of a standard TLI	Exposure depends on trajectory chosen
<b>Available Orbits</b>	TLI (Deployment at 4.5, 6.75, 8 hours); recommend 6.75 hours, when radiation belt cleared	TLI (Deployment at 4, 7, 25 hours); Recommend 7 hours, when radiation belt cleared	Deployment in TLI and Collision Derisked NRHO	Collision Derisked NRHO/Deployment Beforehand on Low-Thrust Trajectory	TLI Collision Derisked NRHO prior to landing	Polar LLO deployment likely Potential option for elliptical orbit	Collision Derisked NRHO/Polar LLO prior to landing
<b>Primary Launches</b>	NET 9/2025, 9/2026 (Artemis II, Artemis III)	9/2028, 9/2029 (Artemis IV, Artemis V)	9/2028, 9/2029 (Artemis VI, VII)	October 2025	9/2028, 9/2028	2026 Test in 2028	Custom Scheduling
<b>Replacement Launches</b>	None	9/2030, 9/2031 (Artemis VI, VII)	9/2030, 9/2031	None	Possible Use on Artemis VI or VII	Possible Use on Artemis VI or VII	Custom Scheduling
<b>Reliability</b>	1/1 successful flights, 6/10 deployed cubesats suffered major issues	Untested upper stage presents added potential risk	1/1 successful Orion mission, Nonevaluated deployment option	Gateway PPE/HALO are one-off payloads Falcon Heavy is regularly flown and reliable	Prototype testing of LV, lander still in development	Untested lander and transfer vehicle Falcon 9 are normally flown and reliable	1/1 success for this configuration 39/43 successes for all Electron rockets
<b>Readiness</b>	Both launches delayed 2+ years Artemis III could be delayed to early 2027	Artemis IV delayed 1 year; upper stage still under development	Nonevaluated deployment option	Nonevaluated deployment option High likelihood of delay following Artemis II/III delays	Nonevaluated deployment option	Still on track for launch 1 year after contract award	Proven vehicle, achieved first launch in 2 years after contract award -\$11.9 million inflation-adjusted (\$9.95 Million)
<b>Cost</b>	N/A	N/A	N/A	N/A	N/A	N/A	N/A
<b>Rudimentary Rating Scale</b>	Best	Good	Ok	Bad	Insufficient Data		

Figure 69: Comparison of Secondary Payload Launch Vehicle Options and RocketLab Electron

## FY 2025 President's Budget Request Moon to Mars Manifest



FY	2023	2024	2025	2026	2027	2028	2029	2030	2031	2032
Exploration Systems Development Mission Directorate			<b>Artemis II</b> (Sep. 2025) Crewed Flight SLS Block 1/ OrionML1	<b>Artemis III</b> (Sep. 2026) Crewed Flight SLS Block 1/ OrionML1	HLS Crewed Lunar Demo x EVA Surface Suits	HLS Uncrewed Lunar Demo Gateway PPEC/HALO Launch	Artemis IV (Sep. 2027) Crewed Flight SLS Block 1B/ OrionML2	I-Hab to Gateway Logistics Services Sustaining HLS Crewed Lunar Demo x EVA Surface Suits	Artemis V (May 2031) Crewed Flight SLS Block 1B/ OrionML2	ESPRIT to Gateway Logistics Services Sustaining HLS Uncrewed Lunar Demo x EVA Surface Suits
Space Operations Mission Directorate	 Completed DSS-36 (Canberra)	Completed DSS-24 (Goldstone)	DSS-34 [Canberra] DSS-56 [Madrid]		Lunar Exploration Ground Sites 1-3 DSS-54 [Madrid]		Ongoing Science, Human Research Program, and Technology Development in LEO (ISS transition to CLD)			
Science Mission Directorate	 CLPS Flights Outlined	 Attempted TO 2-AB Completed TO 190 TO 2-M	 HERMES ready for launch ESA Lunar Pathfinder delivered for launch AVATAR (Artemis II) TO PRIME-1 Lunar Traiblazer	 MMX (MEGANE/P-Sampler)	LRO continued ops TO CS-46	 TO CP-11 TO CS-344   TO CP-12 TO CP-21   TO CP-22 TO CS-6   TO CP-31	TO CP-41   TO CP-42 TO CP-51   TO CP-52	 Rosalind Franklin Mission (RFM) Launch, Landing	 Artemis LTV Science Instruments	 Fission Surface Power demo delivered for launch
Space Technology Mission Directorate	MOXIE; MEDA DSOC		Surface Robotic Scouts (CARDS) TO LIFT-1: Drill/Nokon LTE/4G Comm; IM Deployable Hopper CFM ULA TP Flight Demo CFM space enviro. complete CFM Ela Space TP Flight Demo	CFM Lockheed Martin TP Flight Demo NEP Concept Design	DRACO Demonstration		TO LIFT-1: Lunar Surface Power Demo (i.e., RFC, VSAT, Wireless Charging); Lunar Surface Scaled Construction Demo 1; ISRU Pilot Excavator; ISRU Subscale Demo	SEP qual. complete		TO LIFT-2: Lunar Surface Scaled Construction Demo 2; Artemis External Robotics Demo; Deployable Hopper 2; ISRU Subscale Demo 2

Icons are representative only, and may not reflect final configurations, not to scale | Icons represent the fiscal year in which an event occurs | Based on FY 2025 President's budget request

6

Figure 70: NASA Moon Launch Manifest



ARGOS Primary LV Technical Comparison		
NAME	PSLV	Falcon 9 Block 5 (Reusable)
Mass to TLI	1100 kg to GTO listed 593 kg estimated (208-1034 kg 95% confidence interval)	>1908 kg proven (IM-1) 2708 kg estimated (2082-3398 kg 95% confidence interval)
Volume	29.125 m^3 60 x 70 x 85 cm dimensions for auxiliary payload 1 main, 2 auxillary payloads in User's Guide, launch of more payloads demonstrated but not specified	>143.1 m^3 Volume limits for each payload specified in User's Guide Sufficient attachment points specified in User's Guide
Export Control	Export controls waivers acquired for U.S. small satellite companies	LV manufactured and operated in U.S.
Information	Detailed integration and environmental conditions in User's Guide, but for older PSLV-G variant	Detailed conditions in 2021 User's Guide for rideshare-oriented Transporter missions
Reliability	97% success rate with 60 launches	99% success rate with 317 launches
Cost	\$31 Million	\$49 million (alternative figure of \$67 million)
Deployment Mechanism	Ball lock separation mechanism specified for 50-150 kg payloads	Circular, 4-point, cubesat dispenser interfaces can be provided
Integration	Auxiliary: Trickle charging via umbilical	Rideshares: Battery charging until LV rollout, none during launch
Peak g-Load		<4000 lb main payload: -4, 8.5 g axial, ±3.5 g lateral 50 kg rideshare: Axial ± 10 g, Lateral ± 16 g
Peak Shock	1500 g at 1000-5000 Hz	1000 g at 1000-10000 Hz
Rudimentary Rating Scale	Best	
	Good	
	Ok	
	Bad	
	Insufficient Data	

Figure 71: Full PSLV-XL vs. Falcon 9 Comparison



Table 119: Comparison of Environmental Loads Across Selected LVs

LV	Falcon 9 [55]	Blue Ghost on Falcon 9 [34]	Starship HLS [39]
Acoustic Peak/Overall	132.6 dB at 125 Hz/139.3 dB overall	132.2 dB at 125 Hz/137.6 dB overall	130 dB at 100-200 Hz/137.7 dB overall
Vibrational Peak/Overall	0.03 $g^2$ /Hz at 800-925Hz/5.57 GRMS	0.034 $g^2$ /Hz at 800-925Hz/5.13 GRMS	Not Specified
Peak g-force	Axial $\pm$ 10 g, Lateral $\pm$ 16 g for 20-60 kg payloads	Axial -2, 6 g, Lateral $\pm$ 2 g	Axial -2, 6 g, Lateral $\pm$ 3.5 g
Peak Shock	1000 g at 1000-10000 Hz	1000 g at 1000-10000 Hz	1000 g at 1000-10000 Hz
Natural Frequency Limit	40 Hz	Secondary structure 35 Hz	Not Specified
Temperature	Peak of 95 C	Peak of 84 C Thermal management provided by lander	Not Specified
Radiation	Chandrayaan-1 accumulated 1.3 grays of exposure during its transfer from Earth to Moon. [216]		



## A.4 GNC

### A.4.1 Orbit Literature Review Trade Study

Type of Orbit	Location	Qualities	Pros	Cons	Past Mission Examples
Lyapunov	Lagrange	planar, relatively unstable	Stable near the Lagrange points (less station keeping)	limited coverage, will get eclipsed a lot (especially by the Moon in L2)	Theoretical studies: WIND mission
Halo	Lagrange	inclined, north or south, suited for missions that want broader communication and observation across cislunar space	good coverage of the poles, constant visibility of the earth	not as good coverage of the Moon's equator, requires very precise navigation and control, more stationkeeping	James Webb Telescope, SOHO L1, Aditya-L1
NRHO	Lagrange	nearly vertical halo orbit, closer to the moon, so suited for missions that focus on lunar exploration/support, and has easier access to lunar surface	constant visibility of the earth, LLO accessibility, stable - little stationkeeping, access to the poles	highly elliptical, apoapsis very far from the moon, may be too far for tracking sensors	L2 NRHO for Lunar Gateway
Butterfly Orbit	L2	Only exist for L2 and for this mission we wanted simplicity and symmetry			

Figure 72: Trade Study for Lagrange Point Orbits

Type of Orbit	Location	Qualities	Pros	Cons	Past Mission Examples
LLO (circular)	Moon	Circular orbits at <100-200km in altitude	Close tracking of LLO objects	gravitational instability around the moon, will require active stationkeeping	Lunar Reconnaissance Orbiter
Frozen Orbits	Moon	Circular orbits at certain inclinations that see stable properties in the Moon's uneven gravitational field	Require less propulsion for station keeping, very stable because less perturbations	Only for very specific orbital parameters (i.e. specific inclinations)	ERS-1, ERS-2, and Envisat Earth observation satellites (Frozen satellites around Earth)
Elliptical Lunar orbit	Moon	Increased access time length at locations where satellite's periapsis is	close passes to lunar surface (but not part of our objective/driver)	highly unstable, complex path, precise navigation, seems to be a transition not a mission orbit	Used in Apollo missions and Lunar Reconnaissance Orbiter
Elliptical Frozen Orbit	Moon	Elliptical orbits at certain inclinations and eccentricities that exhibit frozen orbit properties	Stable - requires little stationkeeping, elliptical to allow for longer coverage/access times	Only for very specific orbital parameters (specific inclinations and its corresponding eccentricity)	Molniya (Earth), theoretical studies on Moon
Polar Lunar Orbit	Moon	Elliptical orbits around the poles of the Moon	Full lunar surface coverage (although that is not our objective/driver)	may have longer communication blackouts	Lunar prospector

Figure 73: Trade Study for Lunar Orbits



#### A.4.2 Access Times

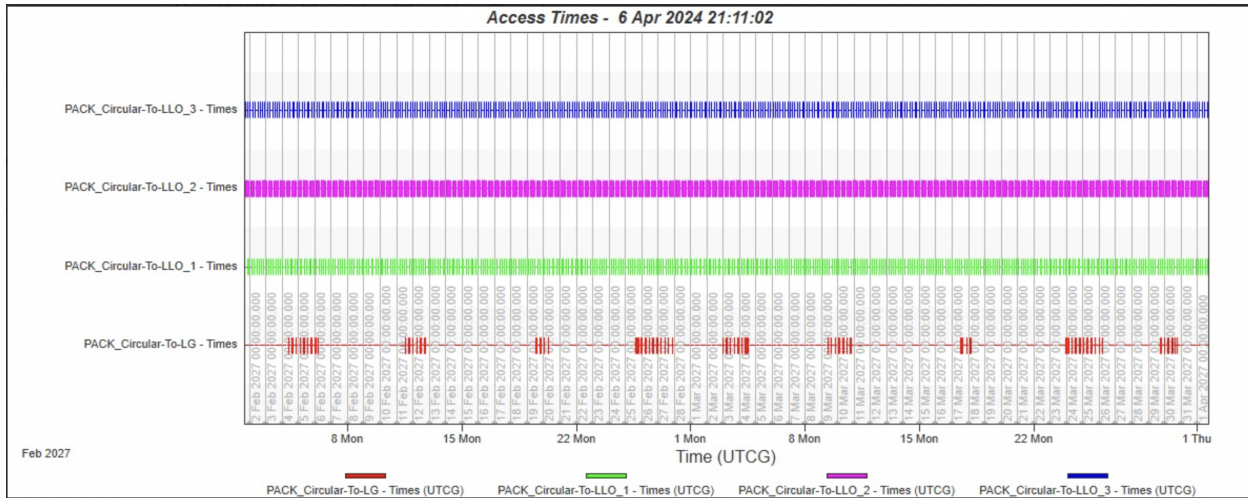


Figure 74: Access Times from PACK-C to LG and LLO Objects

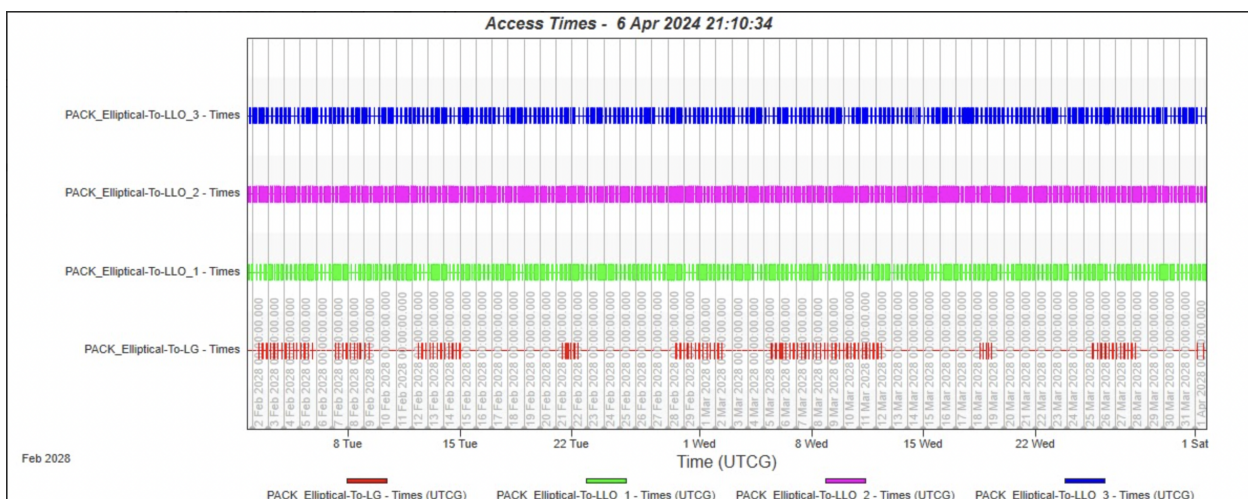


Figure 75: Access Times from PACK-E to LG and LLO Objects

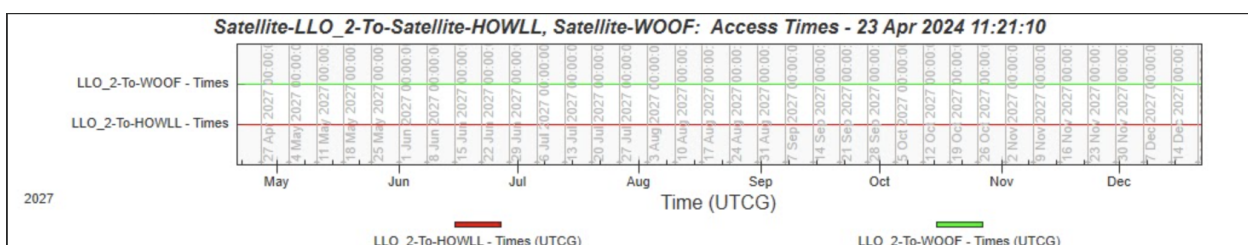


Figure 76: Access Times to LLO-2 Object from HOWLL and WOOF

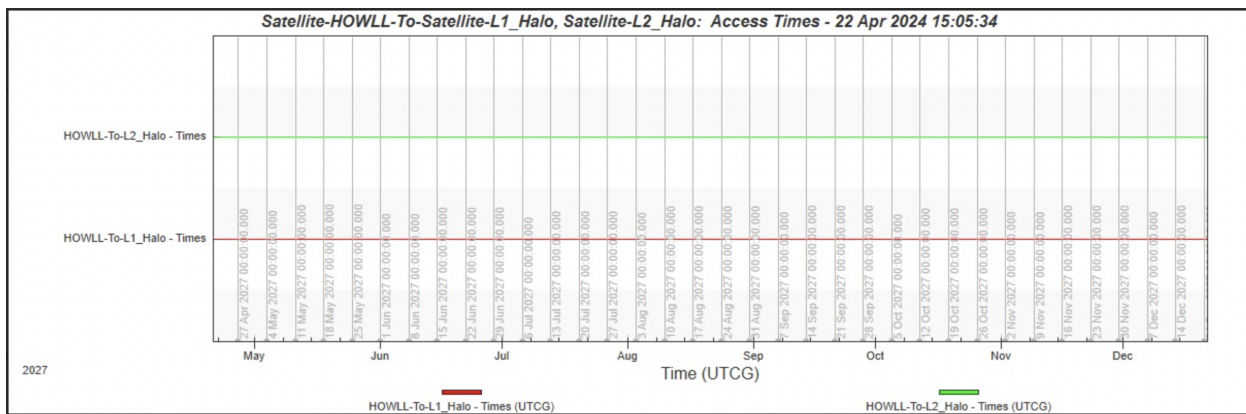


Figure 77: Access Times from HOWLL to L1 and L2 Objects

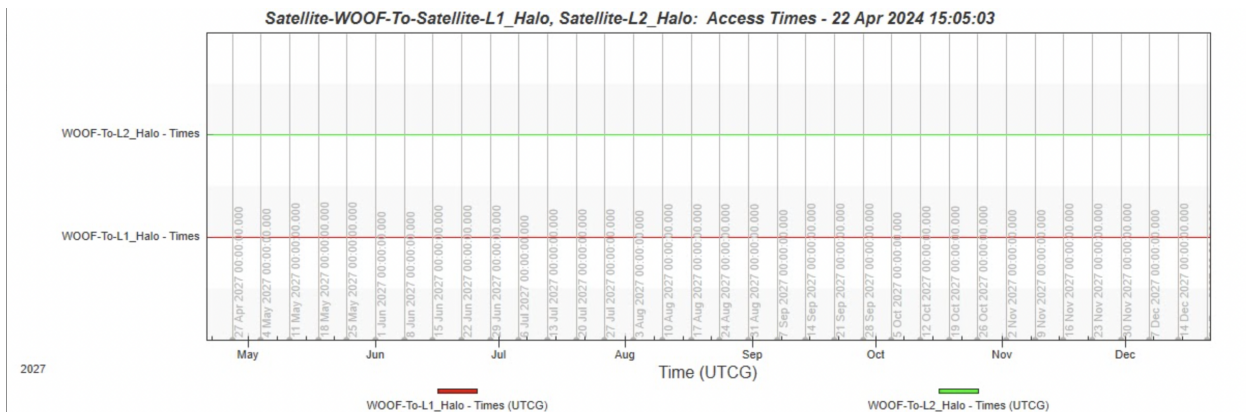


Figure 78: Access Times from WOOF to L1 and L2 Objects

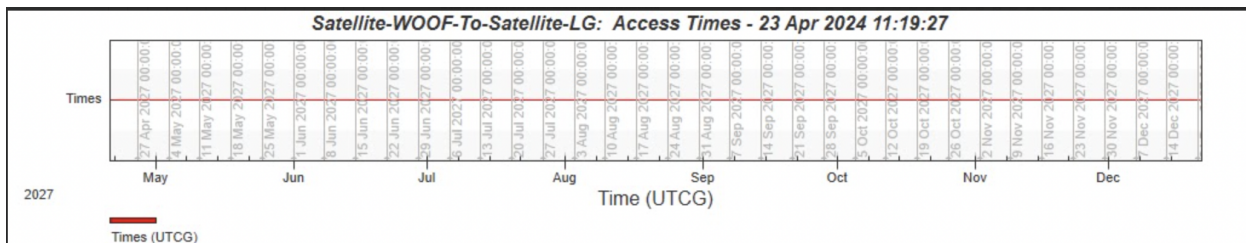


Figure 79: Access Times from WOOF to LG

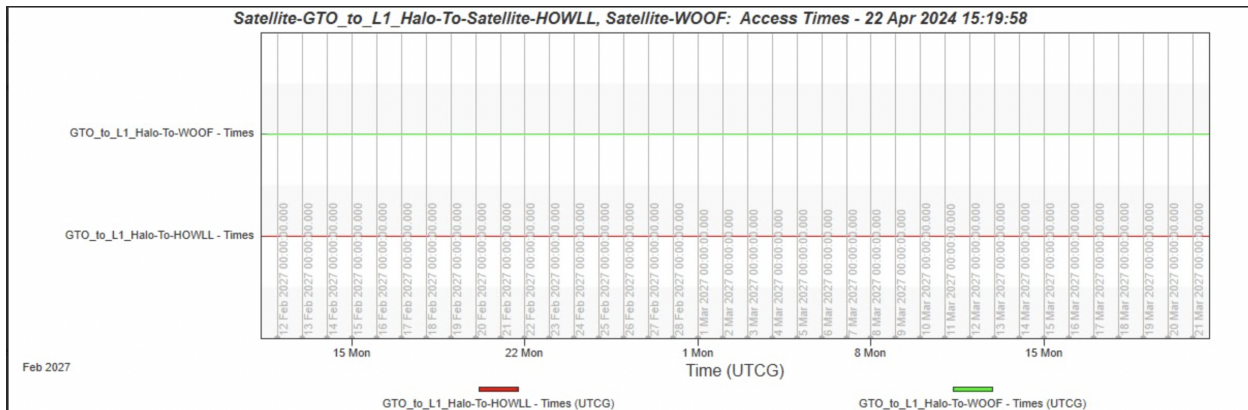


Figure 80: Access Times to GTotoL1 Object from HOWLL and WOOF

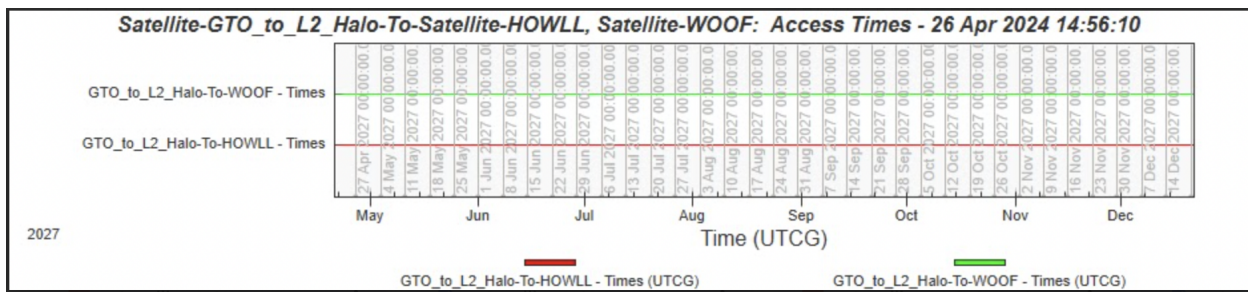


Figure 81: Access Times to GTotoL2 Object from HOWLL and WOOF

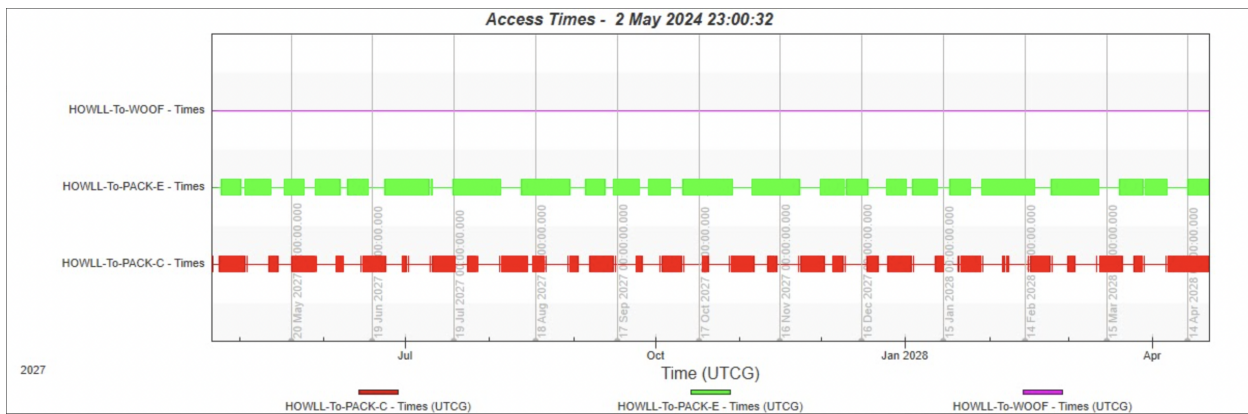


Figure 82: Access Times from HOWLL to WOOF and PACK for Communication Purposes

#### A.4.3 Station-Keeping

1. PACK-C Argument of Periapsis Correction
2. PACK-C Eccentricity Correction
3. PACk-C Inclination Correction
4. PACK-C Semi-major Axis Correction
5. PACK-E First Correction Burn
6. PACK-E Second Correction Burn

4 May 2024 12:43:39  
Satellite-Satellite2

Astrogator MCS Segment Summary Astrogator MCS Target  
Sequence Summary

---

MCS Segment Type: TargeterSequence  
Name: Target Sequence  
User Comment: Sequence that runs targeting profiles

Sequence Start: 4 Jun 2027 04:00:00.000 UTCG; 2461560.66666667 UTC  
Julian Date  
Sequence Stop: 4 Jun 2027 04:00:00.000 UTCG; 2461560.66666667 UTC  
Julian Date

\*\*\*<<< Start of Sequence: Target Sequence >>>\*\*\*

\*\*\*-----  
-----\*\*\*

MCS Segment Type: Maneuver:Impulsive  
Name: Target Sequence.Maneuver  
User Comment: Maneuvers satellite with an impulsive burn or finite  
burn

Maneuver Summary:  
Maneuver Start: 4 Jun 2027 04:00:00.000 UTCG; 2461560.66666667 UTC  
Julian Date  
Maneuver Stop: 4 Jun 2027 04:00:00.000 UTCG; 2461560.66666667 UTC  
Julian Date  
Duration: 0 sec  
Fuel Used: 0 kg  
DeltaV Magnitude: 0.05384938586088892 m/sec  
Estimated Equivalent Finite Burn Duration: 0.05632594212229387  
sec  
Estimated Fuel Used: 0.00957275 kg (Update mass OFF)  
Maneuver Direction Specification: Thrust Vector

DeltaV vector with respect to VNC(Earth) axes:

X (Velocity):	-3.469446951953614e-18	m/sec
Y (Normal):	5.204170427930421e-18	m/sec
Z (Co-Normal):	0.05384938586088892	m/sec
Azimuth:	0	deg
Elevation:	90	deg
Magnitude:	0.05384938586088892	m/sec

4 May 2024 11:51:14  
Satellite-Satellite2

Astrogator MCS Segment Summary Astrogator MCS Target  
Sequence1 Summary

---

MCS Segment Type: TargeterSequence  
Name: Target Sequence1  
User Comment: Sequence that runs targeting profiles

Sequence Start: 4 Jun 2027 16:00:00.000 UTCG; 2461561.16666667 UTC  
Julian Date  
Sequence Stop: 4 Jun 2027 16:00:00.000 UTCG; 2461561.16666667 UTC  
Julian Date

\*\*\*<<< Start of Sequence: Target Sequence1 >>>\*\*\*

\*\*\*-----  
-----\*\*\*

MCS Segment Type: Maneuver:Impulsive  
Name: Target Sequence1.Maneuver  
User Comment: Maneuvers satellite with an impulsive burn or finite  
burn

Maneuver Summary:  
Maneuver Start: 4 Jun 2027 16:00:00.000 UTCG; 2461561.16666667 UTC  
Julian Date  
Maneuver Stop: 4 Jun 2027 16:00:00.000 UTCG; 2461561.16666667 UTC  
Julian Date  
Duration: 0 sec  
Fuel Used: 0 kg  
DeltaV Magnitude: 2.255746195393009 m/sec  
Estimated Equivalent Finite Burn Duration: 2.358606185597137  
sec  
Estimated Fuel Used: 0.400851 kg (Update mass OFF)  
Maneuver Direction Specification: Thrust Vector

DeltaV vector with respect to VNC(Earth) axes:

X (Velocity):	0 m/sec
Y (Normal):	1.387778780781446e-16 m/sec
Z (Co-Normal):	-2.255746195393009 m/sec
Azimuth:	0 deg
Elevation:	-90 deg
Magnitude:	2.255746195393009 m/sec

4 May 2024 11:51:06  
Satellite-Satellite2

Astrogator MCS Segment Summary Astrogator MCS Target  
Sequence Summary

---

MCS Segment Type: TargeterSequence  
Name: Target Sequence  
User Comment: Sequence that runs targeting profiles

Sequence Start: 4 Jun 2027 04:00:00.000 UTCG; 2461560.66666667 UTC  
Julian Date  
Sequence Stop: 4 Jun 2027 04:00:00.000 UTCG; 2461560.66666667 UTC  
Julian Date

\*\*\*<<< Start of Sequence: Target Sequence >>>\*\*\*

\*\*\*-----  
-----\*\*\*

MCS Segment Type: Maneuver:Impulsive  
Name: Target Sequence.Maneuver  
User Comment: Maneuvers satellite with an impulsive burn or finite  
burn

Maneuver Summary:  
Maneuver Start: 4 Jun 2027 04:00:00.000 UTCG; 2461560.66666667 UTC  
Julian Date  
Maneuver Stop: 4 Jun 2027 04:00:00.000 UTCG; 2461560.66666667 UTC  
Julian Date  
Duration: 0 sec  
Fuel Used: 0 kg  
DeltaV Magnitude: 0.01987845389171028 m/sec  
Estimated Equivalent Finite Burn Duration: 0.02079279252419168  
sec  
Estimated Fuel Used: 0.00353379 kg (Update mass OFF)  
Maneuver Direction Specification: Thrust Vector

DeltaV vector with respect to VNC(Earth) axes:

X (Velocity):	-0.01987845389171028	m/sec
Y (Normal):	-1.734723475976807e-18	m/sec
Z (Co-Normal):	0	m/sec
Azimuth:	-180	deg
Elevation:	0	deg
Magnitude:	0.01987845389171028	m/sec

5 May 2024 22:32:48  
Satellite-PACK-C\_Traveler

Astrogator MCS Segment Summary Astrogator MCS Target  
Sequence Summary

---

MCS Segment Type: TargeterSequence  
Name: Target Sequence  
User Comment: Sequence that runs targeting profiles

Sequence Start: 4 Jun 2027 04:00:00.000 UTCG; 2461560.66666667 UTC  
Julian Date  
Sequence Stop: 6 Jun 2027 15:32:43.302 UTCG; 2461563.1477234 UTC  
Julian Date

\*\*\*<<< Start of Sequence: Target Sequence >>>\*\*\*

\*\*\*-----  
-----\*\*\*  
MCS Segment Type: Maneuver:Impulsive  
Name: Target Sequence.Maneuver  
User Comment: Maneuvers satellite with an impulsive burn or finite  
burn

Maneuver Summary:  
Maneuver Start: 4 Jun 2027 04:00:00.000 UTCG; 2461560.66666667 UTC  
Julian Date  
Maneuver Stop: 4 Jun 2027 04:00:00.000 UTCG; 2461560.66666667 UTC  
Julian Date  
Duration: 0 sec  
Fuel Used: 0 kg  
DeltaV Magnitude: 0.002018402583693107 m/sec  
Estimated Equivalent Finite Burn Duration: 0.00211248378158358  
sec  
Estimated Fuel Used: 0.000358812 kg (Update mass OFF)  
Maneuver Direction Specification: Thrust Vector

DeltaV vector with respect to VNC(Earth) axes:

X (Velocity): 0.001848883726384787 m/sec  
Y (Normal): -1.084202172485504e-19 m/sec  
Z (Co-Normal): -0.0008096776865941873 m/sec  
Azimuth: -3.359876434404072e-15 deg  
Elevation: -23.64995047861039 deg  
Magnitude: 0.002018402583693107 m/sec

4 May 2024 21:13:40  
Satellite-Satellite7

Astrogator MCS Segment Summary Astrogator MCS Target  
Sequence Summary

---

MCS Segment Type: TargeterSequence  
Name: Target Sequence  
User Comment: Sequence that runs targeting profiles

Sequence Start: 18 May 2027 04:00:00.000 UTCG; 2461543.66666667 UTC  
Julian Date  
Sequence Stop: 18 May 2027 22:49:00.563 UTCG; 2461544.45070096 UTC  
Julian Date

\*\*\*<<< Start of Sequence: Target Sequence >>>\*\*\*

\*\*\*-----  
-----\*\*\*  
MCS Segment Type: Maneuver:Impulsive  
Name: Target Sequence.Maneuver  
User Comment: Maneuvers satellite with an impulsive burn or finite  
burn

Maneuver Summary:  
Maneuver Start: 18 May 2027 04:00:00.000 UTCG; 2461543.66666667  
UTC Julian Date  
Maneuver Stop: 18 May 2027 04:00:00.000 UTCG; 2461543.66666667  
UTC Julian Date  
Duration: 0 sec  
Fuel Used: 0 kg  
DeltaV Magnitude: 17.52380085202387 m/sec  
Estimated Equivalent Finite Burn Duration: 34.94342926481712  
sec  
Estimated Fuel Used: 5.93873 kg (Update mass OFF)  
Maneuver Direction Specification: Thrust Vector

DeltaV vector with respect to VNC(Earth) axes:

X (Velocity):	2.751539184017987 m/sec
Y (Normal):	-1.77635683940025e-15 m/sec
Z (Co-Normal):	-17.30643315129395 m/sec
Azimuth:	-3.698938775722236e-14 deg
Elevation:	-80.96619052989351 deg
Magnitude:	17.52380085202388 m/sec

Name: Target Sequence.Maneuver1

User Comment: Maneuvers satellite with an impulsive burn or finite burn

Maneuver Summary:

Maneuver Start: 18 May 2027 13:24:41.190 UTCG; 2461544.05881007

UTC Julian Date

Maneuver Stop: 18 May 2027 13:24:41.190 UTCG; 2461544.05881007

UTC Julian Date

Duration: 0 sec

Fuel Used: 0 kg

DeltaV Magnitude: 15.30602462183521 m/sec

Estimated Equivalent Finite Burn Duration: 30.53255602940058 sec

Estimated Fuel Used: 5.18909 kg (Update mass OFF)

Maneuver Direction Specification: Thrust Vector

DeltaV vector with respect to VNC(Earth) axes:

X (Velocity):	1.512232747704073 m/sec
Y (Normal):	1.77635683940025e-15 m/sec
Z (Co-Normal):	-15.23113724713284 m/sec
Azimuth:	6.730296639942182e-14 deg
Elevation:	-84.32993600981402 deg
Magnitude:	15.30602462183522 m/sec

DeltaV vector with respect to Earth Inertial axes:

X:	8.32686226840748 m/sec
Y:	11.07293169358275 m/sec
Z:	6.50599248358377 m/sec
Azimuth:	53.05677584615506 deg
Elevation:	25.1545177579977 deg
Magnitude:	15.30602462183522 m/sec

DeltaV vector with respect to spacecraft body axes:

X:	15.30602462183522 m/sec
Y:	0 m/sec
Z:	0 m/sec
Azimuth:	0 deg
Elevation:	0 deg
Magnitude:	15.30602462183522 m/sec

Attitude with respect to Earth Inertial axes:

-----  
qx: 0.7625954482390803  
qy: 0.2371624964242932  
qz: 0.4144169128481077  
qs: 0.4364180965087004



#### A.4.4 Conjunction Analysis

2 May 2024 21:45:30

AdvCAT-AdvCAT1

### Close Approach Definition

---

Advanced CAT object: AdvCAT1

Close Approach Threshold: 10.000000 (km)

Close Approach Time Interval: 20 Apr 2027 16:00:00.000 to 21 Aug 2027 16:00:00.000

### Settings

---

Out of Date Filter is OFF.

Apo Peri Filter is ON. Pad is 30.000000 (km)

Path Filter is OFF.

Time Filter is ON. Pad is 30.000000 (km)

Secondaries whose SSC number match the primary SSC number have been ignored.

MaxSampleStepSize is 300.000000 secs

MinSampleStepSize is 1.000000 secs

Name Tangential (km)	Status Cross-Track (km)	Type Normal (km)
Satellite/H0WLL 10.000000	Found Scenario Object 10.000000	Scenario Object 10.000000
Satellite/W00F 10.000000	Found Scenario Object 10.000000	Scenario Object 10.000000
Satellite/PACK-C 10.000000	Found Scenario Object 10.000000	Scenario Object 10.000000
Satellite/PACK-E 10.000000	Found Scenario Object 10.000000	Scenario Object 10.000000

Name Tangential (km)	Status Cross-Track (km)	Type Normal (km)
Satellite/H0WLL 10.000000	Found Scenario Object 10.000000	Scenario Object 10.000000
Satellite/L1_Halo	Found Scenario Object	Scenario Object

10.000000	10.000000	10.000000
Satellite/L2_Halo	Found Scenario Object	Scenario Object
10.000000	10.000000	10.000000
Satellite/LG	Found Scenario Object	Scenario Object
10.000000	10.000000	10.000000
Satellite/LL0_1	Found Scenario Object	Scenario Object
10.000000	10.000000	10.000000
Satellite/LL0_2	Found Scenario Object	Scenario Object
10.000000	10.000000	10.000000
Satellite/LL0_3	Found Scenario Object	Scenario Object
10.000000	10.000000	10.000000
Satellite/PACK-C	Found Scenario Object	Scenario Object
10.000000	10.000000	10.000000
Satellite/PACK-E	Found Scenario Object	Scenario Object
10.000000	10.000000	10.000000
Satellite/W00F	Found Scenario Object	Scenario Object
10.000000	10.000000	10.000000

#### Close Approach Report by Min Range

---

Primary Vehicle Satellite/H0WLL: no hits during TimePeriod

---

Primary Vehicle Satellite/W00F: no hits during TimePeriod

---

Primary Vehicle Satellite/PACK-C: no hits during TimePeriod

---

Primary Vehicle Satellite/PACK-E: no hits during TimePeriod

---

2 May 2024 21:58:19  
AdvCAT-AdvCAT1

### Close Approach Definition

---

Advanced CAT object: AdvCAT1

Close Approach Threshold: 10.000000 (km)

Close Approach Time Interval: 20 Aug 2027 16:00:00.000 to 21 Apr 2028 16:00:00.000

### Settings

---

Out of Date Filter is OFF.

Apo Peri Filter is ON. Pad is 30.000000 (km)

Path Filter is OFF.

Time Filter is ON. Pad is 30.000000 (km)

Secondaries whose SSC number match the primary SSC number have been ignored.

MaxSampleStepSize is 300.000000 secs

MinSampleStepSize is 1.000000 secs

Name Tangential (km)	Status Cross-Track (km)	Type Normal (km)
Satellite/H0WLL 10.000000	Found Scenario Object 10.000000	Scenario Object 10.000000
Satellite/W00F 10.000000	Found Scenario Object 10.000000	Scenario Object 10.000000
Satellite/PACK-C 10.000000	Found Scenario Object 10.000000	Scenario Object 10.000000
Satellite/PACK-E 10.000000	Found Scenario Object 10.000000	Scenario Object 10.000000

Name Tangential (km)	Status Cross-Track (km)	Type Normal (km)
Satellite/H0WLL 10.000000	Found Scenario Object 10.000000	Scenario Object 10.000000
Satellite/L1_Halo	Found Scenario Object	Scenario Object

10.000000	10.000000	10.000000
Satellite/L2_Halo	Found Scenario Object	Scenario Object
10.000000	10.000000	10.000000
Satellite/LG	Found Scenario Object	Scenario Object
10.000000	10.000000	10.000000
Satellite/LL0_1	Found Scenario Object	Scenario Object
10.000000	10.000000	10.000000
Satellite/LL0_2	Found Scenario Object	Scenario Object
10.000000	10.000000	10.000000
Satellite/LL0_3	Found Scenario Object	Scenario Object
10.000000	10.000000	10.000000
Satellite/PACK-C	Found Scenario Object	Scenario Object
10.000000	10.000000	10.000000
Satellite/PACK-E	Found Scenario Object	Scenario Object
10.000000	10.000000	10.000000
Satellite/W00F	Found Scenario Object	Scenario Object
10.000000	10.000000	10.000000

#### Close Approach Report by Min Range

---

Primary Vehicle Satellite/H0WLL: no hits during TimePeriod

---

Primary Vehicle Satellite/W00F: no hits during TimePeriod

---

Primary Vehicle Satellite/PACK-C: no hits during TimePeriod

---

Primary Vehicle Satellite/PACK-E: no hits during TimePeriod

---

2 May 2024 22:02:50  
AdvCAT-AdvCAT1

### Close Approach Definition

---

Advanced CAT object: AdvCAT1  
Close Approach Threshold: 10.000000 (km)  
Close Approach Time Interval: 20 Apr 2028 16:00:00.000 to 21 Apr 2029 16:00:00.000

### Settings

---

Out of Date Filter is OFF.  
Apo Peri Filter is ON. Pad is 30.000000 (km)  
Path Filter is OFF.  
Time Filter is ON. Pad is 30.000000 (km)

Secondaries whose SSC number match the primary SSC number have been ignored.

MaxSampleStepSize is 300.000000 secs  
MinSampleStepSize is 1.000000 secs

Name Tangential (km)	Status Cross-Track (km)	Type Normal (km)
Satellite/H0WLL 10.000000	Found Scenario Object 10.000000	Scenario Object 10.000000
Satellite/W00F 10.000000	Found Scenario Object 10.000000	Scenario Object 10.000000
Satellite/PACK-C 10.000000	Found Scenario Object 10.000000	Scenario Object 10.000000
Satellite/PACK-E 10.000000	Found Scenario Object 10.000000	Scenario Object 10.000000

Name Tangential (km)	Status Cross-Track (km)	Type Normal (km)
Satellite/H0WLL 10.000000	Found Scenario Object 10.000000	Scenario Object 10.000000
Satellite/L1_Halo	Found Scenario Object	Scenario Object

10.000000	10.000000	10.000000
Satellite/L2_Halo	Found Scenario Object	Scenario Object
10.000000	10.000000	10.000000
Satellite/LG	Found Scenario Object	Scenario Object
10.000000	10.000000	10.000000
Satellite/LL0_1	Found Scenario Object	Scenario Object
10.000000	10.000000	10.000000
Satellite/LL0_2	Found Scenario Object	Scenario Object
10.000000	10.000000	10.000000
Satellite/LL0_3	Found Scenario Object	Scenario Object
10.000000	10.000000	10.000000
Satellite/PACK-C	Found Scenario Object	Scenario Object
10.000000	10.000000	10.000000
Satellite/PACK-E	Found Scenario Object	Scenario Object
10.000000	10.000000	10.000000
Satellite/W00F	Found Scenario Object	Scenario Object
10.000000	10.000000	10.000000

#### Close Approach Report by Min Range

---

Primary Vehicle Satellite/H0WLL: no hits during TimePeriod

---

Primary Vehicle Satellite/W00F: no hits during TimePeriod

---

Primary Vehicle Satellite/PACK-C: no hits during TimePeriod

---

Primary Vehicle Satellite/PACK-E: no hits during TimePeriod

---

2 May 2024 22:48:28

AdvCAT-AdvCAT1

### Close Approach Definition

---

Advanced CAT object: AdvCAT1

Close Approach Threshold: 10.000000 (km)

Close Approach Time Interval: 20 Apr 2029 16:00:00.000 to 21 Apr 2030 16:00:00.000

### Settings

---

Out of Date Filter is OFF.

Apo Peri Filter is ON. Pad is 30.000000 (km)

Path Filter is OFF.

Time Filter is ON. Pad is 30.000000 (km)

Secondaries whose SSC number match the primary SSC number have been ignored.

MaxSampleStepSize is 300.000000 secs

MinSampleStepSize is 1.000000 secs

Name Tangential (km)	Status Cross-Track (km)	Type Normal (km)
Satellite/H0WLL 10.000000	Found Scenario Object 10.000000	Scenario Object 10.000000
Satellite/W00F 10.000000	Found Scenario Object 10.000000	Scenario Object 10.000000
Satellite/PACK-C 10.000000	Found Scenario Object 10.000000	Scenario Object 10.000000
Satellite/PACK-E 10.000000	Found Scenario Object 10.000000	Scenario Object 10.000000

Name Tangential (km)	Status Cross-Track (km)	Type Normal (km)
Satellite/H0WLL 10.000000	Found Scenario Object 10.000000	Scenario Object 10.000000
Satellite/L1_Halo	Found Scenario Object	Scenario Object

10.000000	10.000000	10.000000
Satellite/L2_Halo	Found Scenario Object	Scenario Object
10.000000	10.000000	10.000000
Satellite/LG	Found Scenario Object	Scenario Object
10.000000	10.000000	10.000000
Satellite/LL0_1	Found Scenario Object	Scenario Object
10.000000	10.000000	10.000000
Satellite/LL0_2	Found Scenario Object	Scenario Object
10.000000	10.000000	10.000000
Satellite/LL0_3	Found Scenario Object	Scenario Object
10.000000	10.000000	10.000000
Satellite/PACK-C	Found Scenario Object	Scenario Object
10.000000	10.000000	10.000000
Satellite/PACK-E	Found Scenario Object	Scenario Object
10.000000	10.000000	10.000000
Satellite/W00F	Found Scenario Object	Scenario Object
10.000000	10.000000	10.000000

#### Close Approach Report by Min Range

---

Primary Vehicle Satellite/H0WLL: no hits during TimePeriod

---

Primary Vehicle Satellite/W00F: no hits during TimePeriod

---

Primary Vehicle Satellite/PACK-C: no hits during TimePeriod

---

Primary Vehicle Satellite/PACK-E: no hits during TimePeriod

---



#### A.4.5 Insertion DeltaV

6 May 2024 14:12:26  
Satellite-PACK-C

Astrogator MCS Segment Summary Astrogator MCS Target  
Sequence Summary

---

MCS Segment Type: TargeterSequence  
Name: Target Sequence  
User Comment: Sequence that runs targeting profiles

Sequence Start: 6 May 2027 18:07:24.862 UTCG; 2461532.25514887 UTC  
Julian Date  
Sequence Stop: 6 May 2027 18:07:24.862 UTCG; 2461532.25514887 UTC  
Julian Date

\*\*\*<<< Start of Sequence: Target Sequence >>>\*\*\*

\*\*\*-----  
-----\*\*\*  
MCS Segment Type: Maneuver:Impulsive  
Name: Target Sequence.Maneuver  
User Comment: Maneuvers satellite with an impulsive burn or finite  
burn

Maneuver Summary:  
Maneuver Start: 6 May 2027 18:07:24.862 UTCG; 2461532.25514887 UTC  
Julian Date  
Maneuver Stop: 6 May 2027 18:07:24.862 UTCG; 2461532.25514887 UTC  
Julian Date  
Duration: 0 sec  
Fuel Used: 0 kg  
DeltaV Magnitude: 200 m/sec  
Estimated Equivalent Finite Burn Duration: 386.7067132166734  
sec  
Estimated Fuel Used: 65.7219 kg (Update mass OFF)  
Maneuver Direction Specification: Thrust Vector

DeltaV vector with respect to VNC(Earth) axes:

X (Velocity):	200 m/sec
Y (Normal):	0 m/sec
Z (Co-Normal):	-1.06581410364015e-14 m/sec
Azimuth:	0 deg
Elevation:	0 deg
Magnitude:	200 m/sec

6 May 2024 11:42:32  
Satellite-PACK-E

Astrogator MCS Segment Summary Astrogator MCS Target  
Sequence Summary

---

MCS Segment Type: TargeterSequence  
Name: Target Sequence  
User Comment: Sequence that runs targeting profiles

Sequence Start: 6 May 2027 18:40:33.499 UTCG; 2461532.2781655 UTC  
Julian Date  
Sequence Stop: 6 May 2027 18:40:33.499 UTCG; 2461532.2781655 UTC  
Julian Date

\*\*\*<<< Start of Sequence: Target Sequence >>>\*\*\*

\*\*\*-----  
-----\*\*\*  
MCS Segment Type: Maneuver:Impulsive  
Name: Target Sequence.Maneuver  
User Comment: Maneuvers satellite with an impulsive burn or finite  
burn

Maneuver Summary:  
Maneuver Start: 6 May 2027 18:40:33.499 UTCG; 2461532.2781655 UTC  
Julian Date  
Maneuver Stop: 6 May 2027 18:40:33.499 UTCG; 2461532.2781655 UTC  
Julian Date  
Duration: 0 sec  
Fuel Used: 0 kg  
DeltaV Magnitude: 51.48529753897967 m/sec  
Estimated Equivalent Finite Burn Duration: 102.0748285878451  
sec  
Estimated Fuel Used: 17.3479 kg (Update mass OFF)  
Maneuver Direction Specification: Thrust Vector

DeltaV vector with respect to VNC(Earth) axes:

X (Velocity):	51.48529753897969 m/sec
Y (Normal):	4.538036613155327e-15 m/sec
Z (Co-Normal):	-3.658531810835086e-15 m/sec
Azimuth:	5.050186318002491e-15 deg
Elevation:	0 deg
Magnitude:	51.48529753897969 m/sec



## A.5 Propulsion

### A.5.1 Propulsion Method Trade Study

Propulsion Type	Propellant	Manufacturer	Product	Mass [kg]	Power Draw [W]	Thrust [N]	Specific Impulse [s]	Initial Mass [kg]	Delta-V [m/s]	Acceleration of Gravity [g]
<b>Chemical</b>										
Monopropellant	Hydrazine	Aerojet Rocketdyne	MR-103	0.37	16	1	202	24	100	9.81
Monopropellant	HPGP	Bradford Space	1N HPGP Thruster	0.38	10	1	235	24	100	9.81
Bipropellant	Nitrous Oxide & Propylene	Dawn Aerospace	SatDrive	—	—	16.7	280	24	100	9.81
Bipropellant	HTP & Alcohol	Benchmark Space Systems	Peregrine	—	—	22	300	24	100	9.81
Hybrid	HTPB/N2O	Parabalis Space Technologies	NanoSat Orbital Transfer System	—	—	9.4	245	24	100	9.81
Hybrid	ABSI/GOX	Utah State University	Green Hybrid Rocket	—	—	8	215	24	100	9.81
Solid Motor	TP-H-3498	Northrop Grumman	STAR 3	1.16	—	461	266	24	100	9.81
Solid Motor	TP-H-3399	Northrop Grumman	STAR 4G	1.5	—	258	269	24	100	9.81
<b>Electrical</b>										
Electrospray	EMI-Im (ionic)	Busek	CMNT (4x heads)	14.8	16.5	8.00E-02	225	24	100	9.81
Electrospray	Indium (FEEP)	Enpulsion	Nano	1.4	45	3.50E-01	2600	24	100	9.81
Electrothermal	Adamantane	AIS	AIS-SWAG1-PQ	0.224	5	1.20E-04	20	24	100	9.81
Electrothermal	Water	Aurora	ARM-A	0.28	10	5.00E-04	100	24	100	9.81
Gridded-Ion	Iodine	Busek	BIT-3	2.9	70	1.10E-03	2150	24	100	9.81
Gridded-Ion	Xenon	QinetiQ	T5	2.00E+00	600	2.00E-02	3000	24	100	9.81
Hall-Effect	Xenon	Busek	BHT-100	1.2	105	6.30E-03	1086	24	100	9.81
Hall-Effect	Krypton	ExoTerra	Halo	0.83	300	1.20E+01	900	24	100	9.81
Pulsed Plasma and Vacuum Arc	Bismuth	AIS	AIS-VAT1-PQ	0.056	5	2.60E-02	87	24	100	9.81
Pulsed Plasma and Vacuum Arc	Metal	Comat	Plasma Jet Pack	1.2	30	1.50E-01	2000	24	100	9.81
Ambipolar	Xenon	Phase Four	Maxwell(Block 1)RF	5.9	450	7.00E-03	400	24	100	9.81
Ambipolar	Iodine	T4i	Refulus-50-12	2.5	50	5.50E-04	550	24	100	9.81
<b>Propellant-less</b>										
Cold Gas	Nitrogen	Benchmark Space Systems	Starling	0.75	4	1	70	24	100	9.81
Cold Gas	Butane	GomSpace	NanoProp CGP3	0.35	2	1	110	24	100	9.81

Figure 83: Propulsion Method Trade Study (1 of 2)

Propulsion Type	Propellant	Manufacturer	Product	Mass Flow Rate [kg/s]	Propellant Escape Velocity [m/s]	Time Required [hr]	Time Required [min]	Time Required [sec]	TOTAL Time Required [s]
<b>Chemical</b>									
Monopropellant	Hydrazine	Aerojet Rocketdyne	MR-103	0.0005046378197	1981.62	0	39	0.4493997038	2340.4494
Monopropellant	HPGP	Bradford Space	1N HPGP Thruster	0.0004337736136	2305.35	0	39	8.691713	2348.691713
Bipropellant	Nitrous Oxide & Propylene	Dawn Aerospace	SatDrive	0.006079891951	2748.8	0	2	21.12883406	141.1288341
Bipropellant	HTP & Alcohol	Benchmark Space Systems	Peregrine	0.007475365274	2943	0	1	47.25832777	187.2583278
Hybrid	HTPB/N2O	Parabalis Space Technologies	NanoSat Orbital Transfer System	0.00391104454	2403.45	0	4	10.08054052	250.0805405
Hybrid	ABSI/GOX	Utah State University	Green Hybrid Rocket	0.003792997179	2109.15	0	4	52.9920766	292.9992077
Solid Motor	TP-H-3498	Northrop Grumman	STAR 3	0.17666494938	2609.46	0	0	5.107582044	5.107582044
Solid Motor	TP-H-3399	Northrop Grumman	STAR 4G	0.09776837989	2638.89	0	0	9.128276504	9.128276504
<b>Electrical</b>									
Electrospray	EMI-Im (ionic)	Busek	CMNT (4x heads)	3.62E-05	2207.25	8	8	5.06E+01	2.93E+04
Electrospray	Indium (FEEP)	Enpulsion	Nano	1.37E-05	25506	1	54	3.72E+00	6.84E+03
Electrothermal	Adamantane	AIS	AIS-SWAG1-PQ	6.12E-07	196.2	4352	31	4.62E+01	1.57E+07
Electrothermal	Water	Aurora	ARM-A	5.10E-07	981	1267	37	3.78E+01	4.56E+06
Gridded-Ion	Iodine	Busek	BIT-3	5.22E-08	21091.5	604	37	3.41E+01	2.18E+06
Gridded-Ion	Xenon	QinetiQ	T5	6.80E-07	29430	33	16	3.64E+01	1.20E+05
Hall-Effect	Xenon	Busek	BHT-100	5.91E-07	10653.66	105	19	3.01E+01	3.79E+05
Hall-Effect	Krypton	ExoTerra	Halo	1.36E-03	8829	0	3	1.89E+01	1.99E+02
Pulsed Plasma and Vacuum Arc	Bismuth	AIS	AIS-VAT1-PQ	3.05E-05	853.47	24	11	4.51E+01	8.71E+04
Pulsed Plasma and Vacuum Arc	Metal	Comat	Plasma Jet Pack	7.85E-06	19620	4	25	5.93E+01	1.60E+04
Ambipolar	Xenon	Phase Four	Maxwell(Block 1)RF	1.78E-06	3924	94	2	5.30E+00	3.39E+05
Ambipolar	Iodine	T4i	Refulus-50-12	1.02E-07	5395.5	1200	57	2.73E+01	4.32E+06
<b>Propellant-less</b>									
Cold Gas	Nitrogen	Benchmark Space Systems	Starling	0.001456239988	686.7	0	37	13.43370603	2233.433706
Cold Gas	Butane	GomSpace	NanoProp CGP3	0.0009266981744	1079.1	0	38	12.15316757	2292.15316757

Figure 84: Propulsion Method Trade Study (2 of 2)



### A.5.2 Monopropellant Thruster Trade Study

Performance Rank	Mass Rank	Power Rank	Merit Index	Propulsion Type	Propellant	Manufacturer	Product
			Sum of Performance, Mass and Power Rankings)	Chemical			
1 22	5	6	33	Monopropellant	HPPG	Bradford Space	1N HPGP Thruster
2 7	—	2	—	Monopropellant	HTP	Benchmark Space Systems	Halcyon
3 5	—	11	—	Monopropellant	HTP + Fuel	Benchmark Space Systems	Halcyon Avant
4 3	—	—	—	Monopropellant	HTP & Alcohol	Benchmark Space Systems	Peregrine
5 17	19	6	42	Monopropellant	LMP-103S	ECAPS	SkySat 1N HPGP Propulsion System
6 26	9	16	51	Monopropellant	ASCENT	Busek	BGT-X5 System
7 28	14	1	43	Monopropellant	(CMP-X) Peroxide/Ethanol blend	CU Aerospace USA	MPUC
8 6	—	—	—	Monopropellant	Nitrous Oxide & Propylene	Dawn Aerospace New Zealand	SatDrive
9 25	6	24	55	Monopropellant	Green or 'Traditional'	Moog USA	Monopropellant Propulsion Module
10 29	10	14	53	Monopropellant	ASCENT	Rubicon Space Systems USA	Sprite
11 32	16	25	73	Monopropellant	ASCENT	NASA MSFC USA	LFPS
12 19	8	5	32	Monopropellant	IADN-blend	NanoAvionics Lithuania	EPSS C1K
13 20	12	—	—	Monopropellant	IADN-blend	NanoAvionics Lithuania	EPSS C2
14 14	13	18	45	Monopropellant	Water (Electrolysis)	Tethers Unlimited USA (Subsidiary of ARKA Group LP)	HYDROS-C
15 14	17	23	54	Monopropellant	Water (Electrolysis)	Tethers Unlimited USA (Subsidiary of ARKA Group LP)	HYDROS-M
16 30	11	16	57	Monopropellant	LMP-103S/R134a	VACCO USA	ArgoMoon Hybrid MIPS
17 30	15	11	56	Monopropellant	LMP-103S	VACCO USA	Green Propulsion System (MIPS)
18 17	18	26	61	Monopropellant	LMP-103S	VACCO USA	Integrated Propulsion System
19 24	—	10	—	Monopropellant	ASCENT	Aerojet Rocketdyne USA	GR-M1
20 12	—	15	—	Monopropellant	ASCENT	Aerojet Rocketdyne USA	GR-1
21 1	—	22	—	Monopropellant	ASCENT	Aerojet Rocketdyne USA	GR-22
22 13	—	—	—	Monopropellant	HTP	Benchmark Space Systems USA	Felicette
23 11	—	—	—	Monopropellant	HTP	Benchmark Space Systems USA	Lynx
24 4	—	—	—	Monopropellant	HTP	Benchmark Space Systems USA	Ocelet
25 33	6	3	42	Monopropellant	LMP-103S	ECAPS Sweden	0.1 N HPGP
26 22	20	6	48	Monopropellant	LMP-103S	ECAPS Sweden	1 N HPGP
27 21	22	6	49	Monopropellant	LMP-103S/LT	ECAPS Sweden	1 N GP
28 10	—	18	—	Monopropellant	LMP-103S	ECAPS Sweden	5 N HPGP
29 2	21	26	49	Monopropellant	LMP-103S	ECAPS Sweden	22 N HPGP
30 27	1	4	32	Monopropellant	ASCENT	Rubicon Space Systems USA	0.1N
31 16	2	11	29	Monopropellant	ASCENT	Rubicon Space Systems USA	1N
32 8	3	18	29	Monopropellant	ASCENT	Rubicon Space Systems USA	5N LT
33 8	4	18	30	Monopropellant	ASCENT	Rubicon Space Systems USA	5N HT

Figure 85: Monopropellant Thruster Trade Study (1 of 4)

Product	Mass [kg]	Volume [Units Variable]	Power Draw [W]	Thrust [N]	Specific Impulse [s]	Initial Mass [kg]	Delta-V [m/s]	Propellant Density [kg/m^3]	Acceleration of Gravity [m/s^2]
1N HPGP Thruster	0.38	—	10	1	235	24	100	1250	9.81
Halcyon	—	—	4	10	170	24	100	1250	9.81
Halcyon Avant	—	—	15	22	310	24	100	1250	9.81
Peregrine	—	—	—	22	300	24	100	1250	9.81
SkySat 1N HPGP Propulsion System	22	55 x 55 x 15 cm	10	1	200	24	100	1250	9.81
BGT-X5 System	1.5	1U	20	0.5	225	24	100	1250	9.81
MPUC	3.3	2U	3	0.23	178	24	100	1250	9.81
SatDrive	—	—	—	16.7	280	24	100	1250	9.81
Monopropellant Propulsion Module	1	1U	45	0.5	224	24	100	1250	9.81
Sprite	2	1.5U	16	0.15	215	24	100	1250	9.81
LFPS	5.5	2.4U	47	0.1	200	24	100	1250	9.81
EPSS C1K	1.2	1.3U	9.6	1	213	24	100	1250	9.81
EPSS C2	2.6	2U	—	1	220	24	100	1250	9.81
HYDROS-C	2.7	19 x 13 x 9.2 cm	25	1.2	310	24	100	1250	9.81
HYDROS-M	13.7	38.1 dia. x 19.1 cm	40	1.2	310	24	100	1250	9.81
ArgoMoon Hybrid MIPS	2.07	1.3U	20	0.1	190	24	100	1250	9.81
Green Propulsion System (MIPS)	5	3U	15	0.1	190	24	100	1250	9.81
Integrated Propulsion System	14.7	11U	50	1	200	24	100	1250	9.81
GR-M1	—	—	14	0.5	206	24	100	1250	9.81
GR-1	—	—	18	1.4	231	24	100	1250	9.81
GR-22	—	—	28	25	250	24	100	1250	9.81
Felicette	—	—	—	1.2	161	24	100	1250	9.81
Lynx	—	—	—	2.5	295	24	100	1250	9.81
Ocelet	—	—	—	22	302	24	100	1250	9.81
0.1 N HPGP	1	0.04	8	0.1	209	24	100	1250	9.81
1 N HPGP	24	0.38	10	1	235	24	100	1250	9.81
1 N GP	2-8	0.38	10	1	227	24	100	1250	9.81
5 N HPGP	—	0.48	25	5.5	253	24	100	1250	9.81
22 N HPGP	150	1.1	50	22	255	24	100	1250	9.81
0.1N	0.06	—	9	0.28	235	24	100	1250	9.81
1N	0.18	—	15	1.1	250	24	100	1250	9.81
5N LT	0.25	—	25	6	261	24	100	1250	9.81
5N HT	0.3	—	25	6	261	24	100	1250	9.81

Figure 86: Monopropellant Thruster Trade Study (2 of 4)

**Final Design Review Report**  
**Advanced Relay for Geolunar Operational Support (ARGOS)**



**PRINCETON**  
**UNIVERSITY**

Product	Mass Flow Rate [kg/s]	Propellant Escape Velocity [m/s]	Time Required [hr]	Time Required [min]	Time Required [sec]	TOTAL Time Required [s]	Total Impulse [Ns]	Propellant Mass [kg]	Propellant Volume [l/cm³]
1N HPGP Thruster	0.0004337736136	2305.35	0	39	8.691713	2348.691713	2348.691713	1.018800491	815.0403932
Halcyon	0.005996282305	1667.7	0	3	52.94615245	232.9461525	2329.461525	1.396810892	1117.448714
Halcyon Avant	0.007234224458	3041.1	0	1	47.31679882	107.3167988	2360.969574	0.7763538108	621.0830486
Peregrine	0.007475365274	2943	0	1	47.25832777	107.2583278	2359.683211	0.8817951787	641.436143
SkySat 1N HPGP Propulsion System	0.0005096839959	1962	0	38	59.86392497	2339.863925	2339.863925	1.192591195	954.0729562
BGT-X5 System	0.002265262204	2287.25	1	18	12.89183518	4692.891035	2346.445518	1.063062869	850.4502952
MPUC	0.0001317160888	1746.18	2	49	1.616683228	10141.61668	2332.571837	1.335814084	1068.451267
SatDrive	0.006979801951	2746.8	0	2	21.12803406	141.1280341	2356.838169	0.8580304969	686.4243975
Monopropellant Propulsion Module	0.0002275374982	2197.44	1	18	12.42068856	4692.420869	2346.210034	1.067701523	854.1612182
Sprite	0.00007111869711	2109.15	4	20	26.62440844	15626.62441	2343.993661	1.111345168	889.0761345
LFPS	0.00005096839959	1962	6	29	58.63924965	23398.63925	2339.863925	1.192591195	954.0729562
EPSS C1K	0.000478576522	2089.53	0	39	3.476182293	2343.476182	2343.476182	1.212532642	897.2261139
EPSS C2	0.0004633490872	2158.2	0	39	5.247022769	2345.247023	2345.247023	1.086668067	869.3344538
HYDROS-C	0.0003945940614	3041.1	0	32	47.47464499	1967.474645	2360.969574	0.7763538108	621.0830486
HYDROS-M	0.0003945940614	3041.1	0	32	47.47464499	1967.474645	2360.969574	0.7763538108	621.0830486
ArgoMoon Hybrid MIPS	0.00005365094694	1863.9	6	29	27.54954534	23367.54955	2336.754955	1.253691161	1002.952929
Green Propulsion System (MIPS)	0.00005365094694	1863.9	6	29	27.54954534	23367.54955	2336.754955	1.253691161	1002.952929
Integrated Propulsion System	0.0005096839959	1962	0	38	59.86392497	2339.863925	2339.863925	1.192591195	954.0729562
GR-M1	0.0002474194155	2028.86	1	18	3.17368395	4683.17368	2341.568604	1.158708077	926.9664615
GR-1	0.0006177987829	2266.11	0	27	57.01159279	1677.011593	2347.81623	1.036055721	828.8445768
GR-22	0.01019367991	2452.5	0	1	34.06914573	94.06914573	2351.728643	0.9589107618	767.1286694
Felicette	0.0007597773852	1579.41	0	32	18.00085865	1938.0008586	2325.600703	1.472449018	1177.959214
Lynx	0.0008638711795	2893.95	0	15	43.60308003	943.60308003	2359.007701	0.815151506	652.1212048
Osclet	0.007425859543	2962.62	0	1	47.27032828	107.2703283	2359.947222	0.796574391	637.2959128
0.1 N HPGP	0.00004877358813	2050.29	6	30	24.11749106	23424.11749	2342.411749	1.142478259	913.982607
1 N HPGP	0.0004337736136	2305.35	0	39	8.691713	2348.691713	2348.691713	0.018800491	815.0403932
1 N GP	0.0004490607894	2226.87	0	39	6.91035281	2346.910353	2346.910353	0.1053905416	843.143325
5 N HPGP	0.002216017374	2481.93	0	7	7.689708128	427.6897081	2352.293935	0.9477678237	758.214259
22 N HPGP	0.008794547381	2581.55	0	1	46.93920961	106.9392096	2352.662611	0.9404819457	752.385556
0.1N	0.0001214566118	2305.35	2	19	48.18468928	8388.184689	2348.691713	1.018800491	815.0403932
1N	0.0004485219164	2452.5	0	35	37.93513027	2137.93513	2351.728643	0.9589107618	767.1286694
SN LT	0.002343374694	2560.41	0	6	32.28945848	392.28945848	2353.736751	0.9192811897	755.4249517
SN HT	0.002343374694	2560.41	0	6	32.28945848	392.28945848	2353.736751	0.9192811897	755.4249517

Figure 87: Monopropellant Thruster Trade Study (3 of 4)

Merit Index Rank	Merit Index	Manufacturer	Product	ACS Capabilities	Selection
1	29	Rubicon Space Systems USA	1N	<input type="checkbox"/>	
2	29	Rubicon Space Systems USA	5N LT	<input type="checkbox"/>	
3	30	Rubicon Space Systems USA	5N HT	<input type="checkbox"/>	
4	32	Rubicon Space Systems USA	0.1N	<input type="checkbox"/>	
5	32	NanoAvionics Lithuania	EPSS C1K	<input type="checkbox"/>	
6	33	Bradford Space	<b>1N HPGP Thruster</b>	<input checked="" type="checkbox"/>	<b>SELECTED SYSTEM</b>
7	42	ECAPS	SkySat 1N HPGP Propulsion System	<input checked="" type="checkbox"/>	
8	42	ECAPS Sweden	0.1 N HPGP	<input type="checkbox"/>	
9	43	CU Aerospace USA	MPUC	<input type="checkbox"/>	
10	45	Tethers Unlimited USA (Subsidiary of ARKA Group LP)	HYDROS-C	<input type="checkbox"/>	
11	48	ECAPS Sweden	1 N HPGP	<input type="checkbox"/>	
12	49	ECAPS Sweden	1 N GP	<input type="checkbox"/>	
13	49	ECAPS Sweden	22 N HPGP	<input type="checkbox"/>	
14	51	Busek	BGT-X5 System	<input type="checkbox"/>	
15	53	Rubicon Space Systems USA	Sprite	<input type="checkbox"/>	
16	54	Tethers Unlimited USA (Subsidiary of ARKA Group LP)	HYDROS-M	<input type="checkbox"/>	
17	55	Moog USA	Monopropellant Propulsion Module	<input type="checkbox"/>	
18	56	VACCO USA	Green Propulsion System (MIPS)	<input checked="" type="checkbox"/>	
19	57	VACCO USA	ArgoMoon Hybrid MIPS	<input checked="" type="checkbox"/>	
20	61	VACCO USA	Integrated Propulsion System	<input checked="" type="checkbox"/>	
21	73	NASA MSFC USA	LFPS	<input checked="" type="checkbox"/>	

Figure 88: Monopropellant Thruster Trade Study (4 of 4)



### A.5.3 Propellant Tank Sizing

Spacecraft	Initial Mass [kg]	Delta-V [m/s]	Thrust [N]	Specific Impulse [s]	Acceleration of Gravity [m/s^2]	Mass Flow Rate [kg/s]	Propellant Escape Velocity [m/s]
Propellant Tanks							
HOWLL	54.0000000000	190.0000000000	1.0000000000	235.0000000000	9.8100000000	0.0004337736	2,305.3500000000
WOOF	54.0000000000	190.0000000000	1.0000000000	235.0000000000	9.8100000000	0.0004337736	2,305.3500000000
PACK (Prograde Circular)	24.0000000000	266.0000000000	1.0000000000	235.0000000000	9.8100000000	0.0004337736	2,305.3500000000
PACK (Elliptical)	24.0000000000	101.8500000000	1.0000000000	235.0000000000	9.8100000000	0.0004337736	2,305.3500000000

Figure 89: Propellant Tank Calculations (1 of 5)

Spacecraft	Time Required [hr]	Time Required [min]	Time Required [sec]	TOTAL Time Required [s]	Total Impulse [Ns]	Propellant Pressure [Pa]	Propellant Temperature [K]	Propellant Density [kg/m^3]
Propellant Tanks								
HOWLL	2.0000000000	44.0000000000	8.5807032019	9,848.5807032019	9,848.5807032019	1,850.000.0000000000	294.1500000000	1,250.0000000000
WOOF	2.0000000000	44.0000000000	8.5807032019	9,848.5807032019	9,848.5807032019	1,850.000.0000000000	294.1500000000	1,250.0000000000
PACK (Prograde Circular)	1.0000000000	49.0000000000	29.4610806646	6,029.4610806646	6,029.4610806646	1,850.000.0000000000	294.1500000000	1,250.0000000000
PACK (Elliptical)	0.0000000000	39.0000000000	51.1898778210	2,391.1898778210	2,391.1898778210	1,850.000.0000000000	294.1500000000	1,250.0000000000

Figure 90: Propellant Tank Calculations (2 of 5)

Spacecraft	Propellant Mass [kg]	Propellant Volume [m^3]	Propellant Volume [cm^3]	Propellant Tank Radius [cm]	Propellant Tank Length [cm]	Propellant Tank Volume [cm^3]	Number of Required Propellant Tanks
Propellant Tanks							
HOWLL	4.2720544400	0.0034176436	3,417.6435519819	4.5550000000	29.3000000000	1,711.8924677969	1.9964125179
WOOF	4.2720544400	0.0034176436	3,417.6435519819	4.5550000000	29.3000000000	1,711.8924677969	1.9964125179
PACK (Prograde Circular)	2.6154211207	0.0020923369	2,092.3368965804	5.0700000000	29.3000000000	2,093.1521040327	0.9996105360
PACK (Elliptical)	1.0372350740	0.0008297881	829.7880591914	4.5600000000	15.7500000000	830.2810169314	0.9994062760

Figure 91: Propellant Tank Calculations (3 of 5)

Spacecraft	Allowable Tank Stress [Pa]	Cylindrical Wall Thickness [cm]	Spherical Endcap Thickness [cm]
Propellant Tanks			
HOWLL	420,000,000.0000000000	0.0200636905	0.0100318452
WOOF	420,000,000.0000000000	0.0200636905	0.0100318452
PACK (Prograde Circular)	420,000,000.0000000000	0.0223321429	0.0111660714
PACK (Elliptical)	420,000,000.0000000000	0.0200857143	0.0100428571

Figure 92: Propellant Tank Calculations (4 of 5)

Spacecraft	Wall Volume Per Tank [cm^3]	Total Tank Wall Volume [cm^3]	Tank Material Density [kg/cm^3]	Total Tank Mass [kg]
Propellant Tanks				
HOWLL	41.9281667937	83.7059170389	0.0027149700	0.2272590536
WOOF	41.9281667937	83.7059170389	0.0027149700	0.2272590536
PACK (Prograde Circular)	46.6686730283	46.6504972589	0.0027149700	0.1266547005
PACK (Elliptical)	22.5629184381	22.5495222926	0.0027149700	0.0612212765

Figure 93: Propellant Tank Calculations (5 of 5)

### A.5.4 Pressurant Tank Sizing

Spacecraft	Pressurant Pressure (g, instantaneous)[Pa]	Pressurant Pressure (i, initial) [Pa]	Pressurant Temperature [K]	Pressurant Molar Mass [kg/mol]	Universal Gas Constant R [J/mol K]
Pressurant Tanks					
HOWLL	3,103,000.0000000000	31,026,000.0000000000	287.5000000000	0.0040030000	8.3144626180
WOOF	3,103,000.0000000000	31,026,000.0000000000	287.5000000000	0.0040030000	8.3144626180
PACK (Prograde Circular)	3,103,000.0000000000	31,026,000.0000000000	287.5000000000	0.0040030000	8.3144626180
PACK (Elliptical)	3,103,000.0000000000	31,026,000.0000000000	287.5000000000	0.0040030000	8.3144626180

Figure 94: Pressurant Tank Calculations (1 of 2)



Spacecraft	Pressurant Tank Radius [cm]	Pressurant Tank Volume [cm^3]	Number of Required Pressurant T	Pressurant Tank Wall Thickness [cm]	Total Tank Wall Volume [cm^3]	Total Tank Mass [kg]
Pressurant Tanks						
HOWLL	4.4857900000	378.0989093707	0.9999927188	0.1656858578	41.8960598648	0.1137465457
WOOF	4.4857900000	378.0989093707	0.9999927188	0.1656858578	41.8960598648	0.1137465457
PACK (Prograde Circular)	3.8089800000	231.4806462647	0.9999825567	0.1406873970	25.6497090393	0.0696381906
PACK (Elliptical)	2.8000000000	91.9523225755	0.9983434541	0.1034200000	10.1889741437	0.0276627591

Figure 95: Pressurant Tank Calculations (2 of 2)

### A.5.5 System Sizing

Total Propellant Tank Mass [kg]	Total Propellant Tank Volume [cm^3]
4.5189580219	3,501.3494690208
4.5189580219	3,501.3494690208
2.7541025206	2,138.9873938393
1.1032259512	852.3375814840
Total Pressurant Tank Mass [kg]	Total Pressurant Tank Volume [cm^3]
0.1333910740	419.9949692355
0.1333910740	419.9949692355
0.0816648899	257.1303553041
0.0324323598	102.1412967191
Feed System Mass [kg]	Feed System Volume [cm^3]
0.4272054440	341.7643551982
0.4272054440	341.7643551982
0.2615421121	209.2336896580
0.1037235074	82.9788059191
Thruster Mass [kg]	Thruster Volume [cm^3]
1.5200000000	221.3172000000
1.5200000000	221.3172000000
1.5200000000	221.3172000000
1.5200000000	221.3172000000
Total Mass [kg]	Total Volume [cm^3]
6.5995545399	4,484.4259934545
6.5995545399	4,484.4259934545
4.6173095226	2,826.6686388014
2.7593818185	1,258.7748841223

Figure 96: Propulsion Subsystem Total Mass and Volume



## A.6 Payload

This section briefly describes the trade study we conducted to select the 90mm and i-SIM 90 cameras as our payload sensors on board PACK, HOWLL, and WOOF. The following tables are referenced to Payload's Subsystem 1 Report [217].

### High Resolution Camera

Instrument	Manufacturer	Mass (g)	Vol (cm3)	Resolution	Swath	Power Usage (W)
Caiman Imager[218]	Dragonfly Aerospace	1800	2450	3m at 500km	13km at 500km	5-10
90mm Camera[110]	KairoSpace	1400	7783	3m at 400km	9.95km at 400km	4.2
JP-P1430G[219]	Panchromatic	4500	N/A	1.9m at 500km	N/A	N/A

Table 120: Design Specifications for High-Resolution Camera

Instrument	CubeSat Compatibility	Mass	Volume	Resolution	Power Usage	Composite Score
Caiman Imager	Yes	2	1	2	2	1.75
90mm Camera	Yes	1	2	3	1	1.75
JP-P1430G	Yes	3	3	1	3	2.5

Table 121: System Comparison and Evaluations for High-Resolution Camera

### Infrared Sensor

Instrument	Mass (g)	Vol (cm3)	Resolution	Swath	Power Usage (W)
iSIM-90[111]	4000	3511	1.65m at 50km	13km at 500km	25.3
HyperScape100[220]	1100	1690	4.75km at 500km	19.4km at 500km	7

Table 122: Design Specifications for Infrared Sensor



Instrument	CubeSat Compatibility	Mass	Resolution	Power Usage	Volume	Composite Score
iSIM-90	Yes	2	1	2	2	1.75
HyperScape100	Yes	1	2	1	1	1.25

Table 123: System Comparison and Evaluations for Infrared Sensor

## A.7 Communications

### A.7.1 Link Margin: Calculated Variables

The first variable to be calculated is the transmitter power in decibel Watts, which is equivalent to  $P_t = 10 \log(T)$ , where T is the transmitter power in Watts.

Assuming an antenna efficiency of 0.55, which was recommended by both SMAD and the course instructional staff, the next variable to be calculated is the peak transmit antenna gain, represented by  $G_t$ . Here,  $\theta$  represents the half-power antenna beamwidth.

$$G_t = \frac{27000}{\theta^2}$$

Then, the loss resulting from the antenna pointing error must be calculated, represented by  $L_t$ . Here,  $\theta$  represents the half-power antenna beamwidth and  $e$  represents the antenna pointing error.

$$L_t = -12\left(\frac{e}{\theta}\right)^2$$

Once these three values are known, the Equivalent Isotropic Radiated Power (*EIRP*) of the transmitter can be calculated:

$$EIRP = G_t + L_t + P_t$$

This is the effective power of the signal being transmitted in a communication link. As the signal travels to its destination, it loses intensity. The loss, calculated by the following equation, is represented by  $L_s$ , where  $S$  represents the path length in kilometers and  $f$  represents the frequency of the signal in GHz.

$$L_s = 147.55 - 20 \log S - 20 \log f$$

An additional loss in signal strength can occur when there is a mismatch between the polarization of the transmitter and receiver. This loss, recommended by SMAD to be around -0.3 dB, is represented by  $L_p$ .

Once the signal reaches its destination, the receiving antenna can strengthen the signal to aid in coherence. This gain is given by the following equation and is represented by  $G_r$ .

$$G_r = -159.59 + 20 \log D + 20 \log f + 10 \log \eta$$



Here, D is the diameter of the receiving antenna in meters, f is the frequency of the signal being received, and  $\eta$  is the antenna efficiency, once again assumed to be 0.55.

The loss of the signal due to the receiving antenna's pointing error can be calculated the same way as it was for the transmitting antenna. This is represented by  $L_r$ . The total gain of the receiving antenna, therefore, is obtained by the following equation and is represented by  $G_{rt}$ .

$$G_{rt} = G_r + L_r$$

Another source of signal loss is the system noise temperature, a theoretical value that communicates the level of noise present in a system by representing it as a temperature that would produce an equivalent level of noise in a system. This value is more opaque to calculate, but suggested values to use are listed in SMAD. The system noise temperature is represented by  $T_s$ .

With all sources of signal gain and loss now accounted for, it is now possible to calculate the signal-to-noise ratio of a communications link by representing it as a normalized quantity,  $\frac{E_b}{N_0}$ .

$$\frac{E_b}{N_0} = EIRP + L_r + L_s + L_p + G_{rt} + 228.6 - 10 \log T_s - 10 \log R$$

Here, R represents the data rate desired by the communications link.

To fully determine the link margin of a communications link, two more values must be determined. The first is the desired  $\frac{E_b}{N_0}_{desired}$  for the bit error rate (BER) desired by the system. We chose 0.00001 as our desired BER, and SMAD recommends an  $\frac{E_b}{N_0}_{desired}$  of at least 2.7. Additionally, the implementation loss of the system, represented by  $L_i$ , also needs to be taken into account. The final calculation to determine the link margin, represented by  $M$ , is below.

$$M = \frac{E_b}{N_0} - \frac{E_b}{N_0}_{desired} + L_i$$

An  $M$  of 3 signifies that the expected signal strength can be attenuated by up to 50% and still be decipherable, and this was the value that the subsystem team tried to achieve for each communication link in the mission.

This analysis was done for each individual link in the mission architecture, and iterated upon by changing the various inputs described above.



## A.8 Command and Data Handling

TECHNICAL SPECIFICATIONS				
General		Interfaces		
Expected Life	5 years in LEO	SpaceWire	50Mbps	2
Processor	32-bit LEON3FT [IEEE-1754 SPARC v8] fault-tolerant processor	Serial Ports	RS422 / RS485 UARTs	3
Processor Clock	50 MHz	Serial Ports	RS485-only UARTs	2
SCET	15.25 us accuracy	PSS Interface	RS485 PPS input	1
SDRAM	64 MB (post-EDAC)	GPIO	3.3 V logic	12
Instruction Cache	8 kB	CCSDS SBand	RS422 level data stream and TRX command and housekeeping	1
Data Cache	8 kB	CCSDC XBand	LVDS level data stream and both RS422 and LVDS level TRX command and housekeeping	1
NVRAM	16 kB (post-EDAC)	CCSDS Umbilical	RS422 level data stream	1
Operating Temperature Range	-30°C to +60°C	Pulse Command Output	RS422 level CPDU pulse output	12
Nonvolatile System	2 GB (post-EDAC)			
Memory Nand Flash				
Mass Memory Storage	32 GB (post-EDAC)			
Power Supply Input	4.5 V to 16 V			

Size, Weight & Power	
Nominal Power Consumption	1.3 W
Mass	130 g
Length	95.89 mm
Width	90.17 mm
Height	17.20 mm

Figure 97: Data Specifications for Sirius OBC&TCM



## A.9 Power

	HOWLL	WOOF	PACK
<b>Peak Power Draw (W):</b>	73.564	73.564	47.064
<b>with Margin (1.1x) (W):</b>	80.9204	80.9204	51.7704
<b>Voltage (V):</b>	28	28	28
<b>Current (A):</b>	2.89	2.89	1.85
<b>EOL Battery Capacity (Ah):</b>	14.45	14.45	9.24
<b>Series Cells:</b>	8	8	8
<b>BOL Capacity (Ah):</b>	26.97	26.97	10.35
<b>Parallel Strings:</b>	10	10	4
<b>Total Batteries:</b>	73	73	28
<b>Total Mass (kg):</b>	3.65	3.65	1.40
<b>Volume (cm^3):</b>	277.61	277.61	106.56
<b>Total output for drain (Wh):</b>	755	755	290

Figure 98: Power storage specifications for each satellite

	HOWLL	WOOF	PACK
<b>Peak Power Draw (W):</b>	73.564	73.564	47.064
<b>with Margin (1.1x) (W):</b>	=B2*1.1	=C2*1.1	=D2*1.1
<b>Voltage (V):</b>	28	28	28
<b>Current (A):</b>	=B3/B4	=C3/C4	=D3/D4
<b>EOL Battery Capacity (Ah):</b>	=B5*5	=C5*5	=D5*5
<b>Series Cells:</b>	=B4/\$H\$2	=C4/\$H\$2	=D4/\$H\$2
<b>BOL Capacity (Ah):</b>	=(B6*1.12)/0.6	=(C6*1.12)/0.6	=(D6*1.12)
<b>Parallel Strings:</b>	=B8/\$J\$2	=C8/\$J\$2	=D8/\$J\$2
<b>Total Batteries:</b>	=B7*B9	=C7*C9	=D7*D9
<b>Total Mass (kg):</b>	=B10*0.05	=C10*0.05	=D10*0.05
<b>Volume (cm^3):</b>	=3.808*B10	=3.808*C10	=3.808*D10
<b>Total output for drain (Wh):</b>	=B8*28	=C8*28	=D8*28

Figure 99: Power storage calculations for each satellite



## A.10 Mechanisms

Table 124: Comparison of Various CubeSat Deployment Systems

Product	Payload Mass (kg)	Payload Volume	Confidence (Redundancy)	Tab vs. Rail	Vibrational Resistance	Notes
P-POD [221]	2kg/U	3U	Redundant deployment signals	Rail	NA	First developed CubeSat dispenser
NRCSD [222]	2kg/U	6U	Three redundant deployment signals	Rail	NA	Deploys CubeSats from ISS
ISIPOD [223]	2kg/U	12U	Redundant deployment signals	Rail	NA	Visual verification of separation
CSD [151]	2kg/U	27U	Redundant deployment, 99.6% confidence	Tab	Tabs prevent movement	Extra payload volume in the +Z direction. Power/Data ports to interface with CubeSat
RAMI [224]	2kg/U	NA	Multiple redundancies	Rail	NA	Interface to charge satellite batteries while integrates
Tyvak [225]	2kg/U	12U	NA	Rail	Reduces LV vibrations by 70-90%	Door is optional, allowing for more payload volume in +Z direction
Maxwell [153]	2kg/U	6U	Redundant actuation mechanism	Rail	NA	Optional rear mounting interface, reduced lead times (receive within 4 weeks of ordering)

Table 125: General Characteristics of Various Solar Array Release Mechanisms

Method	Reliability	Release Time	Shock	Mass	Power Draw
Pin Puller	Electrical and Mechanical Redundancy	almost instant	Medium	Medium	Medium
Frangibolt	Redundant Heating	Slow and imperfectly predictable	Low	Low	Medium
Burnwire	2 Redundant Burnwires	Fast but not instant	Medium	Medium	Low
Pyrotechnic Cable Cutter	99% at 95% confidence level	almost instant	High	High	Medium
Split Spool Release Device	Highly reliable (flight heritage), but not redundant	almost instant	Low	Low	High



Table 126: Specific Characteristics of Various Solar Array Release Mechanisms

Method	Product	Constraint Force (N)	Time to Release	Mass (g)	Power (W)
Pin Puller	EBAD TiNi Pin Puller P25 [226]	1825	130 ms max	75	12
Frangibolt	EBAD TiNi™ Frangi-bolt Actuator FC4 [157]	667	35 s	10	9
Burnwire	Naval Research Lab [227]	600	2.4-7.2 s	TBD	3
Pyrotechnic Cable Cutter	PACSCI EMC Cable Cutter [228]	Unknown	20 ms	173	6
Split Spool Release Device	EBAD NEA Hold Down Release Mechanisms (HDRM) [229]	1100	50 ms	13.6	16

Method	Product	Reliability	Constraint Force	Mass	Power
Pin Pullers	EBAD TiNi™ Pin Puller P25	Electrical and Mechanical Redundancy	1825 N	75g	12W
	EBAD TiNi™ Mini Frangibolt® Actuator FC4	Redundant Heating (and long heritage)	667N	10g	9W
Burnwire	Naval Research Lab	2 Redundant Burnwires (but limited heritage)	600N	20g	3W
Pyrotechnic Cable Cutter	PACSCI EMC	99% at 95% confidence level	TBD	173 g	6W
Split Spool Release Device	EBAD NEA® Hold Down & Release Mechanisms (HDRM)	Highly reliable (flight heritage), but not redundant	1100 N	<13.6g	16W

Figure 101: Release Mechanism Ranked Trade Study [226] [171] [227] [228] [229]



Table 127: Characteristics of Various Solar Array Drive Assemblies

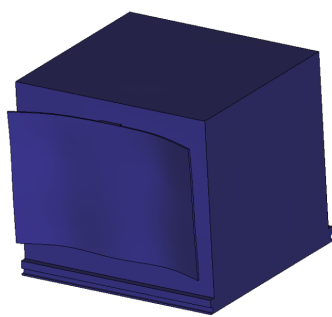
Supplier	Torque	Mass (g)	Power (W)	Precision (deg)	Range (deg)	Power Transmission (W)
Moog [160]	9.4 Nm	1160 kg	8.6 W	+/- 0.36	TBD	Slip Ring (TBD)
Pumpkin [161]	300mNm	TBD	2.4	0.15 degree step size, precision TBD	+/- 200	Slip Ring (TBD)
Beyond Gravity[162]	55 Nm (max)	5400	TBD	+/- 1	0-356	6300
Honeybee Robotics [163]	0.75 Nm	900	5	+/- 1.8	+/- 180	450
COMAT[164]	350mNm	465	TBD	+/- 3	TBD	200
DHV Technology[165]	60 mNm continuous, 120 mNm intermittent	250	5	TBD	+/- 180	84
Revolv Space [166]	TBD	350	6W peak, 3W average	+/- 1	+/- 180	TBD

## A.11 Structures and Materials

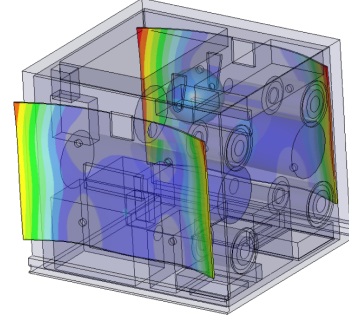
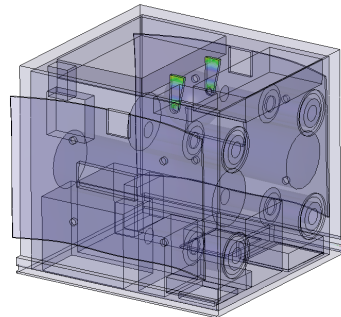
### A.11.1 Advanced Standard for CubeSats

### A.11.2 HOWLL Analysis Results

The following figures are visualizations of the static load analyses on the PACK-C spacecraft. Refer to Table 111 for numerical results.



(a) Stress visualization.

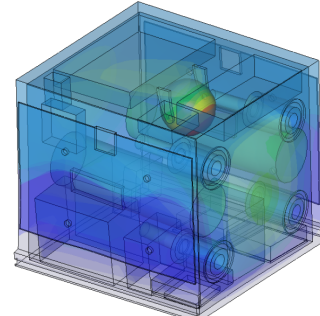
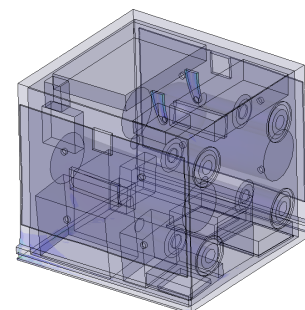


(b) Displacement visualization.

Figure 103: HOWLL static load analysis visualization for XY load case.



(a) Stress visualization.

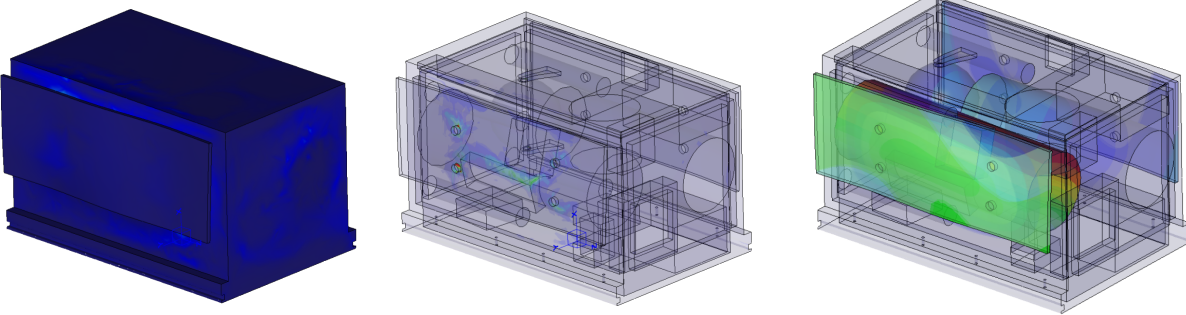


(b) Displacement visualization.

Figure 104: HOWLL static load analysis visualization for XZ load case.

### A.11.3 PACK-C Analysis Results

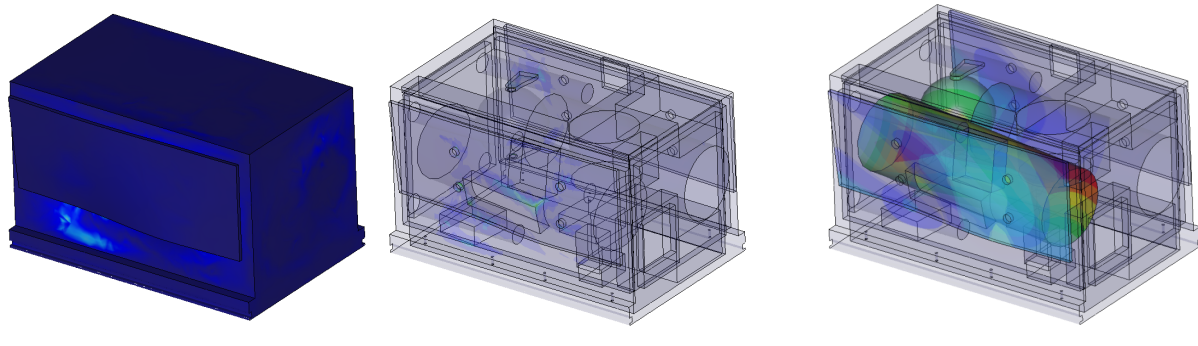
The following figures are visualizations of the static load analyses on the PACK-C spacecraft. Refer to Table 115 for numerical results.



(a) Stress visualization.

(b) Displacement visualization.

Figure 105: PACK static load analysis visualization for XY load case.



(a) Stress visualization.

(b) Displacement visualization.

Figure 106: PACK static load analysis visualization for XZ load case.

#### A.11.4 Falcon 9 Rideshare Environments

The following tables describe the Falcon 9 Rideshare launch and flight environments.

Table 128: Shock Test Environment [202]

Frequency(Hz)	MPE (g)
100	30
1000	1000
1950	1000
10000	1000



Table 129: Random Vibration Environment [214]

Frequency(Hz)	Random Vibration MPE
20	0.01
50	0.0
700	0.015
800	0.03
925	0.03
2000	0.00644

Table 130: Maximum Payload Emission [214]

Frequency MHz	Max Payload Emission by Test (dB $\mu$ V/m)	Max Payload Emission by Analysis (dB $\mu$ V/m)
30 - 1555.42	90	84
1555.42 - 1595.42	48	42
31595.42 - 18000	90	84

Table 131: Temperature Environments [214]

Time (s)	Hot Temperature (°C)	Cold Temperature (°C)
0	40	-5
1000	42	-10
2000	55	-15
3000	69	-20
7200	69	-20

Table 132: Sinusoidal Vibration Environment [214]

Frequency (Hz)	Axial Sinusoidal Vibration MPE (g)	Lateral Sinusoidal Vibration MPE (g)
5	1.4	1.5
100	1.4	1.5



Table 133: Pressure Requirements [214]

	Pressure Vessel	Fully Integrated Pressure System
Test Fluid	<ul style="list-style-type: none"> <li>If working fluid is helium gas: 100% HE</li> <li>If working fluid is liquid: 100% N</li> </ul>	<ul style="list-style-type: none"> <li>If working fluid is gaseous helium: 100% HE</li> <li>If working fluid is liquid: 100% N</li> </ul>
Method	Fully submerge vessel in water	Coat all fittings and connections with Snoop
Success	<ul style="list-style-type: none"> <li>No bubbles</li> <li>Max leak rate is <math>10^{-4}</math></li> </ul>	<ul style="list-style-type: none"> <li>No bubbles</li> <li>Max leak rate is <math>10^{-4}</math></li> </ul>
Minimum Duration	1 hour	5 minutes

### A.11.5 Verification of Requirements and Constraints

Table 134: Verification of technical requirements.

Requirement	Verified?	Justification
SM-F-001	Yes	Spacecraft buses house all mission components as well as the payload.
SM-F-002	Partially	Mounting structures have been designed to the extent of our abilities given the information we have.
SM-F-003	Yes	We have identified and characterized spacecraft bus materials.
SM-F-004	Yes	Components are either in the CAD model of the layout or (for very small components) have designated positions in the spacecraft.
SM-F-005	Yes	Modal analysis complete.
SM-F-006	Yes	Moments of inertia have been characterized.
SM-F-007	Yes	We have determined thermal coefficients for our materials.
SM-P-001	Yes	We use a yield safety factor of 2.
SM-P-002	Partially	We have characterized the modes of the solar arrays but characterizing the modes of other components (e.g. the SADAs) would be out of the scope of this project as this information is not publicly available.



Table 135: Verification of constraints.

Requirement	Verified?	Justification
SM-C-001	Yes	HOWLL SM subsystem has mass of 9.50 kg.
SM-C-002	Yes	WOOF SM subsystem has mass of 9.50 kg.
SM-C-003	Yes	PACK-C SM subsystem has mass of 5.79 kg.
SM-C-004	Yes	PACK-E SM subsystem has mass of 5.79 kg.
SM-C-005	Yes	HOWLL fits in 27U envelope.
SM-C-006	Yes	WOOF fits in 27U envelope.
SM-C-007	Yes	PACK-C fits in 12U envelope.
SM-C-008	Yes	PACK-E fits in 12U envelope.
SM-C-009	Yes	SM subsystems consume no power.
SM-C-010	Yes	SM subsystems consumes no on-board computational power.
SM-C-011	Yes	Spacecraft buses were designed to comply with CDS and ASC.

Table 136: Verification of environmental requirements.

Requirement	Verified?	Justification
SM-E-001	Yes	Spacecraft buses survive flight load environments, which encompass the gravitational environment of cislunar space.
SM-E-002	Yes	Spacecraft buses are designed to survive radiation.
SM-E-003	Yes	Spacecraft bus materials do not have significant changes in material properties in this temperature range.
SM-E-004	Yes	Static load analyses suggest that spacecraft will withstand these loads.
SM-E-005	Yes	Modal analyses suggest that spacecraft will withstand these vibration environments.
SM-E-006	Partially	SM subsystem materials verified to satisfy TML requirement. Verification of other subsystems' components are not possible with publicly available information, but most components have significant flight heritage and are likely to meet outgassing requirements.
SM-E-007	Partially	SM subsystem materials verified to satisfy CVCM requirement. Verification of other subsystems' components are not possible with publicly available information.

Xometry was used to get a quote for the cost breakdown of the SM subsystem. An example of a Xometry quote is also shown.



1
12u-frame-y-plus.prt.14 v0
Configure Part
Revise CAD
+ Upload Drawings
Remove

Repeat Part i

Quantity
-
1
+

**Measurement:** 366.00 mm × 187.80 mm × 12.00 mm,  
242351.73 mm<sup>3</sup> | 14.409 in × 7.394 in × 0.472 in, 14.789 in<sup>3</sup>

**Process:** 3D Printing

**Technology:** Fused Deposition Modeling (FDM)

**Material:** ABS or ASA, Next Available, Color: Next Available, Infill: UltraLight

**Finish:** Standard

**Threads and Tapped Holes:** Threads and Tapped Holes, None

**Inserts:** Inserts: 0

**Inspection:** Formal Inspection with Dimensional Report

**Certificates and Supplier Qualifications:** Certificate of Conformance, Standard Material Certification

Expedite   Made in USA	\$640.20 ea.
12 business days	<b>\$640.20</b>
<hr/>	
Standard   Made in USA	\$321.12 ea.
21 business days	<b>\$321.12</b>
<hr/>	
Economy   Made in USA	\$288.46 ea.
32 business days	<b>\$288.46</b>

Figure 107: Quote for PACK y-plus frame

Table 137: SM subsystem cost breakdown of HOWLL satellite

Component	Cost per Unit (\$)	Quantity	Total Cost of Component
X+ Panel	1155	1	1155
X- Panel	2030	1	2030
Y+ Panel	1285	1	1285
Y- Panel	1285	1	1285
Z- Panel	1210	1	1210
Z+ Panel	1210	1	1210
Secondary Brackets	900	45	40500

**Tot SM subsystem cost for HOWLL: \$48,675**



Table 138: SM subsystem cost breakdown of WOOF satellite

Component	Cost per Unit (\$)	Quantity	Total Cost of Component
X+ Panel	1155	1	1155
X- Panel	2030	1	2030
Y+ Panel	1285	1	1285
Y- Panel	1285	1	1285
Z- Panel	1210	1	1210
Z+ Panel	1210	1	1210
Secondary Brackets	900	43	38700

**Tot SM subsystem cost for WOOF: \$46,875**

Table 139: SM subsystem cost breakdown for each PACK-C and PACK-E satellite

Component	Cost per Unit (\$)	Quantity	Total Cost of Component
X+ Panel	920	1	920
X- Panel	1535	1	1535
Y+ Panel	645	1	645
Y- Panel	645	1	645
Z- Panel	885	1	885
Z+ Panel	885	1	885
Secondary Brackets	900	47	42300

**Total SM subsystem cost for PACK-C and PACK-E: \$47,815 each**



**TiNi™ MINI Frangibolt® FD04 Technical Specifications**

Actuator Family	FD04	
Ti Fastener Size	#4	
Mass	10g	
Power	9W @ 7V	9W @ 12V
Operational Voltage	6V-8V	10.5V-13.5V
Current Draw	.125A @ 7V	.75A @ 12V
Resistance	$5.5 \pm 5 \Omega$	$16 \pm 1.6 \Omega$
Max Load Support	150lbf (667N)	
Function Time	30s @ 7V (23°C)	30s @ 12V (23°C)
Life	50 cycles min	
Operating Temperature	$-50^{\circ}\text{C} + 70^{\circ}\text{C}$	
Compressed Length (X")	.500"	
Diameter (Y")	.450"	
Thruhole (Z")	.116"	

**TiNi™ MINI Frangibolt® FD04 Mechanical Interface Drawing**

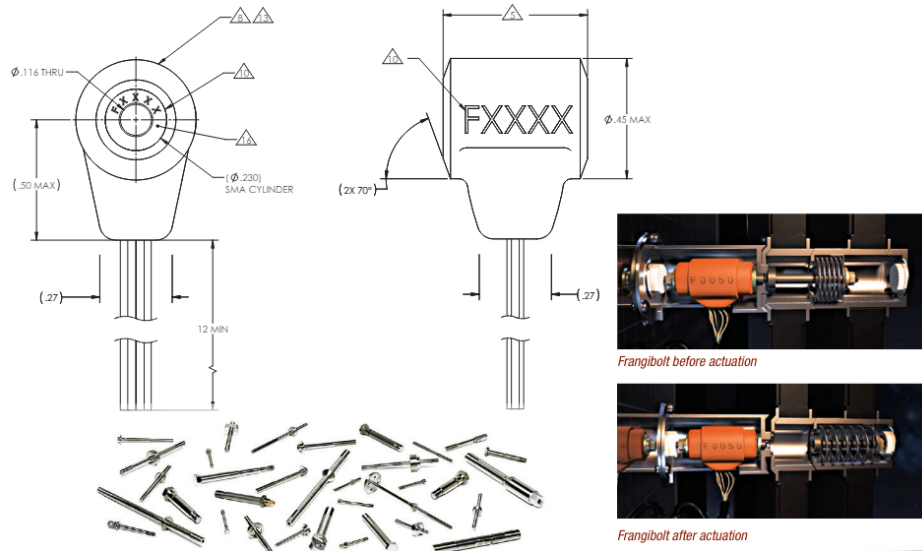


Figure 100: Specifications on the EBAD TiNi Frangibolt



**PARAMETERS**

SYM	Parameter	Conditions	Unit	6U with Rails		6U with Tabs		12U with Tabs		27U with Tabs	
				Min	Max	Min	Max	Min	Max	Min	Max
M	Mass	At launch	kg	0	12	0	12	0	24	0	54
CMx	Center of mass, X	Stowed in canister	mm	30	70	10	70	55	125	100	180
CMy	Center of mass, Y	Stowed in canister	mm	-40	40	-40	40	-40	40	-60	60
CMz	Center of mass, Z	Stowed in canister	mm	133	233	133	233	133	233	133	233
Depth	Maximum payload depth, +X dimension		mm	-	-	0	106.4	0	219.1	0	331.8
Width	Maximum payload width from origin, $\pm Y$ dimension		mm	-	-	0	119.5	0	119.5	0	175.9
Tab Width	$\pm Y$ dimension		mm	-	-	237.6	238.0	237.6	238.0	350.3	350.7
Tab Length	+Z dimension		mm	-	-	360.9	365.9	360.9	365.9	360.9	365.9
DSX	+X dimension defining allowable zone for deployment switches		mm	-	-	-	100	-	212	-	325
FDS	Force from deployment switches, summated, Z axis	When contacting CSD ejection plate	N	0	2.2	0	2.2	0	2.2	0	2.2
DDS	Payload separation from ejection plate necessary to change deployment switch state, Z axis		mm	1.3	12	1.3	12	1.3	12	1.3	12
FFD	Friction force imparted on deployables from canister walls during ejection, summated		N	0	2.0	0	2.0	0	2.0	0	2.0
FND	Normal force deployables impart on canister walls during ejection, per wall		N	0	4.0	0	4.0	0	4.0	0	4.0
EL	External load on payload, any direction	supported solely by tabs or rails	g	29	(1)	29	(1)	23	(1)	16	(1)
TML	Total Mass Loss	Per ASTM E 595-77/84/90	%	0	1.0	0	1.0	0	1.0	0	1.0
CVCM	Collected Volatile Condensable Material	Per ASTM E 595-77/84/90	%	0	0.1	0	0.1	0	0.1	0	0.1
DP	Canister de-pressurization rate	During launch	psi/sec	0	0.5	0	0.5	0	0.5	0	0.5

(1) Load increases with reduced payload mass. Load[g] = 51.8.75\*ln(mass[kg]).

Figure 102: CubeSat parameters from the Advanced Standard for Cubesats [156].

## B Contributions Table

Table 140: Team Contributions

Team Member	Roles	Sections
Sidney Bae	Data Curation, Formal Analysis, Validation, Writing - Original Draft, Review, and Editing	§1.2, 2.1, 6.1, 6.2, 6.3, 6.6, 6.7, 8, 9
Patrick Kozak	Design, Data Curation, Formal Analysis, Validation, Writing - Original Draft, Editing	§9.4, 9.5, 9.6, 9.7, 6, 8
Albert	Data Curation, Formal Analysis, Validation, Writing - Original Draft, Review, and Editing	§, 8.1, 8.2, 8.3, 8.4, 8.5, 8.6, 8.7.1, 8.7.2, 8.7.3, 8.7.4, 6, 9
Ariana Rausch	Data Curation, Formal Analysis, Validation, Writing - Original Draft, Review, and Editing	§1.5, 8.1, 8.2, 8.3, 8.4, 8.5, 8.6, 8.7.1, 8.7.2, 8.7.3, 8.7.4
Sabrina Nicacio	Data Curation, Formal Analysis, Validation, Writing, Editing - Original Draft, Review, and Editing	1.3, 1.5, 6.3, 6.4, 6.5, 6.6, 6.7, 8, 9
Isabel Kim	Design, Data Curation, Formal Analysis, Validation, Writing, Editing	1.2, 9.1, 9.2, 9.3, 9.4, 9.6, 9.7
Mori Ono	Data Curation, Methodology, Formal Analysis, Validation, Writing - Original Draft, Review, and Editing	1.4, 3, 5.3, 5.6, 5.7
Raphael Vogley	Conceptualization, Formal Analysis, Writing - Original Draft, Writing - Reviewing and Editing	Sections 2.5, 12.3, 12.4, 12.7.2, 12.7.4
Sarah Fry	Conceptualization, Investigation, Data Curation, Methodology, Formal Analysis, Validation, Writing - Original Draft, Review, and Editing	1.3, 7.1, 7.2, 7.5, 7.6, 7.6.3, 7.7.1, 7.7.4
Julia Hutto	Conceptualization, Investigation, Writing - Original Draft	5.1 - 5.6, 5.7.4
Kazuki Tojo	Conceptualisation, Formal Analysis, Investigation, Methodology, Project Administration, Supervision, Validation, Visualisation, Writing - Original Draft, Writing - Reviewing & Editing	Abstract, 1, 2, 3, 7.3, 7.4, 7.6.1, 7.6.2, 7.7.2, 7.7.3
Pia DiCenzo	Conceptualization, Data Curation, Formal Analysis, Writing - Original Draft, Writing - Reviewing and Editing	12.1, 12.2, 12.5, 12.6, 12.7.3, 12.7.5
Anna Solzhenitsyn	Conceptualization, Methodology, Data Curation, Formal Analysis, Writing - Original Draft, Writing - Reviewing and Editing	1.2, 13.1, 13.2, 13.4, 13.5, 13.6, 13.6.1, 13.6.5, 13.7.1, 13.7.5
Candace Do	Conceptualization, Methodology, Formal Analysis, Writing - Original Draft, Writing - Reviewing & Editing	15, 2.3, 2.4

Continued on next page



Table 140 – continued from previous page

Team Member	Roles	Sections
Evan Alfandre	Conceptualization, Data Curation, Formal Analysis, Validation, Writing - Original Draft, Reviewing, and Editing	2.1 2.6 13 14 15
Manali Badwe	Conceptualization, Methodology, Formal Analysis, Writing - Original Draft	15.7.4, 15.7.3, 15.7.2, 15.7.1, 15.7.7, 2.4
Rihan Sajid	Formal Analysis, Conceptualization, Writing - Original Draft, Reviewing & Editing, Methodology	4.4, 4.5, 14.1, 14.3, 14.5, 14.7
Ben Kim	Data Curation, Formal Analysis, Investigation, Validation, Writing - original draft, Writing - review & editing	1.1, 14.2, 14.4, 14.6, 14.7.2, 14.7.5, 14.7.6, 14.7.7
Carrie Geisler	Conceptualization, Methodology, Writing - Original Draft, Writing - Reviewing & Editing	2.2, 4, 10, 11
Jack Amen	Conceptualization, Methodology, Data Curation, Formal Analysis, Visualization, Writing - Original Draft, Writing - Reviewing and Editing	2.2, 3, 10
Max Kreidl	Investigation, Writing - Original Draft, Writing - Reviewing & Editing	1.4, 3, 11, 11.6, 11.7
Charlie Rogers	Conceptualization, Methodology, Project Administration, Validation, Writing - Original Draft & Reviewing/Editing	1 1.7 4 10 11
Zoe Koniaris	Conceptualization, Methodology, Project Administration, Validation, Writing - Original Draft	Abstract, 1.6, 4, 4.7.8, 4.7.5, 4.7.6, 4.7.4, 4.7.2, 4.7.7, 4.6, 4.7, 4.1
Andrew Robbins	Conceptualization, Visualization, Writing - Original Draft, Writing - Reviewing & Editing,	



## C Contributions Description

1. **Sidney Bae:** I was the GNC, ADCS, and Payload Co-Team Leader with Sabrina Nicacio. I wrote the Mission Objectives Section (1.2). I finalized our requirements for GNC. I also wrote all of Sections 6.1, 6.2, and 6.6. I did all of the access time, station-keeping, and close approach analysis and wrote those sections accordingly (Sections 6.7.1, 6.7.2, 6.7.3). I also made the simulations for the insertion for PACK and wrote most of 6.7.4. Finally, I generated the date and created the entire Appendix for the GNC team. For oversight, I edited and reviewed Section 2.1, the ADCS (8), and Payload (9) reports.
2. **Patrick Kozak:** My primary focus was on the payload subsystem with Isabel Kim. For this report, I ran and analyzed STK EOIR simulations for the PACK satellites and their space objects, as well as wrote the subsystem constraints, drivers, design approach and PACK section of the formal analysis. I also peer reviewed the remainder of the payload subsystem report, as well as the GNC and ADCS reports.
3. **Albert Kreutzer:** I was working with Ariana on the ADCS design, worked heavily on the design approach 8.6, and edited the requirements in the spreadsheet and as part of Sec. 8.3. I also determined the analysis in 8.7 for the MOI and torque, worked out the control modes 8.7.1 and determined the budget compliance and algorithms 8.7.5.
4. **Ariana Rausch:** I was primarily working on the ADCS system with Albert Kreutzer, wrote the mission drivers section as well as the following sections within the ADCS chapter: 1.5, 8.1, 8.2, 8.3, 8.4, 8.5, 8.6. I wrote and conducted the analysis in the following sections: 8.7.1, 8.7.2, 8.7.3, 8.7.4.
5. **Sabrina Nicacio:** I was the GNC, ADCS, and Payload Co-Team Leader with Sidney Bae, wrote the GNC Constraints and Drivers sections, worked on the requirements spreadsheet, generated STK simulations for insertion and end-of-life, and wrote in the GNC Design and Analysis section. I also generated data on the GNC appendix, reviewed, wrote the list of acronyms, edited chapters 8 and 9 for ADCS and Payload, and edited the overall mission requirements and drivers in Sections 1.3 and 1.5.
6. **Isabel Kim:** I spearheaded the design and analysis of the i-SIM 90 camera on HOWLL and WOOF satellites, which is outlined in Section 9.7.2. I conducted the SNR analysis in STK and calculated the corresponding SNR values by writing a script for the .csv file. I conducted the necessary background research on high-resolution cameras and infrared sensors in order to provide a valid explanation for why these were chosen. I wrote Sections 9.1, 9.2, 9.3, and 9.6. I also described the analysis process in Section 9.7. I wrote Section 9.7.2, which discusses the analysis and results for the L1/L2 Halo objects and GTO to L1/L2 Halo objects.
7. **Mori Ono:** I was the LV, Power, and Propulsion Co-Team Leader with Sarah Fry. I wrote the Launch Vehicle subsystem Sections 5.7.1, 5.7.2, 5.7.3, and 5.7.5. I also wrote most of the Launch Vehicle subsystem sections 5.6 and part of Section 5.7.4. I also compiled information and formatted the tables in Section 5.7. In terms of analysis, I independently reviewed compliance with the subsystem requirements and made adjustments to the requirements. I conducted the STK delta-V analysis and the conjunction analysis and potential opportunities for recouping launch costs. I proofread for the other sections of the Launch Vehicle subsystem. Additionally, I revised the team logo. Finally, I wrote the mission constraints as



described in Section 1.4 and reviewed systems integration in Section 3.

8. **Raphael Vogeley:** I wrote and refined the power subsystem requirements and constraints. I worked with the GNC subsystem and their STK simulation to acquire eclipse and sun times for each satellite. I worked on determining the power loads constraining the power system design through the gathering and analysis of ARGOS mission component nominal power draws and duty cycles. I worked on the power generation for the mission, performing a trade study on available generation methods and performing analysis to
9. **Sarah Fry:** I wrote the original draft of the Mission Requirements section and checked through all mission requirements in the ARGOS Mission Requirements spreadsheet to ensure that no TBC, TBD, or TBR values remained. Additionally, I wrote the original draft of the Propulsion Subsystem Overview, Objectives, and Drivers, adjusting them to fit the current needs of the team for the FDR report. Within the Propulsion subsystem, I was solely responsible for all tank sizing, propellant and pressurant storage feeding and management, and worked very closely with the GNC, ADCS, LV, and SM subsystems to ensure that all delta-V requirements could be achieved while still satisfying spacecraft layout constraints. For the FDR in particular, I redesigned the propellant feed system to correct an error I had made in a previous iteration of the design. I also refined my calculations to further reduce the mass and volume requirements of the PROP subsystem and designed the propellant feeding system. In addition to this, I carried out all PROP Subsystem trade studies related to initial thruster selection and ranking in my ARGOS Propulsion Trade Study [79] spreadsheet. Finally, in terms of team operations and synergy, I served as a PROP subsystem lead, and helped facilitate inter-subsystem communication over the course of the semester. A complete list of the sections I wrote for the FDR is as follows: 1.3, 7.1, 7.2, 7.5, 7.6, 7.6.3, 7.7.1, 7.7.4.
10. **Julia Hutto:** I refined and ensured Launch Vehicle design compliance with ORC. I also contributed to analysis conducted for section 5.7.4 to choose alternative and replacement launch options. I wrote sections 5.1-5.5 and parts of 5.6 and 5.7.
11. **Kazuki Tojo:** As co-lead of Project ARGOS with Zoe Koniaris, I was heavily invested in almost every aspect of this project from start to finish. Leading a 24-person team was incredibly challenging but rewarding, as I multitasked and handled a range of responsibilities from team disputes to team-wide meetings to ensure progress in the right direction. This project was my most substantial time commitment this semester, as leadership for Project ARGOS extended well beyond scheduled sessions to coordinate with all subsystems, sometimes from morning to night. My contributions to this report spanned from the Propulsion subsystem to the general report as a whole. Within Propulsion, I first worked on Subsystem Requirements (7.3) and Constraints (7.4). I went through each of nearly 80 requirements, making adjustments and finalising quantitative values. For the Design Approach, I worked on Thruster Selection, Operation & Layout (7.6.1) and Nozzles (7.6.2), outlining the changes made since the previous design iteration to address important feedback from the PDR, FDR and Goddard. I analysed these changes to demonstrate requirement compliance in the Formal Analysis sections (7.7.1 & 7.7.2). I then reviewed Sarah Fry's writing for the rest of Propulsion as well. I also went through each of nearly 60 Mission Requirements to compile a compliance table for section 2.1, followed by an analysis of each of them to determine compliance and identify which section of this report demonstrates it. More broadly, I reviewed



and added to the Abstract and sections 1-3 to check and polish high-level aspects of the mission. Finally, Max Kreidl and I took charge of creating and shifting over to an entirely new, well-organised Overleaf project to allow for efficient and robust troubleshooting of LaTeX syntax errors that were inevitable with a nearly 300-page document of 24 editors. These syntax errors were causing severe and constant issues for the entire team.

12. **Pia DiCenzo:** I curated and finalized the Power sections 12.1, 12.2, 12.5, 12.6, 12.7.3, 12.7.5. I worked on the power storage system and designed the size and capabilities of the battery packs. I performed a trade study for the optimal batteries to be used in the mission. I also chose the power management and distribution system for the power subsystem, performing a trade study for all of the available options and another for the available COTS PMADs.
13. **Anna Solzhenitsyn:** I reviewed section 1.2 to ensure the mission objectives were correct, and read over the first three sections of the report to ensure cohesion and thoroughness. I wrote sections 13.1, 13.2, 13.4, 13.5, 13.6, 13.6.1, 13.6.5, and 13.7.1 for the mechanisms subsystem. I wrote some new requirements for the Mech subsystem and verified all the traces. I researched costs for each component and made estimates for each component 13.7.5. I reviewed all the Mech sections that I was not responsible for writing, and proof-read and provided comments to the SM and Thermal sections. I spent significant time de-bugging for all subsystems when the entire overleaf document would not compile. I verified that acronyms throughout the entire report, and ensured that citations were compiling correctly, fixing errors for many other subsystems.
14. **Candace Do:** I updated the CAD models of subsystem components as well as the overall layout. I defined and ran static load analyses and modal surveys for both spacecraft models. I wrote Sections 15.7.5 and 15.7.6 (detailing the design and analysis of the spacecraft frames and internal layout). I also verified that the SM subsystem met its objectives and requirements in Section 15.7.8. Finally, I reviewed the rest of Section 15, wrote Section 2.3 on mission mass compliance, and reviewed Section 2.4 (mission volume compliance), Section 13 (Mechanisms), and Section 14 (Thermal).
15. **Evan Alfandre:** I wrote all portions of the Mechanisms section that relate to the three solar array mechanisms. I also wrote and refined the mechanisms requirements and wrote the requirements section, and assisted in the writing of the other mechanisms high-level sections. I was intricately involved in the discussions and decisions surrounding the choice to not include the sensor cover and sensor pointing mechanisms. I reviewed all portions of the mechanisms section that I was not directly responsible for writing. I wrote Section 2.6 and reviewed Section 2.1. I read and reviewed the SM and Thermal sections of the report to provide comments.
16. **Manali Badwe:** I wrote the materials, radiation shielding, solar panel array materials, material outgassing, and verification testing sections in the Section 15. In addition, I wrote the SM subsystem overview, requirements, objectives, constraints, and drivers sections. I also did the mission volume compliance budgets and volume markups.
17. **Rihan Sajid:** I wrote sections 14.1, 14.3, and 14.5 of the Thermal subsystem. I also contributed very heavily to section 14.7 which was the formal analysis. This included the thermal regulation calculations and research regarding suitable components. I also performed trade studies for the components that the thermal team selected. I also reviewed and com-



mented on sections 4.4 and 4.5 to improve the clarity in that section.

18. **Ben Kim:** I was subteam lead of SM/Mech/Thermal. I actively communicated on behalf of Thermal with other subsystems and participated in team-wide discussions. More specific to originally writing the sections mentioned above some of which are unique to the FDR, I rewrote and added various information to supplement clarity and addressed all inter-subteam feedback. I found and integrated all pictures relevant to the thermal subsystem. I performed the entirety of the budget analysis, giving mass, volume, and cost estimates for all components. I helped reorganize and conduct the temperature analysis to account for all varying conditions and classes. I was also responsible for keeping track of tasks and notes in a document to ensure smooth subsystem operation.
19. **Carrie Geisler:** I summarized our subsystem ORCs and provided updates on any changes to them since the PDR. I summarized the process of risk identification and mitigation, and provided updates on the downgrade of most of our medium-high risks, as well as our single points of failure. I summarized and updated the budget distribution, clearly showing subsystem and mission level compliance with the cost budget. I also read and reviewed both the Comms and CDH Design sections.
20. **Jack Amen:** I wrote the Design Approach, Formal Analysis, and Appendix sections of the Comms section, as well as assisted in writing and editing the Overview, Objectives, Requirements, Constraints, and Drivers sections. My focus on analysis this time was the addition of redundancy to the subsystem to fulfill our final requirement. Outside of the Comms sphere, I was the secondary contributor to the Cost Compliance and Systems Integration sections in support of Carrie Geisler and Max Kreidl, assisting with edits and additions where needed. Finally, I reviewed the Ops and CDH sections.
21. **Max Kreidl:** I created the system block diagram in section 3 and wrote the accompanying integration in section 3. I also wrote the CDH design and analysis sections (11.6, 11.7). I was the main reviewer for the rest of the sections in the CDH section (section 11). I also reviewed the mission constraints section (section 1.4). I worked on general debugging within the document as a whole and organizing the source documents so that there were fewer errors with citations during the writing process for the team. Along with Kazuki, I created a structural framework to allow for more cohesive editing and review within our team. I also briefly reviewed the Ops and Comms sections of the report.
22. **Charlie Rogers:** I was group lead for the Comms/CDH/Ops subsystem group, and took a co-project manager role in completion of team reports. In this report my team focused efforts were focused on managing completion of the executive summary section. I also wrote the Key Design Decision section 1.7. Regarding my subsystem group, I first focused on task organization, ensuring everyone has proper sections assigned and were completing work on schedule. The majority of my writing efforts were focused on the C&DH subsystem particularly the first 5 sections and figure generation for the Chapter. I also drafted the compliance portion of the 7th section. I also assisted in writing of the beginning portions of the Comms sections and creating their block diagram. Finally I reviewed and edited all sections of the report pertaining to my subsystem group (Ops/C&DH/Comms).
23. **Zoe Koniaris:** I was one of the co-Project Managers for the ARGOS mission. Throughout the semester, I would regularly plan and lead team meetings and facilitate discussions in



our team communications channel that influenced the trajectory of the mission, subsystem design choices, and technical report writing. I was highly communicative about team needs in the group chat, as well as being very responsive to all questions that I was equipped to answer. I assigned group-level sections of the report to appropriate team members, being conscious of their expertise and experience in each area. I wrote the abstract and the Concept of Operations sections for the FDR Report. For the Ops section, I wrote the subsystem overview, subsystem design approach, and the majority of the formal analysis sections 1.6, 4, 4.7.8, 4.7.5, 4.7.6, 4.7.4, 4.7.2, 4.7.7, 4.6, 4.7, 4.1 (excluding the risk analysis and mission budget). I reviewed all content in the Ops section. I reviewed all sections in the executive summary section, the compliance section, and the systems integration section.

24. **Andrew Robbins:** I wrote the Overview, Objectives, Requirements, Constraints, and Drivers sections. I also helped to review and edit the Design Approach section. My focus when writing sections 11.1 to 11.5 was to ensure that the most pertinent and relevant information from the previous reports was included while refining these sections to be as clear and concise as possible. Outside of COMMS I created and edited the Concept of Operations Image. For the FDR it received changes from the PDR. Lastly I reviewed the OPS and C&DH sections.